

**R**  
**ADIOLOGY**  
**AND**  
**ONCOLOGY**

**vol.51 no.3**

**september 2017**



# NOVO



Cilja na 2 procesa nastanka CINV\* v 1 odmerku  
Zagotavlja učinkovito 5-dnevno preprečevanje CINV<sup>1-5</sup>

## En odmerek Dvojno delovanje 5-dnevno preprečevanje<sup>1-5</sup>

**Akynzeo**<sup>®</sup>  
netupitant/palonosetron

\* CINV: Chemotherapy-induced nausea and vomiting  
[Slabost in bruhanje povzročena s kemoterapijo]

1. Aapro M et al. Ann Oncol. 2014 Jul;25(7):1328-33.
2. Hesketh et al. Ann Oncol. 2014 Jul;25(7):1340-46.
3. Gralla RJ et al. Ann Oncol. 2014 Jul;25(7):1333-39.
4. Rojas C et al. Eur J Pharmacol. 2014 Jan 5;572:26-37.
5. Akynzeo SmPC, junij 2016

### SKRAJŠAN POVZETEK GLAVNIH ZNAČILNOSTI ZDRAVILA

▼ Za to zdravilo se izvaja dodatno spremljanje varnosti. Tako bodo hitreje na voljo nove informacije o njegovi varnosti. Zdravstvene delavce naprošamo, da poročajo o katerem koli domnevnem neželenem učinku zdravila.

#### Akynzeo 300 mg/0,5 mg trde kapsule (netupitant/palonosetron)

**TERAPEVTSKE INDIKACIJE** Pri odraslih za preprečevanje akutne in zakasnjene navzee in bruhanja, povezanih z zelo emetogeno kemoterapijo na osnovi cisplatina za zdravljenje raka ter z zmerno emetogeno kemoterapijo za zdravljenje raka. **ODMERJANJE IN NAČIN UPORABE** Eno 300 mg/0,5 mg kapsulo je treba dati približno eno uro pred začetkom vsakega cikla kemoterapije. Trdo kapsulo je treba pogoltniti celo. Kapsulo je mogoče vzeti s hrano ali brez nje. Priporočeni peroralni odmerek deksametazona je treba ob sočasni uporabi z Akynzeom zmanjšati za približno 50 %. Prilagoditev odmerka pri starejših bolnikih ni potrebna. Pri uporabi tega zdravila pri bolnikih, starejših od 75 let, je potrebna previdnost zaradi dolgega razpolovnega časa zdravilnih učinkovin in omejenih izkušenj s to populacijo. Varnost in učinkovitost Akynzea pri pediatrični populaciji nista bili dokazani. Prilagoditev odmerka pri bolnikih z blago do hudo okvaro ledvic predvidoma ni potrebna. Potrebno se je izogibati uporabi Akynzea pri bolnikih s končnim stadijem boleznih ledvic, ki potrebujejo hemodializo. Pri bolnikih z blago ali zmerno okvaro jeter (stopnje 5-8 po lestvici Child-Pugh) prilagoditev odmerka ni potrebna. Pri bolnikih s hudo okvaro jeter (stopnja  $\geq 9$  po lestvici Child-Pugh) je treba Akynzeo uporabljati previdno. **KONTRAINDIKACIJE** Preobčutljivost na zdravilni učinkovini ali katero koli pomožno snov, nosečnost. **POSEBNA OPOZORILA IN PREVIDNOSTNI UKREPI** Ker lahko palonosetron podaljša čas prehoda skozi debelo črevo, je treba bolnike z anamnezo zaprtja ali znaki subakutne zapore črevesa po dajanju zdravila spremljati. Pri uporabi antagonistov 5-HT<sub>3</sub> samih ali v kombinaciji z drugimi serotonergičnimi zdravili (vključno s selektivnimi zaviralci ponovnega privzema serotonina (SSRI) in zaviralci ponovnega privzema serotonina in noradrenalina (SNRI)) so poročali o serotoninskem sindromu. Priporočamo ustrezno opazovanje bolnikov glede simptomov, podobnih kot pri serotoninskem sindromu. Ker Akynzeo vsebuje antagonist receptorjev 5-HT<sub>3</sub>, je potrebna previdnost pri sočasni uporabi z zdravili, ki sočasno peroralno prejemajo zdravilne učinkovine, ki se primarno presnavljajo prek CYP3A4 in imajo ozko terapevtsko območje. Netupitant je zmeren zaviralec CYP3A4 in lahko poveča izpostavljenost kemoterapevtskim zdravilom, ki so substrati za CYP3A4, npr. docetakselu. Zaradi tega je treba bolnike spremljati glede povečane toksičnosti kemoterapevtskih zdravil, ki so substrati za CYP3A4, vključno z irinotekanom. Poleg tega lahko netupitant vpliva tudi na učinkovitost kemoterapevtskih zdravil, pri katerih je potrebna aktivacija prek presnove s CYP3A4. Akynzeo vsebuje sorbitol in saharozo. Bolniki z redko dedno intoleranco za fruktozo, malabsorpcijo glukoze/galaktoze ali pomanjkanjem saharoze-izomaltaze ne smejo jemati tega zdravila. Poleg tega lahko vsebuje tudi sledi lecitina, pridobljenega iz soje. Zaradi tega je treba bolnike z znano preobčutljivostjo na arašide

ali sojo skrbno spremljati glede znakov alergijske reakcije. Ženske v rodni dobi ne smejo biti noseče ali zanositi med zdravljenjem z Akynzeom. Pred začetkom zdravljenja je treba opraviti test nosečnosti pri vseh ženskah, ki še niso imele menopavze. Ženske v rodni dobi morajo uporabljati učinkovito kontracepcijo med zdravljenjem in še do en mesec po njem. Akynzeo je kontraindiciran med nosečnostjo. Med zdravljenjem z Akynzeom in še 1 mesec po zadnjem odmerku je treba prenehati z dojenjem. **INTERAKCIJE** Ob sočasni uporabi Akynzea z drugim zaviralcem CYP3A4 lahko pride do zvišanja plazemskih koncentracij netupitanta. Pri sočasni uporabi Akynzea in zdravil, ki spodbujajo delovanje CYP3A4, lahko pride do znižanja plazemskih koncentracij netupitanta, kar lahko privede do zmanjšane učinkovitosti. Akynzeo lahko zviša plazemske koncentracije sočasno uporabljenih zdravil, ki se presnavljajo prek CYP3A4. Ob sočasnem dajanju deksametazona z Akynzeom je treba peroralni odmerek deksametazona zmanjšati za približno 50 %. Ob sočasnem dajanju z Akynzeom se je izpostavljenost docetakselu in etopozidu povečala za 37 % oziroma 21 %. Pri ciklofosfamidu po sočasnem dajanju netupitanta niso opazili konsistentnih učinkov. Pri eritromicinu, midazolamu ali drugih benzodiazepinih, ki se presnavljajo prek CYP3A4 (alprazolam, triazolam), je treba ob sočasnem dajanju Akynzea upoštevati možne učinke njihovih zvišanih plazemskih koncentracij. Pri sočasnem dajanju Akynzea z močnimi zaviralci CYP3A4 (npr. ketokonazol) je potrebna previdnost, sočasnemu dajanju z močnimi spodbujevalci CYP3A4 (npr. rifampicin) pa se je treba izogibati. Priporočamo previdnost pri uporabi netupitanta v kombinaciji s peroralnim substratom encima UGT2B7 (npr. zidovudin, valprojska kislina, morfin), ker *in vitro* podatki kažejo, da netupitant zavira UGT2B7. Priporočamo previdnost pri kombiniranju netupitanta z digoksinom ali drugimi substrati P-gp, kot sta dabigatran ali kolhicin, ker podatki *in vitro* kažejo, da je netupitant zaviralec P-gp. **NEŽELENI UČINKI** Pogosti ( $\geq 1/100$  do  $< 1/10$ ): glavobol, zaprtje, utrujenost. *Občasni* ( $\geq 1/1000$  do  $< 1/100$ ): nevropenija, levkocitoza, zmanjšan apetit, nespečnost, omotica, vrtoglavica, atrioventrikularni blok prve stopnje, kardiomiopatija, motnja prevajanja, hipertenzija, kolcanje, bolečina v trebuhu, driska, dispneja, napenjanje, navzea, alopecija, urtikarija, astenija, zvišane jetrne transaminaze, zvišana alkalna fosfataza v krvi, zvišan kreatinin v krvi, podaljšanje QT na elektrokardiogramu. *Redki* ( $\geq 1/10000$  do  $< 1/10000$ ): cistitis, levkopenija, limfocitoza, hipokaliemija, akutna psihoza, sprememba razpoloženja, motnja spanja, hipestezija, konjunktivitis, zamegljen vid, aritmija, atrioventrikularni blok druge stopnje, kračni blok, popuščanje mitralne zaklopke, miokardna ishemija, ventrikularne ekstrasistole, hipotenzija, disgagija, obložen jezik, bolečina v hrbtu, občutek vročine, nekardialna bolečina v prsnem košu, nenormalen okus zdravila, zvišan bilirubin v krvi, zvišana kreatin fosfokinaza MB v krvi, depresija segmenta ST na elektrokardiogramu, nenormalen segment ST-T na elektrokardiogramu, zvišan troponin. **Vrsta ovojnine in vsebina:** Škatla z eno kapsulo v pretisnem omotu iz aluminija. **Režim izdaje:** Rb Imetnik dovoljenja za promet: Helsinn Birex Pharmaceuticals Ltd, Damastown, Mulhuddart, Dublin 15, Irska AKY-062016  
Pred predpisovanjem in uporabo zdravila prosimo preberite celoten povzetek glavnih značilnosti zdravila!

Samo za strokovno javnost!  
AKY0816-01, avgust 2016

 **PharmaSwiss**  
Choose More Life

Odgovoreno za trženje v Sloveniji:  
PharmaSwiss d.o.o., Brodišče 32, 1236 Trzin  
telefon: +386 1 236 47 00, faks: +386 1 283 38 10

 **HEL SIN N**  
Building quality cancer care together



## Publisher

Association of Radiology and Oncology

## Affiliated with

Slovenian Medical Association – Slovenian Association of Radiology, Nuclear Medicine Society,  
Slovenian Society for Radiotherapy and Oncology, and Slovenian Cancer Society  
Croatian Medical Association – Croatian Society of Radiology  
Societas Radiologorum Hungarorum  
Friuli-Venezia Giulia regional groups of S.I.R.M.  
Italian Society of Medical Radiology

## Aims and scope

*Radiology and Oncology is a journal devoted to publication of original contributions in diagnostic and interventional radiology, computerized tomography, ultrasound, magnetic resonance, nuclear medicine, radiotherapy, clinical and experimental oncology, radiobiology, radiophysics and radiation protection.*

## Editor-in-Chief

**Gregor Serša**, Institute of Oncology Ljubljana,  
Department of Experimental Oncology, Ljubljana,  
Slovenia

## Executive Editor

**Viljem Kovač**, Institute of Oncology Ljubljana,  
Department of Radiation Oncology, Ljubljana, Slovenia

## Editorial Board

**Sotirios Bisdas**, National Hospital for Neurology  
and Neurosurgery, University College London  
Hospitals, London, UK

**Karl H. Bohuslavizki**, Facharzt für  
Nuklearmedizin, Hamburg, Germany

**Serena Bonin**, University of Trieste, Department of  
Medical Sciences, Trieste, Italy

**Boris Brkljačić**, University Hospital “Dubrava”,  
Department of Diagnostic and Interventional  
Radiology, Zagreb, Croatia

**Luca Campana**, Veneto Institute of Oncology  
(IOV-IRCCS), Padova, Italy

**Christian Dittreich**, Kaiser Franz Josef - Spital,  
Vienna, Austria

**Metka Filipič**, National Institute of Biology,  
Department of Genetic Toxicology and Cancer Biology,  
Ljubljana, Slovenia

**Maria Gódeny**, National Institute of Oncology,  
Budapest, Hungary

**Janko Kos**, University of Ljubljana, Faculty of  
Pharmacy, Ljubljana, Slovenia

**Robert Jeraj**, University of Wisconsin, Carbone  
Cancer Center, Madison, Wisconsin, USA

## Advisory Committee

**Tullio Girdali**, University of Trieste, Faculty of  
Medicine and Psychology, Trieste, Italy

**Vassil Hadjidekov**, Medical University,  
Department of Diagnostic Imaging, Sofia, Bulgaria

## Deputy Editors

**Andrej Cör**, University of Primorska, Faculty of  
Health Science, Izola, Slovenia

**Maja Čemažar**, Institute of Oncology Ljubljana,  
Department of Experimental Oncology, Ljubljana,  
Slovenia

**Igor Kocijančič**, University Medical Centre  
Ljubljana, Institute of Radiology, Ljubljana, Slovenia

**Karmen Stanič**, Institute of Oncology Ljubljana,  
Department of Radiation Oncology, Ljubljana, Slovenia

**Primož Strojjan**, Institute of Oncology Ljubljana,  
Department of Radiation Oncology, Ljubljana, Slovenia

**Tamara Lah Turnšek**, National Institute of  
Biology, Ljubljana, Slovenia

**Damijan Miklavčič**, University of Ljubljana,  
Faculty of Electrical Engineering, Ljubljana, Slovenia

**Luka Milas**, UT M. D. Anderson Cancer Center,  
Houston, USA

**Damir Miletić**, Clinical Hospital Centre Rijeka,  
Department of Radiology, Rijeka, Croatia

**Håkan Nyström**, Skandionkliniken,  
Uppsala, Sweden

**Maja Osmak**, Ruder Bošković Institute,  
Department of Molecular Biology, Zagreb, Croatia

**Dušan Pavčnik**, Dotter Interventional Institute,  
Oregon Health Science University, Oregon,  
Portland, USA

**Geoffrey J. Pilkington**, University of  
Portsmouth, School of Pharmacy and Biomedical  
Sciences, Portsmouth, UK

**Ervin B. Podgoršak**, McGill University,  
Montreal, Canada

**Matthew Podgorsak**, Roswell Park Cancer  
Institute, Departments of Biophysics and Radiation  
Medicine, Buffalo, NY, USA

**Marko Hočevar**, Institute of Oncology Ljubljana,  
Department of Surgical Oncology, Ljubljana, Slovenia

**Miklós Kásler**, National Institute of Oncology,  
Budapest, Hungary

**Csaba Polgar**, National Institute of Oncology,  
Budapest, Hungary

**Dirk Rades**, University of Lubeck, Department of  
Radiation Oncology, Lubeck, Germany

**Mirjana Rajer**, Institute of Oncology Ljubljana,  
Department of Radiation Oncology, Ljubljana, Slovenia

**Luis Souhami**, McGill University, Montreal,  
Canada

**Borut Štabuc**, University Medical Centre Ljubljana,  
Department of Gastroenterology, Ljubljana, Slovenia

**Katarina Šurlan Popovič**, University Medical  
Center Ljubljana, Clinical Institute of Radiology,  
Ljubljana, Slovenia

**Justin Teissié**, CNRS, IPBS, Toulouse, France

**Gillian M. Tozer**, University of Sheffield,  
Academic Unit of Surgical Oncology, Royal  
Hallamshire Hospital, Sheffield, UK

**Andrea Veronesi**, Centro di Riferimento  
Oncologico - Aviano, Division of Medical Oncology,  
Aviano, Italy

**Branko Zakotnik**, Institute of Oncology Ljubljana,  
Department of Medical Oncology, Ljubljana, Slovenia

**Stojan Plesničar**, Institute of Oncology Ljubljana,  
Department of Radiation Oncology, Ljubljana, Slovenia

**Tomaž Benulič**, Institute of Oncology Ljubljana,  
Department of Radiation Oncology, Ljubljana, Slovenia

Editorial office

**Radiology and Oncology**

Zaloška cesta 2

P. O. Box 2217

SI-1000 Ljubljana

Slovenia

Phone: +386 1 5879 369

Phone/Fax: +386 1 5879 434

E-mail: gsera@onko-i.si

Copyright © Radiology and Oncology. All rights reserved.

Reader for English

**Vida Kološa**

Secretary

**Mira Klemenčič**

**Zvezdana Vukmirović**

Design

**Monika Fink-Serša, Samo Rovar, Ivana Ljubanović**

Layout

**Matjaž Lužar**

Printed by

**Tiskarna Ozimek, Slovenia**

Published quarterly in 400 copies

*Beneficiary name: DRUŠTVO RADIOLOGIJE IN ONKOLOGIJE*

*Zaloška cesta 2*

*1000 Ljubljana*

*Slovenia*

*Beneficiary bank account number: SI56 02010-0090006751*

*IBAN: SI56 0201 0009 0006 751*

*Our bank name: Nova Ljubljanska banka, d.d.,*

*Ljubljana, Trg republike 2,*

*1520 Ljubljana; Slovenia*

SWIFT: LJBASIX

*Subscription fee for institutions EUR 100, individuals EUR 50*

*The publication of this journal is subsidized by the Slovenian Research Agency.*

Indexed and abstracted by:

- *Celdes*
- *Chemical Abstracts Service (CAS)*
- *Chemical Abstracts Service (CAS) - SciFinder*
- *CNKI Scholar (China National Knowledge Infrastructure)*
- *CNPIEC*
- *DOAJ*
- *EBSCO - Biomedical Reference Collection*
- *EBSCO - Cinahl*
- *EBSCO - TOC Premier*
- *EBSCO Discovery Service*
- *Elsevier - EMBASE*
- *Elsevier - SCOPUS*
- *Google Scholar*
- *J-Gate*
- *JournalTOCs*
- *Naviga (Softweco)*
- *Primo Central (ExLibris)*
- *ProQuest - Advanced Technologies Database with Aerospace*
- *ProQuest - Health & Medical Complete*
- *ProQuest - Illustrata: Health Sciences*
- *ProQuest - Illustrata: Technology*
- *ProQuest - Medical Library*
- *ProQuest - Nursing & Allied Health Source*
- *ProQuest - Pharma Collection*
- *ProQuest - Public Health*
- *ProQuest - Science Journals*
- *ProQuest - SciTech Journals*
- *ProQuest - Technology Journals*
- *PubMed*
- *PubsHub*
- *ReadCube*
- *SCImago (SJR)*
- *Summon (Serials Solutions/ProQuest)*
- *TDOne (TDNet)*
- *Thomson Reuters - Journal Citation Reports/Science Edition*
- *Thomson Reuters - Science Citation Index Expanded*
- *Ulrich's Periodicals Directory/ulrichsweb*
- *WorldCat (OCLC)*

*This journal is printed on acid-free paper*

On the web: ISSN 1581-3207

<http://www.degruyter.com/view/j/raon>

<http://www.radioloncol.com>

# contents

## review

- 241 **Selection of non-small cell lung cancer patients for intercalated chemotherapy and tyrosine kinase inhibitors**  
Matjaz Zwitter, Antonio Rossi, Massimo Di Maio, Maja Pohar Perme, Gilberto Lopes
- 252 **Magnetic resonance imaging evaluation in neoadjuvant therapy of locally advanced rectal cancer: a systematic review**  
Roberta Fusco, Mario Petrillo, Vincenza Granata, Salvatore Filice, Mario Sansone, Orlando Catalano, Antonella Petrillo

## radiology

- 263 **An image fusion system for estimating the therapeutic effects of radiofrequency ablation on hepatocellular carcinoma**  
Nobuyuki Toshikuni, Yasuhiro Matsue, Kazuaki Ozaki, Kaho Yamada, Nobuhiko Hayashi, Mutsumi Tsuchishima, Mikihiro Tsutsumi
- 270 **Quantitative aspects of diffusion-weighted magnetic resonance imaging in rectal cancer response to neoadjuvant therapy**  
Thiago Bassaneze, José Eduardo Gonçalves, Juliano Ferreira Faria, Rogério Tadeu Palma, Jaques Waisberg
- 277 **Dynamic susceptibility contrast enhanced (DSC) MRI perfusion and plasma cytokine levels in patients after tonic-clonic seizures**  
Tatjana Filipovic, Katarina Surlan Popovic, Alojz Ihan, David Bozidar Vodusek

## experimental oncology

- 286 **Effects of electrochemotherapy with cisplatin and peritumoral IL-12 gene electrotransfer on canine mast cell tumors: a histopathologic and immunohistochemical study**  
Claudia Salvadori, Tanja Svava, Guido Rocchigiani, Francesca Millanta, Darja Pavlin, Maja Cemazar, Ursa Lamprecht Tratar, Gregor Sersa, Natasa Tozon, Alessandro Poli
- 295 ***In vitro* and *in vivo* evaluation of electrochemotherapy with trans-platinum analogue trans-[PtCl<sub>2</sub>(3-Hmpy)<sub>2</sub>]**  
Simona Kranjc, Maja Cemazar, Gregor Sersa, Janez Scancar, Sabina Grabner
- 307 **Protective/restorative role of the adipose tissue-derived mesenchymal stem cells on the radioiodine-induced salivary gland damage in rats**  
Güleser Saylam, Ömer Bayır, Salih Sinan Gültekin, Ferda Alparlan Pınarlı, Ünsal Han, Mehmet Hakan Korkmaz, Mehmet Eser Sancaktar, İlkan Tatar, Mustafa Fevzi Sargon, Emel Çadallı Tatar

## *clinical oncology*

- 317 **Electrochemotherapy - supplementary treatment for loco-regional metastasized breast carcinoma administered to concomitant systemic therapy**  
Eva-Maria Grischke, Carmen Röhm, Eva Stauß, Florin-Andrei Taran, Sara Y. Brucker, Diethelm Wallwiener
- 324 **High dose hypofractionated proton beam therapy is a safe and feasible treatment for central lung cancer**  
Takashi Ono, Tomonori Yabuuchi, Tatsuya Nakamura, Kanako Kimura, Yusuke Azami, Katsumi Hirose, Motohisa Suzuki, Hitoshi Wada, Yasuhiro Kikuchi, Kenji Nemoto
- 331 **Expression of LOC285758, a potential long non-coding biomarker, is methylation-dependent and correlates with glioma malignancy grade**  
Alenka Matjasic, Mara Popovic, Bostjan Matos and Damjan Glavac
- 342 **Health-related quality of life assessed by the EORTC QLQ-C30 questionnaire in the general Slovenian population**  
Vaneja Velenik, Ajra Secerov-Ermenc, Jasna But-Hadzic, Vesna Zadnik
- 351 **The outcome of the first 100 nasopharyngeal cancer patients in Thailand treated by helical tomotherapy**  
Imjai Chitapanarux, Wannapha Nobnop, Patumrat Sripan, Ausareeya Chumachote, Ekkasit Tharavichitkul, Somvilai Chakrabandhu, Pitchayaponne Klunklin, Wimrak Onchan, Bongkot Jia-Mahasap, Suwapim Janlaor, Patcharawadee Kayan, Patrinee Traisathit, Dirk Van Gestel
- 357 **PD-L1 expression in squamous-cell carcinoma and adenocarcinoma of the lung**  
Urska Janzic, Izidor Kern, Andrej Janzic, Luka Cavka, Tanja Cufer
- 363 **A novel mutation in the FOXC2 gene: a heterozygous insertion of adenosine (c.867insA) in a family with lymphoedema of lower limbs without distichiasis**  
Tanja Planinsek Rucigaj, Matija Rijavec, Jovan Miljkovic, Julij Selb, Peter Korosec

## *slovenian abstracts*

# Selection of non-small cell lung cancer patients for intercalated chemotherapy and tyrosine kinase inhibitors

Matjaz Zwitter<sup>1,2</sup>, Antonio Rossi<sup>3</sup>, Massimo Di Maio<sup>4</sup>, Maja Pohar Perme<sup>5</sup>, Gilberto Lopes<sup>6</sup>

<sup>1</sup> Institute of Oncology Ljubljana, Ljubljana, Slovenia

<sup>2</sup> Faculty of Medicine, University of Maribor, Maribor, Slovenia

<sup>3</sup> Division of Medical Oncology, IRCCS Casa Sollievo della Sofferenza Hospital, San Giovanni Rotondo (FG), Italy

<sup>4</sup> Division of Medical Oncology, Mauriziano Hospital, Oncology Department, University of Turin, Torino, Italy

<sup>5</sup> Institute for Biostatistics and Medical Informatics, Faculty of Medicine, University of Ljubljana, Ljubljana, Slovenia

<sup>6</sup> Centro Paulista de Oncologia e HCor Onco, members of the Oncoclínicas do Brasil Group, Sao Paulo, Brazil and Sylvester Comprehensive Cancer Center, University of Miami, Miami, FL, USA

Radiol Oncol 2017; 51(3): 241-251.

Received 3 May 2017

Accepted 9 June 2017

Correspondence to: Prof. Matjaz Zwitter M.D., Ph.D., Department of Radiation Oncology, Institute of Oncology, Zaloška 2, SI-1000 Ljubljana, Slovenia. E-mail: matjaz.zwitter@guest.arnes.si

Disclosure: MZ has received honoraria for lectures from Roche, AstraZeneca and Merck Soreno and consultancy fee from Boehringer Ingelheim. AR has received honoraria for lectures from Roche, and acted as consultant for AstraZeneca, Roche, and Eli-Lilly. MDM acted as consultant for AstraZeneca, Boehringer Ingelheim, Eli Lilly, Bayer, Merck Sharp & Dohme and Bristol Myers Squibb. MPP and GL did not report any conflict of interest.

**Background.** When treating patients with advanced non-small cell lung cancer (NSCLC) with tyrosine kinase inhibitors and chemotherapy, intercalated schedule with time separation between the two classes of drugs should avoid their mutual antagonism. In a survey of published trials, we focus on relation between eligibility criteria and effectiveness of intercalated treatment.

**Methods.** Published documents were identified using major medical databases, conference proceedings and references of published trials. Median progression-free survival (PFS) was taken as the basic parameter of treatment efficacy. Correlation between characteristics of patients and median PFS was assessed through the Pearson's correlation coefficient and the coefficient of determination, separately for first-line and second-line setting.

**Results.** The series includes 11 single-arm trials and 18 randomized phase II or phase III trials with a total of 2903 patients. Treatment-naïve patients or those in progression after first-line treatment were included in 16 and 13 trials, respectively. In 14 trials, only patients with non-squamous histology were eligible. Proportion of patients with non-squamous carcinoma (in first-line setting), proportion of never-smokers (both in first- and second-line setting) and proportion of epidermal growth factor receptor (EGFR) mutant patients (both in first- and second-line setting) showed a moderate or strong correlation with median PFS. In six trials of intercalated treatment applied to treatment-naïve EGFR-mutant patients, objective response was confirmed in 83.1% of cases and median PFS was 18.6 months.

**Conclusions.** Most suitable candidates for intercalated treatment are treatment-naïve patients with EGFR-mutant tumors, as determined from biopsy or liquid biopsy. For these patients, experience with intercalated treatment is most promising and randomized trials with comparison to the best standard treatment are warranted.

**Key words:** NSCLC; intercalated treatment; EGFR; tyrosine-kinase inhibitors

## Introduction

Soon after the discovery of activating mutations of epidermal growth factor receptor (EGFR) and

of their crucial role in determining sensitivity to tyrosine kinase inhibitors (TKIs), several trials confirmed the advantage of TKIs in comparison to chemotherapy for patients with advanced non-

small cell lung cancer (NSCLC) with activating EGFR mutations.<sup>1-5</sup> Due to higher response rate, longer time to progression and less toxicity, monotherapy with TKIs has been approved as the preferred first-line treatment for these patients. TKIs clearly improve short-term prognosis of patients with EGFR mutant lung cancer. Still, after a median interval of around one year, patients on treatment with TKIs develop resistance and experience disease progression.<sup>6</sup> New treatments, either as first-line or at progression are needed.<sup>7</sup>

After huge disappointment due to four large negative trials of chemotherapy alone versus chemotherapy combined with continuous application of gefitinib or erlotinib<sup>8-11</sup>, the idea of combining TKIs with chemotherapy never fully recovered. Many research groups simply concluded that the two categories of drugs should not be used together and most of current pre-clinical and clinical research focuses on new drugs designed to overcome primary or acquired resistance to TKIs.<sup>12-14</sup> The fact that the four trials were unselected regarding histology and smoking status received little attention. For a quarter of patients in the TRIBUTE trial, the status of EGFR mutations was later determined: when treated with the combination in comparison to chemotherapy alone, EGFR mutant patients had higher response rate and a trend towards longer progression-free survival (PFS), but no advantage in overall survival (OS).<sup>15</sup>

In spite of prevailing disappointment, some researchers insisted that the negative message of the four large trials should be accepted as new knowledge rather than ignored and developed the concept of intercalated treatment. The reasoning was clear: when applied concomitantly with chemotherapy, TKIs induce G1-phase cell-cycle arrest, due to which cell-cycle dependent chemotherapeutic agents will not be effective.<sup>16</sup> Chemorefractoriness of cells harboring sensitizing-EGFR mutations in the presence of gefitinib was confirmed *in vitro*.<sup>17</sup> Time separation with an interval of 6 days without TKIs to restore chemosensitivity of tumor cells should remove this mutual antagonism, so as to benefit from the efficacy of both classes of drugs.<sup>18</sup> Additional support for the concept of intercalated treatment came from laboratory experiments and from a clinical trial of sequential application of chemotherapy and TKI: proper sequence starting with cytotoxic drugs, followed by TKIs leads to their synergistic activity.<sup>19-23</sup>

So far, a few dozen clinical trials on intercalated treatment with chemotherapy and TKIs have been published. A recent review focused on trials with

randomization between intercalated schedules and chemotherapy alone.<sup>24</sup> While such a review is definitively valuable, a reader is confused when facing a list of trials with a wide range of eligibility criteria, leading to diverging conclusions. This review paper has a different goal. We believe that before proceeding with further clinical research, we should understand which patients will most likely benefit from intercalated treatment. Only after defining the optimal target population, future trials can be designed to compare intercalated treatment to the best standard treatment in those selected patients.

## Methods

### Selection of publications for analysis

Published papers and conference reports on intercalated therapy for NSCLC were eligible for review. Intercalated treatment was defined as a treatment with cytotoxic drug(s), combined with an EGFR-TKI during a part of a treatment cycle. Trials on chemotherapy combined with continuous application of TKIs or a gap of less than 4 days, and trials using alternating cycles of cytotoxic drugs and of TKIs were not included in this review.

Pubmed was used to search for published trials on intercalated treatment for NSCLC, with the following descriptors and limits: NSCLC; chemotherapy and (erlotinib and/or gefitinib and/or afatinib); clinical trial; 2006-2016 as the publication period; humans; English language. This initial search led to 686 publications. The list was then manually reviewed. Additional publications were identified using Web of Science cross-citation database, proceedings of major conferences during the past 4 years (IASLC World Lung Cancer Conference, ASCO, ESMO, European Lung Cancer Conference) and the list of references in published trials.

### Analysis of published experience

Selected papers were analyzed, with focus on selection criteria and parameters of efficacy. Information on the proportion of patients with EGFR mutant tumors was often incomplete or missing. If not available in the text, an estimate on the proportion of patients with EGFR mutant disease was made. As the first step, all patients with squamous histology were considered as EGFR wild-type (EGFR wt). In case of non-squamous histology, an estimate was based on proportion of never-smokers vs. smokers

and on ethnicity, using published meta-analysis on global pattern of EGFR mutations.<sup>25</sup>

Due to the wide spectrum of eligibility criteria and of comparator arms, randomized trials were not considered an appropriate basis for analysis of efficacy of the intercalated treatment. We therefore chose a different approach. Experience from single-arm phase II trials and from the intercalated arm of randomized trials was analyzed in relation to histology, smoking status and EGFR mutation status, separately for treatment-naive and pre-treated patients. Median PFS was taken as a conventional indicator of efficacy.

### Statistical analysis

Statistical analysis was limited to intercalated treatment, either in non-randomised trials or in the intercalated arm of randomised trials. The strength of correlation between proportion of non-squamous tumors, proportion of non-smokers and proportion of EGFR-mutation positive cases with median PFS was evaluated calculating the Pearson's correlation coefficient (R) and the coefficient of determination (R-squared; R<sup>2</sup>). Pearson's R is a simple measure of the linear correlation between two variables, giving a value between +1 and -1, where +1 is a total positive correlation, 0 is the absence of correlation, and -1 is a total negative correlation. The coefficient of determination is such that  $0 \leq R^2 \leq 1$ : although there are no specific cut-offs to define a moderate, or a strong correlation, a higher R<sup>2</sup> score indicates a stronger association.

Correlations were graphically described by bubble plots, where each bubble represents a study, with bubble size proportional to the number of patients included in each study. As all the analyses were weighted by sample size of each study, weighted least-squares regression line was calculated and reported in each graph.

Statistical analyses were conducted using SPPlus (S-PLUS 6.0 Professional, release 1; Insightful Corporation, Seattle, WA, USA). Graphs were realized using SigmaPlot (Systat Software, San Jose, CA).

## Results

### Identification of publications for analysis

After the initial search through PubMed, 96 reports were selected to which 4 trials found through conference proceedings and 6 trials identified by cross-citation database were added for a total of

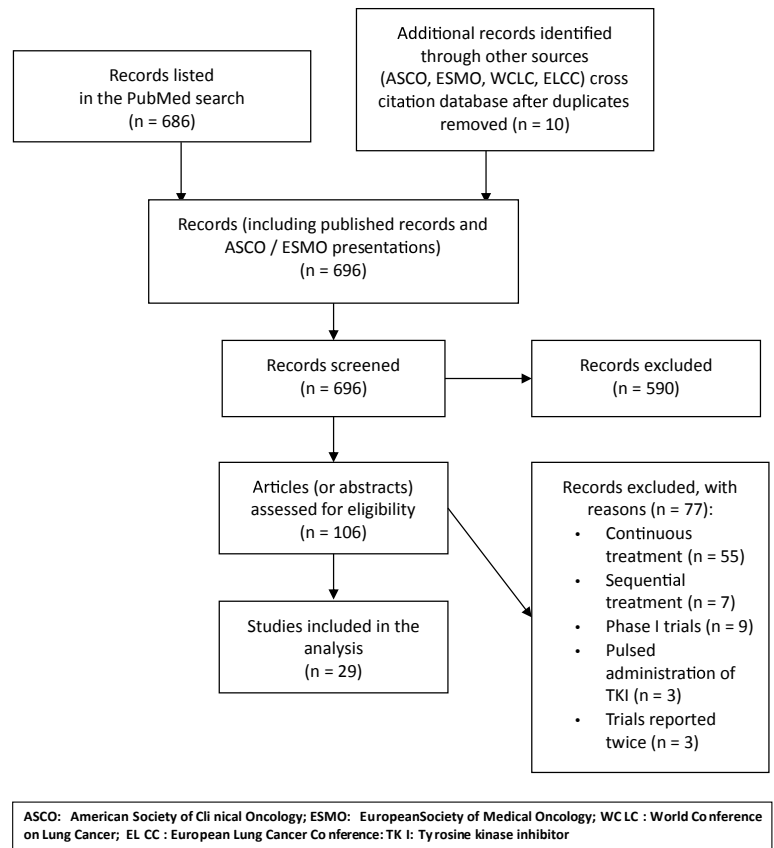


FIGURE 1. Flow diagram on selection of publications for analysis.

106 studies. A total of 29 trials were considered eligible for the analysis (Figure 1). The series includes 11 single-arm phase II trials, 16 randomized phase II trials and 2 phase III randomized trials, with a total of 2903 patients.<sup>26-54</sup>

### Eligibility criteria and treatments used

Fourteen trials were limited to non-squamous histology, while 15 included patients with any histologic type of NSCLC. Sixteen trials were open only for treatment-naive patients, while 13 included those in progression after first-line treatment. The proportion of never-smokers was specified in all but two reports.

Five trials were limited to EGFR mutant disease and 4 to patients with EGFR wild-type or unknown tumors. Another 3 trials included a substantial proportion of EGFR mutant cases and separately reported the experience for this subpopulation of patients. Nine of the remaining 17 trials included information on EGFR status for some of their patients, but the proportion analyzed was usually low and thus inappropriate for any analysis.

TABLE 1. Randomized trials on intercalated chemotherapy and TKIs for non-small cell lung cancer

REFERENCE	TYPE OF TRIAL	# OF PTS	SELECTION OF PATIENTS	TREATMENT REGIMEN(S)	% never-smokers	% EGFR mutant, intercalated arm only	ORR (%)	MEDIAN PFS (months)	MEDIAN OS (months)
<b>Mok 2009 (FASTACT) 26</b>	Randomized Phase 2	154	All histologies, previously untreated	Arm A (76 pts): Gem, d 1 & 8 Cis or Carbo, day 1 Erlotinib, d 15-28 Cycle q 4 weeks Arm B (78 pts): as above, placebo instead of Erlotinib	34%	28%	Arm A: 35.5% Arm B: 24.4%  P = 0.12	Arm A: 6.9 m Arm B: 5.5 m  P = 0.002	Arm A: 17.3 m Arm B: 17.7 m  P: ns
		52	As above, never-smokers	Arm A (24 pts) Arm B (28 pts) Treatment as above	100%	49%	Arm A: 45.8% Arm B: 32.1% P: not reported	Arm A: 11.1 m Arm B: 6.4 m P = 0.002	Not reached
<b>Hirsch 2011 27</b>	Randomized Phase 2	143	Positive for EGFR protein expression and/or with high EGFR gene copy number, previously untreated	Arm A (71 pts): Pacli d 1 Carbo d 1 Erlotinib d 2 - 15 Cycle q 3 weeks Arm B (72 pts): Erlotinib	28%	10%	Arm A: 22.4% Arm B: 11.6%  P = ns	Arm A: 4.6 m Arm B: 2.7 m  P = ns	Arm A: 11.4 m Arm B: 16.7 m  P = ns
<b>Aerts 2012 (NVALT 10) 28</b>	Randomized Phase 2	231	All histologies Progression after platin-based chemotherapy	Arm A (115 pts): Erlotinib Arm B (116 pts): Doce or Pem, d 1 Erlotinib, d 2 - 16 Cycle q 3 weeks	7%	4%	Arm A: 7% Arm B: 13%  P = 0.03	Arm A: 4.9 m Arm B: 6.1 m  P = 0.11	Arm A: 5.5 m Arm B: 7.8 m  P = 0.01
<b>Lee 2013 29</b>	Randomized Phase 2	240	Non-squamous, never-smokers, Progression after 1 <sup>st</sup> line chemotherapy	Arm A (78 pts): Pem d 1 Erlotinib d 2 - 14, Cycle q 3 weeks Arm B (82 pts): Erlotinib continuously Arm C (80 pts): Pem d 1, Cycle q 3 weeks	100%	56%	Arm A: 44.7% Arm B: 29.3% Arm C: 10.0%  P = 0.001	Arm A: 7.4 m Arm B: 3.8 m Arm C: 4.4 m  P = 0.003	Arm A: 20.5 m Arm B: 22.8 m Arm C: 17.7 m  P = 0.19
<b>Wu Y-L 2013 (FASTACT 3) 30</b>	Randomized Phase 3	451	All histologies, previously untreated	Arm A (226 pts): Gem, d 1 & 8 Cis or Carbo, d 1 Erlotinib, d 15-28 Cycle q 4 weeks Arm B (225 pts): as above, placebo instead of Erlotinib	49%	39%	Arm A: 44% Arm B: 16%  P < 0.0001	Arm A: 7.6 m Arm B: 6.0 m  P < 0.0001	Arm A: 18.3 m Arm B: 15.2 m  P = 0.04
		97	As above, subgroup with activating EGFR mutations	Arm A (49 pts): Arm B (48 pts): Treatment as above	Not separately reported	100%	Arm A: 84% Arm B: 15%  P < 0.0001	Arm A: 16.8 m Arm B: 6.9 m  P < 0.0001	Arm A: 31.4 m Arm B: 20.6 m  P = 0.009
<b>Auliac 2014 31</b>	Randomised Phase 2	147	EGFR wild-type or unknown Progression after 1 <sup>st</sup> line chemotherapy	Arm A (73 pts): Doce, d 1 Erlotinib, d 2 - 16 Cycle q 3 weeks Arm B (74 pts): Doce, d 1	7.5%	4%	Arm A: 4.4% Arm B: 1.4%  P = ns	Arm A: 2.2 m Arm B: 2.5 m  P = ns	Arm A: 6.5 m Arm B: 8.3 m  P = ns
<b>Karavasilis 2014 32</b>	Randomized Phase 2	50	All histologies Previously untreated	Arm A (25 pts): Doce, d 1 Erlotinib, d 9 - 20 Arm B (25 pts): Doce, d 1 Erlotinib, d 3 - 14 Cycle q 3 weeks	10%	11%	Arm A: 24% Arm B: 12%  P = ns	Arm A: 2.9 m Arm B: 4.2 m  P = ns	Arm A: 9.9 m Arm B: 10.8 m  P = ns
<b>Mok 2014 33</b>	Randomized Phase 2	123	Unselected, progression after platin-based ChT	Arm A (63 pts): Eribulin mesylate, d1 Erlotinib, d 2-16 Cycle q 3 weeks Arm B (60 pts): Eribulin mesylate, d 1 and 8 Erlotinib, d 15-28 Cycle q 4 weeks	24%	28%	Arm A: 13% Arm B: 17%  P = ns	Arm A: 3.5 m Arm B: 3.8 m  P = ns	Arm A: 7.6 m Arm B: 8.5 m  P = ns

REFERENCE	TYPE OF TRIAL	# OF PTS	SELECTION OF PATIENTS	TREATMENT REGIMEN(s)	% never-smokers	% EGFR mutant, intercalated arm only	ORR (%)	MEDIAN PFS (months)	MEDIAN OS (months)
Yu 2014 <sup>34</sup>	Randomized Phase 2	117	Non-squamous, previously untreated	Arm A (58 pts): Pem, d 1 Cis or Carbo, d 1 Gefitinib, d 3 – 16 Cycle q 3 weeks Arm B (57 pts): As above, no Gefitinib	58%	40%	Arm A: 50.0% Arm B: 47.7%  P = ns	Arm A: 7.9 m Arm B: 7.0 m  P = ns	Arm A: 25.4 m Arm B: 20.8 m  P = ns
		32	As above, subgroup with activating EGFR mutations	Arm A: 14 pts Arm B: 18 pts Treatment as above	Not separately reported	100%	Arm A: 76.9% Arm B: 50.0%  P = 0.13	Arm A: Not reached Arm B: 14.0 m P = 0.017	Not reached
Choi 2015 <sup>35</sup>	Randomized Phase 2	90	NSCLC, EGFR wild. type or unknown, PS 0 – 2, previously untreated	Arm A (44 pts): Pem, d 1 Carbo, d 1 Gefitinib, d 2 – 15 Cycle q 3 weeks x 4 Maintenance Gefitinib Arm B (46 pts): As Arm A, no Gefitinib	10%	10%	Arm A: 41.9% Arm B: 39.5%  P = ns	Arm A: 4.1 m Arm B: 4.1 m  P = ns	Arm A: 9.3 m Arm B: 10.5 m  P = ns
Juan 2015 <sup>36</sup>	Randomized Phase 2	68	All histologies Progression after platin-based chemotherapy	Arm A (33 pts): Doce q 3 weeks Erlotinib, d 2 – 16 Arm B (35 pts): Erlotinib continuously	6%	5%	Arm A: 3% Arm B: 9%  P = 0.19	Arm A: 3.0 m Arm B: 2.1 m  P = 0.09	Arm A: 7.5 m Arm B: 5.2 m  P = 0.19
Lu 2015 <sup>37</sup>	Randomized Phase 3	219	Adenocarcinoma, EGFR unknown, non-smokers, no progression after 2 cycles of gem-carbo	Arm A (109 pts): Gem, d 1 and 8 Carbo, d 1 Gefitinib d 15-25 and maintenance Cycle q 4 weeks x 4 Arm B (110 pts): As above, no Gefitinib	100%	72%	Not reported	Arm A: 10 m Arm B: 4.4 m  P = 0.001	Not reported
Michael 2015 <sup>38</sup>	Randomized Phase 2	54	All histologies PS 2 or elderly Previously untreated	Arm A (28 pts): Gem d 1 and 8 Erlotinib days 15 – 28 Cycle q 4 weeks Arm B (26 pts): Gem d1 and 8 Cycle q 4 weeks	15%	12%	Arm A: 6% Arm B: 23%  P: ns	Arm A: 2.5 m Arm B: 1.9 m  P: ns	Arm A: 3.9 m Arm B: 4.4 m  P: ns
Han 2016 <sup>39</sup>	Randomized Phase 2	121	Adenocarcinoma, EGFR mutant, previously untreated	Arm A (40 pts): Pem, d1 + maintenance Carbo, d1 for ≤ 6 cycles Gefitinib, d 5-21 + maintenance Cycle q 4 weeks Arm B (40 pts): As above, no Gefitinib Arm C (41 pts): Gefitinib alone	Not reported	100%	Arm A: 82.5% Arm B: 32.5% Arm C: 65.9%  P: 0.04	Arm A: 18.8 m Arm B: 5.7 m Arm C: 12.0 m  P: not reported	Not reached
Lara 2016 (SWOG S0709) <sup>40</sup>	Randomized Phase 2	59	PS 2, Proteomics: VeriStrat-good status, previously untreated	Arm A (33 pts): Erlotinib Arm B (26 pts): Pacli d 1 Carbo d 1 Erlotinib d 2 – 16 Cycle q 3 weeks x 4 Maintenance Erlotinib	20%	20%	Arm A: 6% Arm B: 23%  P = 0.06	Arm A: 1.6 m Arm B: 4.6 m  P = 0.06	Arm A: 6.0 m Arm B: 11.0 m  P = 0.27
Li 2016 <sup>41</sup>	Randomized Phase 2	79	Predominantly non-squamous Progression after 1 <sup>st</sup> line chemotherapy	Arm A (27 pts): Pem d 1 Cycle q 3 weeks Arm B (52 pts): Pem d 1 Erlotinib d 2 – 17 Cycle q 3 weeks	Not reported	19%	Arm A: 10% Arm B: 29%  P = 0.17	Arm A: 2.9 m Arm B: 4.7 m  P = 0.26	Arm A: 8.3 m Arm B: 9.7 m  P = 0.28
Lee 2016 <sup>42</sup>	Randomized Phase 2	76	Adenocarcinoma, never-smokers, Previously untreated	Arm A (39 pts): Pem d1 Carbo d 1 Gefitinib d 5 – 18 + maintenance Cycle q 3 weeks x max 9 Arm B (37 pts): As arm A, placebo instead of Gefitinib At progression: Gefitinib for arm B	100%	42%	Arm A: 79.5% Arm B: 51.4%  P = 0.01	Arm A: 12.8 m Arm B: 7.0 m  P = 0.009	Arm A: 29.2 m Arm B: 20.4 m  P = 0.15

REFERENCE	TYPE OF TRIAL	# OF PTS	SELECTION OF PATIENTS	TREATMENT REGIMEN(S)	% never-smokers	% EGFR mutant, intercalated arm only	ORR (%)	MEDIAN PFS (months)	MEDIAN OS (months)
		29	As above, EGFR mutant	Arm A: 15 pts Arm B: 14 pts Treatment as above	100%	100	Arm A: 86.7% Arm B: 42.9%  P = 0.01	Arm A: 13.3 m Arm B: 7.8 m P = 0.08	Arm A: 26.6 m Arm B: 22.2 m P = ns
		37	As above, EGFR wt	Arm A: 22 pts Arm B: 15 pts Treatment as above	100%	0	Arm A: 72.7% Arm B: 57.1% P = ns	Arm A: 6.6 m Arm B: 6.6 m P = 0.08	Arm A: 29.2 m Arm B: 15.9 m P = 0.09
Yoon 2016 <sup>43</sup>	Randomized Phase 2	87	Non-squamous Progression after 1st line chemotherapy	Arm A (57 pts): Pem d 1 Afatinib d 2–15 Arm B (30 pts): Pem d 1	31%	31%	Arm A: 31.8 % Arm B: 13.3% P = 0.074	Arm A: 5.7 m Arm B: 2.9 m P = 0.16	Arm A: 12.1 m Arm B: 15.6 m P = 0.245

Carbo = carboplatin; Cis = cisplatin; Doce = docetaxel; Gem = gemcitabine; ORR = overall response rate; OS = overall survival; Pacli = paclitaxel; PFS = progression-free survival; Pem = pemetrexed; PTS = patient

Erlotinib and gefitinib were used in 17 and 9 trials, respectively. In 2 trials, either erlotinib or gefitinib was used, while afatinib was used in 1 trial.

Among 18 randomized trials (Table 1), chemotherapy alone was the comparator arm in 10 trials. Four trials used TKI alone as the comparator, 2 trials compared two different intercalated schedules, while 2 trials used 3-arm design with comparison among intercalated schedule, chemotherapy alone or TKIs alone. According to PFS as the most common parameter of efficacy, the intercalated schedule was superior to the comparator in 12 trials, crossing the conventional margin of  $P < 0.05$  in 7 trials. No significant difference was seen in 4 other trials and in 2 trials comparing two different intercalated schedules of intercalated therapy.

Basic data on single-arm Phase 2 trials are presented in Table 2.

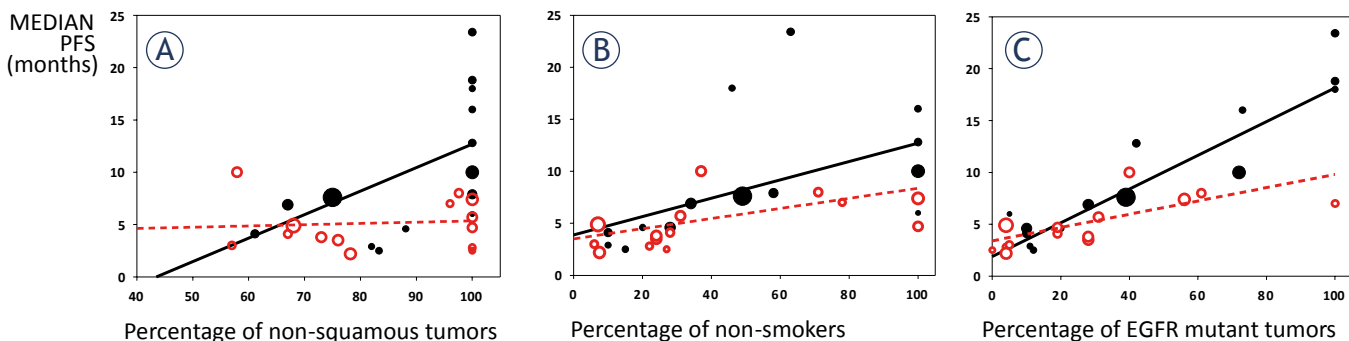
### Efficacy of intercalated treatment

Figure 2 shows correlation between median PFS and proportion of patients with non-squamous

histology (Panel A), proportion of never-smokers (Panel B) and proportion of EGFR mutant patients (Panel C).

As for tumor histology, there was a moderate correlation between proportion of non-squamous tumors and median PFS in the first-line setting ( $R = 0.61$ ,  $R^2 = 0.38$ ,  $p = 0.02$ ). The slope of the regression line (0.23) suggests that a 10% increase in the proportion of non-squamous tumors corresponds to a 2.3-months improvement in median PFS in first-line. On the other hand, the correlation was very weak in the second-line setting ( $R = 0.09$ ,  $R^2 = 0.01$ ,  $p = 0.77$ ).

As for smoking status, there was a moderate correlation between proportion of non-smokers and median PFS, both in the first-line and in the second-line setting (first-line:  $R = 0.55$ ,  $R^2 = 0.30$ ,  $p = 0.04$ ; second-line:  $R = 0.65$ ,  $R^2 = 0.42$ ,  $p = 0.02$ ). In detail, the slope of the regression line (0.09 for the first-line and 0.05 for the second-line) suggests that a 10% increase in the proportion of non-smokers corresponds to a 0.9-months improvement in median PFS in first-line, and to a 0.5-months improvement in median PFS in second-line.



**FIGURE 2.** Correlation between median PFS and proportion of patients with non-squamous histology (A), proportion of never-smokers (B) and proportion of EGFR mutant patients (C). Black solid marks and black solid lines are for 1<sup>st</sup> line treatment; red hollow marks and red interrupted lines for 2<sup>nd</sup> line treatment. Bubble size corresponds to the number of patients in a trial.

TABLE 2. Single-arm Phase II trials on intercalated chemotherapy and TKIs for non-small cell lung cancer

REFERENCE	# OF PTS	SELECTION OF PATIENTS	TREATMENT REGIMEN(s)	% never-smokers	% EGFR mutant	ORR (%)	MEDIAN PFS (months)	MEDIAN OS (months)
Oshita 2010 <sup>44</sup>	16	Unselected, previously untreated	Pacli d 1 Iri d 1 Gefitinib d 8-14 Cycle q 3 weeks	Not reported	25%	43.8%	Not reported	18.1 m
Sangha 2011 <sup>45</sup>	39	All histologies Progression after 1 <sup>st</sup> line chemotherapy	Doce d 1 Erlotinib days 2 – 16 Cycle q 3 weeks	28%	19%	28.2%	4.1 m	18.2 m
Minami 2013 <sup>46</sup>	27	Non-squamous Progression after 1 <sup>st</sup> line chemotherapy	Pem, d 1 Erlotinib, d 2 – 16 Cycle q 3 weeks	22%	4%	11.1%	2.8 m	15.8 m
Yoshimura 2013 <sup>47</sup>	27	Activating EGFR mutations, Progression after TKI	Pem, d 1 Erlotinib or Gefitinib, days 2 – 16 Cycle q 3 weeks	78%	100%	25.9%	7.0 m	11.4 m
Kim 2014 <sup>48</sup>	17	Non-squamous, EGFR wt, progression after 1 <sup>st</sup> line ChT	Pem d 1 Erlotinib d 2-15	27%	0%	27.0%	2.5 m	6.7 m
Fang 2014 <sup>49</sup>	57	Unselected, progression after platinum-based ChT	Gem, d 1 and 8 Cis, d 1-3 Gefitinib, d 10 - 24 Cycle q 4 weeks	37%	40%	11%	10 m	15.2 m
Yang 2014 <sup>50</sup>	29	Adenocarcinoma, non-smokers, EGFR unknown, previously untreated	Pacli, d1 Carbo, d1 Gefitinib, d 8 – 17 + maintenance Cycle q 3 weeks	100%	73%	74.1%	16 m	Not reached
Zwitter 2014 <sup>51</sup>	15	Adenocarcinoma, light/never smokers, EGFR wild-type or unknown Previously untreated	Gem d 1 and 4 Cis d 2 Erlotinib d 5 – 15 Cycle q 3 weeks x 4 – 6 Maintenance Erlotinib	100%	5%	33%	6.0 m	7.6 m
Yoshimura 2015 <sup>52</sup>	26	Activating EGFR mutations Previously untreated	Pem d 1 Gefitinib d 2 – 16	46%	100%	84.6%	18.0 m	32.0 m
Yu 2015 <sup>53</sup>	42	Mostly adenocarcinoma Progression after response to TKI	Pem, d 1 or Pem + Platin, d 1 TKI (Erlotinib or Gefitinib), d 6 – 21 Cycle q 3 weeks	71%	61%	23.8%	8.0 m	11.0 m
Zwitter 2016 (ITAC 2) <sup>54</sup>	38	Activating EGFR mutations Previously untreated	Gem d 1 and 4 Cis d 2 Erlotinib d 5 – 15 Cycle q 3 weeks x 4 – 6 Maintenance Erlotinib	63%	100%	84.2%	23.4 m	38.3 m

Carbo = carboplatin; Cis = cisplatin; Doce = docetaxel; Gem = gemcitabine; Iri = irinotecan; ORR = overall response rate; OS = overall survival; Pacli = paclitaxel; PFS = progression-free survival; Pem = pemetrexed; PTS = patient

As for EGFR mutational status, there was a strong correlation between proportion of EGFR mutation-positive tumors and median PFS, both in the first-line and in the second-line setting (first-line:  $R = 0.91$ ,  $R^2 = 0.83$ ,  $p < 0.0001$ ; second-line:  $R = 0.69$ ,  $R^2 = 0.48$ ,  $p = 0.006$ ). The slope of the regression line (0.16 for the first-line and 0.06 for the second-line) suggests that a 10% increase in the proportion of EGFR mutation-positive tumors corresponds to

a 1.6-months improvement in median PFS in first-line, and to a 0.6-months improvement in median PFS in second-line.

Six trials on treatment-naïve patients with EGFR mutant disease reported excellent response rate of 83.1% (range: 76.9% to 84.2%).<sup>30,34,39,42,52,54</sup> Five of these trials presented data on median PFS ranging from 13.3 to 23.4 months (median PFS for all 5 trials: 18.6 months). This figure does not include an

additional trial from this category which reported 86% PFS at 15 months, with no data on median PFS due to relatively short follow-up.<sup>34</sup>

## Discussion

Most surveys and meta-analyses focus on the question of efficacy and/or toxicity of a particular new treatment in comparison with the standard approach. This was also the case with intercalated treatment for advanced NSCLC. On the basis of published randomized trials, a recent meta-analysis concluded that intercalated treatment is superior to the comparator arm.<sup>24</sup> While this meta-analysis offered a valuable insight into an area which is not in the main stream of current clinical research, the question of efficacy of intercalated treatment is too complex to be answered by a simple comparison.

A critical look at all published trials reveals great heterogeneity in eligibility criteria including treatment-naïve patients or those in progression after first-line therapy. In addition, we see a whole spectrum of biologically divergent disease: all histologic types or only non-squamous histology; exclusively EGFR-mutant disease, only EGFR-wt tumors or, in most trials, both groups. On such a heterogeneous basis and without considering the optimal standard therapy for a particular population of patients, the value of a new approach cannot be assessed. Is the intercalated treatment superior to chemotherapy alone for EGFR-wt patients or superior to TKI alone for EGFR-mutant patients? To be more concrete: it comes as no surprise that intercalated treatment was superior to chemotherapy alone for a population which included a substantial proportion of EGFR-mutant patients,<sup>26,29,30,34,37,39,42</sup> and superior to TKIs alone for a population of predominantly EGFR-wt patients.<sup>36,40</sup> It is not the intercalated approach, but inclusion of an effective drug into the schedule which may be responsible for the positive experience in these trials. We believe that on the basis of randomized clinical trials published so far, the question of superiority of intercalated schedules over the standard treatment cannot be answered.

Our estimate on the proportion of EGFR mutant patients, as used in the analysis, includes a considerable degree of uncertainty. Only half of trials (14/29) included information on the proportion of EGFR-mutant *vs.* EGFR-wt tumors for more than 50% of patients. Other trials reported results of EGFR analysis for a minority of patients, or (in 8

publications) no such information. We therefore made an estimate, based on histologic types of tumors (available for 28/29 trials), on proportion of never-smokers (available for 27/29 trials) and on the country where a trial was performed, using tables from a recent meta-analysis.<sup>25</sup> This approach led us to the best possible estimate, but the results should nevertheless be regarded as exploratory and tentative. In future, precise molecular diagnostics should minimize these uncertainties.

Our survey does not include analysis of toxicity of different schedules of intercalated treatment. This aspect was clearly presented in a recent review: apart from the expected skin toxicity and diarrhea, intercalated schedules do not present a disproportional burden to patients.<sup>24</sup>

Relation between selection criteria and effectiveness of intercalated treatment is shown in Figure 2. On the basis of pooled data on median PFS from randomized and single-arm trials, it is clear that pre-treated patients are not good candidates for a treatment which includes a modality to which resistance has already developed. While the proportion of patients with non-squamous histology and of never-smokers determine efficacy of intercalated treatment, EGFR mutations are clearly the strongest predictive factor for longer PFS. By far the greatest benefit was for treatment-naïve patients with activating EGFR mutations. According to trials in which this group of patients was reported separately, their median PFS after intercalated treatment ranged between 13.3 and 23.4 months; median PFS for the pooled data was 18.4 months. This figure is substantially above PFS of 9 to 13 months, as reported for TKIs as monotherapy for EGFR-mutant NSCLC.<sup>26,55-58</sup> Response rate was also very high: 83.1%, with a substantial proportion of complete remissions. Our survey is in accordance with a recent editorial and with a meta-analysis, which pointed to intercalated regimens as the most promising first-line treatment for EGFR-mutated NSCLC.<sup>59,60</sup>

With the introduction of liquid biopsy from peripheral blood, the category of patients with undetermined EGFR mutant status should be very small.<sup>61</sup> In case this new technique is not available, previously untreated never-smokers with non-squamous histology for whom EGFR status cannot be determined should also be considered for trials testing the role of intercalated treatment. Depending on ethnicity, approximately half of them have EGFR mutant tumors, in which case addition of TKI to cytotoxic drugs would be clearly beneficial; the other half with EGFR negative tu-

mors should benefit from cytotoxic drugs included in the intercalated schedule.

In future trials of intercalated treatment, pemetrexed with platin appears as the preferred option for the cytotoxic component. Regarding the choice of TKI, virtually all current experience is limited to erlotinib and gefitinib. Still, in view of recent very favorable experience for patients who developed resistance mutations, osimertinib intercalated with chemotherapy deserves to be considered either in first-line setting or for patients in progression after first-generation TKIs.<sup>62</sup>

In two recent phase II randomized trials, patients with treatment-naïve advanced EGFR-mutant NSCLC were treated with continuous gefitinib in combination with chemotherapy. As the comparator arm, sequential gefitinib and chemotherapy or gefitinib alone were applied.<sup>63,64</sup> In both trials, patients on the combination with continuous gefitinib and chemotherapy experienced longer PFS. These reports support the advantage of combined treatment with chemotherapy and TKIs and re-open the dilemma between their concomitant and intercalated application. Combination of TKIs with bevacizumab is another possibility which deserves further attention.<sup>65</sup>

We are perfectly aware that the correlation we have reported between the proportion of patients with EGFR mutation positive tumor and the median PFS obtained with the intercalated treatment could be reasonably observed also with EGFR inhibitors alone. The only way to assess the real added value of intercalated treatment is a randomized trial with comparison to TKI alone and overall survival as the principal endpoint.

In conclusion, intercalated treatment with cytotoxic drugs and TKIs is a promising approach for patients with previously untreated advanced NSCLC with activating EGFR mutations, as well as for never-smokers with adenocarcinoma and undetermined EGFR status. For these patients, randomized trials with comparison to the optimal standard treatment, or possibly to a third arm with continuous application of TKIs in combination with chemotherapy should define the preferred treatment approach.

## Funding

This research did not receive any specific grant from funding agencies in the public, commercial, or not-for-profit sectors.

## Acknowledgements

Marjeta Jerala and David Ožura from the Library of the Institute of Oncology Ljubljana provided valuable help in retrieving full-length papers for analysis. Sincere thanks to Lars and Dyanne Søraas for intellectual support and language editing.

## References

- Lynch TJ, Bell DW, Sordella R, Gurubhagavatula S, Okimoto RA, Brannigan BW, et al. Activating mutations in the epidermal growth factor receptor underlying responsiveness of non-small-cell lung cancer to gefitinib. *N Engl J Med* 2004; **350**: 2129-39. doi:10.1056/NEJMoa040938
- Mok TS, Wu YL, Thongprasert S, Yang CH, Chu DT, Saijo N, et al. Gefitinib or carboplatin-paclitaxel in pulmonary adenocarcinoma. *N Engl J Med* 2009; **361**: 947-57. doi:10.1056/NEJMoa0810699
- Zhou C, Wu YL, Chen G, Feng J, Liu XQ, Wang C, et al. Final overall survival results from a randomised, phase III study of erlotinib versus chemotherapy as first-line treatment of EGFR mutation-positive advanced non-small-cell lung cancer (OPTIMAL, CTONG-0802). *Ann Oncol* 2015; **26**: 1877-83. doi:10.1093/annonc/mdv276
- Sequist LV, Yang JC, Yamamoto N, O'Byrne K, Hirsh V, Mok T, et al. Phase III study of afatinib or cisplatin plus pemetrexed in patients with metastatic lung adenocarcinoma with EGFR mutations. *J Clin Oncol* 2013; **31**: 3327-34. doi:10.1200/JCO.2012.44.2806
- Rosell R, Carcereny E, Gervais R, Vergnenegre A, Massuti B, Felip E, et al. Erlotinib versus standard chemotherapy as first-line treatment for European patients with advanced EGFR mutation-positive non-small-cell lung cancer (EURTAC): a multicentre, open-label, randomised phase 3 trial. *Lancet Oncol* 2012; **13**: 239-46. doi:10.1016/S1470-2045(11)70393-X
- Inoue A, Yoshida K, Morita S, Imamura F, Seto T, Okamoto I, et al. Characteristics and overall survival of EGFR mutation-positive non-small cell lung cancer treated with EGFR tyrosine kinase inhibitors: a retrospective analysis for 1660 Japanese patients. *Jpn J Clin Oncol* 2016; **46**: 462-7. doi.org/10.1093/jcco/hyw014
- Zhou C, Yao LD. Strategies to improve outcomes of patients with EGFR-mutant non-small cell lung cancer: Review of the literature. *J Thorac Oncol* 2016; **11**: 174-86. doi:10.1016/j.jtho.2015.10.002
- Giaccone G, Herbst RS, Manegold C, Scagliotti G, Rosell R, Miller V, et al. Gefitinib in combination with gemcitabine and cisplatin in advanced non-small-cell lung cancer: a phase III trial – INTACT 1. *J Clin Oncol* 2004; **22**: 777-84. doi:10.1200/JCO.2004.08.001
- Herbst RS, Giaccone G, Schiller JH, Natale RB, Miller V, Manegold C, et al. Gefitinib in combination with paclitaxel and carboplatin in advanced non-small-cell lung cancer: a phase III trial – INTACT 2. *J Clin Oncol* 2004; **22**: 785-94. doi:10.1200/JCO.2004.07.215
- Herbst RS, Prager D, Herman R, Fehrenbacher L, Johnson BE, Sandler A, et al. TRIBUTE: a phase III trial of erlotinib hydrochloride (OSI-774) combined with carboplatin and paclitaxel chemotherapy in advanced non-small-cell lung cancer. *J Clin Oncol* 2005; **23**: 5892-9. doi:10.1200/JCO.2005.02.840
- Gatzemeier U, Pluzanska A, Szczesna A, Kaukel E, Roubec J, De Rosa F, et al. Phase III study of erlotinib in combination with cisplatin and gemcitabine in advanced non-small-cell lung cancer: The Tarceva Lung Cancer Investigation Trial. *J Clin Oncol* 2007; **25**: 1545-52. doi:10.1200/JCO.2005.05.1474
- Ratti M, Tomasello G. Emerging combination therapies to overcome resistance in EGFR-driven tumors. *Anticancer Drugs* 2014; **25**: 127-39. doi:10.1097/CAD.0000000000000035
- Steuer CE, Khuri FR, Ramalingam SS. The next generation of epidermal growth factor receptor tyrosine kinase inhibitors in the treatment of lung cancer. *Cancer* 2015; **121**: E1-E6. doi:10.1002/cncr.29139
- Jänne PA, Yang JC, Kim DW, Planchard D, Ohe Y, Ramalingam SS, et al. AZD9291 in EGFR inhibitor-resistant non-small-cell lung cancer. *N Engl J Med* 2015; **372**: 1689-99. doi:10.1056/NEJMoa1411817

15. Eberhard DA, Johnson BE, Amler LC, Goddard AD, Heldens SL, Herbst RS, et al. Mutations in the epidermal growth factor receptor and in KRAS are predictive and prognostic indicators in patients with non-small-cell lung cancer treated with chemotherapy alone and in combination with erlotinib. *J Clin Oncol* 2005; **23**: 5900-909. doi:10.1200/JCO.2005.02.857
16. Reck M. Beyond the TRIBUTE trial: integrating HER1/EGFR tyrosine kinase inhibitors with chemotherapy in advanced NSCLC. *Future Oncol* 2006; **2**: 47-51. doi:10.2217/14796694.2.1.47
17. Tsai CM, Chen JT, Chiu CH, Lai CL, Hsiao SY, Chang KT. Combined epidermal growth factor receptor (EGFR)-tyrosine kinase inhibitor and chemotherapy in non-small-cell lung cancer: chemo-refractoriness of cells harboring sensitizing-EGFR mutations in the presence of gefitinib. *Lung Cancer* 2013; **82**: 305-12. doi:10.1016/j.lungcan.2013.08.028
18. Davies AM, Ho C, Lara PN Jr, Mack P, Gumerlock PH, Gandara DR. Pharmacodynamic separation of epidermal growth factor receptor tyrosine kinase inhibitors and chemotherapy in non-small-cell lung cancer. *Clin Lung Cancer* 2006; **7**: 385-8. doi:10.3816/CLC.2006.n.021
19. Mahaffey CM, Davies AM, Lara PN Jr, Pryde B, Holland W, Mack PC, et al. Schedule-dependent apoptosis in K-ras mutant non-small-cell lung cancer cell lines treated with docetaxel and erlotinib: rationale for pharmacodynamic separation. *Clin Lung Cancer* 2007; **8**: 548-53. doi:10.3816/clc.2007.n.041
20. Piperdi B, Ling Y-H, Kroog G, Perez-Soler R. Schedule-dependent interaction between epidermal growth factor inhibitors (EGFR) and G2/M blocking chemotherapeutic agents (G2/MB) on human NSCLC cell lines in vitro. *J Clin Oncol* 2004; **22(14S)**: 7028. PMID: 28016090
21. Solit DB, She Y, Lobo J, Kris MC, Scher HI, Rosen N, et al. Pulsatile administration of epidermal growth factor receptor inhibitor gefitinib is significantly more effective than continuous dosing for sensitizing tumors to paclitaxel. *Clin Cancer Res* 2005; **11**: 1983-9. doi:10.1158/1078-0432.CCR-04-1347
22. Bartholomeusz C, Yamasaki F, Saso H, Kurisu K, Hortobagyi GN, Ueno NT. Gemcitabine overcomes erlotinib resistance in EGFR-overexpressing cancer cells through downregulation of Akt. *J Cancer* 2011; **2**: 435-42. doi:10.7150/jca.2.435
23. Kanda S, Horinouchi H, Fujiwara Y, Nokihara H, Yamamoto N, Sekine I, et al. Cytotoxic chemotherapy may overcome the development of acquired resistance to epidermal growth factor receptor tyrosine kinase inhibitors (EGFR-TKIs) therapy. *Lung Cancer* 2015; **89**: 287-93. doi:10.1016/j.lungcan.2015.06.016
24. La Salvia A, Rossi A, Galetta D, Gobbi E, De Luca E, Novello S, et al. Intercalated chemotherapy and epidermal growth factor receptor inhibitors for patients with advanced non-small-cell lung cancer: A systematic review and meta-analysis. *Clin Lung Cancer* 2017; **18**: 23-33. doi:10.1016/j.clc.2016.08.006
25. Midha A, Dearden S, McCormack R. EGFR mutation incidence in non-small cell lung cancer with adenocarcinoma histology: a systematic review and global map by ethnicity (mutMapII). *Am J Cancer Res* 2015; **5**: 2892-11. PMID: 26609494
26. Mok TS, Wu YL, Yu CJ, Zhou C, Chen YM, Zhang L, et al. Randomized, placebo-controlled, phase II study of sequential erlotinib and chemotherapy as first-line treatment for advanced non-small-cell lung cancer. *J Clin Oncol* 2009; **27**: 5080-7. doi:10.1200/JCO.2008.21.5541
27. Hirsch FR, Kabbinnar F, Eisen T, Martins R, Schnell FM, Dziadziuszko R, et al. A randomized, phase II, biomarker-selected study comparing erlotinib to erlotinib intercalated with chemotherapy in first-line therapy for advanced non-small-cell lung cancer. *J Clin Oncol* 2011; **29**: 3567-73. doi:10.1200/JCO.2010.34.4929
28. Aerts JG, Codrington H, Lankheet NAG, Burgers S, Biesma B, Dingemans AM, et al. A randomized phase II study comparing erlotinib versus erlotinib with alternating chemotherapy in relapsed non-small-cell lung cancer patients: The NVALT-10 study. *Ann Oncol* 2013; **24**: 2860-5. doi:10.1093/annonc/mdt341
29. Lee DH, Lee JS, Kim SW, Rodrigues-Pereira J, Han B, Song XQ, et al. Three-arm randomised controlled phase 2 study comparing pemetrexed and erlotinib to either pemetrexed or erlotinib alone as second-line treatment for never-smokers with non-squamous non-small cell lung cancer. *Eur J Cancer* 2013; **49**: 3111-21. doi:10.1016/j.ejca.2013.06.035
30. Wu YL, Lee JS, Thongprasert S, Yu CJ, Zhang L, Ladrera G, et al. Intercalated combination of chemotherapy and erlotinib for patients with advanced stage non-small-cell lung cancer (FASTACT 2): a randomised, double blind trial. *Lancet Oncol* 2013; **14**: 777-86. doi:10.1016/S1470-2045(13)70254-7
31. Auliac JB, Chouaid C, Greillier L, Monnet I, Le Caer H, Falchero L, et al. Randomized open-label non-comparative multicenter phase II trial of sequential erlotinib and docetaxel versus docetaxel alone in patients with non-small-cell lung cancer after failure of first-line chemotherapy: GFPC 10.02 study. *Lung Cancer* 2014; **85**: 415-9. doi:10.1016/j.lungcan.2014.07.006
32. Karavasilis V, Kosmidis P, Syrigos KN, Mavropoulou P, Dimopoulos MA, Kotoula V, et al. Docetaxel and intermittent erlotinib in patients with metastatic Non-Small Cell Lung Cancer; a phase II study from the Hellenic Cooperative Oncology Group. *Anticancer Res* 2014; **34**: 5649-55. PMID: 25275069
33. Mok TS, Gaeter SL, Iannotti N, Thongprasert S, Spira A, Smith D, et al. Randomized phase II study of two intercalated combinations of eribulin mesylate and erlotinib in patients with previously treated advanced non-small-cell lung cancer. *Ann Oncol* 2014; **25**: 1578-84. doi:10.1093/annonc/mdu174
34. Yu H, Zhang J, Wu X, Luo Z, Wang H, Sun S, et al. A phase II randomized trial evaluating gefitinib intercalated with pemetrexed/platinum chemotherapy or pemetrexed/platinum chemotherapy alone in unselected patients with advanced non-squamous non-small cell lung cancer. *Cancer Biol Ther* 2014; **15**: 832-9. doi:10.4161/cbt.28874
35. Choi YJ, Lee DH, Choi CM, Lee JS, Lee SJ, Ahn JH, et al. Randomized phase II study of paclitaxel/carboplatin intercalated with gefitinib compared to paclitaxel/carboplatin alone for chemotherapy-naïve non-small cell lung cancer in a clinically selected population excluding patients with non-smoking adenocarcinoma or mutated EGFR. *BMC Cancer* 2015; **15**: 763. doi:10.1186/s12885-015-1714y
36. Juan Ó, Aparisi F, Sánchez-Hernández A, Muñoz-Langa J, Esquerdo G, García-Sánchez J, et al. Intercalated dosing schedule of erlotinib and docetaxel as a therapeutic strategy to avoid antagonism and optimize its benefits in advanced non-small-cell lung cancer. A randomized phase II clinical trial. *Clin Lung Cancer* 2015; **16**: 193-9. doi:10.1016/j.clc.2014.11.006
37. Lu S, Jian H, Li W, Yong MZ, Huang JJ, Feng J, et al. Intercalating and maintenance use of gefitinib plus chemotherapy versus chemotherapy alone in selected advanced NSCLC (ISCAN,CTONG-1102): a multicentre, open-label, randomised, phase 3 study. [abstract]. *J Clin Oncol* 2015; **33(Suppl)**: abstr 8042. ClinicalTrials.gov Identifier: NCT01404260
38. Michael M, White SC, Abdi E, Nott L, Clingan P, Zimet A, et al. Multicenter randomized, open-label phase II trial of sequential erlotinib and gemcitabine compared with gemcitabine monotherapy as first-line therapy in elderly or ECOG PS two patients with advanced NSCLC. *Asia Pac J Clin Oncol* 2015; **11**: 4-14. doi:10.1111/ajco.12178
39. Han B, Zhang Y, Jin B, Chu T, Gu A, Xu J. Combination of chemotherapy and gefitinib as first-line treatment of patients with advanced lung adenocarcinoma and sensitive EGFR mutations: a randomized controlled trial. *J Thorac Oncol* 2016; **11(Suppl 4)**: S113-4. doi:10.1016/S1556-0864(16)30244-1
40. Lara PN Jr, Moon J, Hesketh PJ, Redman MW, Williamson SK, Akerley WL 3rd, et al. SWOG S0709: Randomized Phase II trial of erlotinib versus erlotinib plus carboplatin/paclitaxel in patients with advanced non-small cell lung cancer and impaired performance status as selected by a serum proteomics assay. *J Thorac Oncol* 2016; **11**: 420-5. doi:10.1016/j.jtho.2015.11.003
41. Li T, Piperdi B, Walsh WV, Kim M, Beckett A, Gucalp R, et al. Randomized phase II study of pharmacodynamic separation of pemetrexed and intercalated erlotinib versus pemetrexed alone for advanced non-small cell lung cancer. *Clin Lung Cancer* 2017; **18**: 60-7. doi:10.1016/j.clc.2016.10.003
42. Lee JS, Lee YJ, Kim HY, Nam B-H, Lee GK, Kim HT, et al. Randomized phase II trial of intercalated gefitinib (G) and pemetrexed/cisplatin (Pem/Cis) for never-smokers with chemo-naïve stage IIIB/IV lung adenocarcinoma (LADC). [abstract]. *J Clin Oncol* 2016; **34**: e20505. ClinicalTrials.gov Identifier: NCT01502202
43. Yoon S, Lee D-H, Kim D, Choi C-M, Kim S-W. Randomized Phase II trial comparing intercalation of afatinib to pemetrexed with pemetrexed alone after failure of platinum doublet therapy. [abstract] *J Thorac Oncol* 2017; **12(Suppl 1)**: S926. abstr P2.03A-061
44. Oshita F, Saito H, Murakami S, Kondo T, Yamada K. Phase II study of paclitaxel and irinotecan with intercalated gefitinib in patients with advanced non-small-cell lung cancer. *Am J Clin Oncol* 2010; **33**: 66-9. doi:10.1097/COC.0b013e31819ccc6d
45. Sangha R, Davies AM, Lara PN Jr, Mack PC, Beckett LA, Hesketh PJ, et al. Intercalated erlotinib-docetaxel dosing schedules designed to achieve pharmacodynamic separation: results of a phase I/II trial. *J Thorac Oncol* 2011; **6**: 2112-9. doi:10.1097/JTO.0b013e31822ae061

46. Minami S, Kijima T, Hamaguchi M, Nakatani T, Koba T, Takahashi R, et al. Phase II study of pemetrexed plus intermittent erlotinib combination therapy for pretreated advanced non-squamous non-small cell lung cancer with documentation of epidermal growth factor receptor mutation status. *Lung Cancer* 2013; **82**: 271-5. doi:10.1016/j.lungcan.2013.07.022
47. Yoshimura N, Okishio K, Mitsuoka S, Kimura T, Kawaguchi T, Kobayashi M, et al. Prospective assessment of continuation of erlotinib or gefitinib in patients with acquired resistance to erlotinib or gefitinib followed by the addition of pemetrexed. *J Thorac Oncol* 2013; **8**: 96-101. doi:10.1097/JTO.0b013e3182762bfb
48. Kim YH, Nishimura T, Ozasa H, Nagai H, Sakamori Y, Iwata T, et al. Phase II study of pemetrexed and erlotinib in pretreated nonsquamous non-small-cell lung cancer patients without an EGFR mutation. *Chemotherapy* 2013; **59**: 414-9. doi:10.1159/000363731
49. Fang H, Lin RY, Sun MX, Wang Q, Zhao YL, Yu JL, et al. Efficacy and survival-associated factors with gefitinib combined with cisplatin and gemcitabine for advanced non-small cell lung cancer. *Asian Pac J Cancer Prev* 2014; **15**: 10967-70. doi:10.7314/APJCP.2014.15.24.10967
50. Yang J, Shi Y, Zhang X, Xu J, Wang B, Hao X et al. Phase II trial of paclitaxel-carboplatin with intercalated gefitinib for untreated, epidermal growth factor receptor gene mutation status unknown non-small cell lung cancer. *Thorac Cancer* 2014; **5**: 149-54. doi:10.1111/1759-7714.12074
51. Zwitter M, Stanić K, Rajer M, Kern J, Vrankar M, Edelbauer N, et al. Intercalated chemotherapy and erlotinib for advanced NSCLC: high proportion of complete remissions and prolonged progression-free survival among patients with EGFR activating mutations. *Radiol Oncol* 2014; **48**: 361-8. doi:10.2478/raon-2014-0038
52. Yoshimura N, Kudoh S, Mitsuoka S, Yoshimoto N, Oka T, Nakai T, et al. Phase II study of a combination regimen of gefitinib and pemetrexed as first-line treatment in patients with non-small cell lung cancer harbouring a sensitive EGFR mutation. *Lung Cancer* 2015; **90**: 65-70. doi:10.1016/j.lungcan.2015.06.002
53. Yu S, Zhang B, Xiang C, Shu Y, Wu H, Huang X, et al. Prospective assessment of pemetrexed or pemetrexed plus platinum in combination with gefitinib or erlotinib in patients with acquired resistance to gefitinib or erlotinib: a phase II exploratory and preliminary study. *Clin Lung Cancer* 2015; **16**: 121-27. doi:10.1016/j.clc.2014.09.007
54. Zwitter M, Rajer M, Stanic K, Vrankar M, Doma A, Cuderman A, et al. Intercalated chemotherapy and erlotinib for non-small cell lung cancer (NSCLC) with activating epidermal growth factor receptor (EGFR) mutations. *Cancer Biol Ther* 2016; **17**: 833-9. doi:10.1080/15384047.2016.1195049
55. Chen YM, Lai CH, Chang HC, Chao TY, Tseng CC, Fang WF, et al. The impact of clinical parameters on progression-free survival of non-small cell lung cancer patients harboring EGFR-mutations receiving first-line EGFR-tyrosine kinase inhibitors. *Lung Cancer* 2016; **93**: 47-54. doi:10.1016/j.lungcan.2016.01.001
56. De Grève J, Van Meerbeeck J, Vansteenkiste JF, Decoster L, Meert AP, Vuylsteke P, et al. Prospective evaluation of first-line erlotinib in advanced non-small cell lung cancer (NSCLC) carrying an activating EGFR mutation: A multicenter academic phase II study in Caucasian patients (FIELT). *PLoS One* 2016; **11**: e0147599. doi:10.1371/journal.pone.0147599
57. Douillard JY, Ostoros G, Cobo M, Ciuleanu T, McCormack R, Webster A, et al. First-line gefitinib in Caucasian EGFR mutation-positive NSCLC patients: a phase-IV, open-label, single-arm study. *Br J Cancer* 2014; **110**: 55-62. doi:10.1038/bjc.2013.721
58. Inoue A, Yoshida K, Morita S, Imamura F, Seto T, Okamoto I, et al. Characteristics and overall survival of EGFR mutation-positive non-small cell lung cancer treated with EGFR tyrosine kinase inhibitors: a retrospective analysis for 1660 Japanese patients. *Jpn J Clin Oncol* 2016; **46**: 462-7. doi:10.1093/jjco/hyw014
59. Rossi A. Chemotherapy plus intercalated or continuous EGFR-TKI in advanced non-small cell lung cancer. *Transl Cancer Res* 2016; **5(Suppl 4)**: S659-63.
60. Lopes G, Tan PS, Acharyya S, Bilger M, Haaland B. Network meta-analysis comparing first-line therapies and maintenance regimens in EGFR mutated advanced non-small-cell lung cancer (NSCLC). [abstract]. *J Clin Oncol* 2016; **34(Suppl)**: abstr e20570.
61. Sacher AG, Komatsubara KM, Oxnard GR. Application of plasma genotyping technologies in non-small cell lung cancer: a practical review. *J Thorac Oncol* 2017; [Epub ahead of print]. doi:10.1016/j.jtho.2017.05.022
62. Mok TS, Wu Y-L, Ahn M-J, Garassino MC, Kim HR, Ramalingam SS, et al. Osmertinib or platinum-pemetrexed in EGFR T790M-positive lung cancer. *N Engl J Med* 2016; **376**: 629-40. doi:10.1056/NEJMoa1612674
63. Sugawara S, Oizumi S, Minato K, Harada T, Inoue A, Fujita Y, et al. Randomized phase II study of concurrent versus sequential alternating gefitinib and chemotherapy in previously untreated non-small cell lung cancer with sensitive EGFR mutations: NEJ005/TCOG0902. *Ann Oncol* 2015; **26**: 888-94. doi:10.1093/annonc/mdv063
64. Cheng Y, Murakami H, Yang PC, He J, Nakagawa K, Kang JH, et al. Randomized Phase II trial of gefitinib with and without pemetrexed as first-line therapy in patients with advanced nonsquamous non-small-cell lung cancer with activating epidermal growth factor receptor mutations. *J Clin Oncol* 2016; **34**: 3258-66. doi:10.1200/JCO.2016.66.9218
65. Seto T, Kato T, Nishio M, Goto K, Atagi S, Hosomi Y, et al. Erlotinib alone or with bevacizumab as first-line therapy in patients with advanced non-squamous non-small-cell lung cancer harbouring EGFR mutations (JO25567): an open-label, randomised, multicentre, phase 2 study. *Lancet Oncol* 2014; **15**: 1236-44. doi:10.1016/S1470-2045(14)70381-X

# Magnetic resonance imaging evaluation in neoadjuvant therapy of locally advanced rectal cancer: a systematic review

Roberta Fusco<sup>1</sup>, Mario Petrillo<sup>1</sup>, Vincenza Granata<sup>1</sup>, Salvatore Filice<sup>1</sup>, Mario Sansone<sup>2</sup>, Orlando Catalano<sup>1</sup>, Antonella Petrillo<sup>1</sup>

<sup>1</sup> Radiology Unit, Dipartimento di Supporto ai Percorsi Oncologici Area Diagnostica, Istituto Nazionale Tumori - IRCCS - Fondazione G. Pascale, Via Mariano Semmola, Naples, Italy

<sup>2</sup> Department of Electrical Engineering and Information Technologies, Università degli Studi di Napoli Federico II, Via Claudio, Naples, Italy

Radiol Oncol 2017; 51(3): 252-262.

Received 29 December 2016

Accepted 21 June 2017

Correspondence to: Dr. Roberta Fusco, Radiology Unit, Dipartimento di Supporto ai Percorsi Oncologici Area Diagnostica, Istituto Nazionale Tumori - IRCCS - Fondazione G. Pascale, Via Mariano Semmola, Naples, Italy. Phone: +39 8159 0322; Fax: +39 8159 03825; E-mail: r.fusco@istitutotumori.na.it

Disclosure: No potential conflicts of interest were disclosed.

**Background.** The aim of the study was to present an update concerning several imaging modalities in diagnosis, staging and pre-surgery treatment response assessment in locally advanced rectal cancer (LARC). Modalities include: traditional morphological magnetic resonance imaging (MRI), functional MRI such as dynamic contrast enhanced MRI (DCE-MRI) and diffusion weighted imaging (DWI). A systematic review about the diagnostic accuracy in neoadjuvant therapy response assessment of MRI, DCE-MRI, DWI and Positron Emission Tomography/Computed Tomography (PET/CT) has been also reported.

**Methods.** Several electronic databases were searched including PubMed, Scopus, Web of Science, and Google Scholar. All the studies included in this review reported findings about therapy response assessment in LARC by means of MRI, DCE-MRI, DWI and PET/CT with details about diagnostic accuracy, true and false negatives, true and false positives. Forest plot and receiver operating characteristic (ROC) curves analysis were performed. Risk of bias and the applicability at study level were calculated.

**Results.** Twenty-five papers were identified. ROC curves analysis demonstrated that multimodal imaging integrating morphological and functional MRI features had the best accuracy both in term of sensitivity and specificity to evaluate preoperative therapy response in LARC. DCE-MRI following to PET/CT showed high diagnostic accuracy and their results are also more reliable than conventional MRI and DWI alone.

**Conclusions.** Morphological MRI is the modality of choice for rectal cancer staging permitting a correct assessment of the disease extent, of the lymph node involvement, of the mesorectal fascia and of the sphincter complex for surgical planning. Multimodal imaging and functional DCE-MRI may also help in the assessment of treatment response allowing to guide the surgeon versus conservative strategies and/or tailored approach such as "wait and see" policy.

Key words: magnetic resonance imaging; neoadjuvant therapy; evaluation; locally advanced rectal cancer

## Introduction

In the USA 39,220 new cases of rectal cancer occurred in 2016.<sup>1</sup> Despite the introduction of the screening programs, several patients are diagnosed in a locally advanced stage. Mortality has

decreased thanks to prevention and early diagnosis and to effective management of the disease<sup>2-12</sup>, such as the standardization of operative procedures and the introduction of adjuvant and neoadjuvant therapy<sup>13-23</sup>, which determines a reduction of recurrence risk and a decrease of tumour size.

Preoperative chemo-radiotherapy (pCRT) combined with following total mesorectal excision is the standard procedure of care for locally advanced rectal cancer (LARC).<sup>13-24</sup> However, there is an increase of conservative treatment strategies application for patients with substantial tumour regression after pCRT and “wait and see” policy for patients with complete pathological response. The advantage of this strategy is the reduction of morbidity and the possibility to provide a “true” organ-sparing approach. In this scenario, it is necessary to individualize the selection criteria for these strategies that accurately can assess neoadjuvant treatment response. Functional approaches have been exploited by several authors because of their capability to assess the residual tissue “vitality”.<sup>25-35</sup> FDG positron emission tomography coupled with computed tomography (PET/CT) is widely used and it is considered the best technique for early response monitoring after pCRT in LARC.<sup>13-14</sup> However, other functional approaches including dynamic contrast enhanced-MRI (DCE-MRI) and diffusion weighted imaging (DWI) have been adopted to discriminate responder by non-responder patients and complete *vs.* non complete pathological response after pCRT.<sup>13-14</sup>

The objective of this manuscript is to present an update about the imaging modalities used in LARC staging with a specific focus on morphological MRI. Furthermore, a systematic review about the performance of imaging in the tumour response assessment after neoadjuvant therapy has been performed. We report diagnostic accuracy findings in terms of false and true positives, false and true negatives number for morphological MRI, DCE-MRI, DWI and PET/CT.

## Overview about staging and restaging in LARC

The role of imaging is to provide a loco-regional staging as accurate as possible with the aim to assess the degree of tumour infiltration and extension. Moreover, the features detected by radiological imaging allow to evaluate pCRT response for guiding surgeon towards patient tailored strategies.<sup>36-74</sup>

In LARC, CT scan roughly show tumour size and its possible infiltration to internal organs: in fact, it can provide excellent contrast between tissues with large difference in X-ray absorption (bone *vs.* soft tissues); however, it can poorly discriminate between tissues with similar absorption such as different soft tissues, including tumours.<sup>47</sup>

PET/CT provides functional tissue information concerning metabolic activity fused with the morphological details of CT. The integration of tissue metabolic activity with anatomic information can improve its accuracy more than PET or CT when considered alone.<sup>48-49</sup>

Morphological MRI (T2 weighted images) has shown superior potential because it can provide an accurate evaluation not only of the tumour extent, but also of the adjacent soft tissues. Morphological MRI allows for comprehensive evaluation of disease stage including tumour infiltration degree, a precise assessment of the neoplasia distance by mesorectal fascia (circumferential margin) and an effective assessment of lymph nodes involvement and mesorectal infiltration.<sup>26</sup>

Traditionally, tumour response assessments have been achieved measuring the percentage reduction of the tumour size according to the response evaluation criteria in solid tumours (RECIST), as the change in tumour size is generally thought to be correlated with treatment efficacy.<sup>17,50-53</sup> However, this assessment approach is insensitive to early treatment changes, and it makes difficult to distinguish between active tumour and post-treatment fibrosis.

In fact, morphological MRI has been considered not to be conclusive in pCRT tumour response assessment since pathological down-staging is not always accompanied with tumour size effective reduction.<sup>17,23-26,50-53</sup> However, the high temporal resolution obtainable using more powerful sequences has allowed to perform perfusion and dynamic studies after paramagnetic contrast agent administration. The latter MRI techniques permit to obtain functional tissue information concerning the vitality of the tissue essential to differentiate fibrosis from residual tumour after anti-angiogenetic treatments.

## Dynamic contrast MRI

In scientific literature the potential of DCE-MRI has been reported as a promising evaluation tool to monitor and predict therapy response thanks to the relationship between tumour growth and angiogenesis.<sup>5-7,19,24-25</sup> It is well known that angiogenesis is a key factor in the growth and dissemination of cancer. The characterization of the tumour angiogenic status on an individual patient basis could allow patient tailored treatments.<sup>24</sup>

Many clinical trials in rectal cancer have demonstrated that angiogenesis inhibition can increase treatment effectiveness. Consequently, imaging

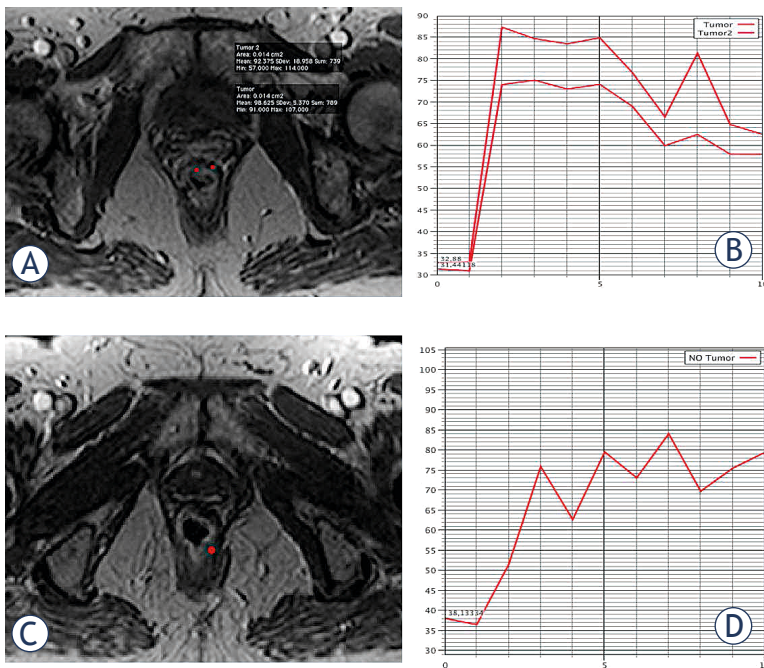


**FIGURE 1.** T1 weighted post contrast scan obtained before (A)-(B) and after (C)-(D) chemo-radiotherapy (CRT). The analysis of time intensity curve (TIC) show areas with rapid contrast uptake and fast discharge (B). After CRT, on the same areas no pathological contrast uptake is present confirming that hypo-intense tissue are tumour nests but only residual inflammation due to CRT.

modalities able to assess tumour vascularization might improve the treatment management in patients affected by LARC.<sup>6-7,24-25</sup>

To assess tissue perfusion by means of DCE-MRI several approaches to analyse time intensity curve (TIC) have been proposed. The most commonly used in the clinical radiological practice is the TIC visual inspection approach.<sup>54</sup> The main drawback of this qualitative approach is its dependence upon the experience of the operator and the absence of reproducibility. Petrillo *et al.*<sup>52</sup> utilized TIC visual inspection to assess pCRT response in LARC (Figure 1). According to<sup>52</sup>, when patients with a partial or complete response to pCRT were included, a sensitivity, specificity and an accuracy of 79%, 76% and 78% respectively have been obtained. Instead, considering the performance of qualitative MRI evaluation in complete responders a sensitivity, a specificity and an accuracy of 94%, 76% and 84% respectively could be reached.

To overcome the limitations related to visual inspection alone, the quantitative or semi-quantitative approach for DCE-MRI data analysis have been proposed and investigated.

Quantitative model-based analysis involves compartmental tracer kinetic modelling<sup>20-21</sup> and

pixel-by-pixel or region of interest based estimation of kinetic features, by means of a non-linear regression. The latter has been introduced to better correlate quantitative model-based features with physiological tissue properties. Kim *et al.*<sup>55</sup> showed that average K<sub>trans</sub> (a parameter associated to contrast agent transfer constant between plasma to extracellular extravascular space) had a large decrease after pCRT; this decrease was linked with a good therapeutic response in LARC. However, being influenced by many variables and since many different models are present in the literature, the quantitative approach still suffers from high output variability, poor clinical consistency and reproducibility.<sup>20</sup> Quantitative analysis findings in the therapy response assessment using 3T scanners are more encouraging as Intven *et al.* and Lim *et al.* have reported in their studies.<sup>56-57</sup>

To overcome previous problems several authors<sup>58-61</sup> performed semi-quantitative analysis. Lavini *et al.*<sup>59</sup>, in order to discriminate benign and malignant pixels, used the following features: maximum signal difference, time to peak, maximum slope of increase, relative final slope and initial signal. Tuncbilek *et al.*<sup>60</sup> demonstrated that time to peak, wash-in intercept and maximum enhancement were strongly correlated to micro vessel density. Petrillo *et al.*<sup>53</sup> investigated a semi-quantitative analysis with a piecewise linear fitting and they individuated a combination of two TIC descriptors named Standardized Index of Shape (SIS). This latter is a linear weighted combination of relative change of maximum signal difference ( $\Delta$ MSD) and relative change of wash-out slope ( $\Delta$ WOS).<sup>53</sup> This index reached a sensitivity of 93.5% and a specificity of 82.1% with relevant gains respect to  $\Delta$ MSD (+20.1% in sensitivity and +11.7% in specificity) and  $\Delta$ WOS (+13.1% in sensitivity and + 4.3% in specificity) alone. Moreover, the standardized index of shape improved negative predictive value to 88.5% and positive predictive value to 89.6%.

Because many of the conducted studies are relatively small and study design is very heterogeneous, the evidence on DCE-MRI is rather inconsistent. Therefore, future research should aim at increasing sample sizes and standardization of imaging techniques and analyses.<sup>61</sup>

### Diffusion weighted imaging

The use of DWI into a standard MR protocol is progressively increasing thanks to its capability in the tumour detection, characterization as well as its potentiality in the monitoring and in the pre-

diction of treatment response.<sup>8-12,62-65</sup> By means of DWI data analysis is possible to estimate water molecules mobility that is related to cell density, vascularity, viscosity of extracellular fluid and cell membrane integrity.<sup>12</sup> By measuring these properties with apparent diffusion coefficient (ADC) and other diffusion coefficients characteristics of intravoxel incoherent motion, the DWI could be used as an imaging biomarker to better select patients with reduced prognosis who will benefit from a more aggressive neoadjuvant treatment.<sup>8-12</sup> It was demonstrated that ADC values in LARC correlate with prognostic factors including the mesorectal fascia status, the nodal stage and the histological differentiation grade.<sup>8,40,62</sup> There are several ways to analyse DWI data including visual evaluation, volumetric assessment, and ADC measurements. Visual DWI evaluation has been shown to improve the MRI performance to differentiate between patients with and without residual tumour after pCRT. Another approach is to measure the volume before and after therapy. Ha *et al.* reported that DWI tumour volumetry offered the best results to predict the complete response to chemoradiation treatment.<sup>11</sup> Furthermore, Sathyakumar *et al.*<sup>19</sup> demonstrated that DWI visual assessment post therapy and DWI tumour volume reduction were the best predictors of complete pathological response. Sensitivity, specificity, positive predictive value, negative predictive value and accuracy of DWI visual assessment to predict complete response were 81.8%, 94.3%, 75%, 96.1% and 76% respectively. Sensitivity, specificity and accuracy of tumour volume reduction (cut off value 95%) were 80%, 84.1% and 64.1%, respectively.

ADC measure (before, during, and after therapy) is the most widely studied approach to assess therapy response. Increases in ADC values after treatment are linked to decreases in tissue cellularity and thus it provides indirect evaluation of chemotherapy induced cell death. Kim *et al.*<sup>62</sup> demonstrated that the addition of DWI to standard MRI protocol yields better diagnostic accuracy than use of conventional MRI alone in the evaluation of pathological complete response. Marouf *et al.*<sup>63</sup> reported for conventional MRI a sensitivity of 60% and specificity of 33% with overall diagnostic accuracy of 46.5% in the assessment of T stage. Overall diagnostic accuracy increased adding DWI to 83.5% with the 87% of sensitivity and 80% of specificity. N stage prediction by conventional MRI had 74% of sensitivity and 80% of specificity with an overall accuracy of 78%. Overall accuracy to predict N stage increased adding DWI to 83%.

However, the evidence regarding the use of pre, during and post treatment ADC measurements to assess tumour response has so far been inconsistent, which is also related to the fact that ADC measurement are influenced by variations in MR scanner hardware, field strength, acquisition protocols and measurement methods. Lack of standardization hampers the implementation of ADC in clinical practice and should be the focus of future studies.<sup>61</sup>

### PET/CT

PET/CT is constantly increasing in rectal cancer management for its ability to predict treatment response.<sup>50</sup> Avallone *et al.*<sup>50</sup> reported that early changes (12 days after the pCRT beginning) of the standardized uptake maximum value ( $\Delta$ SUVmax) were predictive of pathological response with an optimal threshold value of -42.0% and an accuracy of 93.0%. In this study, the authors also observed that the findings obtained from late pre surgical PET/CT scans showed lower accuracy in predicting of pathologic response. Leccisotti *et al.*<sup>70</sup> analysed the metabolic activity modifications by PET/CT during and after pCRT in 124 patients with LARC demonstrating that the areas under ROC curve of the early response index to detect non-complete pathological response was 0.74 (optimal cut-off of  $\Delta$ SUVmax was 61.2%). On the contrary, the optimal cut-off for the late response index was not being found. Niccoli-Asabella *et al.*<sup>71</sup> reported similar findings, with an area under ROC curve for  $\Delta$ SUVmax of 0.67. Therefore, the literature data were discordant detecting in general the poor accuracy of late metabolic response to predict pathological response in LARC.

### Systematic review

The review is the result of autonomous studies without protocol and registration number.

### Search criterion

Several electronic database were searched: PubMed (US National Library of Medicine, <http://www.ncbi.nlm.nih.gov/pubmed>), Scopus (Elsevier, <http://www.scopus.com/>), Web of Science (Thomson Reuters, <http://apps.webofknowledge.com/>) and Google Scholar (<https://scholar.google.it/>). The following search criteria have been used: "rectal cancer" AND "diffusion magnetic resonance imaging" AND "response", "rectal cancer" AND "dynamic

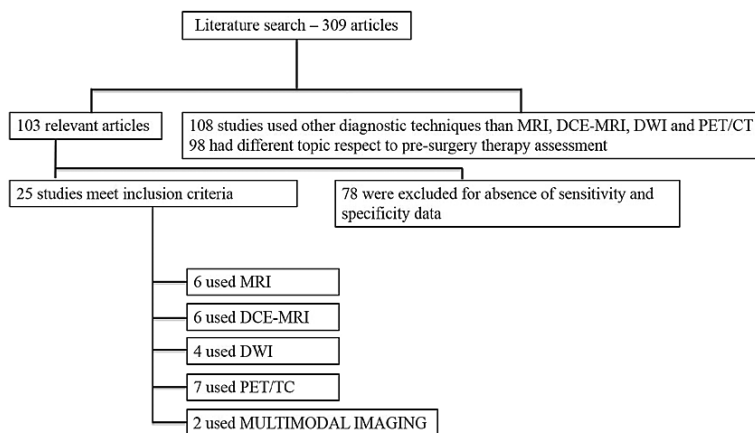


FIGURE 2. Included and excluded studies in systematic review.

DCE-MRI = dynamic contrast enhanced MRI; DWI = diffusion weighted imaging

contrast enhanced magnetic resonance imaging" AND "response", "rectal cancer" AND "positron emission tomography" AND "response", "rectal cancer" AND "multimodal imaging" AND "response". In order to cover the last twelve years of the recent oncologic research literature, the research covered the years from 2005 through 2016. Moreover, the reference lists of the found papers were analysed for papers not indexed in the electronic databases.

All titles and abstracts were analysed and exclusively the studies reporting morphological MRI, DCE-MRI, DWI or PET/CT results in the preoperative therapy response assessment for LARC were retained.

If not otherwise stated, all the studies reviewed herein fulfil the following criteria: English language; thorough clinical characterization of the patients with rectal cancer studied by means morphological MRI, DCE-MRI, DWI and PET/CT to discriminate responders versus non responders to pCRT and exclusion of studies using other diagnostic techniques; articles, reviews and studies that did not present data about specificity, sensibility, positive and negative predictive value of tests treated were excluded; articles, reviews and studies that did not present data about specificity, sensibility, positive and negative predictive value of tests treated were excluded; reviews, general overview articles and congress abstracts were excluded. There was not defining a minimum number of patients as inclusion criteria due to the small number of studies for each imaging modality. Information extracted from each study included

TABLE 1. Number of studies and participants for each diagnostic modality

Diagnostic modality	Studies	Participants
MRI	6	329
DCE-MRI	6	340
DWI	4	133
PET/CT	7	366
MULTIMODAL IMAGING	2	70

DCE-MRI = dynamic contrast enhanced MRI; DWI = diffusion weighted imaging

title, authors, year of publication, sample size, diagnostic modality and approach, reference standard, true and false positives number, true and false negatives number.

### Data analysis

Review Manager (version 5.2) was used to perform data analysis for systematic review. The PRISMA statement for reporting systematic review was used.<sup>75</sup>

True and false positives number, true and false negatives number for each paper were collected and used to obtain the forest plots reporting the sensitivity, specificity values and relative 95% confidence intervals. ROC curves were also constructed. Moreover, to assess the quality and bias risk of diagnostic accuracy studies included in the review was used QUADAS-2 tool.<sup>76</sup>

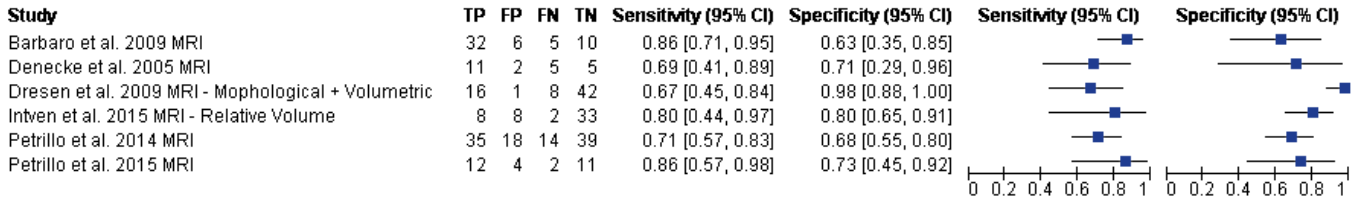
## Results

By using the search terms described earlier, we identified 309 studies from 2005 through 2016. One hundred eight studies used other diagnostic techniques than morphological MRI, DCE-MRI, DWI and PET/CT; 98 had different topic respect to pre-surgery therapy assessment; 78 were excluded for insufficient data (absence of sensibility and specificity value). Twenty-five studies remained for inclusion in our systematic review (Figure 2).

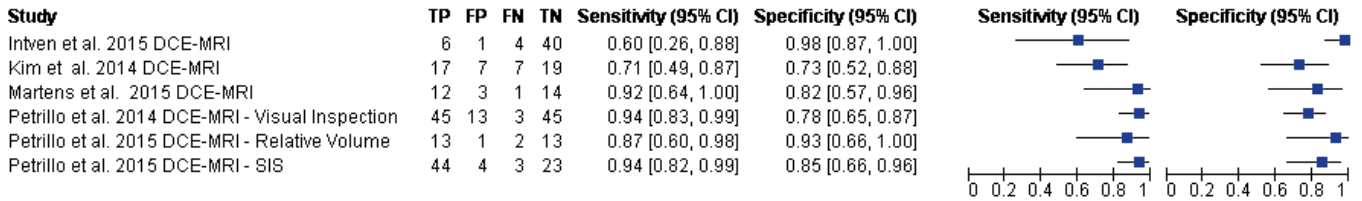
Table 1 shows the number of included studies and the overall number of participants grouped by diagnostic modality.

Details regarding the number of patients, imaging modality, the accuracy values and examined parameters were recorded. Table 2 summarizes the main characteristics of the examined methodologies in LARC studies.

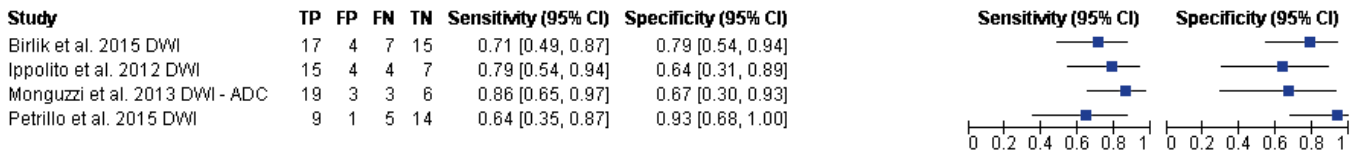
**MRI**



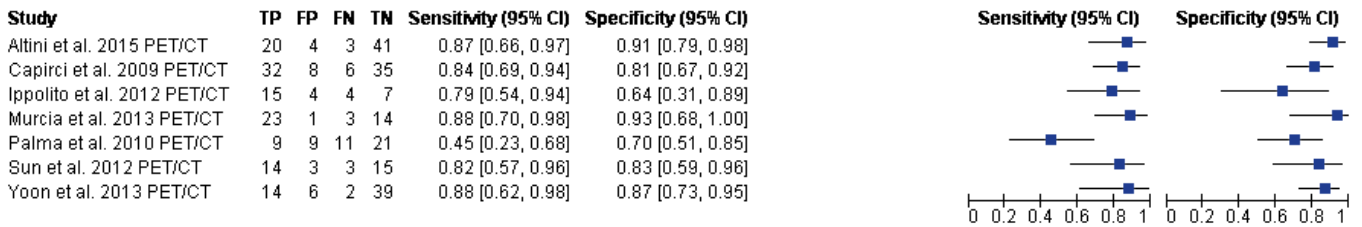
**DCE-MRI**



**DWI**



**PET/CT**



**MULTIMODAL IMAGING**

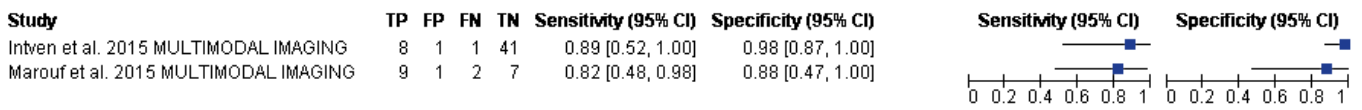


**FIGURE 3.** Forest plot subdivide for imaging modality including sensitivity and specificity estimates and their confidence intervals (95%).

CI = confidence interval; FN = false negative; FP = false positive; SIS = standardized index of shape; TN = true negative; TP = true positive

Figure 3 reports the values of true positive (TP), false positive (FP), false negative (FN), true negative (TN), sensitivity and specificity estimates and their confidence intervals (95%) for each study, subdivided according to the diagnostic modality used for therapy response assessment in LARC. Figure 4 shows ROC for each diagnostic modality.

Table 3 reports the diagnostic performance for each imaging modality in terms of sensitivity, specificity, positive predictive value and negative predictive value.

Figure 5 shows the bias risk and applicability analysis results. A very low risk of bias was present for the studies included in this systematic review.

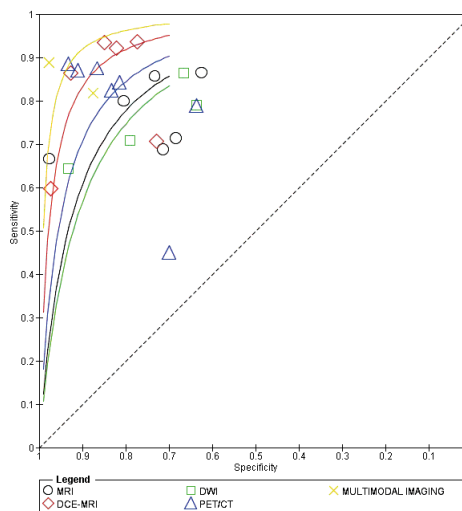


**FIGURE 4.** Estimated summary ROC curves and original data points for imaging techniques.

DCE-MRI = dynamic contrast enhanced MRI; DWI = diffusion weighted imaging

**TABLE 2.** Main characteristics summary of included studies in the systematic review: for each study the table reports imaging modality used; number of patients examined; parameters examined

Imaging modality	Authors	Approach	N. patients	Gold standard
MRI	Barbaro <i>et al.</i> <sup>69</sup>	Score system	53	TNM
	Denecke <i>et al.</i> <sup>46</sup>	Morphologic criteria	23	TNM
	Dresen <i>et al.</i> <sup>45</sup>	Morphologic + volumetric criteria	67	TNM
	Intven <i>et al.</i> <sup>56</sup>	Relative volume	51	TRG
	Petrillo <i>et al.</i> <sup>52</sup>	Score system	106	TRG
	Petrillo <i>et al.</i> <sup>64</sup>	Relative volume	29	TRG
DCE-MRI	Intven <i>et al.</i> <sup>56</sup>	Relative Ktrans	51	TRG
	Kim <i>et al.</i> <sup>55</sup>	Relative Ktrans	50	TNM
	Martens <i>et al.</i> <sup>67</sup>	TIC slope	30	TRG
	Petrillo <i>et al.</i> <sup>52</sup>	TIC visual inspection	106	TRG
	Petrillo <i>et al.</i> <sup>64</sup>	Relative volume	29	TRG
	Petrillo <i>et al.</i> <sup>53</sup>	Standardized index of shape	74	TRG
DWI	Birlik <i>et al.</i> <sup>65</sup>	ADC	43	TRG
	Ippolito <i>et al.</i> <sup>40</sup>	ADC	30	TRG
	Monguzzi <i>et al.</i> <sup>68</sup>	ADC	31	TRG
	Petrillo <i>et al.</i> <sup>64</sup>	Relative volume	29	TRG
MULTIMODAL IMAGING	Intven <i>et al.</i> <sup>56</sup>	Relative volume + relative Ktrans	51	TRG
	Marouf <i>et al.</i> <sup>63</sup>	MRI + DWI Score system	19	TNM
PET/CT	Altini <i>et al.</i> <sup>36</sup>	SUV	68	TRG
	Capirci <i>et al.</i> <sup>42</sup>	SUV	81	TRG
	Ippolito <i>et al.</i> <sup>40</sup>	SUV	30	TRG
	Murcia <i>et al.</i> <sup>43</sup>	SUV	41	TRG
	Sun <i>et al.</i> <sup>41</sup>	Total lesion glycolysis	35	TRG
	Yoon <i>et al.</i> <sup>66</sup>	Dual-point index	61	TRG
	Palma <i>et al.</i> <sup>73</sup>	SUV	50	TRG

ADC = apparent diffusion coefficient; DWI = diffusion weighted imaging; SUV = standardized uptake value; TIC = time intensity curve; TRG = tumour regression grade

## Discussions

The objective of this systematic review was to evaluate the different imaging modalities (morphological MRI, DWI, DCE-MRI, PET/CT and multimodal imaging) in LARC management after pCRT. We collected the current evidence of the role of functional MRI and PET/CT in the assessment of pathological response after pCRT in LARC. The objective was linked to the potentiality of imaging to guide surgeon choice. In fact, patients with substantial (partial response) tumour regression after pCRT could be candidate to conservative strategy while patients reporting a complete response could be subjected to a “wait and see” policy. The advantage

is the reduction of morbidity and the possibility to provide a “true” organ-sparing approach.

Our results, using a systematic review of literature and the ROC curves analysis, showed that multimodal imaging combining morphological and functional might achieve better results having the best accuracy in term of sensitivity and specificity (85% and 96%, respectively). However, it should be noted that only two studies have been retrieved from the literature for a total number of only 70 participants subjected to multimodal MRI examination.<sup>56,63</sup> Intven *et al.*<sup>56</sup> demonstrated on 51 patients with LARC that both the post therapy tumour volume and post therapy Ktrans values and their relative changes were predictive for patho-

**TABLE 3.** Performance pooled analysis for MRI, diffusion weighted imaging (DWI), dynamic contrast enhanced MRI (DCE-MRI), PET/CT and multimodal imaging

Performance Pooled Analysis	Sensitivity	Specificity	Positive predictive value	Negative predictive value	Accuracy
MRI	75,84	78,21	74,34	79,55	77,13
DCE-MRI	87,18	84,15	82,42	88,51	85,55
DWI	75,95	79,25	84,51	68,85	77,27
PET/CT	80,25	83,08	79,27	83,92	81,82
<b>MULTIMODAL IMAGING</b>	<b>85,00</b>	<b>96,08</b>	<b>89,47</b>	<b>94,23</b>	<b>92,96</b>

DCE-MRI = dynamic contrast enhanced MRI; DWI = diffusion weighted imaging

logical response. For the relative Ktrans, Intven *et al.*<sup>56</sup> reported a positive predictive value of 100% (with a Ktrans cut-off of 32%) to discriminate good responders. However, for pathological complete response, the best positive predictive value was 80% obtained with a multiparameter model of relative volume and relative Ktrans. Marouf *et al.*<sup>63</sup> reported an increase of diagnostic accuracy for the combination of morphological MRI and DWI from 84.2% to 94.7%. Although the number of patients is relatively small multimodal imaging seems to give promising results whose reliability is to be confirmed in future studies.

Moreover, DCE-MRI following to PET/CT showed a high diagnostic accuracy (sensitivity 87% and 80% respectively, specificity 84% and 83% respectively) and their results are also more reliable than conventional MRI and DWI alone (Figure 3 and 4). Instead, for morphological MRI alone, the sensitivity was of 76% and specificity of 78%. For DWI, the sensitivity was of 76% and specificity was of 79%. Our findings are comparable with recent meta-analysis that indicated that addition of DWI to standard MRI in a multimodal approach improves the sensitivity for T-staging after pCRT from 50% to 84%.<sup>12</sup>

Instead, Ippolito *et al.*<sup>40</sup> reported that the best predictors cut-off values for tumour regression grade (TRG) response were for PET/CT SUVmax of 4.4 and for ADC of  $1.28 \times 10^3 \text{ mm}^2 \text{ s}^{-1}$ . ADC obtained sensitivity, specificity, accuracy, negative and positive predictive values of 77.3%, 88.9%, 80.7%, 61.5%, and 94.4%, respectively.

However, PET/CT showed an inferior diagnostic accuracy in comparison of DCE-MRI in pre-surgical assessment of therapy response in LARC but it had a high predict value in the early evaluation of therapy response. The early response assessment by PET/CT was a predictor of non-complete

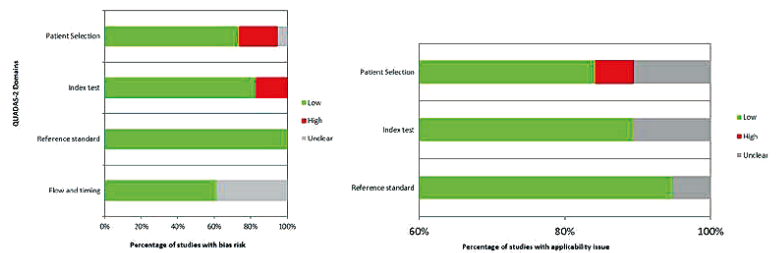


**FIGURE 5.** Assessment of bias risk and applicability analysis.

pathological therapy response allowing practical modification of treatment.

Kim *et al.*<sup>72</sup> revealed that SUVmax post therapy had a sensitivity of 60.4%, a specificity of 65.0%, and an accuracy of 55.9% to discriminate pathological complete response. Palma *et al.*<sup>73</sup> reported that maximum  $\Delta\text{SUVmax}$  had a sensitivity of 45.0%, a specificity of 67.0%, and an accuracy of 89.0% while Altini *et al.*<sup>36</sup> shown a sensitivity of 87.0%, a specificity of 70.0% and an accuracy of 60.0%. Similar results were also observed in others advanced cancers such as esophageal cancer.<sup>74</sup> On the contrary, late response index was not sufficiently precise to guide the surgeon choice versus radical or local excision or versus a “wait and see” strategy.<sup>50,70-73</sup>

As well as PET/CT, DWI technology can be efficient for predicting pathological complete response in LARC<sup>77-80</sup> but inefficient to assess late response in pre-surgical phase. Chen *et al.*<sup>79</sup> reported DWI sensitivity, specificity, positive predictive value, negative predictive value, and accuracy of 60%, 64%, 60%, 60%, and 60%, respectively, in pathological complete response discrimination using a cut-off value of  $0.866 \times 10^{-3} \text{ mm}^2/\text{s}$  for pre-treatment ADC value. Using a cut-off value for ADC percentage change of 58% the sensitivity, specificity, positive predictive value, negative predictive value, and accuracy were 80%, 76%, 77%, 79% and 78%, respectively.<sup>79</sup> Moreover, the mean pre-treatment

tumour ADC correlates with the degree of tumour response after therapy and patients who respond to treatment seem to have a lower ADC at presentation than do those who do not respond.<sup>5</sup> The association between high tumour ADC and poor response is consistent with the known relationship between necrosis and poor response to cancer treatment. However, both PET/CT and DWI had an important role in therapy prediction and in early therapy response assessment but showed a low accuracy in pre-surgical therapy evaluation.

Therefore, multimodal assessment combining different imaging modalities might be the best option for local restaging of locally advanced rectal cancer after CRT in pre-surgical phase.<sup>81</sup> According to this theory, recently Ippolito *et al.*<sup>82</sup> reported that the functional imaging combining ADC and SUVmax in a single analysis permits to detect changes in cellular tissue structures useful for the assessment of tumour response after the neoadjuvant therapy in rectal cancer, increasing the sensitivity in correct depiction of treatment response than either method alone.

A number of limitations of this analysis must be recognized. Most papers report on a limited number of patients and heterogeneity within the included studies with respect to patient selection, neoadjuvant treatment and imaging protocols and analyses. This pooled analysis should be regarded as an indicator of the general performance of functional MRI and PET/CT in the therapy response assessment. Validation and implementation in a multicenter setting are still awaited. Standardization of MRI acquisition protocols and data post processing approaches is mandatory to guarantee results reproducibility. Multicenter studies using large patient populations are needed to validate the role of functional imaging in order to identify those patients who may benefit from a less aggressive therapeutic approach after CRT.

We can conclude that in local staging, morphological MRI is superior respect to CT and PET/CT permitting a correct assessment of the disease extent, of the lymph node involvement, of the mesorectal fascia and of the sphincter complex for surgical planning. On the other side, in restaging for therapy response assessment, Multimodal MRI followed by DCE-MRI seem to give more promising results respect to PET/CT, DWI and conventional MRI. Multimodal Imaging including morphological and functional MRI and DCE-MRI alone could allow to better discriminate responder by non responders patients after neoadjuvant therapy with a high diagnostic accuracy.

In the future, the scientific research should be focused on the integration and combination of functional imaging modalities including also clinical data and molecular biomarkers. A greater number of studies should be performed in the future for each modality to improve the reliability of any conclusion.

## References

1. Siegel RL, Miller KD, Jemal A. Cancer statistics, 2016. *CA Cancer J Clin* 2016; **66**: 7-30. doi:10.3322/caac.21332
2. Folkman J. Tumour angiogenesis: therapeutic implications. *N Engl J Med* 1971; **285**: 1182-86. doi:10.1056/NEJM197111182852108
3. Choi HJ, Hyun MS, Jung GJ, Kim SS, Hong SH. Tumor angiogenesis as a prognostic predictor in colorectal carcinoma with special reference to mode of metastasis and recurrence. *Oncology* 1998; **55**: 575-81.
4. Dvorak HF, Brown LF, Detmar M, Dvorak AM. Vascular permeability factor/vascular endothelial growth factor, microvascular hyperpermeability, and angiogenesis. *Am J Pathol* 1995; **146**: 1029-39.
5. Dzik-Jurasz A, Domenig C, George M, Wolber J, Padhani A, Brown G, et al. Diffusion MRI for prediction of response of rectal cancer to chemoradiation. *Lancet* 2002; **360**: 307-8. doi:10.1016/S0140-6736(02)09520-X
6. Devries AF, Griebel J, Kremser C, Judmaier W, Gneiting T, Kreczy A, et al. Tumor microcirculation evaluated by dynamic magnetic resonance imaging predicts therapy outcome for primary rectal carcinoma. *Cancer Res* 2001; **61**: 2513-6.
7. DeVries AF, Kremser C, Hein PA, Griebel J, Kreczy A, Ofner D, et al. Tumor microcirculation and diffusion predict therapy outcome for primary rectal carcinoma. *Int J Radiat Oncol Biol Phys* 2003; **56**: 958-65.
8. Foti PV, Privitera G, Piana S, Palmucci S, Spatola C, Bevilacqua R, et al. Locally advanced rectal cancer: qualitative and quantitative evaluation of diffusion-weighted MR imaging in the response assessment after neoadjuvant chemo-radiotherapy. *Eur J Radiol Open* 2016; **3**: 145-52. doi:10.1016/j.ejro.2016.06.003
9. Koh DM, Collins DJ. Diffusion-weighted MRI in the body: applications and challenges in oncology. *AJR Am J Roentgenol* 2007; **188**: 1622-35. doi:10.2214/AJR.06.1403
10. Padhani AR, Liu G, Koh DM, Chenevert TL, Thoeny HC, Takahara T, et al. Diffusion-weighted magnetic resonance imaging as a cancer biomarker: consensus and recommendations. *Neoplasia* 2009; **11**: 102-25.
11. Ha HI, Kim AY, Yu CS, Park SH, Ha HK. Locally advanced rectal cancer: diffusion-weighted MR tumour volumetry and the apparent diffusion coefficient for evaluating complete remission after preoperative chemoradiation therapy. *Eur Radiol* 2013; **23**: 3345-53. doi:10.1007/s00330-013-2936-5
12. van der Paardt MP, Zagers MB, Beets-Tan RG, Stoker J, Bipat S. Patients who undergo preoperative chemoradiotherapy for locally advanced rectal cancer restaged by using diagnostic MR imaging: a systematic review and meta-analysis. *Radiology* 2013; **269**: 101-12. doi:10.1148/radiol.13122833
13. Avallone A, Delrio P, Guida C, Tatangelo F, Petrillo A, Marone P, et al. Biweekly oxaliplatin, raltitrexed, 5-fluorouracil and folinic acid combination chemotherapy during preoperative radiation therapy for locally advanced rectal cancer: a phase I-II study. *Brit J Cancer* 2006; **94**: 1809-15. doi:10.1038/sj.bjc.6603195
14. Avallone A, Delrio P, Pecori B, Tatangelo F, Petrillo A, Scott N, et al. Oxaliplatin plus dual inhibition of thymidilate synthase during preoperative pelvic radiotherapy for locally advanced rectal carcinoma: long-term outcome. *Int J Radiat Oncol* 2011; **79**: 670-6. doi:10.1016/j.ijrobp.2009.12.007
15. van Gijn W, Marijnen CA, Nagtegaal ID, Kranenbarg EM, Putter H, Wiggers T, et al; Dutch Colorectal Cancer Group. Preoperative radiotherapy combined with total mesorectal excision for resectable rectal cancer: 12-year follow-up of the multicentre, randomised controlled TME trial. *Lancet Oncol* 2011; **12**: 575-82. doi:10.1016/S1470-2045(11)70097-3

16. Vermaas M, Ferenschild FT, Nuytens JJ, Marinelli AW, Wiggers T, van der Sijp JR, et al. Preoperative radiotherapy improves outcome in recurrent rectal cancer. *Dis Colon Rectum* 2005; **48**: 918-28. doi:10.1007/s10350-004-0891-6
17. Gérard JP, Conroy T, Bonnetain F, Bouché O, Chapet O, Closon-Dejardin MT, et al. Preoperative radiotherapy with or without concurrent fluorouracil and leucovorin in T3-4 rectal cancers: results of FFCO 9203. *J Clin Oncol* 2006; **24**: 4620-5. doi:10.1200/JCO.2006.06.7629
18. Bosset JF, Collette L, Calais G, Mineur L, Maingon P, Radosevic-Jelic L, et al; EORTC Radiotherapy Group Trial 22921. Chemotherapy with preoperative radiotherapy in rectal cancer. *N Engl J Med* 2006; **355**: 1114-23. doi:10.1056/NEJMoa060829
19. Sathyakumar K, Chandramohan A, Masih D, Jesudasan MR, Pulimood A, Eapen A. Best MRI predictors of complete response to neoadjuvant chemoradiation in locally advanced rectal cancer. *Br J Radiol* 2016; **89**: 20150328. doi:10.1259/bjr.20150328
20. Willett CG, Boucher Y, di Tomaso E, Duda DG, Munn LL, Tong RT, et al. Direct evidence that the VEGF-specific antibody bevacizumab has antivasular effects in human rectal cancer. *Nat Med* 2004; **10**: 145-7. doi:10.1038/nm988
21. Vermaas M, Ferenschild FT, Verhoef C, Nuytens JJ, Marinelli AW, Wiggers T, et al. Total pelvic exenteration for primary locally advanced and locally recurrent rectal cancer. *Eur J Surg Oncol* 2007; **33**: 452-8. doi:10.1016/j.ejso.2006.09.021
22. Wiig JN, Poulsen JP, Larsen S, Braendengen M, Waehre H, Giercksky KE. Total pelvic exenteration with preoperative irradiation for advanced primary and recurrent rectal cancer. *Eur J Surg* 2002; **168**: 42-8. doi:10.1080/110241502317307562
23. Luna-Perez P, Delgado S, Labastida S, Ortiz N, Rodriguez D, Herrera L. Patterns of recurrence following pelvic exenteration and external radiotherapy for locally advanced primary rectal adenocarcinoma. *Ann Surg Oncol* 1996; **3**: 526-33.
24. Delrio P, Avallone A, Guida C, Lastoria S, Tatangelo F, Cascini GM, et al. Multidisciplinary approach to locally advanced rectal cancer: results of a single institution trial. *Suppl Tumori* 2005; **4**: S8.
25. Delrio P, Lastoria S, Avallone A, Ravo V, Guida C, Cremona F, et al. Early evaluation using PET-FDG of the efficiency of neoadjuvant radiochemotherapy treatment in locally advanced neoplasia of the lower rectum. *Tumori* 2003; **89**(4 Suppl): 50-3.
26. Petrillo A, Catalano O, Delrio P, Avallone A, Guida C, Filice S, et al. Post-treatment fistulas in patients with rectal cancer: MRI with rectal superparamagnetic contrast agent. *Abdom Imaging* 2007; **32**: 328-31. doi:10.1007/s00261-006-9028-9
27. Pecori B, Lastoria S, Caracò C, Celentani M, Tatangelo F, Avallone A, et al. Sequential PET/CT with [18F]-FDG predicts pathological tumor response to preoperative short course radiotherapy with delayed Surgery in patients with locally advanced rectal cancer using logistic regression analysis. *PLoS One* 2017; **12**: e0169462. doi:10.1371/journal.pone.0169462
28. Sansone M, Fusco R, Petrillo A, Petrillo M, Bracale M. An expectation-maximisation approach for simultaneous pixel classification and tracer kinetic modelling in dynamic contrast enhanced-magnetic resonance imaging. *Med Biol Eng Comput* 2011; **49**: 485-95. doi:10.1007/s11517-010-0695-x
29. Fusco R, Sansone M, Petrillo M, Antonella Petrillo. Influence of parameterization on tracer kinetic modeling in DCE-MRI. *J Med Biol Eng* 2012; **34**: 157-63. doi:10.5405/jmbe.1097
30. Fusco R, Sansone M, Maffei S, Petrillo A. Dynamic contrast-enhanced MRI in breast cancer: a comparison between distributed and compartmental tracer kinetic models. *J Biomed Graph Comput* 2012; **2**: 23. doi:10.5430/jbgc.v2n2p23
31. Gunderson LL, Sargent DJ, Tepper JE, O'Connell MJ, Allmer C, Smalley SR, et al. Impact of T and N substage on survival and disease relapse in adjuvant rectal cancer: a pooled analysis. *Int J Radiat Oncol* 2002; **54**: 386-96.
32. Gunderson LL, Sargent DJ, Tepper JE, Wolmark N, O'Connell MJ, Begovic M, et al. Impact of T and N stage and treatment on survival and relapse in adjuvant rectal cancer: a pooled analysis. *J Clin Oncol* 2004; **22**: 1785-96. doi:10.1200/JCO.2004.08.173
33. Goh V, Padhani AR, Rasheed S. Functional imaging of colorectal cancer angiogenesis. *Lancet Oncol* 2007; **8**: 245-55. doi:10.1016/S1470-2045(07)70075-X
34. Kremser C, Trieb T, Rudisch A, Judmaier W, de Vries A. Dynamic t(1) mapping predicts outcome of chemoradiation therapy in primary rectal carcinoma: sequence implementation and data analysis. *J Magn Reson Imaging* 2007; **26**: 662-71. doi:10.1002/jmri.21034
35. Beets-Tan RG, Beets GL. Rectal cancer: review with emphasis on MR imaging. *Radiology* 2004; **232**: 335-46. doi:10.1148/radiol.2322021326
36. Altini C, Niccoli Asabella A, De Luca R, Fanelli M, Callandro C, Quartuccio N, et al. Comparison of (18)F-FDG PET/CT methods of analysis for predicting response to neoadjuvant chemoradiation therapy in patients with locally advanced low rectal cancer. *Abdom Imaging* 2015; **40**: 1190-202. doi:10.1007/s00261-014-0277-8
37. Chen CC, Lee RC, Lin JK, Wang LW, Yang SH. How accurate is magnetic resonance imaging in restaging rectal cancer in patients receiving preoperative combined Chemoradiotherapy? *Dis Colon Rectum* 2005; **48**: 722-8. doi:10.1007/s10350-004-0851-1
38. Capirci C, Rampin L, Erba PA, Galeotti G, Banti E, et al. Sequential FDG-PET/CT reliably predicts response of locally advanced rectal cancer to neo-adjuvant chemo-radiation therapy. *Nucl Med Mol Imaging* 2007; **34**: 1583-93. doi:10.1007/s00259-007-0426-1
39. Kristiansen C, Loft A, Berthelsen AK, Graff J, Lindebjerg J, Bisgaard C, et al. PET/CT and histopathologic response to preoperative chemoradiation therapy in locally advanced rectal cancer. *Dis Colon Rectum* 2008; **51**: 21-5. doi:10.1007/s10350-007-9095-1
40. Ippolito D, Monguzzi L, Guerra L, Deponti E, Gardani G, Messa C, et al. Response to neoadjuvant therapy in locally advanced rectal cancer: assessment with diffusion-weighted MR imaging and 18FDG PET/CT. *Abdom Imaging* 2012; **37**: 1032-40. doi:10.1007/s00261-011-9839-1
41. Sun W, Xu J, Hu W, Zhang Z, Shen W. The role of sequential 18(F)-FDG PET/CT in predicting tumour response after preoperative chemoradiation for rectal cancer. *Colorectal Dis* 2013; **15**: e231-8. doi:10.1111/codi.12165
42. Capirci C, Rubello D, Pasini F, Galeotti F, Bianchini E, Del Favero G, et al. The role of dual-time combined 18-fluorodeoxyglucose positron emission tomography and computed tomography in the staging and restaging workup of locally advanced rectal cancer, treated with preoperative chemoradiation therapy and radical surgery. *Int J Radiat Oncol Biol Phys* 2009; **74**: 1461-9. doi:10.1016/j.ijrobp.2008.10.064
43. Murcia MJ, Duréndez L, Frutos Esteban J, Luján MD, Frutos G, Valero JL, et al. The value of 18F-FDG PET/CT for assessing the response to neoadjuvant therapy in locally advanced rectal cancer. *Eur J Nucl Med Mol Imaging*; **40**: 91-7. doi:10.1007/s00259-012-2257-y
44. Rosenberg R, Herrmann K, Gertler R, Künzli B, Essler M, Lordick F, et al. The predictive value of metabolic response to preoperative radiochemotherapy in locally advanced rectal cancer measured by PET/CT. *Int J Colorectal Dis* 2009; **24**: 191-200. doi:10.1007/s00384-008-0616-8
45. Dresen RC, Beets GL, Rutten HJT, Engelen SME, Lahaye MJ, Vliegen RFA, et al. Locally advanced rectal cancer: MR imaging for restaging after neoadjuvant radiation therapy with concomitant chemotherapy Part I. Are we able to predict tumor confined to the rectal wall? *Radiology* 2009; **252**: 71-80. doi:10.1148/radiol.2521081200
46. Denecke T, Rau B, Hoffmann KT, Hildebrandt B, Ruf J, Gutberlet M, et al. Comparison of CT, and FDG-PET in response prediction of patients with locally advanced rectal cancer after multimodal preoperative therapy: is there a benefit in using functional imaging? *Eur Radiol* 2005; **15**: 1658-66. doi:10.1007/s00330-005-2658-4
47. Beets-Tan RG, Beets GL, Borstlap AC, Oei TK, Teune TM, von Meyenfildt MF, et al. Preoperative assessment of local tumour extent in advanced rectal cancer: CT or high-resolution MRI? *Abdom Imaging* 2000; **25**: 533-41. doi:10.1107/s0026100000086
48. Wiering B, Ruers TJ, Oyen WJ. Role of FDG PET in the diagnosis and treatment of colorectal liver metastases. *Expert Rev Anticancer Ther* 2004; **4**: 607-13. doi:10.1586/14737140.4.4.607
49. Park IJ, Kim HC, Yu CS, Ryu MH, Chang HM, Kim JH, et al. Efficacy of PET/CT in the accurate evaluation of primary colorectal carcinoma. *Eur J Surg Oncol* 2006; **32**: 941-7. doi:10.1016/j.ejso.2006.05.019
50. Avallone A, Aloj L, Caracò C, Delrio P, Pecori B, Tatangelo F, et al. Early FDG PET response assessment of preoperative radiochemotherapy in locally advanced rectal cancer: correlation with long-term outcome. *Eur J Nucl Med Mol Imaging* 2012; **39**: 1848-57. doi:10.1007/s00259-012-2229-2

51. Avallone A, Aloj L, Delrio P, Pecori B, Leone A, Tatangelo F, et al. Multidisciplinary approach to rectal cancer: are we ready for selective treatment strategies? *Anticancer Agents Med Chem* 2013; **13**: 852-60.
52. Petrillo A, Fusco R, Petrillo M, Granata V, Filice S, Delrio P, et al. Dynamic contrast enhanced-MRI in locally advanced rectal cancer: value of time intensity curve visual inspection to assess neo-adjuvant therapy response. *J Physiol Health Photon* 2014; **110**: 255-67.
53. Petrillo A, Fusco R, Petrillo M, Granata V, Sansone M, Avallone A, et al. Standardized index of shape (SIS): a quantitative DCE-MRI parameter to discriminate responders by non-responders after neoadjuvant therapy in LARC. *Eur Radiol* 2015; **25**: 1935-45. doi:10.1007/s00330-014-3581-3
54. Fusco R, Petrillo A, Petrillo M, Sansone M. Use of tracer kinetic models for selection of semi-quantitative features for DCE-MRI data classification. *Appl Magn Reson* 2013; **44**: 1311-24. doi:10.1007/s00723-013-0481-7
55. Kim SH, Lee JM, Gupta SN, Han JK, Choi BI. Dynamic contrast-enhanced MRI to evaluate the therapeutic response to neoadjuvant chemoradiation therapy in locally advanced rectal cancer. *J Magn Reson Imaging* 2014; **40**: 730-7. doi:10.1002/jmri.24387
56. Intven M, Reerink O, Philippens ME. Dynamic contrast enhanced MR imaging for rectal cancer response assessment after neo-adjuvant chemoradiation. *J Magn Reson Imaging* 2015; **41**: 1646-53. doi:10.1002/jmri.24718
57. Lim JS, Kim D, Baek SE, Myoung S, Choi J, Shin SJ, et al. Perfusion MRI for the prediction of treatment response after preoperative chemoradiotherapy in locally advanced rectal cancer. *Eur Radiol* 2012; **22**: 1693-700. doi:10.1007/s00330-012-2416-3
58. Guo JY, Reddick WE. DCE-MRI pixel-by-pixel quantitative curve pattern analysis and its application to osteosarcoma. *J Magn Reson Imaging* 2009; **30**: 177-84. doi:10.1002/jmri.21785
59. Lavini C, de Jonge MC, van de Sande MG, Tak PP, Nederveen AJ, Maas M. Pixel-by-pixel analysis of DCE MRI curve patterns and an illustration of its application to the imaging of the musculoskeletal system. *Magn Reson Imaging* 2007; **25**: 604-12. doi:10.1016/j.mri.2006.10.021
60. Tuncbilek N, Karakas HM, Altaner S. Dynamic MRI in indirect estimation of microvessel density, histologic grade, and prognosis in colorectal adenocarcinomas. *Abdom Imaging* 2004; **29**: 166-72. doi:10.1007/s00261-003-0090-2
61. Lambregts DM, Maas M, Stokkel MP, Beets-Tan RG. Magnetic Resonance Imaging and Other Imaging Modalities in Diagnostic and Tumor Response Evaluation. *Semin Radiat Oncol* 2016; **26**: 193-8. doi:10.1016/j.semradonc.2016.02.001
62. Kim SH, Lee JM, Hong SH, Kim GH, Lee JY, Han JK, et al. Locally advanced rectal cancer: added value of diffusion-weighted MR imaging in the evaluation of tumor response to neoadjuvant chemo- and radiation therapy. *Radiology* 2009; **253**: 116-25. doi:10.1148/radiol.2532090027
63. Marouf RA, Tadrosa MY, Ahmedb TY. Value of diffusion-weighted MR imaging in assessing response of neoadjuvant chemo and radiation therapy in locally advanced rectal cancer. *EJRN* 2015; **46**: 553-61. doi:10.1016/j.ejrn.2015.03.005
64. Petrillo M, Fusco R, Catalano O, Sansone M, Avallone A, Delrio P, et al. MRI for assessing response to neoadjuvant therapy in locally advanced rectal cancer using DCE-MR and DW-MR data sets: a preliminary report. *Biomed Res Int* 2015; **2015**: 514740. doi:10.1155/2015/514740
65. Biriik B, Obuz F, Elibol FD, Celik AO, Sokmen S, Terzi C, et al. Diffusion-weighted MRI and MR- volumetry - in the evaluation of tumor response after preoperative chemoradiotherapy in patients with locally advanced rectal cancer. *Magn Reson Imaging* 2015; **33**: 201-12. doi:10.1016/j.mri.2014.08.041
66. Yoon HJ, Kim SK, Kim TS, Im HJ, Lee ES, Kim HC, et al. New application of dual point 18F-FDG PET/CT in the evaluation of neoadjuvant chemoradiation response of locally advanced rectal cancer. *Clin Nucl Med* 2013; **38**: 7-12. doi:10.1097/RLU.0b013e3182639a58
67. Martens MH, Subhani S, Heijnen LA, Lambregts DM, Buijns J, Maas M, et al. Can perfusion MRI predict response to preoperative treatment in rectal cancer? *Radiother Oncol* 2015; **114**: 218-23. doi:10.1016/j.radonc.2014.11.044
68. Monguzzi L, Ippolito D, Bernasconi DP, Trattenero C, Galimberti S, Sironi S. Locally advanced rectal cancer: value of ADC mapping in prediction of tumor response to radiochemotherapy. *Eur J Radiol* 2013; **82**: 234-40. doi:10.1016/j.ejrad.2012.09.027
69. Barbaro B, Fiorucci C, Tebala C, Valentini V, Gambacorta MA, Vecchio FM, et al. Locally advanced rectal cancer: MR imaging in prediction of response after preoperative chemotherapy and radiation therapy. *Radiology* 2009; **250**: 730-9. doi:10.1148/radiol.2503080310
70. Leccisotti L, Gambacorta MA, de Waure C, Stefanelli A, Barbaro B, Vecchio FM, et al. The predictive value of 18F-FDG PET/CT for assessing pathological response and survival in locally advanced rectal cancer after neoadjuvant radiochemotherapy. *Eur J Nucl Med Mol Imaging* 2015; **42**: 657-66. doi:10.1007/s00259-014-2820-9
71. Niccoli-Asabella A, Altini C, De Luca R, Fanelli M, Rubini D, Caliandro C, et al. Prospective analysis of 18F-FDG PET/CT predictive value in patients with low rectal cancer treated with neoadjuvant chemoradiotherapy and conservative surgery. *Biomed Res Int* 2014; **2014**: 952843. doi:10.1155/2014/952843
72. Kim JW, Kim HC, Park JW, Park SC, Sohn DK, Choi HS, et al. Predictive value of (18)F-FDG PET-CT for tumour response in patients with locally advanced rectal cancer treated by preoperative chemoradiotherapy. *Int J Colorectal Dis* 2013; **28**: 1217-24. doi:10.1007/s00384-013-1657-1
73. Palma P, Conde-Muñoz R, Rodríguez-Fernández A, Segura-Jiménez J, Sánchez-Sánchez R, Martín-Cano J, et al. The value of metabolic imaging to predict tumour response after chemoradiation in locally advanced rectal cancer. *Radiat Oncol* 2010; **5**: 119. doi:10.1186/1748-717X-5-119
74. Wieder HA, Brücher BL, Zimmermann F, Becker K, Lordick F, Beer A, et al. Time course of tumor metabolic activity during chemoradiotherapy of esophageal squamous cell carcinoma and response to treatment. *J Clin Oncol* 2004; **22**: 900-8. doi:10.1200/JCO.2004.07.122
75. Liberati A, Altman DG, Tetzlaff J, Mulrow C, Gøtzsche PC, Ioannidis JP, et al. The PRISMA statement for reporting systematic reviews and meta-analyses of studies that evaluate healthcare interventions: explanation and elaboration. *BMJ* 2009; **339**: b2700.
76. Whiting PF, Rutjes AW, Westwood ME, Mallett S, Deeks JJ, Reitsma JB, et al; QUADAS-2 Group. QUADAS-2: a revised tool for the quality assessment of diagnostic accuracy studies. *Ann Intern Med* 2011; **155**: 529-36. doi:10.7326/0003-4819-155-8-201110180-00009
77. Sathyakumar K, Chandramohan A, Masih D, Jesudasan MR, Pulimood A, Eapen A. Best MRI predictors of complete response to neoadjuvant chemoradiation in locally advanced rectal cancer. *Br J Radiol* 2016; **89**: 20150328. doi:10.1259/bjr.20150328
78. Jacobs L, Intven M, van Lelyveld N, Philippens M, Burbach M, Seldenrijk K, et al. Diffusion-weighted MRI for early prediction of treatment response on preoperative chemoradiotherapy for patients with locally advanced rectal cancer: a feasibility study. *Ann Surg* 2016; **263**: 522-8. doi:10.1097/SLA.0000000000001311
79. Chen YG, Chen MQ, Guo YY, Li SC, Wu JX, Xu BH. Apparent diffusion coefficient predicts pathology complete response of rectal cancer treated with neoadjuvant chemoradiotherapy. *PLoS One* 2016; **11**: e0153944. doi:10.1371/journal.pone.0153944
80. Choi MH, Oh SN, Rha SE, Choi JJ, Lee SH, Jang HS, et al. Diffusion-weighted imaging: apparent diffusion coefficient histogram analysis for detecting pathologic complete response to chemoradiotherapy in locally advanced rectal cancer. *J Magn Reson Imaging* 2016; **44**: 212-20. doi:10.1002/jmri.25117
81. Kye BH, Kim HJ, Kim G, Kim JG, Cho HM. Multimodal assessments are needed for restaging after neoadjuvant chemoradiation therapy in rectal cancer patients. *Cancer Res Treat* 2016; **48**: 561-6. doi:10.4143/crt.2015.114
82. Ippolito D, Fior D, Trattenero C, Ponti ED, Drago S, Guerra L, et al. Combined value of apparent diffusion coefficient-standardized uptake value max in evaluation of post-treated locally advanced rectal cancer. *World J Radiol* 2015; **7**: 509-20. doi:10.4329/wjr.v7.i12.509

# An image fusion system for estimating the therapeutic effects of radiofrequency ablation on hepatocellular carcinoma

Nobuyuki Toshikuni, Yasuhiro Matsue, Kazuaki Ozaki, Kaho Yamada, Nobuhiko Hayashi, Mutsumi Tsuchishima, Mikihiro Tsutsumi

Department of Hepatology, Kanazawa Medical University, Uchinada, Ishikawa, Japan

Radiol Oncol 2017; 51(3): 263-269.

Received 3 December 2016

Accepted 29 June 2017

Correspondence to: Nobuyuki Toshikuni, M.D., Ph.D., Department of Hepatology, Kanazawa Medical University, 1-1 Daigaku, Uchinada-machi, Kahoku, Ishikawa 920-0293, Japan. Phone: +81 76 286 2211; Fax: +81 76 286 0892; E-mail: n.toshikuni@gmail.com

Disclosure: The authors declare no potential conflicts of interest.

**Background.** During ultrasound-guided radiofrequency ablation (RFA) of hepatocellular carcinoma (HCC), high echoic areas due to RFA-induced microbubbles can help calculate the extent of ablation. However, these areas also decrease visualization of target tumors, making it difficult to assess whether they completely cover the tumors. To estimate the effects of RFA more precisely, we used an image fusion system (IFS).

**Patients and methods.** We enrolled patients with a single HCC who received RFA with or without the IFS. In the IFS group, we drew a spherical marker along the contour of a target tumor on reference images immediately after administering RFA so that the synchronized spherical marker represented the contour of the target tumor on real-time ultrasound images. When the high echoic area completely covered the marker, we considered the ablation to be complete. We compared outcomes between the IFS and control groups.

**Results.** We enrolled 25 patients and 20 controls, and the baseline characteristics were similar between the two groups. The complete ablation rates during the first RFA session were significantly higher in the IFS group compared with those in the control group (88.0% vs. 60.0%,  $P = 0.041$ ). The number of RFA sessions was significantly smaller in the IFS group compared with that in the control group ( $1.1 \pm 0.3$  vs.  $1.5 \pm 0.7$ ,  $P = 0.016$ ).

**Conclusions.** The study suggested that the IFS enables a more precise estimation of the effects of RFA on HCC, contributing to enhanced treatment efficacy and minimized patient burden.

Key words: image fusion; hepatocellular carcinoma; radiofrequency ablation

## Introduction

Radiofrequency ablation (RFA) is an established curative, non-surgical method for treating small hepatocellular carcinoma (HCC)<sup>1</sup>, and ultrasound (US) is the most widely used imaging modality for RFA procedures because of its convenience and simplicity. During US-guided RFA, a high echoic area due to RFA-induced microbubbles emerges and then enables calculation of the ablation extent.<sup>2,3</sup> However, the high echoic area also decreases visualization of target tumors, making it difficult to assess whether the area completely covers the tumor. A method that can overcome this issue would

increase the efficiency of RFA and thus decrease the number of treatments required and prevent further distress to patients due to re-treatment.

Recent advances in imaging technologies have enabled image fusion among stored computed tomography (CT), magnetic resonance imaging (MRI), US images and real-time US images on the same US monitor, called real-time image fusion (RTIF).<sup>4,5</sup> Numerous studies on RFA for HCC have shown that RTIF can help target tumors that are inconspicuous on US but detectable on CT and/or MRI. These studies reported that tumor targeting was successful (53–100%) for detecting several inconspicuous tumor cases.<sup>6–12</sup>

In this study, we hypothesized that tumor marking with an image fusion system (IFS) may be useful for assessing the positional relationship between target tumors and high echoic areas during RFA and could thereby more precisely estimate the effects of RFA on HCC. The primary aim of this study was to compare complete ablation rates in the first RFA session between patients receiving RFA with or without use of this method. The secondary aim was to compare the number of RF electrode insertions, number of RFA sessions, and local recurrence rates among patients.

## Patients and methods

### Patients

We performed a historically controlled study by prospectively enrolling patients with a single HCC who received RFA with the IFS between April 2012 and May 2016. HCC patients who received RFA without the method between October 2011 and March 2012 served as controls. We diagnosed HCC based on the results of contrast enhanced US (CEUS), dynamic CT, and dynamic MRI in combination with serum tumor markers.<sup>13</sup> For CEUS, we used perflurobutane (Sonazoid; GE Healthcare, Amersham Place, UK) as an US contrast agent.<sup>14,15</sup> We selected RFA as a curative treatment for HCC according to the Clinical Practice Guidelines for Hepatocellular Carcinoma (the J-HCC guidelines), which were the first evidence-based clinical practice guidelines for the treatment of HCC in Japan.<sup>16</sup>

This study protocol was approved by the Ethical Committee of Kanazawa Medical University (approval number 236). We obtained informed consent from all patients and performed all procedures according to the guidelines of the Helsinki Declaration.

### RFA procedure

Three experienced operators (N.T., Y.M., and N.H.) performed RFA using a cooled-tip RFA system (Covidien, Mansfield, MA, USA) in which a 480-kHz monopolar RF generator was connected to a 17-gauge, internally cooled-tip electrode with a 2- or 3-cm tip. After administration of a sedative agent, an operator percutaneously inserted the electrode into the target tumor under US guidance using an US machine (HI VISION Preirus, Hitachi Ltd., Tokyo, Japan) and a 3.5-MHz microconvex probe (EUP-B512, Hitachi Ltd.). In the event an

inconspicuous tumor was identified upon US, we performed RFA under CEUS guidance.<sup>17</sup> After the operator appropriately placed the RF electrode, assistants slowly increased the generator output to 80-120 watts and maintained this output for up to 12 minutes. If the tumor was located under the diaphragm (segment VII or VIII according to the Couinaud classification) or near the liver surface, we performed RFA using artificial ascites and/or pleural effusion to facilitate US guidance and avoid damaging the diaphragm or the parietal peritoneum.<sup>18</sup> We performed RFA following transcatheter arterial chemoembolization for tumors approximately 25-mm or more in size.<sup>19</sup>

### Estimation of the RFA effects with the IFS

To estimate the effects of RFA more precisely, we used Real-time Virtual Sonography™ (Hitachi Ltd.), which is an RTIF system consisting of an US machine (HI VISION Preirus, Hitachi Ltd.), a 3.5-MHz microconvex probe (EUP-B512, Hitachi Ltd.) equipped with a magnetic sensor, a transmitter to generate a magnetic field, and a magnetic position detection unit.<sup>5</sup> To create reference images for RTIF, we obtained and stored CEUS and dynamic CT and/or MRI images acquired prior to treatment as three-dimensional volume data in the US machine. We selected an image series that clearly depicted the target tumor and landmark structures of the hepatic parenchyma, such as intrahepatic vessels. To obtain the CEUS volume data, we performed a sweep scan with the 3.5-MHz microconvex probe after injecting Sonazoid™ (GE Healthcare) to ensure the scan covered both the target tumor and the surrounding hepatic parenchyma and then stored the scanned data.<sup>15</sup>

During RFA, a high echoic area due to RFA-induced microbubbles emerged around the position of the RF electrode tip and decreased visualization of the target tumor. Moreover, an acoustic shadow occurred behind the high echoic area, which obscured the posterior boundary line between the area and the hepatic parenchyma; however, approximately 5 minutes after RFA, this acoustic shadow had almost disappeared.

Immediately after RFA, operators retrieved the stored volume data and created reference images or planar images showing the target tumor and the surrounding hepatic parenchyma prior to treatment. We selected the data set that most clearly depicted the target tumor and landmark structures of the hepatic parenchyma. Using Real-time Virtual Sonography™ (Hitachi Ltd.), operators performed

an image fusion between the reference images and real-time US images as follows: As the first step of image fusion, operators matched the tip of the xiphoid process on reference images to the structure on real-time US images and coregistered the reference images and the real-time US images in the sagittal plane of the left hepatic lobe. Next, while scanning on or around the insertion site, operators repeated the coregistration until they achieved correct image fusion. During coregistration, operators asked patients to hold their breath. The US machine had a marking function that automatically displayed synchronized straight and spherical markers on reference images and real-time US images, respectively. Operators drew straight markers along intrahepatic vessels and ensured correct image fusion. They also drew a spherical marker along the target tumor contour on the reference images to show its maximum diameter. The size of the spherical marker was designed to change inversely with the distance between the center of the marker and the scanning section. Thus, the synchronized spherical marker was drawn on real-time US images in all directions, indicating the exact position of the tumor contour that had been poorly visualized immediately after RFA (Figure 1).

After performing image fusion and tumor marking, operators scanned the ablation area and assessed the positional relationship between the high echoic area and the spherical marker. Once the high echoic area surrounded the spherical marker in all directions with a margin of several millimeters, we considered the ablation to be complete. If the target tumor was located adjacent to vessels or near the liver surface, a partially insufficient margin at the sites was acceptable. If the ablation was deemed incomplete, operators performed additional RF electrode insertions.

### Assessment of the RFA effects

We performed dynamic CT or MRI scans 1 or 2 days after RFA. Experienced radiologists blinded to whether the patients received RFA with or without the IFS assessed the RFA effects by viewing images acquired pre-treatment and post-treatment side by side. The complete ablation criteria included that an RFA-induced avascular area surrounded the original target tumor with a margin of several millimeters.<sup>20</sup> When tumors were located adjacent to vessels or near the liver surface, partially insufficient margins at the sites were acceptable. After the radiologists assessed the RFA effects, we evaluated the assessment results. If difficulty was encoun-

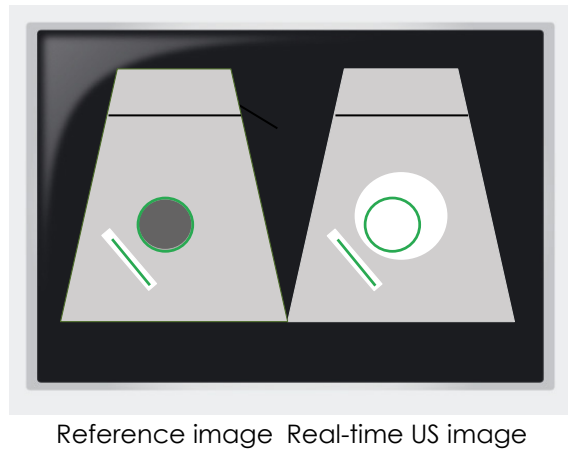


**FIGURE 1.** Schema of our IFS. An US monitor shows a reference image (left) and a real-time US image (right) immediately after RFA. Two synchronized straight markers depicted in identical positions in the same intrahepatic vessels ensure correct image fusion. On the reference image, a spherical marker (unfilled green circle) was drawn along the contour of a target tumor (filled black circle). On the real-time US image, a high echoic area (filled white circle) due to RFA-induced microbubbles completely covers the synchronized spherical marker, indicating the exact position of the tumor contour, suggesting potential complete ablation.

IFS = image fusion system; RFA = radiofrequency ablation; US = ultrasound

tered when assessing treatment completeness, we discussed the treatment effects with the radiologists. If the effects did not meet the above criteria, we performed an additional RFA.

### Surveillance after RFA

After completing RFA, patients were subjected to imaging and laboratory examinations every 3–6 months. When recurrent HCCs were detected, the patients received appropriate treatment according to the J-HCC guidelines.<sup>16</sup> HCCs detected adjacent to ablated tumors were considered local recurrence tumors.

### Statistical analysis

Data are expressed as the mean  $\pm$  standard deviation. We used Student's t-test and the Fisher's exact probability test to compare continuous variables and categorical variables, respectively. We used the Kaplan-Meier method to calculate local recurrence rates and performed log-rank tests to evaluate the rate differences. We considered a *P*-value  $< 0.05$  as significant. We performed statistical analysis using

STATA version 13.1 software (StataCorp, College Station, TX, USA).

## Results

We enrolled 25 patients who received RFA in combination with the IFS, and 20 patients who received conventional RFA as controls. The baseline characteristics were similar between the two patient groups (Table 1). We were able to use the image fusion method for all 25 patients, and retrieving the stored data, performing image fusion and tumor marking, and estimating the effects of RFA took approximately 10 minutes. The complete ablation rate during the first RFA session was significantly higher in the IFS group than in the control group (88% [22/25] vs. 60% [12/20],  $P = 0.041$ ). Incomplete ablation during the first RFA session in the IFS group was due to an insufficient margin ( $n = 3$ ),

while incomplete ablation during the first RFA session in the control group was due to an unablated residual tumor ( $n = 4$ ) and an insufficient margin ( $n = 4$ ). The number of RFA sessions was significantly smaller in the IFS group than in the control group ( $1.1 \pm 0.3$  [1,  $n = 22$ ; 2,  $n = 3$ ] vs.  $1.5 \pm 0.7$  [1,  $n = 12$ ; 2,  $n = 6$ ; 3,  $n = 2$ ],  $P = 0.016$ ), and the total number of RF electrode insertions was not significantly different between the two groups ( $2.0 \pm 0.9$  [1,  $n = 9$ ; 2,  $n = 9$ ; 3,  $n = 6$ ; 4,  $n = 1$ ] vs.  $2.3 \pm 1.5$  [1,  $n = 7$ ; 2,  $n = 5$ ; 3,  $n = 6$ ; 4,  $n = 1$ ; 7,  $n = 1$ ],  $P = 0.18$ ). There were no severe RFA-related complications in any of the patients. In this study, we presented two HCC cases in which we performed RFA using this method (Figures 2 and 3). In case 2, we considered the ablation incomplete after the first RF electrode insertion during the first RFA session. Owing to the positional information gained from the image fusion method, we could easily identify portions of the tumor requiring additional RF electrode in-

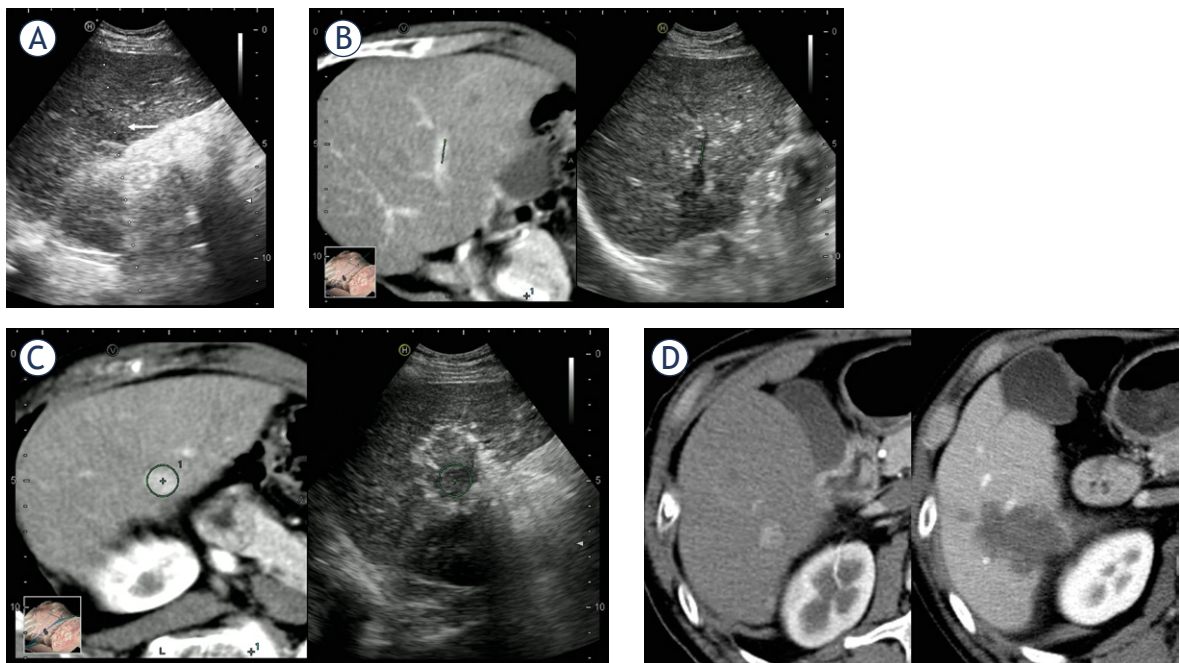


**FIGURE 2.** Case 1. A 67-year-old male patient had a 15-mm HCC in segment VI. **(A)** The HCC is depicted as a low echoic tumor (white arrow) on US. A dot-line represents a puncture line for RFA. **(B)** A reference CT image (left) and a real-time US image (right) immediately after the first RF electrode insertion in the first RFA session. In this case, reference images were created by retrieving pre-treatment arterial phase images from a dynamic CT. Two synchronized straight markers depicted at the same positions in the same portal vein branches ensured correct image fusion. **(C)** Another reference CT image depicting the tumor (right) and the corresponding real-time US image (left). On the reference image, a spherical marker was drawn along the tumor contour. On the real-time US image, the tumor is almost invisible because of a high echoic area due to RFA-induced microbubbles. However, the synchronized spherical marker indicates the exact position of the tumor contour. The high echoic area completely covers the synchronized spherical marker, thus suggesting the potential complete ablation. **(D)** Pre-treatment (left) and post-treatment (right) dynamic CT images. The pre-treatment arterial phase image depicts a hypervascular tumor, while the post-treatment portal phase image depicts an RFA-induced avascular area larger than the original tumor. These findings are suggestive of the achievement of complete ablation after the first RFA session.

CT = computed tomography; HCC = hepatocellular carcinoma; RFA = radiofrequency ablation; US = ultrasound

TABLE 1. Baseline characteristics of patients

	IFS group (n = 25)	Control group (n = 20)	P-value *
Age (years)	73 ± 8 <sup>a</sup>	74 ± 9 <sup>a</sup>	0.39
Sex, male/female	14/11	8/12	0.37
Etiology, viral/non-viral	15/10	17/3	0.10
Child-Pugh grade, A/B	22/3	16/4	0.68
Occurrence, new/recurrent	23/2	18/2	1.00
Tumor size (mm)	19 ± 6 <sup>a</sup>	19 ± 8 <sup>a</sup>	0.42
Tumor location, L/M/A/P	2/4/11/8	0/2/11/7	0.53
Tumor vascularity, hypo/hyper	3/22	1/19	0.62
Electrode tip, 2 cm/3 cm	9/16	2/18	0.08
CEUS guidance for RFA, no/yes	22/3	18/2	1.00
Artificial ascites and/or pleural effusion, no/yes	12/13	8/12	0.76
Combined with TACE, no/yes	21/4	18/2	0.68

IFS = image fusion system; L = lateral segment; M = medial segment; A = anterior segment; P = posterior segment; CEUS = contrast enhanced ultrasound; RFA = radiofrequency ablation; TACE = transcatheter arterial chemoembolization. <sup>a</sup> Data are expressed as the mean ± standard deviation. \* Student's t-tests and Fisher's exact probability tests were used for continuous variables and categorical variables, respectively.

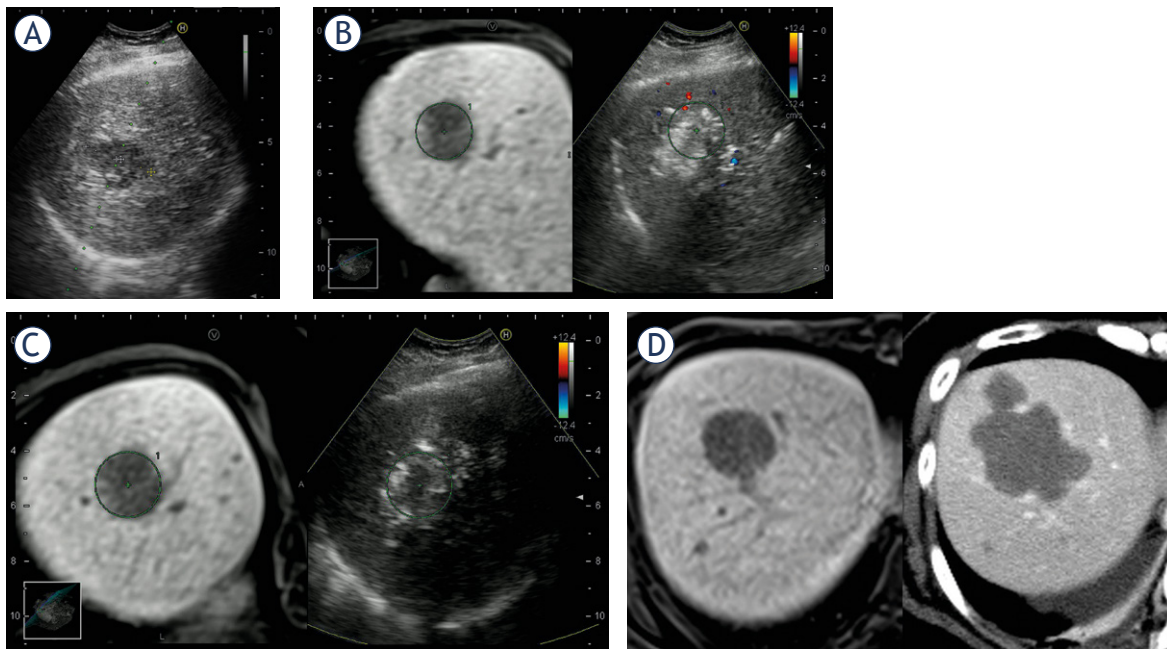


**FIGURE 3.** Case 2. A 66-year-old female patient had a 28-mm HCC in segment VIII. **(A)** The HCC is depicted as a low echoic tumor on US. A dot-line represents a puncture line for RFA. **(B)** A reference MRI image (left) and a real-time US image (right) immediately after the first RF electrode insertion in the first RFA session. In this case, reference images were created by retrieving pre-treatment hepatobiliary phase images of Gd-EOB-DTPA-enhanced MRI. On the reference image, a spherical marker was drawn along the tumor contour. Although the tumor is almost invisible on the real-time US image because of a high echoic area due to RFA-induced microbubbles, the synchronized spherical marker indicates the exact position of the tumor contour. The positional relationship between the high echoic area and the synchronized spherical marker suggests incomplete ablation. **(C)** A reference MRI image (left) and a real-time US image (right) immediately after the fourth RF electrode insertion in the first RFA session. The extent of the high echoic area due to RFA-induced microbubbles is larger than that after the first RF electrode insertion. The positional relationship between the high echoic area and the synchronized spherical marker suggests potential complete ablation. **(D)** A pre-treatment MRI image (left) and a post-treatment dynamic CT image (right). The pre-treatment hepatobiliary image depicts a hypointense tumor, while the post-treatment portal phase image depicts an RFA-induced avascular area larger than the original tumor. These findings are suggestive of the achievement of complete ablation after the first RFA session.

CT = computed tomography; Gd-EOB-DTPA = gadolinium-ethoxybenzyl-diethylenetriamine pentaacetic acid; HCC = hepatocellular carcinoma; MRI = magnetic resonance imaging; RFA = radiofrequency ablation; US = ultrasound

sertions. Thus, we performed additional ablations and completely ablated the tumor in a single RFA session.

During a mean follow-up period of 27 months (IFS group, 21 months [range 1–36 months]; control group, 34 months [range 2–63 months]), the cumulative local recurrence rates at 36 months were 8.3% in the IFS group and 12.6% in the control group, which were not significantly different ( $P = 0.98$ ).

## Discussion

The present study demonstrated that using an IFS permits precise estimation of the effects of RFA on HCC and thus aids in deciding whether to perform additional RF electrode insertions in an RFA session and identifying tumor portions requiring additional RF electrode insertions. In most cases, use of our method resulted in complete ablation in a single RFA session. Minimizing the number of treatment sessions would reduce patient distress, the risk of treatment complications and treatment costs. In an earlier study, Hiraoka *et al.* succeeded in precisely estimating the effects of RFA on HCC via an RTIF method using a workstation.<sup>21</sup> In accordance with the results of our study, Hiraoka *et al.* demonstrated that RFA using their method decreased the number of treatment sessions required. Because of recent advances in imaging modalities, clinicians can now perform RTIF on a single US machine without a workstation, which may facilitate routine use of this IFS in RFA of HCC.

Our IFS is advantageous for performing RFA for HCC. A major limitation of RFA is poor conspicuity on US. Isoechoic tumors, small tumors, and surrounding coarse, nodular liver parenchyma are reported causes of poor conspicuity.<sup>5</sup> Conventional RTIF has overcome this issue, leading to successful RFA for tumors undetectable via US.<sup>6–12</sup> High echoic areas due to RFA-induced microbubbles are another cause of poor target tumor conspicuity, which makes precise estimation of therapeutic effects difficult. Using a marking function in our IFS provides a solution to poor conspicuity during RFA, as this technology allows operators to recognize the exact position of poorly visualized target tumors in high echoic areas, thus leading to precise estimation of the effects of RFA.

We previously reported the utility of the IFS in assessing the effects of RFA on HCC.<sup>15</sup> In a previous study, we discussed the possibility of reducing the number of dynamic CT scans when assessing the effects of RFA, and several studies have pre-

sented similar results to this effect.<sup>22</sup> The results of past and present studies regarding this method will enable US to be used more frequently for diagnosing HCC, performing RFA, and assessing RFA effects, especially when US volume data can be the reference image source for image fusion. In a recent study, Minami *et al.* reported that an image fusion method using US reference images could allow precise estimation of the effects of RFA on liver metastases.<sup>23</sup> Hence, the IFS may potentially increase the efficiency of using RFA for HCC.

Our method does, however, have several limitations. First, we used spherical markers so that the markers indicated the exact positions of tumor contours that are poorly visualized on real-time US images immediately after RFA. However, tumor contours are not perfectly spherical, and discrepancy between the markers and actual tumor contours may occasionally make estimating ablation margins difficult. Indeed, there were three cases of incomplete ablation after the first RFA session in the IFS group. Second, correct image fusion may be difficult for patients who cannot hold their breath for a certain amount of time (approximately 10 seconds). Third, patients with pacemakers are not eligible for RFA with RTIF because this method uses a magnetic field. Fourth, only high-end US machines currently incorporate RTIF systems, and additional time would be required for such systems to be readily available in clinical practice.

In conclusion, our study suggested that the present method could enhance the efficiency of RFA for HCC and minimize patient burden. Further studies with a larger number of patients would confirm the benefits of RFA with the IFS for the treatment of HCC.

## Acknowledgements

We are most grateful to Mr. Makoto Mishita and Ms. Eriko Matsuoka, Hitachi Ltd., for their excellent technical support.

## References

1. Tiong L, Maddern GJ. Systematic review and meta-analysis of survival and disease recurrence after radiofrequency ablation for hepatocellular carcinoma. *Br J Surg* 2011; **98**: 1210–24. doi:10.1002/bjs.7669
2. Nouse K, Shiraga K, Uematsu S, Okamoto R, Harada R, Takayama S, et al. Prediction of the ablated area by the spread of microbubbles during radiofrequency ablation of hepatocellular carcinoma. *Liver Int* 2005; **25**: 967–72. doi:10.1111/j.1478-3231.2005.01145.x

3. Koda M, Mandai M, Matono T, Sugihara T, Nagahara T, Ueki M, et al. Assessment of the ablated area after radiofrequency ablation by the spread of bubbles: comparison with virtual sonography with magnetic navigation. *Hepatogastroenterology* 2011; **58**: 1638-42. doi:10.5754/hge08641
4. Minami Y, Kudo M. Ultrasound fusion imaging of hepatocellular carcinoma: a review of current evidence. *Dig Dis* 2014; **32**: 690-5. doi:10.1159/000368001
5. Toshikuni N, Tsutsumi M, Takuma Y, Arisawa T. Real-time image fusion for successful percutaneous radiofrequency ablation of hepatocellular carcinoma. *J Ultrasound Med* 2014; **33**: 2005-10. doi:10.7863/ultra.33.11.2005
6. Kawasoe H, Eguchi Y, Mizuta T, Yasutake T, Ozaki I, Shimonishi T, et al. Radiofrequency ablation with the real-time virtual sonography system for treating hepatocellular carcinoma difficult to detect by ultrasonography. *J Clin Biochem Nutr* 2007; **40**: 66-72. doi:10.3164/jcbn.40.66
7. Kitada T, Murakami T, Kuzushita N, Minamitani K, Nakajo K, Osuga K, et al. Effectiveness of real-time virtual sonography-guided radiofrequency ablation treatment for patients with hepatocellular carcinomas. *Hepatol Res* 2008; **38**: 565-71. doi:10.1111/j.1872-034X.2007.00308.x
8. Minami Y, Chung H, Kudo M, Kitai S, Takahashi S, Inoue T, et al. Radiofrequency ablation of hepatocellular carcinoma: value of virtual CT sonography with magnetic navigation. *AJR Am J Roentgenol* 2008; **190**: W335-41. doi:10.2214/ajr.07.3092
9. Nakai M, Sato M, Sahara S, Takasaka I, Kawai N, Minamiguchi H, et al. Radiofrequency ablation assisted by real-time virtual sonography and CT for hepatocellular carcinoma undetectable by conventional sonography. *Cardiovasc Intervent Radiol* 2009; **32**: 62-9. doi:10.1007/s00270-008-9462-x
10. Lee MW, Rhim H, Cha DI, Kim YJ, Choi D, Kim YS, et al. Percutaneous radiofrequency ablation of hepatocellular carcinoma: fusion imaging guidance for management of lesions with poor conspicuity at conventional sonography. *AJR Am J Roentgenol* 2012; **198**: 1438-44. doi:10.2214/ajr.11.7568
11. Song KD, Lee MW, Rhim H, Cha DI, Chong Y, Lim HK. Fusion imaging-guided radiofrequency ablation for hepatocellular carcinomas not visible on conventional ultrasound. *AJR Am J Roentgenol* 2013; **201**: 1141-7. doi:10.2214/ajr.13.10532
12. Ahn SJ, Lee JM, Lee DH, Lee SM, Yoon JH, Kim YJ, et al. Real-time US-CT/MR Fusion Imaging for Percutaneous Radiofrequency Ablation of Hepatocellular Carcinoma. *J Hepatol* 2016. doi:10.1016/j.jhep.2016.09.003
13. Bruix J, Sherman M, Practice Guidelines Committee, American Association for the Study of Liver Diseases. Management of hepatocellular carcinoma. *Hepatology* 2005; **42**: 1208-36. doi:10.1002/hep.20933
14. Hatanaka K, Kudo M, Minami Y, Ueda T, Tatsumi C, Kitai S, et al. Differential diagnosis of hepatic tumors: value of contrast-enhanced harmonic sonography using the newly developed contrast agent, Sonazoid. *Intervirol* 2008; **51(Suppl 1)**: 61-9. doi:10.1159/000122600
15. Toshikuni N, Shiroeda H, Ozaki K, Matsue Y, Minato T, Nomura T, et al. Advanced ultrasonography technologies to assess the effects of radiofrequency ablation on hepatocellular carcinoma. *Radiol Oncol* 2013; **47**: 224-9. doi:10.2478/raon-2013-0033
16. Kudo M, Izumi N, Kokudo N, Matsui O, Sakamoto M, Nakashima O, et al. Management of hepatocellular carcinoma in Japan: Consensus-Based Clinical Practice Guidelines proposed by the Japan Society of Hepatology (JSH) 2010 updated version. *Dig Dis* 2011; **29**: 339-64. doi:10.1159/000327577
17. Minami T, Minami Y, Chishina H, Arizumi T, Takita M, Kitai S, et al. Combination guidance of contrast-enhanced US and fusion imaging in radiofrequency ablation for hepatocellular carcinoma with poor conspicuity on contrast-enhanced US/fusion imaging. *Oncology* 2014; **87(Suppl 1)**: 55-62. doi:10.1159/000368146
18. Uehara T, Hirooka M, Ishida K, Hiraoka A, Kumagi T, Kisaka Y, et al. Percutaneous ultrasound-guided radiofrequency ablation of hepatocellular carcinoma with artificially induced pleural effusion and ascites. *J Gastroenterol* 2007; **42**: 306-11. doi:10.1007/s00535-006-1949-0
19. Takuma Y, Takabatake H, Morimoto Y, Toshikuni N, Kayahara T, Makino Y, et al. Comparison of combined transcatheter arterial chemoembolization and radiofrequency ablation with surgical resection by using propensity score matching in patients with hepatocellular carcinoma within Milan criteria. *Radiology* 2013; **269**: 927-37. doi:10.1148/radiol.13130387
20. Kim YS, Lee WJ, Rhim H, Lim HK, Choi D, Lee JY. The minimal ablative margin of radiofrequency ablation of hepatocellular carcinoma (> 2 and < 5 cm) needed to prevent local tumor progression: 3D quantitative assessment using CT image fusion. *AJR Am J Roentgenol* 2010; **195**: 758-65. doi:10.2214/AJR.09.2954
21. Hiraoka A, Hirooka M, Koizumi Y, Hidaka S, Uehara T, Ichikawa S, et al. Modified technique for determining therapeutic response to radiofrequency ablation therapy for hepatocellular carcinoma using US-volume system. *Oncol Rep* 2010; **23**: 493-7.
22. Numata K, Fukuda H, Morimoto M, Kondo M, Nozaki A, Oshima T, et al. Use of fusion imaging combining contrast-enhanced ultrasonography with a perflubutane-based contrast agent and contrast-enhanced computed tomography for the evaluation of percutaneous radiofrequency ablation of hypervascular hepatocellular carcinoma. *Eur J Radiol* 2012; **81**: 2746-53. doi:10.1016/j.ejrad.2011.11.052
23. Minami Y, Minami T, Chishina H, Kono M, Arizumi T, Takita M, et al. US-US Fusion Imaging in Radiofrequency Ablation for Liver Metastases. *Dig Dis* 2016; **34**: 687-91. doi:10.1159/000448857

# Quantitative aspects of diffusion-weighted magnetic resonance imaging in rectal cancer response to neoadjuvant therapy

Thiago Bassaneze<sup>1</sup>, José Eduardo Gonçalves<sup>1</sup>, Juliano Ferreira Faria<sup>2</sup>, Rogério Tadeu Palma<sup>1,3</sup>, Jaques Waisberg<sup>1,3</sup>

<sup>1</sup> Department of Gastrointestinal Surgery, State Public Servant Hospital of São Paulo, São Paulo, Brazil

<sup>2</sup> Department of Diagnostic Imaging, Federal University of São Paulo, São Paulo, Brazil

<sup>3</sup> Department of Gastrointestinal Surgery, ABC Medical School, Santo André, Brazil

Radiol Oncol 2017; 51(3): 270-276.

Received 6 December 2016

Accepted 1 June 2017

Correspondence to: Thiago Bassaneze, M.D., Postgraduate Program in Health Science, Department of Gastrointestinal Surgery, State Public Servant Hospital, Avenida Ibirapuera, 981, São Paulo 04029-000, São Paulo, Brazil. Phone: +55 11 4573 8251; E-mail: drthiagobassaneze@gmail.com

Disclosure: No potential conflicts of interest were disclosed.

**Background.** The aim of the study was to evaluate the added value of the apparent diffusion coefficient (ADC) of diffusion-weighted magnetic resonance imaging (DW-MRI) in patients with rectal cancer who received neoadjuvant chemoradiotherapy (CRT). The use of DW-MRI for response evaluation in rectal cancer still remains a widely investigated issue, as the accurate detection of pathologic complete response (pCR) is critical in making therapeutic decisions. **Patients and methods.** Thirty-three patients with locally advanced rectal cancer were evaluated retrospectively by MRI in addition to diffusion-weighted images (DWI) and its ADC pre- and post- neoadjuvant CRT. These patients subsequently underwent curative-intent surgery. Tumor staging by MRI and ADC value were compared with histopathological findings of the surgical specimen.

**Results.** MRI in addition to DWI had a sensitivity of 96.1%, specificity of 71.4%, positive predictive value of 92.5%, and negative predictive value of 83.3% in the detection of pCR. The pre-CRT ADC alone could not reliably predict the pCR group. Post-CRT ADC cutoff value of  $1.49 \times 10^{-3} \text{ mm}^2/\text{s}$  had the highest accuracy and allowed a 16.7% increase in negative predictive value and 3.9% increase in sensitivity. Patients with pCR to neoadjuvant treatment differed from the other groups in their absolute values of post-CRT ADC ( $p < 0.01$ ).

**Conclusions.** The use of post-CRT ADC increased the diagnostic performance of MRI in addition to DWI in predicting the final pathologic staging of rectal carcinoma.

Key words: rectal cancer; neoadjuvant therapy; diffusion MRI

## Introduction

Restaging locally advanced rectal cancer after neoadjuvant chemoradiotherapy (CRT) is critical in making therapeutic decisions based on magnetic resonance imaging (MRI). The diagnostic performance of this radiological method is reduced in the restaging of patients undergoing neoadjuvant therapy, because of the difficulty in differentiating residual tumour within radiotherapy induced fibrosis.<sup>1-3</sup>

Several publications of the last decade reported the potential use of diffusion-weighted magnetic resonance imaging (DW-MRI) through its apparent diffusion coefficient (ADC) as an additional way to clarify the radiological and biological behavior of these tumors.<sup>4</sup> This technique measures the characteristics of water diffusion in a tissue, which depends on the cell density, vascularization, extracellular viscosity, and integrity of the cell membrane. Any change in tissue components, including the ratio of protons of water molecules between the

extracellular and intracellular environment, may modify the diffusion coefficient of water.<sup>5-7</sup>

Previous studies of different tumor types have suggested that this quantitative interpretation of the ADC could be used as a reliable biomarker of response to neoadjuvant treatment.<sup>5,7-9</sup>

However, there is no consensus regarding the use of different ADC cutoff values or their eventual clinical use in daily practice in the evaluation of response to CRT in rectal cancer. Small-scale studies with varying methodologies and conflicting conclusions have contributed to the wide range of results.<sup>1-10</sup>

Given this knowledge gap, the objective of this study was to evaluate the diagnostic performance of MRI in addition to diffusion-weighted images (DWI) and measure the tumor's ADC, before and after CRT, through a pathological correlation with the surgical specimen.

## Patients and methods

### Patients

Forty-four patients were diagnosed and treated for rectal cancer in the State Public Servant Hospital of São Paulo (Brazil), from February 2010 to May 2014. This study was performed in accordance with the guidelines of the Helsinki Declaration, fulfilling all requirements for retrospective studies in humans. All the images were accessed in the hospital database, with the approval of the Ethics Committee of our institution (number 04989912.8.0000.5463). Informed consent was not obtained as patient records and information was anonymized and de-identified prior to all the analysis of this pure retrospective study.

The inclusion criteria were the following: patient with histological biopsy of rectal adenocarcinoma, completion of a full course of neoadjuvant CRT, and having undergone MRI and DW-MRI pre- and post-CRT. Thirty-eight patients met the above criteria. The exclusion criteria were the following: failure to obtain a specimen for pathological examination when the surgery was contraindicated during treatment, a history of previous pelvic irradiation, and subjects with missing data. Among 38 patients, 5 patients were excluded due to disease progression (n = 1), missing data (n = 1) and previous pelvic irradiation (n = 3). Thirty-three patients remained in the final study population, 18 males and 15 females. The median age was 59 (± 11.53) years with a range of 36–80 years. Surgery performed included low anterior resection (n = 15),

abdominoperineal resection (n = 15), and pelvic exenteration (n = 3). The clinical characteristics are summarized in Table 1.

### Neoadjuvant chemoradiation therapy

The neoadjuvant CRT regime used in all patients consisted of radiation to a total dose of 4500 cGy, divided into 5 days per week, a 28-day treatment period, and one boost of 540 cGy. This regimen was associated with the use of 5-fluorouracil at a dose of 350 mg/m<sup>2</sup>/day and folinic acid at a dose of 20 mg/m<sup>2</sup>/day, in bolus for 5 days in the first and fifth weeks of radiation therapy.

### Histopathological examination of the surgical specimens

The histopathological analyzes were performed by expert colorectal pathologists subspecialized in gastro-intestinal pathology, who had no radiographic information. Hematoxylin and eosin (H&E)-stained slides were used for microscopic analysis in all 33 subjects. The standard of reference was based on pathological staging (TNM staging system).<sup>11</sup> The histopathological parameters used

**TABLE 1.** The patients' clinical characteristics and pathologic characteristics of the tumor

	All	pCR	non-pCR
<b>Average age, years</b>	59.6 ± 11.5	58.5 ± 11.2	59.9 ± 11.8
<b>Gender*</b>			
Male	18	5	13
Female	15	2	13
<b>Clinical T stage pre-CRT (MRI classification)*</b>			
T2	3	1	2
T3	23	5	18
T4	7	1	6
<b>Average tumor distance to the anus (cm)*</b>	5.1 (± 2.2)	6.1 (± 1.3)	4.8 (± 2.3)
<b>Type of resection*</b>			
Low anterior resection	15	3	12
Abdominoperineal resection	15	4	11
Pelvic exenteration	3	0	3
<b>Histologic grade (biopsy)*</b>			
Well differentiated	6	2	4
Moderately differentiated	23	4	19
Poorly differentiated	4	1	3

\* = number of individuals; CRT = chemoradiotherapy; pCR = pathologic complete response

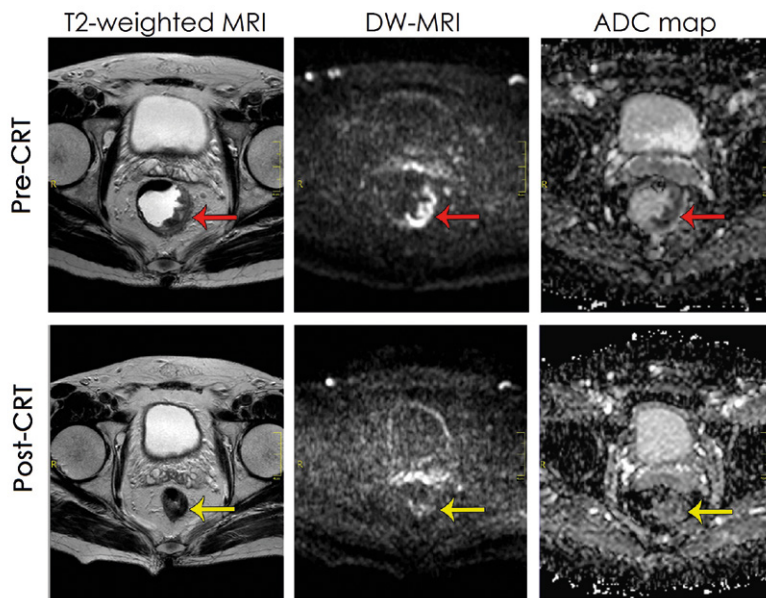


**FIGURE 1.** Sample of a T2-weighted MRI, DW-MRI (b-value 1000 s/mm<sup>2</sup>), and ADC map from a locally advanced rectal tumor. The red arrows point to different aspects of the left lateral pre-CRT tumor area. The yellow arrows point to the cancer shrinkage in the post-CRT. Pre- and post-CRT ADC values were  $0.92 \times 10^{-3}$  mm<sup>2</sup>/s and  $1.50 \times 10^{-3}$  mm<sup>2</sup>/s, with pCR in the surgical specimen.

in this study were the maximum degree of tumor penetration in the rectal wall, the circumferential and longitudinal resection margin, and the presence or absence of intramural mucin. A pathologic complete response (pCR) was defined as no viable cells present on pathological examination of the surgical specimens.<sup>11</sup>

### Imaging technique

The mean interval between pre-CRT MRI and the start of the neoadjuvant treatment was  $20 \pm 3$  days. The mean interval between the completion of CRT and post-CRT MRI for response evaluation was  $58 \pm 8.8$  days.

The MRI equipment used in the study was a 1.5 Tesla whole-body system (Achieva®/Philips Medical Systems, Best, Netherlands), with a 16-channel phased-array coil. The sequences used and their specifications were sagittal T2-weighted (T2W) MRI fast spin echo (repetition time/echo time [TR/TE]: 5030/100 ms; field of view [FOV]: 20 cm; gap: 0.5 mm; section thickness: 3 mm; matrix size: 268 x 210; axial T2W MRI fast spin echo; TR/TE: 4681/90 ms; FOV: 20 cm; gap: 0.3 mm; section thickness: 3 mm; and matrix size: 212 x 168). Axial DW-MRI were obtained using the single-shot echo planar imaging technique with the following pa-

rameters: TR/TE: 2800/70 ms; gap: 1 mm; slice thickness: 3 mm; matrix size: 104 x 100; and field of view: 20 cm. The axial sequences were obtained in the perpendicular plane to the longitudinal axis of rectal cancer. All sequences (including DW-MRI) were used for conventional MRI reading. In all MRIs the standard of reference was based on previous radiologic staging protocols and T2W images were used to help correctly identify the tumor, if that was the case.<sup>10,21</sup>

The diffusion-weighted images were acquired using four different b-values ( $b = 0, 50, 500$  and  $1000$  s/mm<sup>2</sup>). Patients did not receive antispasmodic medication or bowel preparation before MRI examinations. Two experienced researchers in pelvic MRI and DW-MRI (JFF and TB), in consensus, blinded to patients' data and surgical or pathological results, reviewed the anonymized DICOM files, using computer software (iQ-View, version 2.7, IMAGE Information Systems, London, UK).

### Image analysis

The diffusion-restricted area was characterized on one single slice, as the region with the most prominent restrictive diffusion (hyperintense signal) on DW-MRI ( $b = 1000$  s/mm<sup>2</sup>). This same region of interest (ROI) was identified and superimposed on the ADC map as a low signal area, which was reconstructed automatically by the computer software on a pixel-by-pixel basis, avoiding T2 shine-through effect. The tumors' ADC value was obtained through the calculation of the ROI, manually designed, in which the whole tumor area was depicted and delineated, excluding visible necrotic or cystic portions and distortion artifacts. For criteria of magnetic resonance complete response, the residual tumor was absent in all sequences, and the ROI included the areas of fibrosis, which was characterized by the hypointense area on T2W and no residual hyperintense signal on high b-value DW-MRI (Figure 1).

### Statistical analysis

The statistical analysis investigated the following aspects: calculation of diagnostic performance of conventional MRI and combined set of conventional MRI in addition to DWI (sensitivity, specificity, positive predictive value and negative predictive value); Hypothesis test - two-way ANOVA (Analysis of Variance) using two factors: staging (ranging from ypT0 to ypT4) and treatment status (pre- or post-CRT) with Bonferroni test post-

hoc; Student t-test for comparison after normality test; Correlation between post-CRT ADC values and final T staging with Spearman correlation; Gaussianity tests and the estimation of a Gaussian distribution of post-CRT ADC.

Statistical analyzes were performed using the t and ANOVA tests, conducted with Epi Info software (version 3.3.2, Control Diseases Center, Atlanta, GA, USA). The receiver operating characteristics (ROC) curves were used to analyze the different cutoff values, aiming at the point of highest sensitivity and specificity to the differentiation between pCR and non-pCR. The analyzes of ROC curves and the gaussianity tests were performed using SPSS for Windows (version 10, IBM SPSS, Chicago, IL, USA). Estimates of power analysis were calculated for each sample using Stata software version 8.2 (Stata, College Station, TX, USA). The study had a 95% confidence level ( $\alpha = 0.05$ ), and the value of  $p \leq 0.05$  determined the significance in all tests.

## Results

### Treatment characteristics

All patients were operated on with the total mesorectal excision technique.<sup>12</sup> The mean interval between the end of neoadjuvant CRT and surgery was  $77 \pm 9.1$  days. The longitudinal and circumferential resection margins of the specimen were free of cancer in all 33 patients. pCR occurred in 21.2% (7/33); ypT1 in 3.0% (1/33), ypT2 in 30.3% (10/33), ypT3 in 27.3% (9/33) and ypT4 in 18.2% (6/33) patients. Small amount of intramural mucin occurred in 8 (24.2%) patients, and half of these had pCR. Mesorectal fascia involvement occurred in 8 (24.2%) cases. The mean time interval between the restaging MRI and surgery was  $21 \pm 13.7$  days.

### Diagnostic performance of conventional MRI and combined set of conventional MRI in addition to DWI

For detecting the pCR group, conventional post-CRT T2W MRI had a sensitivity of 86.9% (20/23; 95% CI: 0.65 to 0.96), specificity of 50% (5/10; 95% CI: 0.20 to 0.79), positive predictive value of 80% (20/25; 95% CI: 0.58 to 0.92), and negative predictive value of 62.5% (5/8; 95% CI: 0.25 to 0.89). Post-CRT MRI in addition to DWI had a sensitivity of 96.1% (25/26; 95% CI: 0.78 to 0.99), specificity of 71.4% (5/7; 95% CI: 0.30 to 0.94), positive predictive value of 92.6% (25/27; 95% CI: 0.74 to 0.98), and negative

**TABLE 2.** Calculation of diagnostic performance of conventional T2W MRI and combined set of conventional T2W MRI in addition to DWI for the diagnosis of complete rectal cancer response to neoadjuvant therapy

	T2W	95% CI	T2W + DWI	95% CI
Sensitivity%	86.9	(0.65–0.96)	96.1	(0.78–0.99)
Specificity%	50	(0.20–0.79)	71.4	(0.30–0.94)
PPV%	80	(0.58–0.92)	92.6	(0.74–0.98)
NPV%	62.5	(0.25–0.89)	83.3	(0.36–0.99)
Accuracy%	75.7	(0.57–0.88)	81.8	(0.63–0.92)

95% CI = 95% confidence interval; DWI = diffusion-weighted imaging; T2W = T2-weighted; NPV = negative predictive value; PPV = positive predictive value

predictive value of 83.3% (5/6; 95% CI: 0.36 to 0.99). MRI in addition to DWI also increased the overall accuracy of conventional MRI from 75.7% to 81.8%. These aspects are summarized in Table 2.

### Pre-CRT ADC value

The average pre-CRT ADC value was  $1.01 \pm 0.05 \times 10^{-3} \text{ mm}^2/\text{s}$  and did not vary as a function of tumor staging found in the surgical specimen ( $p > 0.05$ ).

### Post-CRT ADC value

Post-CRT ADC values differed in each T stage group ( $p < 0.01$ ). Due to the small sample of ypT1, this comparison was impaired, and there was no statistical difference ( $p > 0.05$ ).

Analyzing the distribution of the post-CRT ADC values and its correlation with the result of the pathological examination, we found a significant statistical correlation between them (Spearman's Rho = -0.54 which indicate a moderate negative correlation; 95% confidence interval -0.75 to -0.24). The pCR ADC-median value ( $1.53 \times 10^{-3} \text{ mm}^2/\text{s}$ ) is far away from the lower ( $1.04 \times 10^{-3} \text{ mm}^2/\text{s}$ ) and upper ( $1.31 \times 10^{-3} \text{ mm}^2/\text{s}$ ) quartiles - 25th and 75th percentiles, respectively - of the non-pCR box (unpaired t test,  $p < 0.01$ ).

These quantitative aspects of the ADC and the rectal cancer pathological findings are shown in Figure 2 A, B, C.

Using the post-CRT ADC values, the ROC curve was constructed. The cutoff value of  $1.32 \times 10^{-3} \text{ mm}^2/\text{s}$  obtained a specificity of 100.0% (95% CI: 0.56 to 1.00) and sensitivity of 80.8% (95% CI: 0.60 to 0.92), with 84.8% accuracy. All patients who had pCR were allocated above this value. The cutoff value with highest accuracy (93.9%) was  $1.49 \times 10^{-3}$

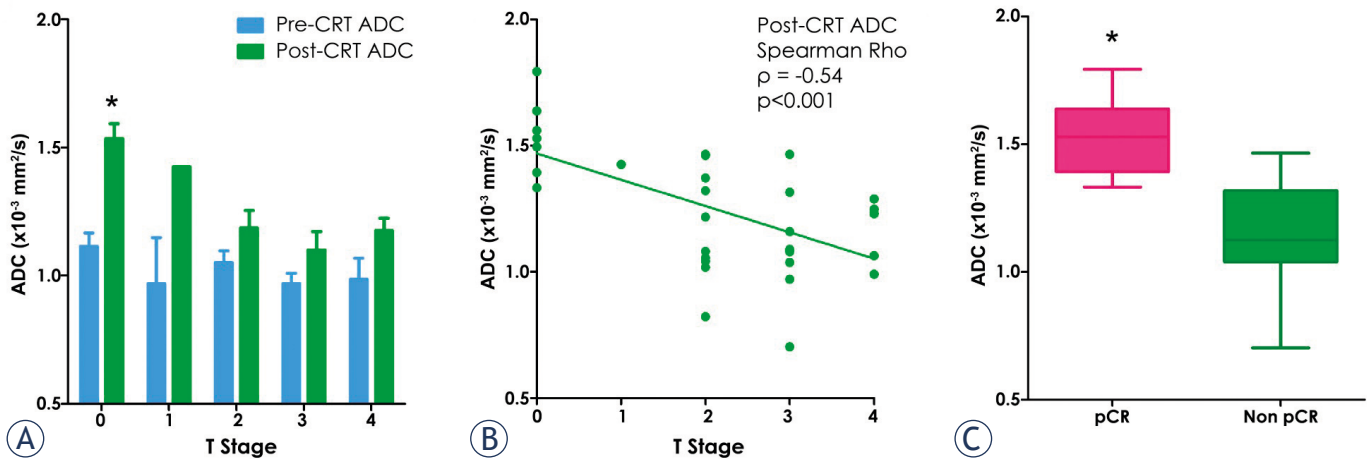


**FIGURE 2.** Correlation between ADC values and final T staging. **(A)** The pre-CRT ADC values were similar in the different groups (blue bars,  $p > 0.05$ ), although post-CRT ADC values differed in each group (green bars,  $p < 0.01$ ); statistical significance (\*). **(B)** Post-CRT ADC values with a moderate negative correlation and slope different from zero degrees (Spearman's Rho = -0.54; 95% confidence interval -0.75 to -0.24). **(C)** Box plot analysis between post-CRT ADC values and final T staging. The pCR ADC-median value ( $1.53 \times 10^{-3} \text{ mm}^2/\text{s}$ ) is far away from the lower and upper boundaries of the non-pCR box ( $p < 0.01$ ).

$3 \text{ mm}^2/\text{s}$ , with a sensitivity of 100% (95% CI: 0.83 to 1.00) and specificity of 71.4% (95% CI: 0.30 to 0.94) (Figure 3A). All patients with residual tumor in the surgical specimen were allocated below this threshold.

A histogram was created to estimate the post-CRT ADC values distribution in a following Gaussian distribution population. Its coefficient of variation (which is the ratio of the standard deviation to the mean) was 10% and 16% respectively, for non-pCR and pCR groups, both values being considered sufficient for high forecastability.

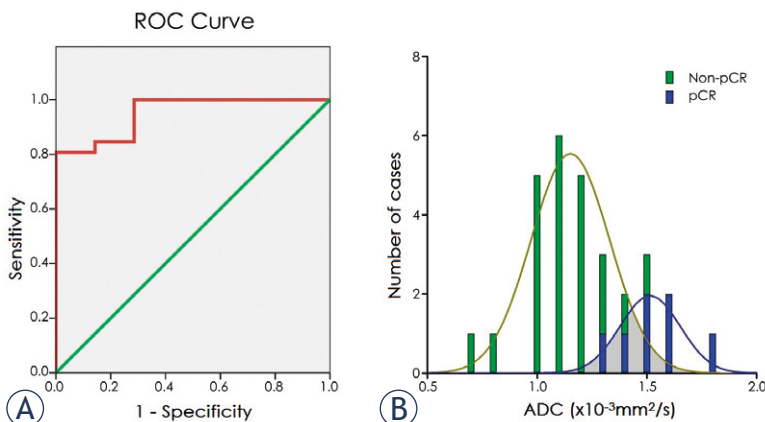


**FIGURE 3.** Receiver operating characteristic (ROC) curve and histogram in patients with rectal carcinoma with a normal distribution. **(A)** The optimal post-CRT ADC cutoff value  $1.49 \times 10^{-3} \text{ mm}^2/\text{s}$  (area under the curve = 0.95). **(B)** Histogram. The mean post-CRT ADC values of patients with pCR was  $1.53 (\pm 1.96 \times 0.15 \times 10^{-3} \text{ mm}^2/\text{s})$  and of patients with non-pCR  $1.16 (\pm 1.96 \times 0.19 \times 10^{-3} \text{ mm}^2/\text{s})$ ; the area in gray highlights the possible overlap in these values.

Figure 3B depicts the normal distribution based on the sample size of this study.

## Discussion

The growing interest in using DW-MRI through its ADC to study tumor behavior is a reality. This method is sensitive to the motion of water molecules, which vary in function in cell membranes and intracellular elements, providing potential access to the cellular architecture on a millimetric scale. Promising results have been described for breast cancer, liver metastasis, sarcoma and brain tumor.<sup>13-17</sup>

The demand for an image that allows a reliable interpretation of tumor aggressiveness and the need for a safety reevaluation of the response to neoadjuvant CRT in rectal cancer have stimulated research.<sup>1-10,18-23</sup> DW-MRI has advantages, such as the absence of the use of exogenous contrast and irradiation, it does not induce pain or cause discomfort in the patient, besides the fact that DW-MRI can be obtained relatively quickly if incorporated into routine standard MRI.<sup>24,25</sup>

This study explored quantitative aspects of the ADC in patients with rectal cancer who received CRT and it is in line with the growing use of potentially powerful imaging biomarker. This kind of radiological approach may allow a better understanding of the biological tumors cells behavior, and enable a more personalized management, in an era focused at less extensive surgeries.<sup>24</sup>

However, many challenges still exist for widespread implementation of DW-MRI to reevaluate rectal cancer after CRT. Koh *et al.*<sup>1</sup>, Lambregts *et al.*<sup>2</sup>, and Engin *et al.*<sup>3</sup> warned that because the measurements and analyzes of this radiological method are not yet standardized, the validation and reproduction of several studies is difficult due to the lack of a uniform methodology among them, thus quality assurance is placed at risk. This plurality of results was the target of a recent systematic review in which we observed a wide range of conflicting results.<sup>4</sup>

In the present study, we first retrospectively evaluated the use of conventional MRI alone and in addition to DWI in patients undergoing neoadjuvant CRT and subsequently performed surgery for rectal adenocarcinoma. We observed that adding DWI can improve the diagnostic performance of conventional MRI, increasing its sensitivity, positive and negative predictive value, specificity and accuracy. Foti *et al.*<sup>31</sup> recently published and described the same positive impact of using DWI sequences in conventional MRI reading for radiological re-assessment of rectal cancer response to CRT.

Other important focus of this study was to evaluate the diagnostic performance of ADC values pre- and post- neoadjuvant CRT to assess the response to treatment, through the correlation with histopathological parameters.

No difference was found in the distribution of pre-CRT ADC values between pCR and non-pCR groups. The possible use of pre-CRT ADC value to predict tumor response to CRT was first published by Andrzej Dzik-Jurasz *et al.*<sup>28</sup> However, this correlation is controversial, and it was not reproduced later, in 6 of 9 published papers, compiled in a recent systematic review.<sup>4</sup> Our results also suggest lack of differences for pre-CRT ADC to predict the final response to therapy. These findings are in line with those of Engin *et al.*<sup>3</sup>, Kim *et al.*<sup>5</sup>, Curvo-Semedo *et al.*<sup>6</sup>, as recently published by Blazic *et al.*<sup>29</sup>

Moreover, the analysis of post-CRT ADC values was significantly different between patients with pCR and those in which the tumor was identified in the specimen. The ypT0 group was statistically different from the other patients, corroborating the findings of Song *et al.*<sup>7</sup> Sun *et al.*<sup>8</sup> proposed that this ADC increase reflects the local necrosis and sensitivity of tumors to treatment and is greater in patients with ypT0 staging, which was also observed in this study.

The importance of post-CRT ADC values was evident by the increase in the specificity of MRI in addition to DWI in 28.6% of scans, increasing from

71.4% to 100%, considering the cutoff value of  $1.32 \times 10^{-3} \text{ mm}^2/\text{s}$ . Thus, all ypT0 patients were above this threshold. This fact has already been described by other authors.<sup>3,5,9</sup> The maximum sensitivity and diagnostic performance of post-CRT ADC values was achieved with the cutoff of  $1.49 \times 10^{-3} \text{ mm}^2/\text{s}$ , below which all subjects who had viable tumor in the surgical specimen were allocated. Other cutoff values available in the literature ranged from 1.04 to  $1.41 \times 10^{-3} \text{ mm}^2/\text{s}$ .<sup>4</sup>

The histogram obtained in this study characterized this previous phenomenon and allowed an inference from the behavior of the curves of post-CRT ADC values in a population with normal distribution. Based on the sample in this study, 95% of patients with non-pCR had post-CRT ADC values between 0.77 and  $1.54 \times 10^{-3} \text{ mm}^2/\text{s}$ .

This study has some limitations. First, this was a single center, retrospective study that had an overall small population without a validation set, which may lead inevitable bias. Second, the ADC values were obtained in a single slice ROI containing the whole visible tumor area, which may not be fully representative of the overall profile of the tumor. Variations in ROI size and positioning can affect tumor ADC measurements. However in recent previous studies single slice ROI and whole-tumor volume methods had comparable diagnostic performance levels with similar AUCs. In this context, single slice ROI can be used as a less time consuming alternative and relatively efficient approach for clinical practice, in the assessment of tumor response to CRT.<sup>29,30</sup> Third, the presence of small amount of mucin in specimen, as tumor regresses, may have changed the post-CRT ADC value, as already observed by others authors.<sup>10,26-27</sup> Fourth, because of the retrospective nature of this study, all patients had already been operated on when we analyzed the MRIs, thus it was not possible to perform the dissection and histopathological evaluation of each of the suspicious lymph nodes.

## Conclusions

This study provides quantitative aspects of the use of DW-MRI through the pre- and post-CRT ADC values. Our data support the fact that post-CRT ADC values increased the overall diagnostic performance of MRI in addition to DWI. In the future, larger studies may separate these populations with greater precision, revealing and making clear the area of interception between the pCR and non-pCR groups.

## References

- Koh DM, Collins DJ. Diffusion-weighted MRI in the body: applications and challenges in oncology. *Am J Roentgenol* 2007; **188**: 1622-35. doi:10.2214/AJR.06.1403
- Lambrechts DM, Beets GL, Maas M, Curvo-Semedo L, Kessels AG, Thywissen T, et al. Tumour ADC measurements in rectal cancer: effect of ROI methods on ADC values and interobserver variability. *Eur Radiol* 2011; **21**: 2567-74. doi:10.1007/s00330-011-2220-5
- Engin G, Sharifov R, Güral Z, Sağlam EK, Sağlam S, Balık E, et al. Can diffusion-weighted MRI determine complete responders after neoadjuvant chemoradiation for locally advanced rectal cancer? *Diagn Interv Radiol* 2012; **18**: 574-81. doi:10.4261/1305-3825.DIR.5755-12.1
- Joye I, Deroose MC, Vandecaveye V, Haustermans K. The role of diffusion-weighted MRI and 18F-FDG PET/CT in the prediction of pathologic complete response after radiochemotherapy for rectal cancer: a systematic review. *Radiother Oncol* 2014; **113**: 158-65. doi:10.1016/j.radonc.2014.11.026
- Kim SH, Lee JY, Lee JM, Han JK, Choi BI. Apparent diffusion coefficient for evaluating tumour response to neoadjuvant chemoradiation therapy for locally advanced rectal cancer. *Eur Radiol* 2011; **21**: 987-95. doi:10.1007/s00330-010-1989-y
- Curvo-Semedo L, Lambrechts DM, Maas M, Thywissen T, Mehsen RT, Lammering G, et al. Rectal cancer: assessment of complete response to preoperative combined radiation therapy with chemotherapy—conventional MR volumetry versus diffusion-weighted MR imaging. *Radiology* 2011; **260**: 734-43. doi:10.1148/radiol.11102467
- Song I, Kim SH, Lee SJ, Choi JY, Kim MJ, Rhim H. Value of diffusion-weighted imaging in the detection of viable tumour after neoadjuvant chemoradiation therapy in patients with locally advanced rectal cancer: comparison with T2-weighted and PET/CT imaging. *Br J Radiol* 2012; **85**: 577-86. doi:10.1259/bjr/68424021
- Sun YS, Zhang XP, Tang L, Ji JF, Gu J, Cai Y, et al. Locally advanced rectal carcinoma treated with preoperative chemotherapy and radiation therapy: preliminary analysis of diffusion-weighted MR imaging for early detection of tumor histopathologic downstaging. *Radiology* 2010; **254**: 170-8. doi:10.1148/radiol.2541082230
- Lambrechts DM, Vandecaveye V, Barbaro B, Bakers FC, Lambrecht M, Maas M, et al. Diffusion-weighted MRI for selection of complete responders after chemoradiation for locally advanced rectal cancer: a multicenter study. *Ann Surg Oncol* 2011; **18**: 2224-31. doi:10.1245/s10434-011-1607-5
- Jang KM, Kim SH, Choi D, Lee SJ, Park MJ, Min K. Pathological correlation with diffusion-weighted MRI on diffusion weighted imaging in patients with pathological complete response after neoadjuvant chemoradiation therapy for locally advanced rectal cancer: preliminary results. *Br J Radiol* 2012; **85**: 566-572. doi:10.1259/bjr/24557556
- Edge SB, Byrd DR, Compton CC, Fritz AG, Greene FL, Trotti A. *AJCC Cancer Staging Manual*. New York: Springer; 2010. p. 143-464.
- Lin HH, Lin JK, Lin CC, Lan YT, Wang HS, Yang SH, et al. Circumferential margin plays an independent impact on the outcome of rectal cancer patients receiving curative total mesorectal excision. *Am J Surg* 2013; **206**: 771-7. doi:10.1016/j.amjsurg.2013.03.009
- Theilmann RJ, Borders R, Trouard TP, Xia G, Outwater E, Ranger-Moore J, et al. Changes in water mobility measured by diffusion MRI predict response of metastatic breast cancer to chemotherapy. *Neoplasia* 2004; **6**: 831-37. doi:10.1593/neo.03343
- Kamel IR, Reyes DK, Liapi E, Bluemke DA, Geschwind JF. Functional MR imaging assessment of tumor response after 90Y microsphere treatment in patients with unresectable hepatocellular carcinoma. *J Vasc Interv Radiol* 2007; **18**: 49-56. doi:10.1016/j.jvir.2006.10.005
- Uhl M, Saueressig U, van Buijen M, Kontny U, Niemeyer C, Köhler G, et al. Osteosarcoma: preliminary results of in vivo assessment of tumor necrosis after chemotherapy with diffusion- and perfusion weighted magnetic resonance imaging. *Invest Radiol* 2006; **41**: 618-23. doi:10.1097/01.rli.0000225398.17315.68
- Mardor Y, Pfeffer R, Spiegelmann R, Roth Y, Maier SE, Nissim O, et al. Early detection of response to radiation therapy in patients with brain malignancies using conventional and high b-value diffusion-weighted magnetic resonance imaging. *J Clin Oncol* 2003; **21**: 1094-100. doi:10.1200/JCO.2003.05.069
- Yankeelov TE, Lepage M, Chakravarthy A, Broome EE, Niernmann KJ, Kelley MC, et al. Integration of quantitative DCE-MRI and ADC mapping to monitor treatment response in human breast cancer: initial results. *Magn Reson Imaging* 2007; **25**: 1-13. doi:10.1016/j.mri.2006.09.006
- Kim SH, Lee JM, Hong SH, Kim GH, Lee JY, Han JK, et al. Locally advanced rectal cancer: added value of diffusion-weighted MR imaging in the evaluation of tumor response to neoadjuvant chemo- and radiation therapy. *Radiology* 2009; **253**: 116-25. doi:10.1148/radiol.2532090027
- Habr-Gama A, Gama-Rodrigues J, Perez RO. Is tailoring treatment of rectal cancer the only true benefit of long-course neoadjuvant chemoradiation? *Dis Colon Rectum* 2013; **56**: 264-66. doi:10.1097/DCR.0b013e318277e8e4
- DeVries AF, Kremser C, Hein PA, Griebel J, Krezcy A, Ofner D, et al. Tumor microcirculation and diffusion predict therapy outcome for primary rectal carcinoma. *Int J Radiat Oncol Biol Phys* 2003; **56**: 958-65. doi:10.1016/S0360-3016(03)00208-6
- Taylor FG, Swift RI, Blomqvist L, Brown G. A systematic approach to the interpretation of preoperative staging MRI for rectal cancer. *Am J Roentgenol* 2008; **191**: 1827-35. doi:10.2214/AJR.08.1004
- Torkzad MR, Suzuki C, Tanaka S, Palmer G, Holm T, Blomqvist L. Morphological assessment of the interface between tumor and neighboring tissues, by magnetic resonance imaging, before and after radiotherapy in patients with locally advanced rectal cancer. *Acta Radiol* 2008; **49**: 1099-103. doi:10.1080/02841850802477916
- Dresen RC, Beets GL, Rutten HJ, Engelen SM, Lahaye MJ, Vliegen RF, et al. Locally advanced rectal cancer: MR imaging for restaging after neoadjuvant radiation therapy with concomitant chemotherapy. Part I. Are we able to predict tumor confined to the rectal wall? *Radiology* 2009; **252**: 71-80. doi:10.1148/radiol.2521081200
- Padhani AR, Liu G, Koh DM, Chenevert TL, Thoeny HC, Takahara T, et al. Diffusion-weighted magnetic resonance imaging as a cancer biomarker: consensus and recommendations. *Neoplasia* 2009; **11**: 102-25. doi:10.1593/neo.81328
- Yang E, Nucifora PG, Melhem ER. Diffusion MR imaging: basic principles. *Neuroimaging Clin N Am* 2011; **21**: 1-25. doi:10.1016/j.nic.2011.02.001
- Allen SD, Padhani AR, Dzik-Jurasz AS, Glynn-Jones R. Rectal carcinoma: MRI with histologic correlation before and after chemoradiation therapy. *Am J Roentgenol* 2007; **188**: 442-51. doi:10.2214/AJR.05.1967
- Smith KD, Tan D, Das P, Chang GJ, Kattepogu K, Feig BW, et al. Clinical significance of acellular mucin in rectal adenocarcinoma patients with a pathologic complete response to preoperative chemoradiation. *Ann Surg* 2010; **251**: 261-4. doi:10.1097/SLA.0b013e3181bdfc27
- Dzik-Jurasz A, Domenig C, George M, Wolber J, Padhani A, Brown G, et al. Diffusion MRI for prediction of response of rectal cancer to chemoradiation. *Lancet* 2002; **360**: 307-8. doi:10.1016/S0140-6736(02)09520-X
- Blazic IM, Lilić GB, Gajic MM. Quantitative assessment of rectal cancer response to neoadjuvant combined chemotherapy and radiation therapy: comparison of three methods of positioning region of interest for ADC measurements at diffusion-weighted MR imaging. *Radiology* 2017; **282**: 418-28. doi:10.1148/radiol.2016151908
- Lambrechts DM, Beets GL, Maas M, Curvo-Semedo L, Kessels AG, Thywissen T, et al. Tumour ADC measurements in rectal cancer: effect of ROI methods on ADC values and interobserver variability. *Eur Radiol* 2011; **21**: 2567-74. doi:10.1007/s00330-011-2220-5
- Foti PV, Privitera G, Piana S, Palmucci S, Spatola C, Bevilacqua R, et al. Locally advanced rectal cancer: Qualitative and quantitative evaluation of diffusion-weighted MR imaging in the response assessment after neoadjuvant chemo-radiotherapy. *Eur J Radiol* 2016; **3**: 145-52. doi:10.1016/j.ejro.2016.06.003

# Dynamic susceptibility contrast enhanced (DSC) MRI perfusion and plasma cytokine levels in patients after tonic-clonic seizures

Tatjana Filipovic<sup>1</sup>, Katarina Surlan Popovic<sup>2</sup>, Alojz Ihan<sup>3</sup>, David Bozidar Vodusek<sup>1</sup>

<sup>1</sup> Division of Neurology, University Medical Centre Ljubljana, Ljubljana, Slovenia

<sup>2</sup> Institute of Radiology, University Medical Centre Ljubljana, Ljubljana, Slovenia

<sup>3</sup> Institute of Immunology, Medical School, University of Ljubljana, Ljubljana, Slovenia

Radiol Oncol 2017; 51(3): 277-285.

Received 17 April 2017

Accepted 14 June 2017

Correspondence to: Filipović Tatjana, M.D., Division of Neurology, University Medical Centre Ljubljana, Zaloška cesta 7a, SI-1000 Ljubljana, Slovenia. Phone: +386 5 223 195; E-mail: tatjana.filipovic@kclj.si

Disclosure: No potential conflicts of interest were disclosed.

**Background.** Inflammatory events in brain parenchyma and glial tissue are involved in epileptogenesis. Blood concentration of cytokines is shown to be elevated after tonic-clonic seizures. As a result of inflammation, blood-brain barrier leakage occurs. This can be documented by imaging techniques, such is dynamic susceptibility contrast enhanced (DSC) MRI perfusion. Our aim was to check for postictal brain inflammation by studying DSC MRI perfusion and plasma level of cytokines. We looked for correlations between number and type of introducing seizures, postictal plasma level of cytokines and parameters of DSC MRI perfusion. Furthermore, we looked for correlation of those parameters and course of the disease over one year follow up.

**Patients and methods.** We prospectively enrolled 30 patients, 8–24 hours after single or repeated tonic-clonic seizures.

**Results.** 25 of them had normal perfusion parameters, while 5 had hyperperfusion. Patients with hyperperfusion were tested again, 3 months later. Two of 5 had hyperperfusion also on control measurements. Number of index seizures negatively correlated with concentration of proinflammatory cytokines IL-10, IFN- $\gamma$  and TNF- $\alpha$  in a whole cohort. In patients with hyperperfusion, there were significantly lower concentrations of antiinflammatory cytokine IL-4 and higher concentrations of proinflammatory TNF- $\alpha$ .

**Conclusions.** Long lasting blood- brain barrier disruption may be crucial for epileptogenesis in selected patients.

Key words: seizure; blood-brain barrier; cytokines; DSC MRI

## Introduction

Epilepsy is a chronic disorder characterized by the recurrence of unprovoked seizures. The consequences of epilepsy are not only neurobiological but also cognitive, physiological and social.<sup>1</sup> Epilepsy affects roughly 50 million people worldwide.<sup>2</sup> One third of all affected persons suffer from intractable seizures. With the exception of surgical resection, in most instances treatment is only symptomatic.<sup>3</sup>

A single seizure is not yet epilepsy; it may be a symptom of infection, trauma, stroke, metabolic derangements etc., and may never repeat.<sup>4</sup>

The crucial process leading to repeated seizures is epileptogenesis; a process from initial brain damage to the first seizure and beyond, consisting of a sequence of chemical and structural alterations resulting in transformation of normal to epileptogenic brain tissue. Epileptogenesis may last years.<sup>5</sup> The initial event can be a seizure per se.<sup>6,7</sup>

Indices of inflammation in epilepsy have been repeatedly demonstrated but there is no clear answer as to whether inflammation is the cause or a consequence of the disease.<sup>8,9</sup> There is evidence that a single seizure promotes a surge of cytokine production in brain tissue.<sup>10,11</sup> Repeated seizures

tend to be accompanied by a higher level of brain cytokine production.<sup>12</sup> Elevated peripheral blood levels of cytokines, mostly interleukin-6 (IL-6) and antagonist of IL-1 Receptor (IL-1Ra) have been reported after secondarily generalized<sup>13</sup> and focal epileptic seizures.<sup>14,15</sup> Blood perfusion changes have so far been extensively studied in patients with acute ischemic stroke<sup>16,17</sup>, and there have also been studies in patients with epilepsy.<sup>18,19</sup> In animal studies, early brain perfusion changes after status epilepticus have been suggested to be of prognostic value in relation to future hippocampal shrinkage and degeneration.<sup>20,21</sup> Vascular perfusion changes were not localized but spread throughout wide brain areas; in a model of prolonged focal seizures, the effect was explained by diffuse changes in neurovascular coupling.<sup>22,23</sup> Changes in cerebral blood perfusion related to seizures have also been attributed to higher metabolic demand<sup>24</sup> and leucocyte-endothelial interaction.<sup>25</sup> In humans, assessment of perfusion changes after a single seizure<sup>26</sup> or status epilepticus<sup>27</sup> has been reported to be helpful in localizing the epileptic focus.

It was our aim to check for postictal brain inflammation indices by studying MR perfusion and blood cytokines, and to determine whether the type and number of index seizures, postictal blood concentrations of cytokines and parameters of MR perfusion are predictive for the seizure burden over a one year follow-up.

## Patients and methods

### Patients

We *prospectively* enrolled 30 patients presenting in the Emergency Service of the Division of Neurology, University Medical Centre Ljubljana, Slovenia after one or multiple seizures, from 1. 6. 2011 to 31. 12. 2014.

*Inclusion criteria were:* one or more witnessed seizures in the last 24 hours, age 18–65 years, informed written consent for study enrolment and informed written consent for the contrast MRI examination. *Exclusion criteria were:* brain injury, haemorrhage or stroke in the last 6 months, primary or secondary brain tumour any time in the past, known autoimmune disease or any immune modifying therapy in the last 6 months, pregnancy or lactation, alcohol or drug abuse, liver or kidney failure, clinical signs of infection or CRP > 20 (mg/l) and inability to obtain informed written consent (dementia, mental retardation, altered consciousness, psychosis).

The study was approved by the National Medical Ethics Committee.

### Study protocol

Written consent was signed; a full history was recorded, including smoking status. Patients were given an Epilepsy Diary with instructions for its use. A minimum 8 and maximum 24 hours after the last seizure, 2 ml of venous blood in EDTA buffer were taken and transported for immediate processing. C-reactive protein (CRP) was checked on a Point of Care device. Brain MRI with contrast was performed. Routine 32-channel EEG with scalp electrodes was recorded. Patients with reported »hyperperfusion« after visual MRI analysis were invited for a control blood and MRI examination after three months. One year after the index event, patients were contacted by phone and relevant information about disease activity was collected.

Individual researchers (clinicians, immunologist and radiologist) were unaware of the results of investigations performed by other researchers in the course of the study.

### Assessment of clinical and EEG data

The severity of the disease in the year prior to the study was assessed by the National Hospital Seizure Severity (NHS) 3 score<sup>28</sup>; if two types of seizures were reported, the »lesser« one (including aura) being chosen first. The frequency of seizures in the year prior to the study was defined as: 1. Rare (R) < 1 seizure per year, 2. Often (O) > 1 seizure per year and 3. Very often (V) > 1 seizure per month.

EEG findings were categorized as: 1. Normal, 2. Focal changes (location included), 3. Generalized changes and 4. Nonspecific abnormalities. Syndromological classification was performed based on International League Against Epilepsy (ILAE) criteria.<sup>1,29</sup> The category »probable focal symptomatic« was used if the semiology of the seizures strongly suggested focal onset (*e.g.*, »déjà vu«, head turn) in the presence of generalized or unspecific EEG changes. Generalized changes were categorized either as IGE (*e.g.* multiple spikes/waves) or nonspecific generalized (*e.g.* short generalized delta/theta rhythm).

### Immunological methods

The concentrations of interleukins: 4 (IL-4), 6 (IL-6), 10 (IL-10) and 12 (IL-12), antagonist of IL-1 receptor (IL-1Ra), tumour necrosis factor- $\alpha$  (TNF- $\alpha$ ) and

interferon  $\gamma$  (IFN- $\gamma$ ) were measured. The concentration of high sensitivity CRP was used additionally to rule out acute infections and autoimmune disorders.

Two ml of blood were taken in a test tube recoated with ethylenediaminetetraacetic acid (EDTA), immediately centrifuged and stored until processing at  $-20^{\circ}\text{C}$ . A chemoluminescent immunometry assay based on tagged monoclonal antibodies was performed. In brief, the system adds serum and reagent (cytokine specific antibody conjugated with alkaline phosphatase) into a test tube containing the carrier covered with cytokine specific antibody. The whole sample is then incubated until complex *cytokine specific antibody-cytokine-alkaline phosphatase conjugated cytokine specific antibody* is formed. The sample is then rinsed (to remove the non-bound reagent) and the luminogenous substrate is added. Alkaline phosphatase bound via cytokine to a carrier splits the substrate into an unstable luminescent intermediary. The level of luminescence corresponds to the serum level of cytokine. The test was performed using the commercial Immulite 1000 and Immulite 2000 XPI systems (Siemens, Germany; detailed description available in: N CEL 19 and N CEL-18 Siemens Manual). Controls were performed with the commercial IMMULITE Cytokine Control Module (Siemens). The concentration of cytokine is calculated by a calibration curve generated by the manufacturer for each lot of reagents and saved at the bar code of the test kit. Reference values are given by the manufacturer for each cytokine and soluble receptor.

## MRI Methods

All MRI images were obtained on a 1.5T MRI scanner (Philips Achieva Nova, Netherlands). Morphological brain studies were obtained using the following sequence protocol: T1 weighted spin echo (SE), T2 weighted fast field echo (FFE) and diffusion weighted imaging (DWI) in transversal plane; fluid attenuated inversion recovery (FLAIR), T1 weighted inversion recovery (IR) echoplanar imaging (EPI) and T2 weighted fast spin echo (FSE) in coronal and transversal planes; T1 weighted three dimensional (3D) in sagittal plane. MR perfusion was performed by fast field echo (FFE) echo planar imaging (EPI) sequence.

Each subject obtained a 16 G cubital *i.v.* line. Gadolinium-based contrast agent (Gadovist; Bayer HealthCare Pharmaceuticals, Germany) was used in the standard dose (0.1 mmol/kg), with flow ve-

locity 4 ml/s. At the end of the contrast bolus, 20 ml of normal saline with the same flow was given. Contrast agent and normal saline were given by automatic injector. First-pass dynamic susceptibility-weighted contrast-enhanced perfusion-weighted imaging (DSC-MRI) was then performed. DSC-MRI was done using the planar echo 3D method: the signal from the whole k-plane was acquired after a single  $90^{\circ}$  radiofrequency pulse in order to reach maximum study speed. Data acquisition was done before, during and after contrast bolus (20 slices with 5 mm thickness, matrix size  $128 \times 128$  and size of examined field 224 mm). The repetition time (TR) was 1501 ms, the acquisition time for each dynamic volume was 1.6 s. The echo time (TE) was 40 ms, flip angle  $75^{\circ}$ . Each perfusion sequence consisted of 40 dynamic images, lasting 66 s for each first-pass.

First, two experienced neuroradiologists independently visually interpreted the morphological MRI sequences and then the functional colour maps of perfusion parameters. An automatic deconvolution program (Neuro T2\* perfusion package, Philips Achieva Nova, Netherlands), which is a part of the MRI scanner software, was used. The program automatically calculated the perfusion parameters: negative integral, *i.e.*, blood volume (BV), mean transit time (MTT), time to peak (TTP) and an index representing blood flow (BF). The deconvolution method is based on a predetermined arterial input function (AIF). AIF was set on the medial cerebral artery (MCA) at the side of the brain with larger diameter and more prominent flat course. According to methods previously described<sup>30, 31</sup>, we manually chose and marked two regions of grey matter with either higher blood flow or higher blood volume, so called regions of interest (ROIs), and calculated the relative values of perfusion parameters.

## Statistical methods

The commercially available SPSS version 21.0 program was used. All values are given as absolute (N) and percentage (%). Mean values are expressed as median (Me) and/or mean (M) with standard deviation (SD). The normality of the data was tested by Kolmogorov-Smirnov and Shapiro-Wilk tests. Since most of the data was not normally distributed, nonparametric statistical methods were used. Correlation was tested with Pearson's correlation and Eta coefficient. For group comparison, the Wilcoxon, Kruskal-Wallis, Chi-square and Mann-Whitney U tests were used.

## Results

Demographical and clinical data are summarized in Table 1, EEG and syndrome data in Table 2.

In four patients (13.3%) the index seizure was their first seizure; patient 3 had only had one seizure in the past.

None of the 30 patients had hypoperfusion on MRI, 25 had normal MRI perfusion parameters (»normoperfusion« patients); five (17%) (Patients 2, 3, 7, 15 and 25) had hyperperfusion (»hyperperfusion« patients) (Figure 1). All »hyperperfusion« patients had normal structural MRI; 9 of the remaining 25 patients with normal perfusion parameters had structural abnormalities. Two had more diffuse structural abnormalities: patient 1 had leucopathy, patient 28 had cerebellar atrophy. Patient 5 had had resection of the right frontal lobe in childhood; patient 26 had an aneurysm of the left medial cerebral artery. We did not find associations between structural MRI abnormalities and

either postictal cytokine level or MRI perfusion parameters. Patients 7 and 15 also had hyperperfusion also on the control MRI examination after three months (»control hyperperfusion«). During this period, both patients were seizure free (*i.e.*, the date of the last seizure was the date of enrolling in the study).

MRI parameters after index seizure(s) are shown in Table 3.

Blood samples were drawn 8 hours after the last seizure in most patients, except in patient 1 (24 h), patient 9 (13 h), patient 14 (15 h) and patient 16 (20 h). The blood sample of patient 3 was accidentally lost.

The tested cytokines, including concentrations of IL-6, showed marked variability.

Cytokine levels after the index seizure(s) are summarized in Table 4. Median concentrations of cytokines in the three subgroups of patients (»normoperfusion«, »hyperperfusion«, and »control hyperperfusion«) are provided in Table 5.

Postictal (1<sup>st</sup>) and control levels of cytokines in patients with hyperperfusion after the index seizure(s) are summarized in Table 6. The number of index seizures significantly negatively correlated with concentrations of IL-10, IFN- $\gamma$  and TNF- $\alpha$  (Table 7).

There was a significant correlation among concentrations of the following cytokines: IL-6 and IL-12 ( $\rho = 0.37$ ,  $p < 0.05$ ); TNF- $\alpha$  and hsCRP ( $\rho = 0.71$ ,  $p < 0.01$ ); TNF- $\alpha$  and IL-1Ra ( $\rho = 0.51$ ,  $p < 0.01$ ), and IL-1Ra and IFN- $\gamma$  ( $\rho = 0.39$ ,  $p < 0.05$ ).

Taking into account the whole cohort of patients, cytokine concentrations did not correlate with postictal MRI perfusion parameters. Postictal MRI perfusion parameters were furthermore not correlated with any other tested variable (age, gender, smoking status, number of index seizures, antiepileptic drug, epileptic syndrome, EEG, structural MRI or seizure frequency in the previous year).

Analysis was then performed for the two subgroups of patients - »normoperfusion« (25 patients), and »hyperperfusion« (5 patients). There were a slightly higher proportion of smokers in the »hyperperfusion« group: (60% *vs.* 40% in the »normoperfusion« group). The percentage of idiopathic generalized epilepsy was identical between the two groups (20%). Overall, 12 patients had focal EEG abnormalities but there was only one of these in the »hyperperfusion« group (left temporal changes).

In the »hyperperfusion« group, concentrations of most of the cytokines were lower but the difference reached significance only for IL-4 ( $Z = -1.98$ ;

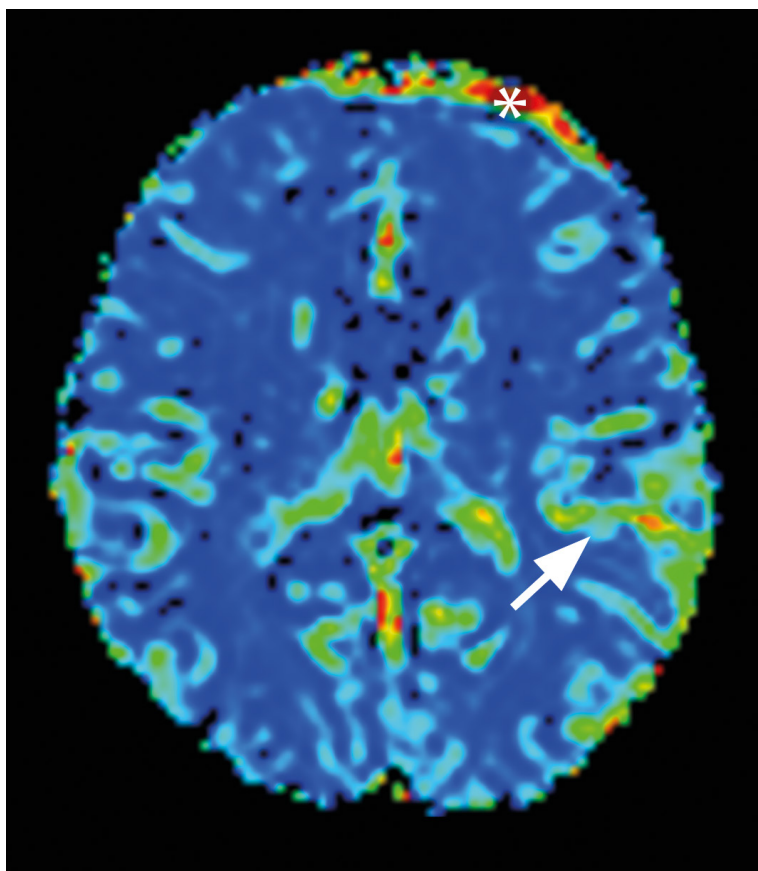


FIGURE 1: increased blood flow (arrow) in the region of the left medial cerebral artery; signal changes adjacent to left frontal bone (asterisk) are the artefact (patient 15)

TABLE 1. Demographical and clinical data

	Sex age,	Smoking status	Illness Duration (yr)	syndrome	EEG	FREQUENCY	N-INDEX	AED	TYPE /NHS3	Structural MRI	Follow up
1	F 65	/	7	PFS	G	V	4	LAM, LEV	2(5/10)	Leucopathy	0
2	F 38	5	7	PFS	G	R	1	LEV*	2 (2/10)	N	0
3	M 26	/	3	/	N	R	1	LEV*	2(2/12)	N	0
4	F 65	/	/	/	G	1 <sup>ST</sup>	1	/	1(11)	N	0
5	F 23	/	15	FS	F (RF)	V	1	TPM, LAM, DPH	2 (2/12)	Resection RF	>100
6	M 35	/	20	FS	F (RF)	R	1	LAM	2(2/10)	N	0
7	M 42	/	1	FS	F(RT)	1 <sup>ST</sup>	1	LEV*	1(18)	N	5
8	F 20	10	7	IGE	G	O	1	VA	2(2/13)	N	0
9	F 24	/	1	/	N	2 <sup>nd</sup>	1	/	1(12)	N	0
10	M 21	20	6	PFS	N	O	1	LEV*	1(13)	N	0
11	M 29	/	12	IGE	G	O	1	VA	2(2/14)	N	0
12	M 46	/	/	FS	F(LT)	1 <sup>ST</sup>	1	LEV* PREG**	1(13)	Encephalomalacy LT	0
13	F 57	/	/	/	F(RF)	1 <sup>ST</sup>	1	/			
14	M 27	/	7	FS	F(LT)	R	1	LEV*	1(18)	N	6
15	F 54	/	8	PFS	N	O	1	LEV	1 (11)	N	0
16	M 44	10	5	FS	F(LF)	O	3	LAM	1(12)	N	0
17	F 45	/	20	PFS	N	R	1	LAM	1(15)	N	0
18	M 30	10	12	FS	F(RF)	O	1	LAM	1(18)	Gliosis RF	5
19	M 63	/	4	FS	F(RT)	O	5	LEV	2(2/18)	MTS R	12
20	M 40	/	20	FS	F(RT)	O	1	CBZ	2(2/15)	N	12
21	M 41	/	20	FS	F(LT)	V	5	CBZ,VA	1(10)	N	50
22	M 23	/	8	IGE	G	V	3	LAM	1(18)	N	47
23	F 29	/	11	FS	F(RT)	V	2	TPM,LAM	1(20)	Cortical. Dysplasia RT	5
24	M 27	/	12	IGE	G	O	7	VA*	1(9)	N	2
25	M 21	10	6	IGE	G	O	6	VA	2(2/8)	N	0
26	F 50	20	34	FS	F(LT)	R	1	/	1(8)	Aneurysm L MCA	0
27	F 43	/	25	PFS	N	V	3	LAM	1(11)	Gliosis RF	0
28	M 50	/	40	IGE	G	V	1	LAM,LEV	1(19)	Cerebellar atrophy	18
29	M 39	/	32	/	G	R	1	/	1(8)	N	0
30	M 19	10	5	/	G	R	1	CBZ*	1(9)	N	0

AED = antiepileptic drugs; CBZ = carbamazepine; DPH = diphenylhydantoin; F = female; Follow up = seizure burden in one year after study inclusion; F = frontal; FS = focal symptomatic; G = generalized; IGE = idiopathic generalized epilepsy; L = left; LAM = lamotrigine; LEV = levetiracetam; M = male; MCA = middle cerebral artery; N = index; number of index seizures; NHS3 score = National Hospital Seizure Severity 3 score; N = normal; O = often (1/month); PFS = probable focal symptomatic; PREG = pregabalin; R = right, R = rare(1/year); Type/NHS3 = number of types/National Hospital Seizure Severity 3 score; T = temporal; TPM = topiramate; V = very often (> 1/month); VA = valproate

$p < 0.05$ ); concentrations of TNF- $\alpha$  were higher ( $Z = -2, 18$ ;  $p < 0.05$ ) and also hsCRP but the latter did not reach significance.

Patients 7 and 15 («control hyperperfusion») had the highest median concentrations of IL-6, IL-12, TNF- $\alpha$ , IFN- $\gamma$ , IL-1Ra and hsCRP among the three groups («normoperfusion», «hyperperfu-

sion», «control hyperperfusion»). Conversely, their concentration of IL-10 was the lowest among the three groups. These differences, however, did not reach statistical significance (Table 6).

The number of seizures during the follow up year correlated significantly only with the number of antiepileptic drugs ( $\rho = 0.60$ ,  $p < 0.01$ ).

TABLE 2. EEG and syndrome

EEG and syndrome		N (%)
Frequency	R	8 (27)
	O	11 (37)
	V	6 (20)
Syndrome	PFS	6 (20)
	FS	12 (40)
	IGE	6 (20)
	undetermined	6 (20)
EEG	Normal	4 (13)
	Focal	12 (40)
	Generalized	5 (17)
	IGE	6 (20)
	undetermined	3 (10)
Focus	RT	4(33)
	LT	5(41)
	RF	2(16)
	LF	1(8)

FS = focal symptomatic; F = frontal; IGE = idiopathic generalized epilepsy; L = left; O = often; PFS = probable focal symptomatic; R = rare; R = right; T = temporal; V = very often

Patients with a *first seizure* were analysed separately. They had a lower number of seizure types, lower NHS3-1 score, lower number of index seizures and lower number of antiepileptic drugs; but differences were not statistically significant.

TABLE 3. MRI perfusion parameters after index seizures (grey matter)

	N	M	Me	SD
<b>N</b> BF	25	101,7	93	40,8
<b>N</b> BV	25	8	7	3,9
<b>N</b> MTT	25	6,9	6,9	2,9
<b>N</b> TTP	25	13,9	13,8	2,3
<b>P</b> BF	5	265,8**	234	56,3
<b>P</b> BV	5	25,5**	27,6	4,7
<b>P</b> MTT	5	5,7	5	1,2
<b>P</b> TTP	5	14,5	13,5	4,5

BF = blood flow; BV = blood volume; M = mean; Me = median; MTT = mean transit time; N = »negative« (»normoperfusion«); P = »positive« patients (»hyperperfusion«); SD = standard deviation; TTP = time to peak; \*\* statistically significant difference (p < 0,001)

## Discussion

Elevated cytokine levels have been demonstrated after epileptic seizures in brain tissue<sup>10,11</sup> and in peripheral blood.<sup>13-15</sup> Similarly, our study found an abnormal blood level of IL-6 in 14 out of 29 patients 8–24 hours after index seizure(s).

Alapirtti *et al.*<sup>32</sup> found an increased level of IL-6 only in the group of patients with temporal lobe epilepsy, whereas in patients with extra-temporal foci cytokine the level remained unchanged. This was not the case in our patient group, in which only four (out of 30) subjects had temporal lobe epilepsy and the level of IL-6 was elevated in 14/29 patients. However, it has previously been reported that patients with active epilepsy, regardless of epilepsy type, duration or frequency of seizures, have elevated levels of IL-6.<sup>33</sup> Lehtimäki *et al.*<sup>14</sup> found an increased level of IL-6 in all but two patients with partial seizures, with the greatest magnitude in patients who suffered repeated tonic-clonic seizures; but since patients with alcohol withdrawal and tumour provoked seizures were included in their study group, the interpretation of their results is difficult.

In another study (in the emergency setting), proinflammatory cytokines were elevated postictally in half of the subjects; however, patients with brain infections, cerebral venous thrombosis and brain tumour were included<sup>34</sup>; such patients were excluded in our study.

We found a highly significant correlation not only between proinflammatory cytokines IL-6 and IL-12; TNF- $\alpha$  and hsCRP but also between proinflammatory cytokines (TNF- $\alpha$  and IFN- $\gamma$ ) and IL-1Ra. This is consistent with the hypothesis of the inflammatory damage mitigation role of IL-1Ra.<sup>35</sup>

In contrast to previous reports<sup>10,14,36,37</sup>, we found an inverse correlation between the number of index seizures and the level of proinflammatory cytokines IL-10, TNF- $\alpha$  and IFN- $\gamma$ . We suggest that this may be a consequence of the design of our study; we tested a single cytokine level and not cytokine level dynamics. Two patients with idiopathic generalized epilepsy had the highest reported number of index seizures in our group. Since we relied solely on eyewitness observational data, we did not measure the auras, exact number of index seizures or their duration, which may be a crucial factor in measurement of the postictal cytokine level. Our study was performed at emergency settings where video-EEG was not available.

MRI »normo-« and »hyperperfusion« groups of patients demonstrated different concentrations

TABLE 4. Blood cytokine concentration after index seizure(s)

	N	M	Me	SD	Ref.	No (%) above/below reference
IL-4(pg/ml)	29*	0.9	0.6	1.3	≤ 1	7(24)
IL-6 (pg/ml)	29*	5.7	3.7	5.1	≤ 3.9	15(52)
IL-10 (pg/ml)	29*	42.8	11.4	10.2	≤ 10.9	16(55)
IL-12 (pg/ml)	29*	66	58.5	40.3	≤ 204	29(100)
TNFα (pg/ml)	29*	8.5	7.6	4	4.7–12.4	1(3)
IFN-γ (pg/ml)	29*	27.5	15	54.4	≤ 1.2	7(24)
IL-1Ra (pg/ml)	29*	1302.7	676	1797	168–744	14(48)
Hs CRP (mg/l)	29*	2.9	1.1	4.5	<3	29(100)

M = mean; Me = median; N = number; Ref = reference values; SD = standard deviation; \*patient 3 is not included

TABLE 5. Median concentrations of cytokines (pg/ml) and hs CRP(mg/l) in three subgroups of patients (see text for details)

	IL-4	IL-6	IL-10	IL-12	TNF-α	IFN-γ	IL-1Ra	hsCRP
Normoperfusion	0,6	4,3	11	60,1	7,3	15,1	677	0,9
Hyperperfusion	0,3*	1,5	63,7	44,5	9,7*	14	407*	1,3
Control hyperperfusion <sup>1</sup>	0,5	6,0	5,1	110,4	10,6	27,7	868	1,6

\* Statistically significant difference ( $p < 0.05$ )

TABLE 6. Basic and control concentrations of cytokines (pg/ml) in patients with hyperperfusion after index seizure(s)

Patient	IL-4	IL-6	IL-10	IL-12	TNF-α	IFN-γ	IL-1Ra	hsCRP
2 (1 <sup>st</sup> )	0,08	<2	116	54,5	8,19	13,08	352	1,5
(control)	0,3	<2	134	99,6	8,97	9,23	822	1,7
3 (1 <sup>st</sup> )	/	/	/	/	/	/	/	/
(control)	1,77	<2	12,6	127	11,5	108	1479	0,9
7* (1 <sup>st</sup> )	0,41	2,47	10,02	24,8	11,7	44,56	676	1,9
(control)	0,35	<2	29,8	41,8	12,1	31	361	1,8
15* (1 <sup>st</sup> )	0,61	9,49	0,22	196	9,57	10,81	1060	1,4
(control)	0,00	<2	0,58	150	14,1	14,7	593	0,7
25 (1 <sup>st</sup> )	0,38	<2	11,51	34,6	11,1	14,97	462	1,1
(control)	1,01	<2	12,0	42,5	20,2	16,2	660	1,4

\* Patient demonstrated hyperperfusion also on control MRI after three months.

of cytokines IL-4 and TNF-α: patients with hyperperfusion had significantly lower concentrations of IL-4 and a higher concentration of TNF-α. The two »control hyperperfusion« patients had the highest concentrations of TNF-α and other pro-inflammatory cytokines - IL-6, IL-12, IFN-γ, IL-1Ra and hsCRP. It is tempting to speculate that »hyperperfusion« and »control hyperperfusion« patients had the highest intensity of brain inflammation but further studies will have to check this hypothesis.

There are experimental<sup>38</sup> and clinical<sup>24</sup> evidences that long lasting blood-brain barrier disruption is linked to epileptogenesis. Increased postictal blood levels of proinflammatory cytokines - as also demonstrated in our study - have been attributed to postictal blood-brain barrier affection. DSC MRI is a noninvasive surrogate biomarker of brain inflammation, capable of demonstrating endothelial dysfunction or increased blood-brain barrier permeability.<sup>35</sup> In patients with high frequency seizures, Pizzini *et al.*<sup>26</sup> demonstrated periictal hyperperfu-

TABLE 7. Correlation between cytokine concentrations and number of index seizures

Cytokine concentration	Pearson's coefficient of correlation $\rho$
IL-4 (pg/ml)	0,07
IL-6 (pg/ml)	0,23
IL-10 (pg/ml)	-0,37*
IL-12 (pg/ml)	0,24
TNF $\alpha$ (pg/ml)	-0,41**
IFN- $\gamma$ (pg/ml)	-0,39*
IL-1Ra (pg/ml)	-0,22
hsCRP	-0,16

\*weak correlation; \*\*moderate correlation

sion (up to 5 hours after seizure) and in patients with low frequency seizures postictal hypoperfusion (up to 15-28 hours) on both DSC MRI and non-contrast arterial spin labelling (ASL) MRI. No patient in our study had hypoperfusion. Because we chose a minimum of 8-hour postictal delay for MRI imaging (in order to avoid postictal perfusion changes that may represent ongoing epileptic activity)<sup>18,19</sup> we may have missed contralateral hypoperfusion that has proposed to be a consequence of widespread dissociation of cerebral neurovascular coupling.<sup>22</sup> We did demonstrate postictal hyperperfusion in a subgroup of patients.

MRI perfusion parameters from our group taken as a whole did not correlate with any tested variable (including seizure frequency or syndrome). Hyperperfusion on MRI - perfusion with a 12-hour delay after a 4-hour pilocarpine induced status epilepticus in rats - correlated with histological signs of neurodegeneration in certain brain areas (not seen on T2 MRI).<sup>20</sup>

Looking at the clinical data, cytokine blood levels and DSC MRI parameters, we failed to find prognostic factors for the course of disease over a one-year follow up. The main limitation of our study is the smallness and heterogeneity of our group. We propose, however, that the trends shown in our study are worth following up.

## Conclusions

In conclusion, our study revealed a subgroup of patients with brain postictal hyperperfusion and higher plasma cytokine values, indicating a probable long lasting blood-brain barrier alteration.

Larger studies are needed to validate the hypothesis that post seizure brain tissue inflammation is a crucial factor of epileptogenesis in selected patients and to determine the diagnostic and prognostic values of the various parameters studied.

## Acknowledgement

The study was partially financed with grant ID TP 20120095.

## References

1. Fisher RS, Boas WVE, Blume W, Elger C, Genton P, Lee P, et al. Epileptic seizures and epilepsy: definitions proposed by the International League against Epilepsy (ILAE) and the International Bureau for Epilepsy (IBE). *Epilepsia* 2005; **46**: 470-47. doi:10.1111/j.0013-9580.2005.66104.x
2. WHO. Neurological disorders: public health challenges. Available at: [http://www.who.int/mental\\_health/publications/neurological\\_disorders\\_ph\\_challenges](http://www.who.int/mental_health/publications/neurological_disorders_ph_challenges) [cited 2016 Feb 22]. p. 56-69. ISBN: 978 92 4 156336 9
3. Lerche H, Vezzani A, Beck H, Blümcke I, Weber Y, Elger C. [New developments in epileptogenesis and therapeutic perspectives]. [German]. *Nervenarzt* 2011; **82**: 978-85. doi:10.1007/s00115-011-3260-4
4. Berg AT. Risk of recurrence after a first unprovoked seizure. *Epilepsia* 2008; **49**: 13-18. doi:10.1111/j.1528-1167.2008.01444.x
5. Pitkänen A, Sutula TP. Is epilepsy a progressive disorder? Prospects for new therapeutic approaches in temporal-lobe epilepsy. *Lancet Neurol* 2002; **1**: 173-81. doi:10.1016/S1474-4422(02)00073-X
6. Ravizza T, Boer K, Redeker S, Spliet WGM, Van Rijen PC, Troost D, et al. The IL-1 $\beta$  system in epilepsy-associated malformations of cortical development. *Neurobiol Dis* 2006; **24**: 128-43. doi:10.1016/j.nbd.2006.06.003
7. Vezzani A, Aronica E, Mazarati A, Pittman QJ. Epilepsy and brain inflammation. *Exp Neurol* 2013; **13**: 11-21. doi:10.1016/j.expneurol.2011.09.033
8. Vezzani A. Epilepsy and inflammation in the brain: Overview and pathophysiology. *Epilepsy Curr* 2014; **14**(Suppl. 2): 3-7. doi:10.5698/1535-7511-14.s2.3
9. Vezzani A. Finding the epileptogenesis switch. *Nat Med* 2012; **11**: 1626-7. doi:10.1038/nm.2982
10. Librizzi L, Noè F, Vezzani A, de Curtis M, Ravizza T. Seizure-induced brain-borne inflammation sustains seizure recurrence and blood-brain barrier damage. *Ann Neurol* 2012; **72**: 82-90. doi:10.1002/ana.23567
11. Turrin NP, Rivest S. Innate immune reaction in response to seizures: implications for the neuropathology associated with epilepsy. *Neurobiol Dis* 2004; **16**: 321-34. doi:10.1016/j.nbd.2004.03.010
12. Kan AA, de Jager W, de Wit M, Heijnen C, van Zuiden M, Ferrier C, et al. Protein expression profiling of inflammatory mediators in human temporal lobe epilepsy reveals co-activation of multiple chemokines and cytokines. *J Neuroinflamm* 2012; **9**: 207-29. doi:10.1186/1742-2094-9-207
13. Bauer S, Cepok S, Todorova-Rudolph A, Nowak M, Köller M, Lorenz R, et al. Etiology and site of temporal lobe epilepsy influence postictal cytokine release. *Epilepsy Res* 2009; **86**: 82-8. doi:10.1016/j.eplepsyres.2009.05.009
14. Lehtimäki KA, Keränen T, Palmio J, Mäkinen R, Hurme M, Honkaniemi J, et al. Increased plasma levels of cytokines after seizures in localisation-related epilepsy. *Acta Neur Scand* 2007; **116**: 226-30. doi:10.1111/j.1600-0404.2007.00882.x
15. Liimatainen S, Fallah M, Kharazmi E, Peltola M, Peltola J. Interleukin-6 levels are increased in temporal lobe epilepsy, but not in extratemporal lobe epilepsy. *Jour Neurol* 2009; **256**: 796-802. doi:10.1007/s00415-009-5021-x
16. Wintermark M, Reichhart M, Thiran J P, Maeder P, Chalaron M, Schnyder P, et al. Prognostic accuracy of cerebral blood flow measurement by perfusion computed tomography, at the time of emergency room admission, in acute stroke patients. *Ann Neurol* 2002; **51**: 417-32. doi:10.1002/ana.10136

17. Avsenik, J, Bisdas S, Popovic KS. Blood-brain barrier permeability imaging using perfusion computed tomography. *Radiol Oncol* 2015; **49**: 107-14. doi:10.2478/raon-2014-0029
18. Wiest R, von Bredow F, Schindler K, Schauble B, Slotboom J, Brekenfeld C, et al. Detection of regional blood perfusion changes in epileptic seizures with dynamic brain perfusion CT-a pilot study. *Epilepsy Res* 2006; **72**: 2-3. doi:10.1016/j.eplepsyres.2006.07.017
19. Hauf M, Wiest R, Nirkko A, Strozzi S, Federspiel A. Cortical regional hyperperfusion in nonconvulsive status epilepticus measured by dynamic brain perfusion CT. *Am J Neuroradiol* 2009; **30**: 693-8. doi:10.3174/ajnr.A1456
20. Fabene PF, Marzola P, Sbarbati A, Bentivoglio M. Magnetic resonance imaging of changes elicited by status epilepticus in the rat brain: diffusion-weighted and T2-weighted images, regional blood volume maps, and direct correlation with tissue and cell damage. *Neuroimage* 2003; **18**: 375-89. doi:10.1016/S1053-8119(02)00025-3
21. Choy M, Cheung KK, Thomas DL, Gadian DG, Lythgoe MF, Scott RC. Quantitative MRI predicts status epilepticus-induced hippocampal injury in the lithium-pilocarpine rat model. *Epilepsy Res* 2010; **88**: 221-30. doi:10.1016/j.eplepsyres.2009.11.013
22. Harris S, Boorman L, Bruyns-Haylett M, Kennerley A, Ma H, Zhao M, et al. Contralateral dissociation between neural activity and cerebral blood volume during recurrent acute focal neocortical seizures. *Epilepsia* 2014; **55**: 1423-30. doi:10.1111/epi.12726
23. Zhao M, Nguyen J, Ma H, Nishimura N, Schaffer C B, Schwartz TH. Preictal and ictal neurovascular and metabolic coupling surrounding a seizure focus. *J Neurosci* 2011; **31**: 13292-300. doi:10.1523/JNEUROSCI.2597-11.2011
24. Leonhardt G, De Greiff A, Weber J, Ludwig T, Wiedemayer H, Forsting M, et al. Brain perfusion following single seizures. *Epilepsia* 2005; **46**: 1943-9. doi:10.1111/j.1528-1167.2005.00336.x
25. Fabene PF, Laudanna C, Constantin G. Leukocyte trafficking mechanisms in epilepsy. *Mol Immunol* 2013; **55**: 100-4. doi:10.1016/j.molimm.2012.12.009
26. Pizzini FB, Farace P, Manganotti P, Zoccatelli G, Bongiovanni LG, Golay X, et al. Cerebral perfusion alterations in epileptic patients during peri-ictal and post-ictal phase: PASL vs. DSC-MRI. *Magn Reson Imaging* 2013; **31**: 1001-5. doi:10.1016/j.mri.2013.03.023
27. Matsuura K, Maeda M, Okamoto K, Araki T, Miura Y, Hamada K, et al. Usefulness of arterial spin-labeling images in periictal state diagnosis of epilepsy. *Jour Neural Sci* 2015; **359**: 424-9. doi:10.1016/j.jns.2015.10.009
28. O'Donoghue MF, Duncan JS, Sander JW. The National Hospital Seizure Severity Scale: a further development of the Chalfont Seizure Severity Scale. *Epilepsia* 1996; **37**: 563-7. doi:10.1111/j.1528-1157.1996.tb00610.x
29. Engel J Jr. ILAE Classification of epilepsy syndromes. *Epilepsy Res* 2006; **70**: S5-10. doi:10.1016/j.eplepsyres.2005.11.014
30. Spampinato MV, Wooten C, Dorton M, Besenski N, Rumboldt Z. Comparison of first-pass and second-bolus dynamic susceptibility perfusion MRI in brain tumors. *Neuroradiology* 2006; **48**: 867-74. doi:10.1007/s00234-006-0134-8
31. Wetzel SG, Cha S, Johnson G, Lee P, Law M, Kasow DL, et al. Relative cerebral blood volume measurements in intracranial mass lesions: interobserver and intraobserver reproducibility study. *Radiology* 2002; **224**: 797-803. doi:10.1148/radiol.2243011014
32. Alapirtti T, Rinta S, Hulkkonen J, Mäkinen R, Keränen T, Peltola J. Interleukin-6, interleukin-1 receptor antagonist and interleukin-1beta production in patients with focal epilepsy: a video-EEG study. *J Neural Sci* 2009; **280**: 94-7. doi:10.1016/j.jns.2009.02.355
33. Nowak M, Bauer S, Haag A, Cepok S, Todorova-Rudolph A, Tackenberg B, et al. Interictal alterations of cytokines and leukocytes in patients with active epilepsy. *Brain Behav Immun* 2011; **25**: 423-9. doi:10.1016/j.bbi.2010.10.022
34. Sinha S, Patil SA, Jayalekshmy V, Satishchandra P. Do cytokines have any role in epilepsy? *Epilepsy Res* 2008; **82**: 171-6. doi:10.1016/j.eplepsyres.2008.07.018
35. Vezzani A, Friedman A. Brain inflammation as a biomarker in epilepsy. *Biomark Med* 2011; **5**: 607-14. doi:10.1016/j.expneurol.2011.09.033
36. Peltola J, Laaksonen J, Haapala AM, Hurme M, Rainesalo S, Keränen T. Indicators of inflammation after recent tonic-clonic seizures correlate with plasma interleukin-6 levels. *Seizure* 2002; **11**: 44-6. doi:10.1053/seiz.2001.0575
37. Maroso M, Balosso S, Ravizza T, Liu J, Aronica E, Iyer AM. Toll-like receptor 4 and high-mobility group box-1 are involved in ictogenesis and can be targeted to reduce seizures. *Nat Med* 2010; **16**: 413-9. doi:10.1038/nm.2127
38. Seiffert E, Dreier JP, Ivens S, Bechmann I, Tomkins O, Heinemann U, et al. Lasting blood-brain barrier disruption induces epileptic focus in the rat somatosensory cortex. *Jour Neurosci* 2004; **24**: 7829-36. doi:10.1523/JNEUROSCI.1751-04.2004

# Effects of electrochemotherapy with cisplatin and peritumoral IL-12 gene electrotransfer on canine mast cell tumors: a histopathologic and immunohistochemical study

Claudia Salvadori<sup>1</sup>, Tanja Svava<sup>2</sup>, Guido Rocchigiani<sup>1</sup>, Francesca Millanta<sup>1</sup>, Darja Pavlin<sup>3</sup>, Maja Cemazar<sup>4</sup>, Ursa Lamprecht Tratar<sup>4</sup>, Gregor Sersa<sup>4</sup>, Natasa Tozon<sup>3</sup>, Alessandro Poli<sup>1</sup>

<sup>1</sup> Department of Veterinary Sciences, University of Pisa, Italy

<sup>2</sup> Institute of Pathology, Forensic and Administrative Veterinary Medicine, Veterinary Faculty, University of Ljubljana, Ljubljana, Slovenia

<sup>3</sup> Veterinary Faculty, Clinic for Companion Animals, University of Ljubljana, Ljubljana, Slovenia

<sup>4</sup> Institute of Oncology Ljubljana, Ljubljana, Slovenia

Radiol Oncol 2017; 51(3): 286-294.

Received 12 July 2017

Accepted 10 August 2017

Correspondence to: Prof. Alessandro Poli, Dipartimento di Scienze Veterinarie, Università di Pisa, Viale delle Piagge 2, 56124 Pisa, Italia. Phone: +39 50 2216982; Fax: +39 50 2216941, E mail: alessandro.poli@unipi.it

Disclosure. The authors declare no potential conflicts of interest.

**Background.** The study was aimed to characterize tumor response after combined treatment employing electrochemotherapy with IL-12 gene electrotransfer in dogs with spontaneous mast cell tumors (MCT).

**Materials and methods.** Eleven dogs with eleven MCTs were included in the study. Histological changes were investigated in biopsy specimens collected before the treatment ( $T_0$ ), and 4 ( $T_1$ ) and 8 weeks ( $T_2$ ) later. Cellular infiltrates were characterized immunohistochemically by using anti CD3, CD20, Foxp3 (Treg), CD68 and anti MHC-class II antibodies. Proliferation and anti-apoptotic activity of neoplastic cells were assessed using anti Ki-67 and Bcl-2 antibodies. Angiogenetic processes were investigated immunohistochemically by using anti Factor VIII and anti CD31 antibodies and micro vessel density quantification.

**Results.** Histopathological examination of samples at  $T_0$  confirmed the diagnosis and the presence of scanty infiltrates consisted mainly of T-lymphocytes and macrophages. At  $T_1$  and  $T_2$  neoplastic cells were drastically reduced in 7/11 cases, small clusters of neoplastic cells were detected in 3/11 cases and 1/11 cases neoplastic cells were still evident. Proliferation activity of neoplastic cells was significantly reduced at  $T_1$  and  $T_2$  and expression of anti-apoptotic protein at  $T_1$ . Microvessel density was drastically reduced in all samples after treatment. The number of T-lymphocytes increased at  $T_1$ , although not significant, while Treg were significant higher at  $T_1$  and macrophages at  $T_2$ .

**Conclusions.** The combined electrochemotherapy and IL-12 gene electrotransfer effectively induced a cellular response against neoplastic cells characterized mainly by the recruitment of T-lymphocytes and macrophages and a fibrotic proliferation with reduction of microvessels.

Key words: electrochemotherapy; histopathology; immune cells; interleukin-12; mast cell tumor; microvessel density

## Introduction

Electrochemotherapy is an ablative technique for the treatment of solid tumors of different histotypes in human and veterinary oncology, with approximately 80% objective response of the treated

tumors.<sup>1,2</sup> It is based on electroporation as drug delivery method to tumors for the chemotherapeutic drugs bleomycin or cisplatin to improve the anti-tumoral efficacy.<sup>1</sup>

Another biomedical application of electroporation is plasmid DNA delivery to tumors (gene elec-

trotransfer) for gene therapy. Preclinical and clinical studies demonstrated effectiveness of different therapeutic plasmid DNA electrotransfer to tumors as effective and safe method for local as well as loco-regional control of the cutaneous tumors.<sup>3</sup> The most studies explored gene electrotransfer of plasmid DNA coding for IL-12 cytokine.<sup>4,6</sup> Its effectiveness was demonstrated also in treatment of spontaneous tumors in dogs.<sup>7-10</sup>

A new treatment approach is combining local tumor electrochemotherapy with gene therapy with plasmid coding for IL-12 peritumorally to skin.<sup>11</sup> Some preclinical data indicate that this approach provides in situ vaccination by electrochemotherapy that is boosted by immunogene IL-12 peritumoral gene electrotransfer.<sup>3</sup>

Our previous report has provided evidence for this approach in MCT with excellent local tumor control and long lasting progression free survival of the treated dogs.<sup>11</sup> To provide further evidence on the mechanisms of action, this study evaluates the histopathological features of those tumors in more detail to characterize whether this approach provides antitumor response also due to boosting the immune response. Therefore, we characterized tumor response including the cellular infiltrates at different time points post-electrochemotherapy with cisplatin combined with peritumoral IL-12 electrotransfer in dogs, spontaneously affected by MCT and compared these results with those observed in biopsies collected before the treatment. Proliferation and anti-apoptotic activity of neoplastic cells as well as the changes in microvessel density were also investigated, at the same timing.

## Materials and methods

### Animals and tumors

Between January and December 2010 eleven subjects, 4 males and 7 females of different breeds ranging from 5 to 9 year-old (mean 6.5 years  $\pm$  1.3 years) complied with inclusion criteria for the clinical survey (histologically confirmed MCT in different anatomical locations, good general health conditions with normal routine hematologic and biochemical profile without cardiac dysfunctions), were included in the study. The animals included in the study were those that owners refused any other type of standard treatment/surgery with wide excision of nodules.

Before the treatment a staging in all patients was performed according to modified WHO staging criteria with physical examination, examination of tho-

racic radiographs, abdominal ultrasonography and basic bloodwork, consisting of a complete blood count with differential white cell count. Biochemical parameters (urea, creatinine, serum alkaline phosphatase and alanine aminotransferase) were determined using an automated chemical analyzer.

The study was approved by the Ethical Committee of the Ministry of Agriculture, Forestry and Food of the Republic of Slovenia (approval No. 323-451/2004-9). Prior to the inclusion a written consent for participation in the clinical study for each animal was obtained from their owners.

### Electrochemotherapy and gene transfer

Electrochemotherapy and IL-12 gene electrotransfer were performed as previously described.<sup>11</sup> Briefly, electrochemotherapy with intratumoral injection of cisplatin (*cis*-diamminedichloroplatinum II, Cisplatyl; Aventis, Paris, France), at a concentration of 2 mg/ml in a dose of  $\sim$ 1 mg/cm<sup>3</sup> was performed just before electric pulses were delivered (8 pulses each of 100  $\mu$ s duration and amplitude to electrode distance ratio of 1300 V/cm and frequency of repetition 5 kHz with electric pulses generator Cliniporator<sup>TM</sup> (IGEA s.r.l., Carpi, Italy)). Two parallel stainless steel plate electrodes with 6 mm distance between them or 4 needle row electrodes with 4 mm distance according to the tumor size was used. Immediately after the electrochemotherapy 2 mg of the IL-12 plasmid was injected intradermally in equidistant locations around tumor nodule in two locations.<sup>10</sup> One high voltage pulse (amplitude to electrode distance ratio 1200 V/cm, duration 100  $\mu$ s) and one low voltage pulse (amplitude to electrode distance ratio 140 V/cm, duration 400  $\mu$ s)<sup>12</sup> were delivered immediately after plasmid injection, using the same electric pulse generator and electrodes as mentioned above.

### Tissue sampling and processing

All the subjects were submitted to biopsy before ( $T_0$ ) the combined therapy and at 4 ( $T_1$ ) and 8 weeks ( $T_2$ ) post-treatment. Biopsies were fixed into 10% neutral buffered formalin and then processed routinely for paraffin embedding. Five-micrometers serial sections from all specimens were stained for haematoxylin and eosin (HE), Gomori's modified trichrome stain and also mounted on treated glass slides (Superfrost Plus; Menzel-Glaser, Germany) for immunohistochemistry. Mast cell tumors were classified according to the Kiupel *et al.* (2011) classification.<sup>13</sup>

TABLE 1. Antibodies used in the study

Antibody	Specificity	Type	Species	Source	Dilution	Pretreatment
Anti-human CD3	Pan-T lymphocytes	Polyclonal	Rabbit	(A0552) Dako UK Ltd. Ely UK	1:50	Citrate buffer pH6
Anti-human CD20	Pan-B lymphocytes	Polyclonal	Rabbit	(RB-9013-PO) Thermo Scientific, Chesire, UK	1:400	None
Anti-human Foxp3	T-reg lymphocytes	Monoclonal	Mouse	(7979) Affymetrix eBioscience, san Diego, CA USA	1:100	Triss-EDTA pH9
Anti-human CD68	Macrophages	Monoclonal	Mouse	(PG-M1) Thermo Scientific, Chesire, UK	1:100	Proteinase K
Anti-human Ki-67	Proliferating cells	Monoclonal	Mouse	(MIB1; M7240) Dako UK Ltd. Ely UK	1:100	Citrate buffer pH6
Anti-human Bcl-2	Anti-apoptotic protein	Monoclonal	Mouse	(610538) BD Biosciences, Wyckoff, NJ, USA5	1:100	Citrate buffer pH6
Anti-human Von Willebrand Factor -	Endothelial cells	Polyclonal	Rabbit	(A0082) Dako UK Ltd. Ely UK	1:300	Citrate buffer pH6
Anti-human CD31	Endothelial cells	Monoclonal	Mouse	(JC70A) Dako UK Ltd. Ely UK	1:100	Citrate buffer pH6

## Immunohistochemistry

Sections were dewaxed in xylene and rehydrated through graded alcohols prior to quenching endogenous peroxidase activity with 3% H<sub>2</sub>O<sub>2</sub> in distilled water for 20 minutes. Heat induced epitope retrieval with citrate buffer pH 6 was performed. Immunohistochemical labelling was performed manually with the Sequenza slide rack and cover-plate system (Shandon, Runcorn, UK). Non-specific antigen binding was blocked by incubation with UltraVision Protein Block (TA-125-PBQ; Thermo Scientific, Cheshire, UK). A panel of primary antibodies was applied to serial sections and incubated overnight at 4°C (Table 1). Antibody binding was detected by the Biotinylated Goat Polyvalent Secondary (TP-125-BN; Thermo Scientific, Cheshire, UK), Streptavidin Peroxidase (TS-125-HR; Thermo Scientific, Cheshire, UK) and DAB chromogen (SK-4105; ImmPact DAB, Vector, Burlingame, CA) as indicated by manufacturer's instructions and slides were counterstained with haematoxylin. Substitution of the primary antibody with unrelated matched primary antibody was used to provide a negative control. Serial sections of canine lymph node were used as positive control.

Slides were examined by two pathologists (C.S. and A.P.) without knowledge of the corresponding clinical and pathological data.

## Quantification of immunolabeling

Bright field images were acquired at x20 magnification with a Leica Microsystem DFC490 digital camera mounted on Leica DMR microscope (Wetzlar,

Germany). Counting were performed using a semiautomatic analysis system (LASV 4.3, Leica). Six 10,000 µm<sup>2</sup> random fields of the central and periphery parts of the biopsies were used for counting the number of infiltrating CD3+, CD20+, Foxp3+ (Treg+), CD68+ and MHC Class II+ cells and Bcl-2+ and Ki-67+ neoplastic cells. Microvessel density was determined with Factor VIII and CD31 immunostained section in six 50,000 µm<sup>2</sup> random fields.

## Statistical analysis

Statistical analysis was performed using the statistical package SPSS Advanced Statistics 21.0 (SPSS Inc., Chicago, IL, USA). ANOVA test was used to compare the composition of cell infiltrates and microvessel density at the different times of observation and post hoc analysis was made by Bonferroni Test. Statistical significance was based on a 5% (0.05) significance level.

## Results

### Histologic features

At T<sub>0</sub> all eleven skin tumors of different volumes (ranged from 0.2 to 16.9 cm<sup>3</sup>) were diagnosed as low grade MCTs and were characterized by sheets of polygonal neoplastic cells with abundant cytoplasm containing variable number of metachromatic granules, associated with moderate to massive infiltration of eosinophils, in the superficial and deep dermis, sometimes extending also to deep muscular layer (Figure 1A). Mitotic index was low (1 to 2 mitoses/10 HPF). Scanty multinucleated cells were observed. Rarely necrotic areas

were present. Neoplastic cells were associated with reactive proliferation of connective tissue.

At  $T_1$  in biopsies collected from seven dogs with complete response, the neoplastic tissue was substituted by a fibrotic tissue composed by horizontally oriented wavy collagen fibers associated with inflammatory infiltrates mainly constituted by lymphocytes and macrophages (Figure 1B). In three cases (partial response), single or small clusters of neoplastic cells were still evident scattered among the fibrotic connective tissue, while in one dog neoplastic mast cells were still evident with features similar to  $T_0$ .

At  $T_2$  biopsies collected from the seven dogs which did not present tumor cells at  $T_1$  were still free of neoplastic cells and consisted of a dense fibrous tissue still infiltrated by mononuclear cells. In other three cases (one with stable disease and two with partial response), thin aggregates of neoplastic mast cells between connective tissue bundles, were still evident (Figure 1C), while in one case with partial response, neoplastic cells were numerous as at  $T_0$  and  $T_1$ .

### Immunohistochemistry

Immunohistochemical analysis of biopsies collected before the treatment and at different times of post-treatment revealed, in dermal infiltrates the presence of CD3+ T lymphocytes (Figure 2A, B), CD20+ B lymphocytes, Treg Lymphocytes (Figure 2C, D), and macrophages (Figure 2E, F), in different percentages, with T lymphocytes and macrophages representing the predominant cell populations. Results of immunohistochemical evaluation of inflammatory infiltrates at  $T_0$  and at  $T_1$  and  $T_2$  intervals are presented in the Figure 3. Overall, the T lymphocyte number increased at  $T_1$ , even this difference was not statistically significant and was reduced at  $T_2$ . Specifically, in biopsies collected from subjects with complete remission, the number of CD3+ lymphocytes was significantly higher than from dogs with stable or progressive disease both at both  $T_1$  ( $8.1 \pm 8.2$  CD3+cells/ 10,000  $\text{mm}^2$  vs  $3.4 \pm 1.9$  CD3+cells/ 10,000  $\text{mm}^2$ ;  $p = 0.008$ ) both at  $T_2$  ( $6.6 \pm 4.4$  CD3+cells/ 10,000  $\text{mm}^2$  vs  $3.2 \pm 1.9$  CD3+cells/ 10,000  $\text{mm}^2$ ;  $p = 0.001$ ). Macrophages significantly increased at  $T_2$  ( $P = 0.006$ ) and Treg lymphocytes significantly increased at  $T_1$  ( $p = 0.0001$ ), but no differences were observed at  $T_2$ . No differences were observed in the presence of CD20 lymphocytes at  $T_1$  and  $T_2$ .

Immunohistochemical studies allowed to determine also the presence of proliferative and anti-ap-

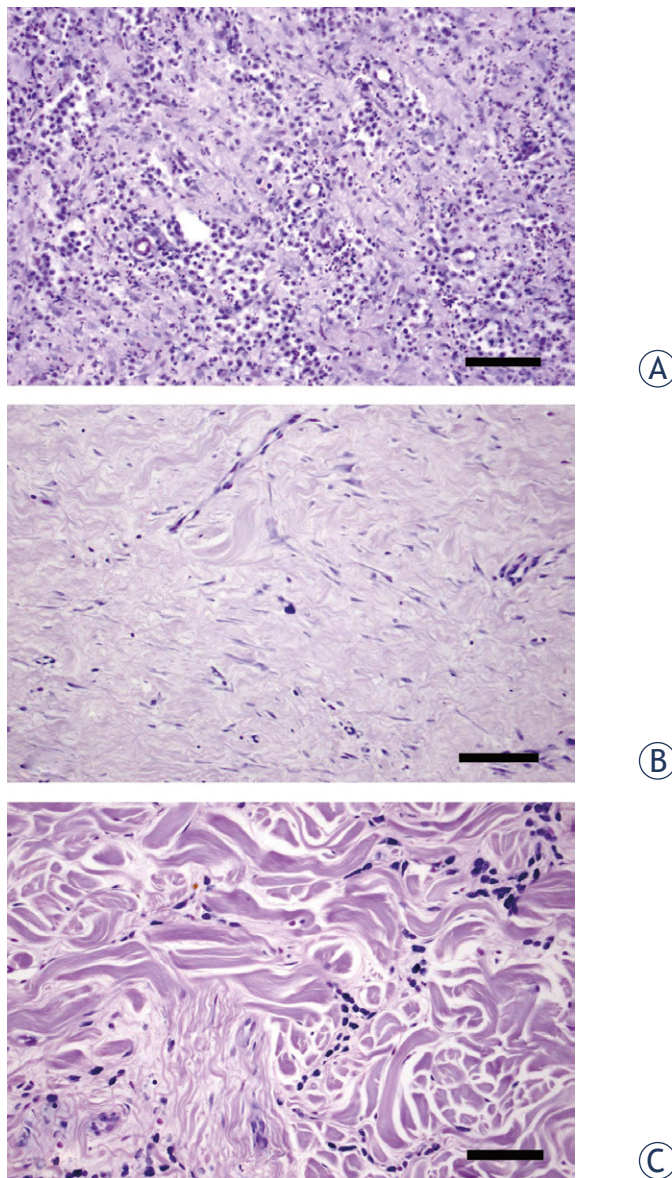


**FIGURE 1.** Histology of tissue samples collected before the combined therapy ( $T_0$ ) and at 4 ( $T_1$ ) and 8 weeks ( $T_2$ ) post-treatment. **(A)** At  $T_0$  sheets of neoplastic cells with abundant cytoplasm containing variable number of metachromatic granules were present in the superficial and deep dermis; **(B)** At  $T_1$  the neoplastic tissue was substituted by a fibrotic tissue associated with scanty inflammatory infiltrates mainly constituted by mononuclear cells; **(C)** At  $T_2$  in dogs with partial response between connective tissue bundles were evident thin aggregates of neoplastic mast cells. Haematoxylin Eosin; bar = 100  $\mu\text{m}$ .

optotic activities of neoplastic cells (Figure 4A, B; and C, D, respectively) as well as the micro-vessel density (Figure 4E, F) at  $T_0$ ,  $T_1$  and  $T_2$ . Results were summarized in the Figure 5.

Proliferation activity of neoplastic cells was statistically reduced at  $T_1$  ( $p = 0.0001$ ) and  $T_2$  ( $p = 0.0001$ ), while the number of neoplastic cells ex-

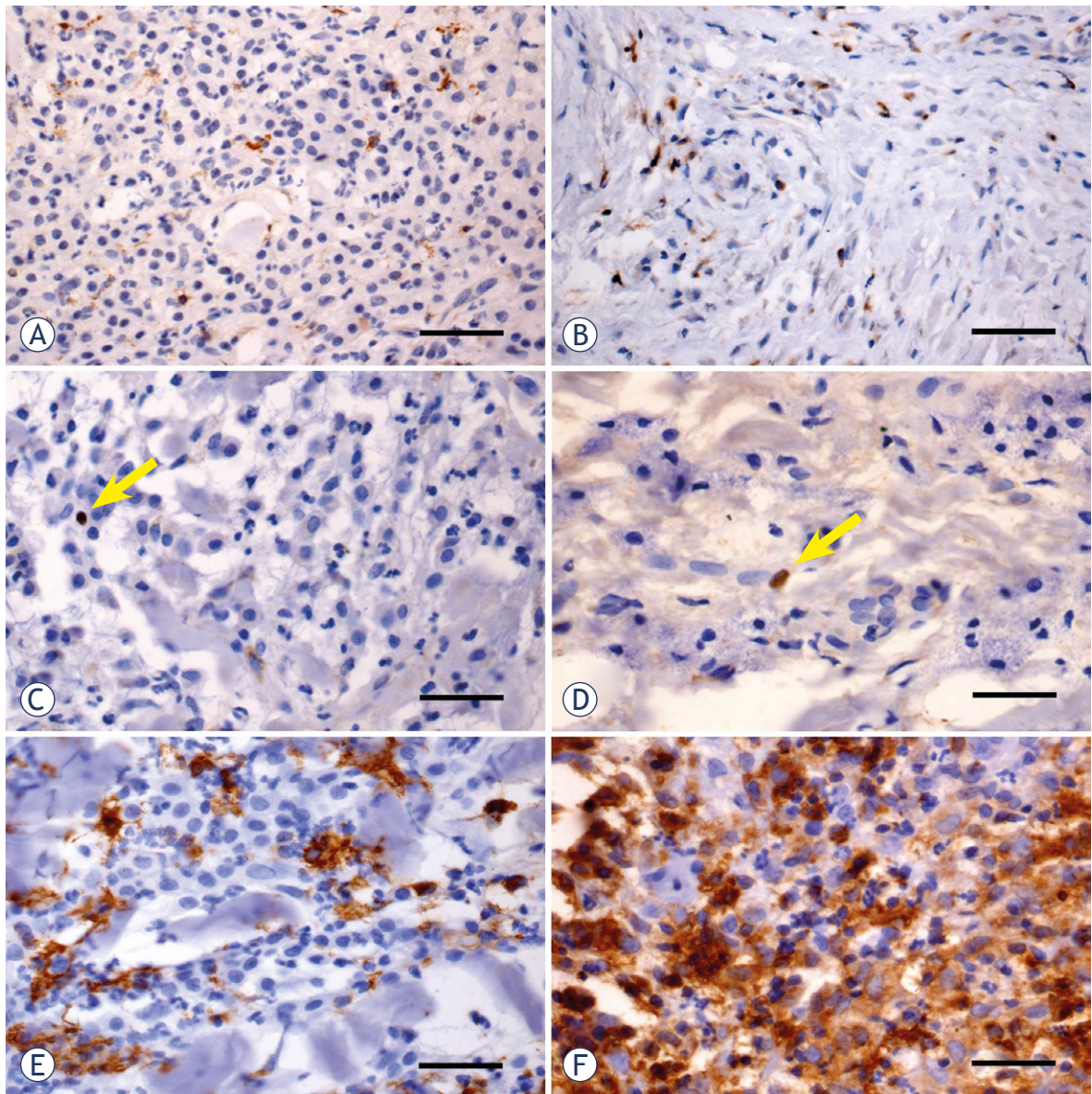


**FIGURE 2.** Immunohistochemical staining of tissue samples collected at T<sub>0</sub> (A, C and E) and T<sub>1</sub> (B, D and E). CD3+ lymphocytes infiltrating the neoplastic tissue at T<sub>0</sub> (A) and the fibrotic tissue at T<sub>1</sub> (B). Scanty Foxp3+ Treg lymphocytes at the periphery of neoplastic tissue at T<sub>0</sub> (C) and in a tissue sample collected at T<sub>1</sub> (D). CD68+ macrophages in the neoplastic tissue at T<sub>0</sub> (E) and in the fibrotic tissue at T<sub>1</sub> (F). Immunohistochemical staining using DAB chromogen and haematoxylin counterstain. Bar = 100  $\mu$ m.

pressing the Bcl-2 anti-apoptotic protein was increased at T<sub>1</sub> ( $p = 0.0001$ ), while was reduced 4 weeks later. Proliferation activity of neoplastic cells in the biopsies collected from subjects with complete response was significantly lower than in the biopsies collected from dogs with stable or progressive disease both at T<sub>1</sub> ( $1.5 \pm 2.1$  Ki-67+cells/10,000 mm<sup>2</sup> vs  $2.5 \pm 0.7$  Ki-67+cells/10,000 mm<sup>2</sup>;  $p = 0.012$ ) both at T<sub>2</sub> ( $0.4 \pm 0.6$  Ki-67+cells/10,000 mm<sup>2</sup> vs  $2.2 \pm 1.0$  Ki-67+cells/10,000 mm<sup>2</sup>;  $p = 0.0001$ ), as

well as the expression of anti-apoptotic Bcl-2 protein both at both T<sub>1</sub> ( $1.9 \pm 2.0$  Bcl-2+cells/10,000 mm<sup>2</sup> vs  $3.2 \pm 0.9$  Bcl-2+cells/10,000 mm<sup>2</sup>;  $p = 0.004$ ) both at T<sub>2</sub> ( $1.4 \pm 1.5$  Ki-67+cells/10,000 mm<sup>2</sup> vs  $2.8 \pm 1.2$  Ki-67+cells/10,000 mm<sup>2</sup>;  $p = 0.0001$ ).

Microvessel density, determined using both anti-Factor VIII and anti-CD31 antibodies, was drastically reduced at T<sub>1</sub> ( $p = 0.000$ ) and T<sub>2</sub> ( $p = 0.0001$ ), when compared with the samples collected before the treatment.

## Discussion

Histopathological evaluation of tissue biopsies after electrochemotherapy with cisplatin combined with peritumoral IL-12 gene electrotransfer demonstrates that in the tumors with complete clinical response, pronouncedly reduced number and proliferation rate of the tumor cells was obtained with significantly enhanced immune and anti-vascular response, which confirm our previously reported clinical results.<sup>11</sup>

At the best of our knowledge this is the first clinical study that describes the histopathological and cellular changes induced *in vivo* by electrochemotherapy and peritumoral IL-12 electrotransfer in dogs bearing MCT, performed with the consent of the owners. The number of biopsies was reduced and made at distance from treatment with the aim to verify its effectiveness.

Already at four weeks post-treatment, in dogs with a complete responses histopathologic examination revealed a marked reduction of neoplastic cells, confirming the anticancer efficacy of the combined electrochemotherapy and gene therapy. This reduction was even more evident four weeks later. On the contrary, in dogs with a partial response the reduction of neoplastic cell was lower at four weeks after treatment and this reduction was absent in dog with stable disease.

The reduced presence of neoplastic cells detected in the tissue samples from dogs with complete response was also associated with a reduced proliferative activity of remnant neoplastic mast cells, characterized by a significant reduction of positivity to Ki-67 antibody and by a significant reduced expression of the anti-apoptotic Bcl-2 protein. The major mechanism of cisplatin tumor destruction consists of the formation of intrastrand and inter-strand DNA adducts leading to DNA fragmentation that can ultimately lead to an apoptotic mediate cell death as demonstrated *in vitro* and *in vivo* in murine models<sup>14</sup> and the decreased expression of anti-apoptotic factor as the Bcl-2 protein promotes higher death rate of the cancer cells.<sup>15</sup>

The time interval of 4 weeks of the first post-treatment biopsy did not allow evaluation of the tumor necrosis, since at this time point dense fibrotic connective tissue with progressive reduction of microvessel density was already present. In experimental animal models has been demonstrated that electroporation induces a higher internalization of cisplatin molecules with a rapid necrosis of neoplastic cells<sup>16</sup> and vascular disrupting action by causing a rapid shutdown of tumour blood flow

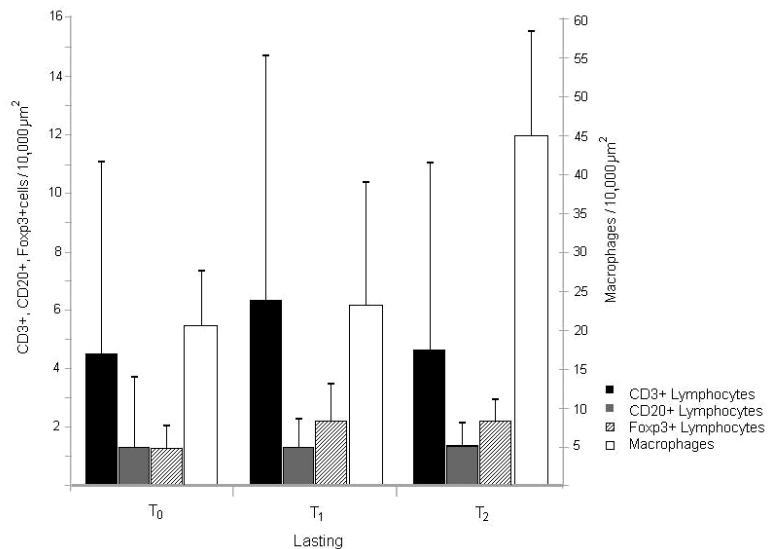


**FIGURE 3.** Histogram of number of immune cells in 10,000  $\mu\text{m}^2$  of tissue samples collected at T<sub>0</sub>, T<sub>1</sub> and T<sub>2</sub>. Slight increase of CD3+ lymphocytes at T<sub>1</sub>, while macrophages significantly increased at T<sub>2</sub> and Treg lymphocytes at T<sub>1</sub>.

leading to reduced tumour oxygenation, increased tumour hypoxia and tumour necrosis.<sup>17</sup>

In this study, electrochemotherapy was associated with IL-12 gene electrotransfer with proven good local and locoregional antitumor effects.<sup>11</sup> The potential for inducing an antitumoral immune response to treat neoplastic disorders is well known, but the application of this technology has not yet been meaningfully transferred to the clinic. Local administration of recombinant cytokines directly into the tumor has proven to be much safer than systemic delivery.<sup>13</sup> IL-12 is a natural occurring cytokine that showed potential success for treating cancer by inducing a specific anti-tumoral immune response.<sup>18</sup> Gene therapy with IL-12 pDNA showed to be effective to treat multiple tumor histotype in rodent models and induce an anti-tumoral immune response capable of affecting neoplastic tissues.<sup>14-16</sup> Likewise, IL-12 gene therapy in canine species can induce tumor regression in spontaneous neoplasms of different histotypes.<sup>17,19,20</sup>

Another therapeutic approach that is currently extensively explored is combination of the ablative techniques with different immunomodulatory approaches, either with immune checkpoint inhibitors, Treg depletion or immunostimulation.<sup>3</sup> In this context ablative techniques are considered as *in situ* vaccination with further boosting of the immune responsiveness of the organism. For this purpose, we postulated that electrochemotherapy

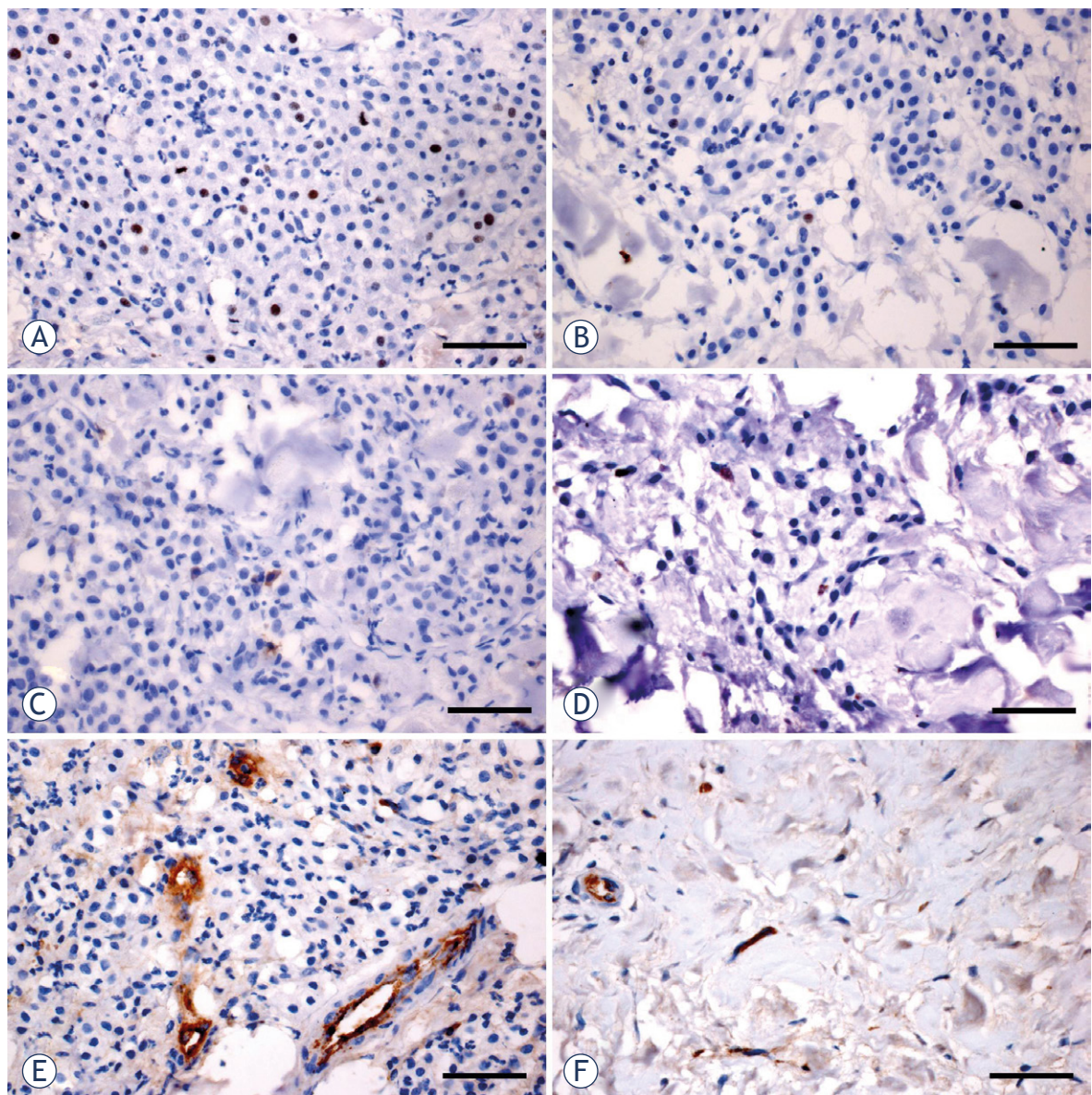


FIGURE 4. Immunohistochemical staining of tissue samples collected at  $T_0$  (A, C and E) and  $T_1$  (B, D and F). Ki-67+ neoplastic cells at  $T_0$  (A) and at  $T_1$  in a dog with partial response (B). Bcl-2+ neoplastic cells at  $T_0$  (C) and at  $T_1$  in a dog with partial response (D). Microvessels stained using an anti-CD31 primary antibody at  $T_0$  (E) and in the fibrotic tissue at  $T_1$  in a dog with a complete response (F). Immunohistochemical staining using DAB chromogen and haematoxylin counterstain. Bar = 100  $\mu$ m.

could be in situ vaccination, which can be boosted with peritumoral IL-12 gene electrotransfer, given peritumorally.<sup>3</sup> Our clinical study on MCT supports this hypothesis, providing evidence that this treatment combination has excellent local tumor control and also the long lasting disease free interval (between 3 and 4 years). Furthermore the present study immunohistologically supports the value of peritumoral IL-12 gene electrotransfer in boosting immune response of the organism, providing evidence of the presence of immune cells

(T-lymphocytes and macrophages) in the tumors treated with electrochemotherapy and peritumoral IL-12 gene electrotransfer compared to tumors before therapy. There is also another study on sarcoids in horses, using the same combined treatment in which increased number of CD4 and CD8 lymphocytes sub-population confirmed induction of local immune response in treated tumors.<sup>21</sup>

Even though in our study the number of examined biopsies was limited, at 4 weeks post-treatment our immunohistochemical results unequivocally

cally demonstrated an increase of T-lymphocytes in cellular infiltrates, higher in subjects with a complete response. T cells are the essential components of the adaptive immune response and they interact closely with antigen presenting cells to release various cytokines that characterize the specific immune response also to neoplastic cells. The T-lymphocyte increase detected after four weeks post treatment was not evident 4 weeks later, indicating that probably the anti-tumoral immune response induced by IL-12 is only transient as previously hypothesized or that due to the complete tumor regression, they could not be observed in higher numbers in the biopsies.<sup>15</sup>

The presence of B cells in examined subjects was not affected by IL-12 gene electrotransfer 4 as well as 8 weeks after the treatment. On the contrary, macrophages increased 8 weeks post-treatment, which was not related with the response to the therapy. The macrophages, as any innate immune cells, act when tissue homeostasis is perturbed, releasing soluble mediators such as cytokines, chemokines, matrix remodeling proteases and reactive oxygen species and contribute to the maintenance of the inflammation and this late increase of these cells detected in treated subjects should be related with the tissue damage induced by the therapy.

Tregs play an important role in down regulating immune responses and an imbalance between numbers of Tregs and CD4+ and CD8+ T-lymphocytes contributes to the outcomes in cancer and infectious diseases. Many studies have demonstrated the *in vivo* role of these cells in the suppression of the immune response to the cancer in human<sup>22,23</sup> and veterinary oncology.<sup>24,25</sup> While Treg are immunosuppressive at sites of inflammation, the increase detected in our study should be explained by previous studies demonstrating that the adjuvant activity of IL-12 is short-lived due to regulatory Treg re-infiltration. In fact, quantitative analysis of Treg kinetics in IL-12 treated tumors revealed a transient loss of these cells followed by a rapid fold expansion of tumor Treg between days 3 and 10 post treatment.<sup>26</sup> So the increase of Treg observed in our study should be related with the timing of tissue sampling after the treatment or due to the presence of inflammation.

In conclusion, our study confirmed the synergic power of electrochemotherapy and IL-12 gene electrotransfer in canine species at immunohistopathological level. It led to number of complete responses and extends survival through the induction of interferon gamma, inhibiting angiogenesis and increasing cytotoxic activity.<sup>3</sup>

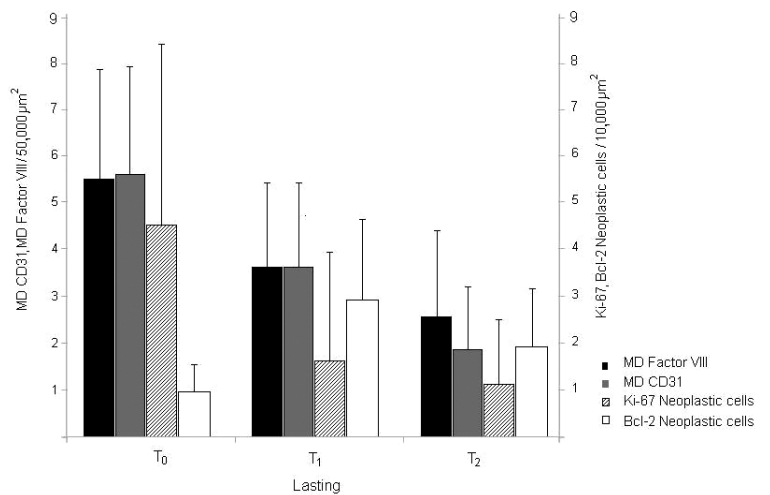


**FIGURE 5.** Histogram of microvessel density determined using both primary antibodies against Factor VIII and CD31 positive-cells in 50,000  $\mu\text{m}^2$  of tissue samples and number of Ki-67+ and Bcl-2+ neoplastic cells in 10,000  $\mu\text{m}^2$  of tissue samples collected at T<sub>0</sub>, T<sub>1</sub> and T<sub>2</sub>. Microvessel density was drastically reduced at T<sub>1</sub> and T<sub>2</sub>, as well as the proliferation activity of neoplastic cells, while Bcl-2 expression was increased at T<sub>1</sub>.

## Acknowledgements

Slovenian Research Agency has supported this research by grants P3-0003 (Gregor Sersa), P4-0053 (Milka Vrecl Fazarinc), J3-6796 (Maja Cemazar). Research was conducted in the scope of the EBAM European Associated Laboratory (LEA) and resulted from the networking efforts of the COST Action TD1104 ([www.electroporation.net](http://www.electroporation.net)).

## References

- Campana L, Clover AJP, Valpione S, Quaglino P, Gehl J, Kunte C, et al. Recommendations for improving the quality of reporting clinical electrochemotherapy studies based on qualitative systematic review. *Radiol Oncol* 2016; **50**: 1-12. doi:10.1515/raon-2016-0006
- Cemazar M, Tamzali Y, Sersa G, Tozon N, Mir LM, Miklavcic D, et al. Electrochemotherapy in veterinary oncology. *J Vet Int Med* 2008; **22**: 826-31. doi:10.1111/j.1939-1676.2008.01117.x
- Sersa G, Teissie J, Cemazar M, Signori E, Kamensek U, Marshall G, et al. Electrochemotherapy of tumors as in situ vaccination boosted by immunogene electrotransfer. *Cancer Immunol Immunother* 2015; **64**: 1315-27. doi:10.1007/s00262-015-1724-2
- Sedlar A, Dolinsek T, Markelc B, Prosen L, Kranjc S, Bosnjak M, et al. Potentiation of electrochemotherapy by intramuscular IL-12 gene electrotransfer in murine sarcoma and carcinoma with different immunogenicity. *Radio Oncol* 2012; **46**: 302-11. doi:10.2478/v10019-012-0044-9
- Kishida T, Asada H, Itokawa Y, Yasutomi K, Shin-Ya M, Gojo S, et al. Potentiation of electrochemotherapy of cancer: intratumoral delivery of interleukin-12 gene and bleomycin synergistically induced therapeutic immunity and suppressed subcutaneous and metastatic melanomas in mice. *Mol Ther* 2003; **8**: 738-45.
- Torrero MN, Henk WG, Li S. Regression of high-grade malignancy in mice by bleomycin and interleukin-12 electrochemotherapy. *Clin Cancer Res* 2006; **12**: 257-63. doi:10.1158/1078-0432.CCR-05-1514

- 7 Cutrera J, Torrero M, Shiomitsu K, Mauldin N, Li S. Intratumoral bleomycin and IL-12 electrochemogenetherapy for treating head and neck tumors in dogs. *Methods Mol Biol* 2008; **423**: 319-25. doi:10.1007/978-1-59745-194-9\_24
- 8 Cutrera J, King G, Jones P, Kicenuik K, Gumpel E, Xia X, et al. Safety and efficacy of tumor-targeted interleukin 12 gene therapy in treated and non-treated, metastatic lesions. *Curr Gene Ther* 2015; **15**: 44-54.
- 9 Cutrera J, King G, Jones P, Kicenuik K, Gumpel E, Xia X, et al. Safe and effective treatment of spontaneous neoplasms with interleukin 12 electrochemo-gene therapy. *J Cell Mol Med* 2015, **19**: 664-75. doi:10.1111/jcmm.12382
- 10 Pavlin D, Cemazar M, Coer A, Sersa G, Pogacnik A, Tozon N. Electrogene therapy with interleukin-12 in canine mast cell tumors. *Radiol Oncol* 2011; **45**: 31-9. doi:10.2478/v10019-010-0041-9
- 11 Cemazar M, Ambrozic Avgustin J, Pavlin D, Sersa G, Poli A, Krhac Levacic A, et al. Efficacy and safety of electrochemotherapy combined with peritumoral IL-12 electrotransfer of canine mast cell tumors. *Vet Comp Oncol* 2017; **15**: 641-4. doi:10.1111/vco.12208
- 12 Pavselj N, Preat V. DNA electrotransfer into the skin using a combination of one high- and one low-voltage pulse. *J Control Release* 2005; **106**: 407-15. doi:10.1016/j.jconrel.2005.05.003
- 13 Kiupel M, Webster JD, Bailey KL, Best S, DeLay J, Detrisac CJ, et al. Proposal of a 2-tier histologic grading system for canine cutaneous mast cell tumors to more accurately predict biological behavior. *Vet Pathol* 2011; **48**: 147-55. doi:10.1177/0300985810386469
- 14 Jamieson ER, Lippard SJ. Structure, recognition, and processing of cisplatin-DNA adducts. *Chem Rev* 1999; **99**: 2467-98.
- 15 Scarfò L, Ghia P. Reprogramming cell death. BCL2 family inhibition in hematological malignancies. *Immunol Lett* 2013; **155**: 36-9. doi:10.1016/j.imlet.2013.09.015
- 16 Belehradec J, Orłowski S, Poddevin B, Paoletti C, Mir LM. Electrochemotherapy of spontaneous mammary tumours in mice. *Eur J Cancer* 1991; **27**: 73-6.
- 17 Sersa G, Jarm T, Kotnik T, Coer A, Podkrajek M, Sentjurc M. Vascular disrupting action of electroporation and electrochemotherapy with bleomycin in murine sarcoma. *Br J Cancer* 2008; **98**: 388-98. doi:10.1038/sj.bjc.6604168
- 18 Trinchieri G. Interleukin-12 and the regulation of innate resistance and adaptive immunity. *Nat Rev Immunol* 2003; **3**:133-46. doi:10.1038/nri1001
- 19 Cutrera J, Li S. Passive and active tumor homing cytokine therapy. In: Lustgarten J, Cui Y, Li S, editors. *Targeted cancer immune therapy*. New York: Springer; 2009. p. 97-113.
- 20 Del Vecchio M, Bajetta E, Canova S, Lotze MT, Wesa A, Parmiani G, et al. Interleukin-12: biological properties and clinical application. *Clin Cancer Res* 2007; **13**: 4677-85. doi:10.1158/1078-0432.CCR-07-0776
- 21 Tamzali Y, Borde L, Rols MP, Golzio M, Lyazrhi F, Teissie J. Successful treatment of equine sarcoids with cisplatin electrochemotherapy: a retrospective study of 48 cases. *Equine Vet J* 2012; **44**: 214-20. doi:10.1111/j.2042-3306.2011.00425.x
- 22 Curiel TJ, Coukos G, Zou L, Alvarez X, Cheng P, Mottram P, et al. Specific recruitment of regulatory T cells in ovarian carcinoma fosters immune privilege and predicts reduced survival. *Nat Med* 2004; **10**: 942-9. doi:10.1038/nm1093
- 23 Zhou J, Ding T, Pan W, Zhu LY, Li L, Zheng L. Increased intratumoral regulatory T cells are related to intratumoral macrophages and poor prognosis in hepatocellular carcinoma patient. *Int J cancer* 2009, **125**: 1640-8. doi:10.1002/ijc.24556
- 24 Kim JH, Hur JH, Lee SM, Im KS, Kim NH, Sur JH. Correlation of Foxp3 positive regulatory T cells with prognostic factors in canine mammary carcinomas. *Vet J* 2012; **193**: 222-7. doi:10.1016/j.tvjl.2011.10.022
- 25 Oh SY, Ryu HH, Yoo DY, Hwang IK, Kweon OK, Kim WH. Evaluation of FOXP3 expression in canine mammary gland tumours. *Vet Comp Oncol* 2014; **12**: 20-8. doi:10.1111/j.1476-5829.2012.00327.x
- 26 Li Q, Virtuoso LP, Anderson CD, Egilmez NK. Regulatory rebound in IL-12 treated tumors is driven by uncommitted peripheral regulatory T cells. *J Immunol* 2015, **195**: 1293-1300. doi:10.4049/jimmunol.1403078

# *In vitro* and *in vivo* evaluation of electrochemotherapy with *trans*-platinum analogue *trans*-[PtCl<sub>2</sub>(3-Hmpy)<sub>2</sub>]

Simona Kranjc<sup>1</sup>, Maja Cemazar<sup>1,2</sup>, Gregor Sersa<sup>1,3</sup>, Janez Scancar<sup>4</sup>, Sabina Grabner<sup>5</sup>

<sup>1</sup> Institute of Oncology Ljubljana, Department of Experimental Oncology, Ljubljana, Slovenia

<sup>2</sup> University of Primorska, Faculty of Health Sciences, Izola, Slovenia

<sup>3</sup> Faculty of Health Sciences, University of Ljubljana, Ljubljana, Slovenia

<sup>4</sup> Department of Environmental Sciences, Jozef Stefan Institute, Ljubljana, Slovenia

<sup>5</sup> Faculty of Chemistry and Chemical Technology, University of Ljubljana, Ljubljana, Slovenia

Radiol Oncol 2017; 51(3): 295-306.

Received 20 July 2017

Accepted 4 August 2017

Correspondence to: Simona Kranjc, Ph.D., Department of Experimental Oncology, Institute of Oncology Ljubljana, Zaloška 2, SI-1000 Ljubljana, Slovenia. Phone/Fax: +386 1 5879 434; E-mail: skranjc@onko-i.si

Disclosure: No potential conflicts of interest were disclosed.

**Background.** Cisplatin is used in cancer therapy, but its side effects and acquired resistance to cisplatin have led to the synthesis and evaluation of new platinum compounds. Recently, the synthesized platinum compound *trans*-[PtCl<sub>2</sub>(3-Hmpy)<sub>2</sub>] (3-Hmpy = 3-hydroxymethylpyridine) (compound **2**) showed a considerable cytotoxic and antitumour effectiveness. To improve compound **2** cytotoxicity *in vitro* and antitumour effectiveness *in vivo*, electroporation was used as drug delivery approach to increase membrane permeability (electrochemotherapy).

**Materials and methods.** *In vitro*, survival of sarcoma cells with different intrinsic sensitivity to cisplatin (TBLCI2 sensitive, TBLCI2Pt resistant and SA-1 moderately sensitive) was determined using a clonogenic assay after treatment with compound **2** or cisplatin electrochemotherapy. *In vivo*, the antitumour effectiveness of electrochemotherapy with compound **2** or cisplatin was evaluated using a tumour growth delay assay. In addition, platinum in the serum, tumours and platinum bound to the DNA in the cells were performed using inductively coupled plasma mass spectrometry.

**Results.** *In vitro*, cell survival after treatment with compound **2** electrochemotherapy was significantly decreased in all tested sarcoma cells with different intrinsic sensitivity to cisplatin (TBLCI2 sensitive, TBLCI2Pt resistant and SA-1 moderately sensitive). However, this effect was less pronounced compared to cisplatin. Interestingly, the enhancement factor (5-fold) of compound **2** cytotoxicity was equal in cisplatin-sensitive TBLCI2 and cisplatin-resistant TBLCI2Pt cells. *In vivo*, the growth delay of subcutaneous tumours after treatment with compound **2** electrochemotherapy was lower compared to cisplatin. The highest antitumour effectiveness after cisplatin or compound **2** electrochemotherapy was obtained in TBLCI2 tumours, resulting in 67% and 11% of tumour cures, respectively. Compound **2** induced significantly smaller loss of animal body weight compared to cisplatin. Furthermore, platinum amounts in tumours after compound **2** or cisplatin electrochemotherapy were approximately 2-fold higher compared to the drug treatment only, and the same increase of platinum bound to DNA was observed.

**Conclusions.** The obtained results *in vitro* and *in vivo* suggest compound **2** as a potential antitumour agent in electrochemotherapy.

Key words: platinum analogue; cisplatin; 3-Hmpy; electroporation; electrochemotherapy; mouse sarcoma

## Introduction

Cisplatin is used for the treatment of variable types of cancers (testicular, bladder, ovarian, en-

dometrial, cervical, lung, head and neck), and primarily systemically used as single drug or in combination with other drugs and/or in combination with radiation therapy, immunotherapy or

other targeted therapies.<sup>1-3</sup> Despite many efforts in adapting an appropriate therapy schedule with cisplatin, the treatment of patients with cisplatin induces side effects, and cancer cells can acquire resistance to cisplatin through different mechanisms. Among these mechanisms, the inactivation of cisplatin via thiol-containing molecules, such as glutathione and metallothionein, increased the repair of cisplatin-DNA adducts, enhanced tolerance to cisplatin-DNA adducts, resulting in the failure of apoptotic pathways and reduction of platinum accumulation through decreased drug uptake or increased drug efflux.<sup>4-8</sup> Therefore, overcoming side effects and acquired resistance of cells to cisplatin during the treatment of patients with cisplatin still remains the main challenge in studies of platinum analogues. Modification of platinum compounds with variable ligands (iminoethers, aliphatic amines, amine piperazine and pyridine) in the *trans* position of ligands resulted in variable cytotoxic effects.<sup>9-17</sup> Pyridine ligands with hydroxyl groups, which participate in the formation of stable complex between DNA and platinum compounds, were demonstrated as promising ligands in activating platinum (II) compound cytotoxicity.<sup>9,11,14,18-20</sup> Recently, we reported that two 3-hydroxymethylpyridine (3-Hmpy) ligand in the *trans* position in the platinum (II) complex increased cytotoxicity *in vitro* and antitumour effectiveness *in vivo*.<sup>21</sup>

The effectiveness of chemotherapeutic drugs relies on their uptake into tumour cells. For poorly permeable drugs, higher doses are needed for effective cytotoxicity to tumour cells, consequently producing higher side effects. Cisplatin is a poorly permeable drug; therefore, many approaches have been examined to increase its uptake, *i.e.*, using nanoparticles, magnetic particles, liposomes, and tumour-specific antibodies and chemically or physically inducing pores in the cell membrane.<sup>16,22-23</sup> Among physical approaches, electroporation, inducing pores in the cell membrane via electric pulses, could be used.<sup>24</sup> Electroporation increases the cytotoxicity up to 80-fold in cisplatin-sensitive and cisplatin-resistant tumour models, *in vitro* and *in vivo*.<sup>25-29</sup> The treatment of tumour nodules with the local application of electric pulses after systemic or local administration of drug is referred to as electrochemotherapy. Electrochemotherapy with cisplatin is currently used for the treatment of variable cutaneous and subcutaneous tumours in human and veterinary clinics, showing a local effectiveness of up to 80% of local tumour control.<sup>30-33</sup> The antitumour effectiveness of electrochemotherapy primarily relies on increased drug uptake and

platinum binding to DNA.<sup>25,29,34</sup> However, some effects might be attributed to immune system modulation and changes in tumour blood flow.<sup>27,35-36</sup>

Thus far, electroporation has been used to increase antitumour effectiveness of platinum (II) analogue 3P-SK containing squarato (skv = 3,4-dioxocyclobut-1-ene-1,2-diolate) and 3-Hmpy ligands (3P-SK, [Pt(3-Hmpy)<sub>2</sub>(skv)]). Indeed, 3P-SK electrochemotherapy treatment had a profound antitumour effectiveness in mouse MCA mammary carcinoma, demonstrating 3P-SK as the first biologically active squarato compound with two 3-Hmpy ligands *in vivo*.<sup>19</sup>

The promising cytotoxic and antitumour effectiveness of compound **2** from a previous study<sup>21</sup> encouraged us to assess the electroporation, as drug delivery method, for compound **2** in *in vitro* and *in vivo* tumour models with different intrinsic sensitivities to cisplatin. *In vitro*, clonogenic assays were performed to demonstrate the cytotoxicity of compound **2**. The cytotoxicity of compound **2** alone or in combination with electroporation was investigated in sarcoma cisplatin-sensitive TBLCl2 cells and the cisplatin-resistant subclone TBLCl2Pt, and in sarcoma SA-1 cells with moderate sensitivity to cisplatin, based on *in vitro* data.<sup>25,37</sup> Furthermore, the antitumour effectiveness of compound **2** electrochemotherapy using tumour growth delay assay was determined in the same sarcoma tumour models *in vivo*. In addition, the animal body weight loss was monitored to estimate the influence of the intratumoural administration of compound **2** and local application of electric pulses to the tumour on animal wellbeing. To clarify the underlying mechanism of antitumour effectiveness of compound **2** electrochemotherapy, the amount of platinum in serum and the platinum uptake into tumours, and platinum binding to DNA were measured.

## Materials and methods

### Drugs

Cisplatin (CDDP, Cysplatyl, Aventis Laboratory, Paris, France) was dissolved in sterile water at concentration of 10 mM and frozen in aliquots at -20°C until further use. The compound **2** (*trans*-[PtCl<sub>2</sub>(3-Hmpy)<sub>2</sub>]) was synthesized at the Faculty of Chemistry and Chemical Technology, University of Ljubljana (Ljubljana, Slovenia)<sup>21</sup> and dissolved in *N,N*-dimethyl-formamide (DMF, Sigma-Aldrich Co. LCC, St. Louis, MO) at a concentration of 10 mM and frozen in aliquots at -20°C until further use.

In the *in vitro* experiments, concentrations of CDDP and compound **2** ranging from 1.7  $\mu\text{M}$  to 1333  $\mu\text{M}$  were prepared in a sterile electroporation buffer (EP buffer, 125 mM sucrose, 10 mM  $\text{K}_2\text{HPO}_4$ , 2.5 mM  $\text{KH}_2\text{PO}_4$ , and 2 mM  $\text{MgCl}_2 \times 6 \text{H}_2\text{O}$ ) immediately prior to the experiments.

In the *in vivo* experiments, fresh solutions of CDDP and compound **2** were prepared in sterile NaCl solution (0.9%) at a final concentration of 13.3 mmol/kg.

### Tumour cell lines

Mouse SA-1 sarcoma cells (Jackson Laboratory, Bar Harbor, ME, USA), mouse TBLCl2 sarcoma cells and the cisplatin-resistant subclone TBLCl2Pt (generously provided by J. Belehradec of the Institute Gustave Roussy, Villejuif, France)<sup>38</sup> were used for the *in vitro* experiments. The SA-1, TBLCl2 and TBLCl2Pt cells were cultured in a humidified incubator at 37°C and 5%  $\text{CO}_2$  in advanced minimum essential media (AMEM, Gibco, Life Technologies Corporation, Grand Island, NY, USA), supplemented with 5% of foetal bovine serum (FBS, Gibco). Two days after sub-culturing, the cells in the exponential phase of growth were obtained and used for the cytotoxicity experiments or for the induction of subcutaneous tumours.

### Animals and tumour models

Animal experiments were conducted in accordance with the Veterinary Administration of the Republic of Slovenia (permission No: 34401-10/2009/6). Inbred A/J and C57Bl/6 mice, females 10-12 weeks old, were purchased from the Institute of Pathology, Medical Faculty, University of Ljubljana (Ljubljana, Slovenia) and acclimated to the facility for 10 days. The mice were maintained under specific pathogen-free conditions, at a constant room temperature in a 12-hour day/night light cycle. Food and water were provided *ad libitum*. Subcutaneous tumours were induced via the injection of 100  $\mu\text{L}$  of cell suspension in the right shaved flank of mice; injection of SA-1 sarcoma tumour cell suspension ( $5 \times 10^6$  cells/mL; obtained from ascites of the donor animal) in A/J mice; injection of TBLCl2 sarcoma ( $25 \times 10^6$  cells/mL; obtained *in vitro*) and TBLCl2Pt cell suspension ( $40 \times 10^6$  cells/mL; obtained *in vitro*) in C57Bl/6 mice.

### Cytotoxicity of electrochemotherapy *in vitro*

In the experiments, variable groups were used: control (untreated cells), CDDP or compound

**2** (5 minutes incubation of cells with drug), electroporation (EP, cells exposed to application of electric pulses), electrochemotherapy (ECT, cells exposed to combination of EP and drug, CDDP or compound **2**). Briefly, cell suspensions of SA-1, TBLCl2 and TBLCl2Pt sarcoma cells in EP buffer at concentration  $2.2 \times 10^7$  cells/mL were prepared via the trypsinization (Trypsin, Gibco) of two day-old monolayers. The cytotoxicity of treatments was determined using a clonogenic assay. In the EP group, 5  $\mu\text{L}$  of EP buffer was added to 45  $\mu\text{L}$  ( $1 \times 10^6$ ) of cell suspension and subsequently placed between two parallel stainless-steel plate electrodes at a 2-mm distance and thereafter exposed to 8 electric pulses (electric field over distance ratio of 1300 V/cm, duration time of each pulse 100  $\mu\text{s}$ , at frequency of 1 Hz; generated at Jouan GHT 1287, St. Herblain, France).<sup>26,27</sup> In CDDP or compound **2** groups, 45  $\mu\text{L}$  ( $1 \times 10^6$ ) of cell suspension was diluted with 5  $\mu\text{L}$  of drug solution at a ten times higher final concentration (1.7  $\mu\text{M}$ -1333  $\mu\text{M}$ ). In the ECT group, 45  $\mu\text{L}$  ( $1 \times 10^6$ ) of cell suspension was diluted with 5  $\mu\text{L}$  of drug solution at a ten times higher final concentration (1.7  $\mu\text{M}$ -1333  $\mu\text{M}$ ) and immediately exposed to electric pulses. Regardless of the treatment, the cells were incubated for 5 minutes at room temperature (22°C) in an ultra-low attachment 24-well plate. Subsequently, the cells (50  $\mu\text{L}$ ) were diluted in 1 mL of fresh medium and a variable number of cells were seeded onto a Petri dish (diameter = 6 cm; 200 to 800 cells/Petri dish) for clonogenic assay. In 7-14 days, viable clonogenic cells formed colonies that were stained with crystal violet (0.005%, Sigma, St. Louis, USA), and only the colonies containing at least 50 cells were counted. The experiment was repeated three times, and each group comprised three replicates.

### Electrochemotherapy of tumours *in vivo*

The antitumour effectiveness of electrochemotherapy was evaluated using a tumour growth delay assay. When subcutaneous tumours grew to a volume of 40  $\text{mm}^3$  in approximately 7-14 days, the animals were divided randomly in experimental groups: control (untreated tumours), CDDP or compound **2** group (intratumoural injection of 50  $\mu\text{L}$  drug solution, CDDP or compound **2**), EP (local application of 8 electric pulses in two perpendicular directions (4+4), with electric field over distance ratio of 1300 V/cm, 100  $\mu\text{s}$  long, 1 Hz, using two plate parallel stainless-steel electrodes 7 mm apart placed percutaneously at the opposite margins of tumour; generated by Jouan GHT 1287,

St. Herblain, France) and combined treatment, electrochemotherapy, *i.e.*, 60 seconds after intratumoural injection of 50  $\mu\text{L}$  drug solution electric pulses were applied. Each experimental group comprised 6 to 12 animals. The antitumour effectiveness of therapies was followed by measuring three orthogonal tumour diameters (a, b, c) every other day after therapy using a Vernier calliper and the tumour volume was subsequently calculated using the formula  $a \times b \times c \times \pi / 6$ . The tumour doubling time for each experimental group based on, tumour growth delay (the tumour doubling time for each experimental group subtracted from the tumour growth delay of control group), was determined as the endpoint of antitumour effectiveness of electrochemotherapy with cisplatin or compound **2**. Growth of treated tumours was followed up to a volume of 350  $\text{mm}^3$  or in the case of completely regressed tumours, up to 100 days after the treatment (complete response, CR). At these times, the animals were humanely sacrificed via cervical dislocation. Potential side effects of therapies were determined after weighing the animals and assessing behaviour and locomotion.

### Platinum determination in tumour and serum

Measurements of platinum in the serum, tumours and platinum bound to the DNA in the cells were performed using inductively coupled plasma mass spectrometry (ICP-MS, Agilent Technologies, model 7700x, Tokyo, Japan), which monitored the  $^{195}\text{Pt}$  isotope. To determine platinum accumulation in the serum at different time points after treatment (3 minutes, 1 hour, 8 and 24 hours), the blood was collected using a glass capillary from intraorbital sinus (8 samples per group) and coagulated at room temperature for two hours. Subsequently, the blood was centrifuged at 3000 rpm for 10 minutes, and the serum was collected and stored at  $-20^\circ\text{C}$ . Furthermore, the total volume of serum samples was digested in 1 mL of 1:1 mixture of 65% nitric acid (MERCK KgaA, Darmstadt, Germany) and 30% hydrogen peroxide (MERCK KgaA, Darmstadt, Germany) at  $90^\circ\text{C}$  for 48 hours. The obtained clear solutions were diluted with Milli-Q water and analysed using ICP-MS.

To obtain tumour samples for platinum determination, the animals were humanely sacrificed immediately after the blood was collected. Tumours were excised (8 samples per group), removed from the overlying skin, weighed and stored at  $-20^\circ\text{C}$ . Subsequently, the tumours were digested in 2 mL

of 1:1 mixture of 65% nitric and 30% hydrogen peroxide) at  $90^\circ\text{C}$  for 48 hours, diluted with Milli-Q water and analysed using ICP-MS.

For measurements of platinum binding to the DNA in the tumour cells, the tumours were obtained as described above. However, the tumours were weighed, immediately mechanically degraded and washed with 3 mL of freshly prepared PBS. Collected samples were filtered through a cell strainer with a pore size of 40  $\mu\text{m}$  (Corning Incorporated, Life Sciences, Durham, USA) and centrifuged at 1500 rpm for 10 minutes. The collected cells were used for the fast DNA isolation using a salting-out protocol. First, the cells were lysed with lysis buffer (10 mM Tris-HCl, 1 mM EDTA, and 1% SDS) containing proteinase K (0.2  $\mu\text{g}/\text{mL}$ ) at  $55^\circ\text{C}$  and constant shaking for 30 minutes. The proteins in the cooled samples were precipitated using 120  $\mu\text{L}$  of 4 M NaCl and shaking for 15 seconds. The precipitated proteins were two times centrifuged at 13000 rpm for 6 minutes. DNA was precipitated from the obtained supernatant using 1 mL of ethanol (70%) for 2 minutes by gentle mixing of tube and centrifugation at 13000 rpm for 2 minutes. The precipitated DNA was washed with an additional 1 mL of ethanol (70%) and centrifuged at 13000 rpm for 2 minutes. The pellet of DNA was dried, dissolved in 100  $\mu\text{L}$  of distilled water. The concentration of DNA in the samples was spectrophotometrically determined at 260 nm (Epoch, Take3, Bio Tek Germany). Finally, the samples of DNA were digested using the same procedure described above and the platinum binding to DNA was determined in the diluted samples using ICP-MS.

### Statistical analysis

Statistical analysis was performed using SigmaPlot software (Systat Software, Chicago, IL, USA). The Shapiro-Wilk test was used to determine the normality of data distribution. The differences between mean values of experimental groups were tested using the t-test or one-way ANOVA, followed by the Holm-Sidak test for multiple comparisons. Values of  $p < 0.05$  were considered significant.

## Results and discussion

Recently, discovered biological activity of *trans* platinum complexes with planar aromatic N-donor base<sup>21</sup>, encouraged us to examine compound **2** with electroporation (electrochemotherapy) as a drug delivery approach in tumour cells with different

TABLE 1. IC<sub>50</sub> values after electrochemotherapy with cisplatin or compound 2 in various mouse tumour cell lines

Group	SA-1		TBLCl2		TBLCl2Pt	
	IC <sub>50</sub> (μM)	EF	IC <sub>50</sub> (μM)	EF	IC <sub>50</sub> (μM)	EF
CDDP	276.7 <sup>†</sup>		180.0 <sup>†</sup>		926.6 <sup>†</sup>	
Compound 2	500.0 <sup>*</sup>		220.0 <sup>*</sup>		1066.6 <sup>*</sup>	
ECT CDDP	28.3 <sup>*</sup>	9.8	8.0 <sup>*</sup>	22.5	12.0 <sup>*</sup>	77.2
ECT Compound 2	80.0	6.3	41.0	5.4	206.7	5.2

IC<sub>50</sub> = dose of drug which reduced cell survival to 50%; EF = enhancement factor for electroporation of cells, calculated on the bases of IC<sub>50</sub> of electroporated and non-electroporated cells; <sup>†</sup>p (< 0.05) statistically significant difference compared to treatment with cisplatin electrochemotherapy (ECT CDDP); <sup>\*</sup>p (< 0.05) significant difference compared to treatment with compound 2 electrochemotherapy (ECT Compound 2); <sup>†</sup>p (< 0.05) statistically difference compared to treatment with compound 2 electrochemotherapy.

intrinsic sensitivities to cisplatin *in vitro* and tumour models *in vivo*. *In vitro*, compound 2 electrochemotherapy was effective in cisplatin-sensitive and cisplatin-resistant cells. However, its cytotoxic effect (at the IC<sub>50</sub> level) was less evident compared to cisplatin electrochemotherapy, with up to 4-fold in cisplatin-sensitive TBLCl2 cells, up to 1.6-fold in moderately cisplatin-sensitive SA-1 cells and up to 15-fold in cisplatin-resistant TBLCl2Pt cells. Similar to *in vitro* data, growth of tumours with variable intrinsic sensitivity to cisplatin (sensitive, moderately sensitive and resistant) after compound 2 electrochemotherapy was less delayed (up to 9.7 days) compared to cisplatin electrochemotherapy. As expected, the most evident antitumour effectiveness of compound 2 and cisplatin electrochemotherapy was obtained in cisplatin-sensitive TBLCl2 tumours, resulting in 11% and 67% of cured tumours, respectively. However, compound 2 electrochemotherapy induced less animal body weight loss compared to cisplatin electrochemotherapy and considering its antitumour effectiveness could be potentially used in further investigation.

### Electrochemotherapy with cisplatin or compound 2 efficiently decreased cell survival, *in vitro*

Cytotoxicity of platinum compound with 3-hydroxymethylpyridine ligands in *cis* and *trans* position has previously been demonstrated in various human and mouse tumour cells.<sup>19-21</sup> First, in mouse B16 melanoma cells, *cis* platinum (II) compound with acyclovir (acv, (9-[(2-hydroxyetoxy)methyl] guanine)) and 3-Hmpy ([Pt([(acv-N7)<sub>2</sub>(3-Hmpy)<sub>2</sub>](NO<sub>3</sub>)<sub>2</sub>) was 1600-fold less cytotoxic compared to cisplatin. Furthermore, an increase of cytotoxicity

in cisplatin-sensitive and cisplatin-resistant human tumour cell lines was obtained using another platinum (II) compound 3P-SK containing 3-Hmpy and squarato ligands.<sup>19</sup> However, the enhancement of cytotoxicity was less pronounced compared to cisplatin, particularly in cisplatin-sensitive cells, with a 42-fold enhancement in MCF7 mammary carcinoma, and a 10-fold enhancement in T24 bladder carcinoma and IGROV ovarian carcinoma cells. The compound 3P-SK was least effective in cisplatin-resistant IGROV/RDDP ovarian carcinoma cells, showing only a 3-fold increase in IC<sub>50</sub> value compared to cisplatin.<sup>19</sup> Further synthesis of platinum analogues with 3-hmpy ligands led to the discovery of biological active platinum (II) compound with *trans* geometry possessing two 3-Hmpy ligands, compound 2. Recently, compound 2 was demonstrated as equally cytotoxic in various human cisplatin-sensitive T24 bladder carcinoma cells and IGROV 1 ovarian carcinoma cells, and in cisplatin-resistant IGROV 1/RDDP ovarian carcinoma cells compared to cisplatin.<sup>21</sup> In the present study, the cytotoxicity of compound 2 using clonogenic assay was determined in another pair of cisplatin-sensitive and cisplatin-resistant cells, TBLCl2 and TBLCl2Pt, respectively. Similarly, equal sensitivity of cisplatin-sensitive TBLCl2 and cisplatin-resistant TBLCl2Pt cells was observed, suggesting that compound 2 partially overcomes the mechanisms of resistance to cisplatin (Table 1, Figure 1). Thus, compound 2 could be potentially used in treatment to cisplatin resistant tumours alone or combined with other treatments, such as irradiation, in combination with other chemotherapeutics.

Knowing that cell membrane is the main barrier for drug import in cells, electroporation as the drug delivery method (electrochemotherapy)

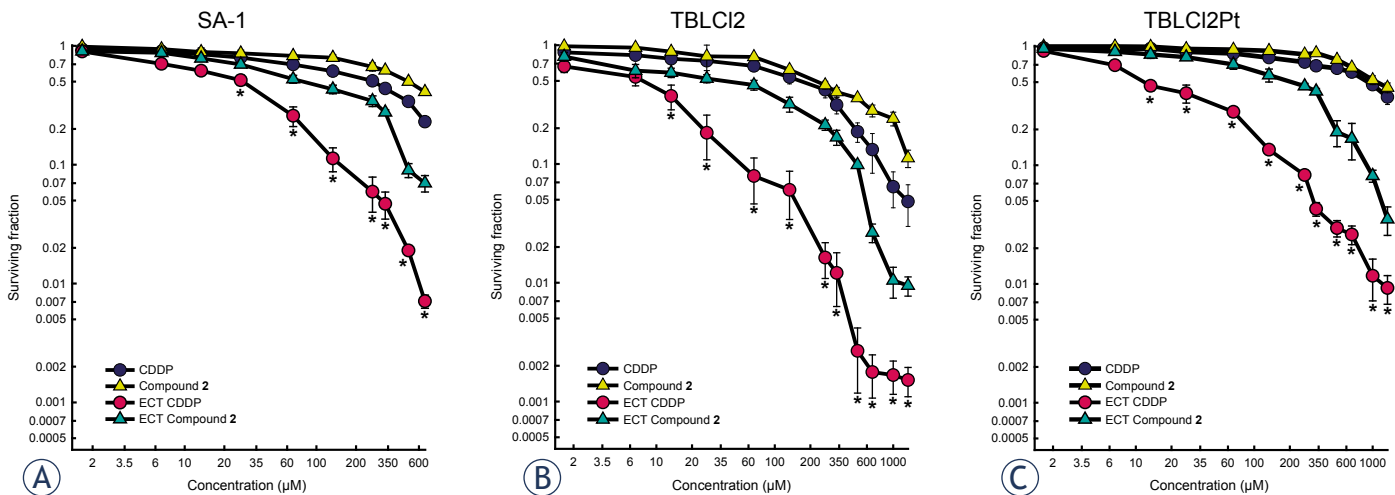


**FIGURE 1.** Survival of SA-1 sarcoma (A), TBLCl2 sarcoma (B) and TBLCl2Pt sarcoma cells (C) after treatment with cisplatin (CDDP) or compound 2 or cisplatin electrochemotherapy (ECT CDDP) or compound 2 electrochemotherapy (ECT Compound 2), determined using a clonogenic assay. Data are presented as the arithmetic mean and standard error of the mean (AM±SE) of triplicates pooled from three independent experiments. The survival of cells treated with electrochemotherapy was normalized to the survival of cells treated with electric pulses alone. The survival of SA-1, TBLCl2 and TBLCl2Pt cells treated with electric pulses alone was  $0.96 \pm 0.05$ ,  $0.93 \pm 0.09$  and  $0.92 \pm 0.10$ , respectively.

could be used for increasing the amount of compound 2 in the cell, thereby achieving the increased cytotoxic effectiveness of compound 2. The cytotoxicity of cisplatin or compound 2 electrochemotherapy was evaluated using a clonogenic assay in cell lines with different intrinsic sensitivities to cisplatin (sensitive TBLCl2, moderate sensitive SA-1 and resistant TBLCl2Pt cells) to obtain reliable results for the cytotoxic effect of compound 2 compared to cisplatin. Electrochemotherapy using either drug significantly decreased  $IC_{50}$  value in all tested cell lines. The most potentiated cytotoxic effect of cisplatin electrochemotherapy was observed in cisplatin-resistant TBLCl2Pt cells, resulting in a 77-fold decrease in  $IC_{50}$  value, as previously demonstrated (79-fold).<sup>25</sup> However, in moderately cisplatin-sensitive SA-1 cells and cisplatin-sensitive TBLCl2 cells, the reduction in  $IC_{50}$  value was less pronounced in cells exposed to cisplatin electrochemotherapy, and the determined decrease in  $IC_{50}$  up to 23-fold (Table 1), was in the range of previously published data (10.5-fold in SA-1 and 24-fold in TBLCl2 cells).<sup>25,37</sup> Using electroporation to increase compound 2 uptake into the cells improved cytotoxicity, resulting in an enhancement factor of 6.3-fold in SA-1 cells, 5.4-fold in TBLCl2 and 5.2-fold in TBLCl2Pt cells. However, the potentiation in the cytotoxic effect of compound 2 electrochemotherapy was significantly lower compared to cisplatin electrochemotherapy, but reflecting a similar enhancement factor in cisplatin-resistant TBLCl2Pt and cisplatin-sensitive TBLCl2 cells

(Table 1, Figure 1), compound 2 still represents a promising drug for further testing.

Since electroporation of cells with cisplatin renders cisplatin-resistant TBLCl2Pt cells to equal level of sensitivity as cisplatin-sensitive cells, and  $IC_{50}$  values were statistically non-significant, consistent with the data obtained in a previous study.<sup>25</sup> These data indicate increased membrane permeability as the predominant mechanism for the improved cytotoxicity of cisplatin. In fact, the same amount of platinum in both, cisplatin-sensitive TBLCl2 or cisplatin-resistant TBLCl2Pt cells induced equal cell killing.<sup>25</sup> Furthermore, the platinum content measured after electrochemotherapy with cisplatin or short 5 minutes incubation with cisplatin alone was comparable in both, cisplatin-sensitive TBLCl2 and cisplatin-resistant TBLCl2Pt cells.<sup>25</sup> In contrast, significant higher  $IC_{50}$  value determined after compound 2 electrochemotherapy (5-fold higher) in cisplatin-resistant TBLCl2Pt cells compared to cisplatin-sensitive TBLCl2 cells suggests the involvement of other mechanisms besides membrane permeability, such as transport mechanisms (influx or efflux of drug), increased level of thiol molecules in cells, enhanced DNA repair, tolerance to DNA damage and cell death decrease.<sup>4-6</sup> The function of compound 2 differs from that of cisplatin. Compound 2 induces severe conformational changes in plasmid DNA, suggesting that once in the cell, compound 2 likely induces few repairable or irreparable DNA damages, which are reflected in delayed apoptosis.<sup>21</sup>

**TABLE 2.** Antitumour effectiveness of electrochemotherapy with cisplatin or compound 2 in mouse sarcoma tumours; SA-1, TBLCI2 and TBLCI2Pt

Group	n	SA-1			TBLCI2			TBLCI2Pt				
		DT (days) (AM±SE)	GD (days)	CR (n, %)	n	DT (days) (AM±SE)	GD (days)	CR (n, %)	n	DT (days) (AM±SE)	GD (days)	CR (n, %)
Control	10	1.7±0.2		0	8	2.8±0.3		0	6	3.1±0.2		0
EP	10	3.1±0.3	1.4	0	8	5.1±1.0	2.3	0	6	4.2±0.9	1.1	0
CDDP	10	5.2±1.0 <sup>†</sup>	3.5	0	8	5.3±0.7 <sup>†</sup>	2.5	0	6	3.4±0.5 <sup>†</sup>	0.3	0
Compound 2	12	2.3±0.3 <sup>*</sup>	0.6	0	9	3.5±0.5 <sup>*</sup>	0.7	0	6	3.2±0.3 <sup>*</sup>	0.1	0
ECT CDDP	12	15.8±2.2 <sup>*</sup>	14.1	0	9	11.6±1.0	8.8	6, 66.6	6	7.6±0.9 <sup>*</sup>	4.5	0
ECT Compound 2	12	5.1±0.4	3.4	0	9	9.4±1.8	6.6	1, 11.1	6	5.1±0.6	2.0	0

EP = application of electric pulses; CDDP = cisplatin, intratumoural injection at a dose of 13.3 mmol/kg; Compound 2: intratumoural injection at a dose 13.3 mmol/kg; ECT = electrochemotherapy, application of EP at 1 minute after intratumoural injection of CDDP or compound 2; DT = tumour doubling time; GD = tumour growth delay; CR = complete response; AM = mean; SE = standard error of the mean; <sup>†</sup>p (< 0.05) significant difference compared to treatment with CDDP electrochemotherapy; <sup>\*</sup>p (< 0.05) significant difference compared to treatment with compound 2 electrochemotherapy.

### Electrochemotherapy with cisplatin or compound 2 efficiently delayed tumour growth *in vivo*

Until recently, few trans-Pt(II) complexes were evaluated *in vivo*. The analogues of transplatin (*trans*-[PtCl<sub>2</sub>(NH<sub>3</sub>)<sub>2</sub>]) with one NH<sub>3</sub> exchanged with pyridine or 4-methylpyridine had no effect in the S180 sarcoma tumour model.<sup>39</sup> In P388 leukaemia an evident antitumour effectiveness was obtained with compound having one iminoether instead of an amine ligand.<sup>40</sup> However, the replacement of two amine ligands with dimethylamine and isopropylamine failed to improve the antitumour activity in human CH ovarian carcinoma, reflecting its extracellular inactivation after binding to plasma proteins.<sup>41</sup> These results indicate the nature of the ligand as an important player in the biological activation of *trans*-Pt(II) compounds. Recently, we showed the promising biological activity of *trans*-Pt compound 2 with both amino groups replaced with pyridine derivate containing hydroxyl group, 3-Hmpy. Interestingly, a comparable antitumour effectiveness of treatment with triple intravenously administered compound 2 in sarcoma SA-1 tumours to cisplatin was obtained.<sup>21</sup>

To evaluate compound 2 as a potential chemotherapeutic drug in combination with electroporation, for the induction of subcutaneous tumours, the same mouse sarcoma tumour cell lines as used *in vitro* (moderately cisplatin-sensitive SA-1 cells, cisplatin-sensitive TBLCI2 and -resistant TBLCI2Pt cells) were selected. Since *in vitro* data have shown sarcoma cells as resistant to compound 2 (high IC<sub>50</sub>), the purpose of the research

was to evaluate whether the intrinsic resistance of these cells is reflected in tumours *in vivo*. The route (intratumoural or intravenous) of drug administration plays an important role in drug distribution and toxicity to normal tissues. In some cases, electrochemotherapy with intratumoural injection of cisplatin showed evident antitumour potential over systemic administration, reflecting a higher concentration of the drug obtained in tumours and lower concentration in normal tissues during electroporation.<sup>34,42</sup> Furthermore, compound 2 pharmacologically behaves differently compared to cisplatin, and more platinum in serum and tumour was observed.<sup>21</sup> According to these observations, in the present study, the single intratumoural administration of drug was used to potentially induce less side effects of the treatment and achieve the highest drug concentration in the tumours at the time of electroporation. In general, the antitumour effectiveness of treatment with compound 2 alone was less pronounced compared to cisplatin in all tumour models with intrinsically different sensitivity to cisplatin (Table 2, Figure 2). Treatment of moderately cisplatin-sensitive SA-1 tumours with cisplatin alone resulted in a significant delay of tumour growth compared to compound 2. Regarding the route of drug administration in SA-1 tumours, triple intravenous<sup>21</sup> or single intratumoural injection resulted in comparable antitumour effectiveness of cisplatin alone. However, the delay of tumour growth after triple intravenous administration of compound 2<sup>21</sup> was more pronounced (up to 2.2 days) compared to single intratumoural administration of compound 2 in the present study. Furthermore, antitumour

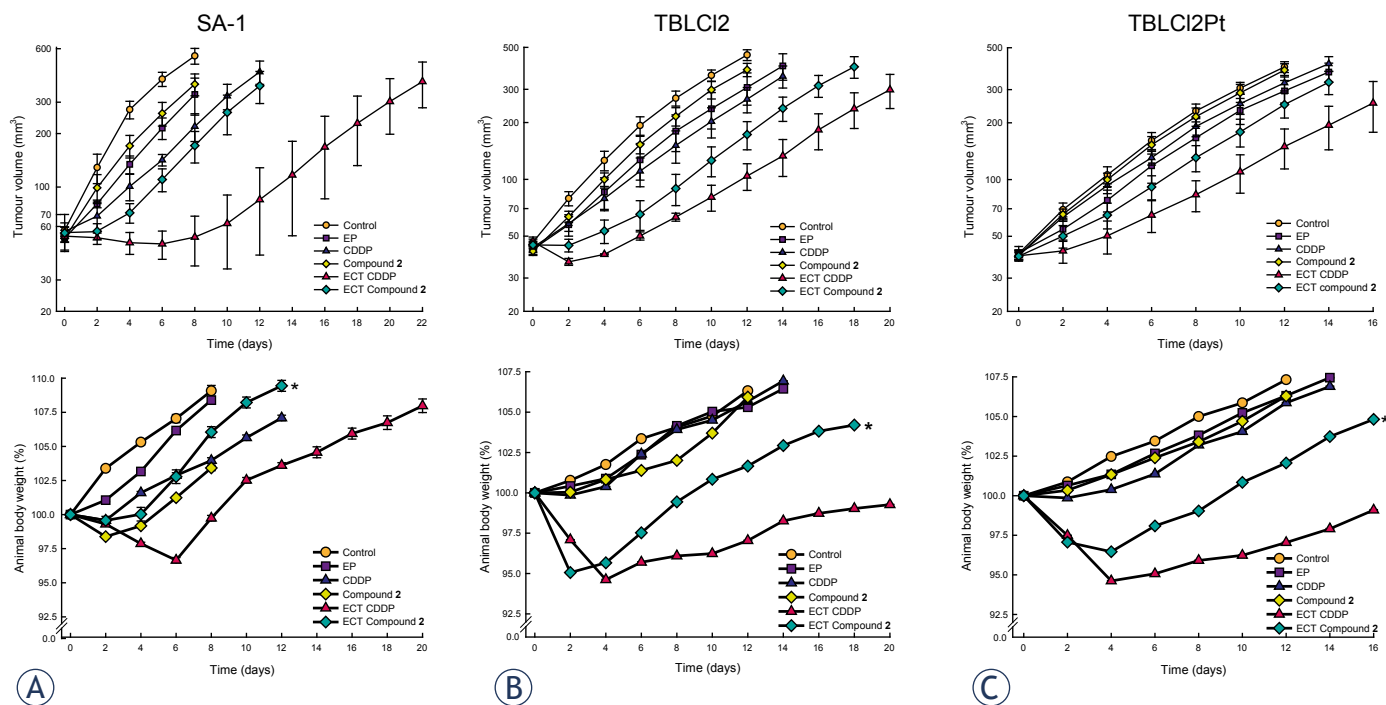


**FIGURE 2.** Tumour growth and animal body weight change after cisplatin or compound **2** electrochemotherapy in mouse sarcoma tumours; SA-1, TBLCl2 and TBLCl2Pt. Mice (6-12 per group) were treated with intratumoural injection of cisplatin (CDDP, 13.3 mmol/kg) or compound **2** (13.3 mmol/kg) or with local application of electric pulses at 1 minute after drug injection (ECT CDDP; ECT Compound **2**; 8 pulses, 1300 V/cm, 100  $\mu$ s, 1 Hz). Data are presented as the arithmetic mean and standard error of the mean (AM $\pm$ SE) of tumour volumes. \*p (< 0.05) significant difference compared to treatment with cisplatin electrochemotherapy

effectiveness was less evident in cisplatin-sensitive TBLCl2 and cisplatin-resistant TBLCl2Pt as in moderately cisplatin-sensitive SA-1 tumours, indicating different intrinsic features of the tumour models examined, particularly the mechanisms of resistance to cisplatin. Several efforts to overcome the mechanisms of cisplatin resistance, *i.e.*, using approaches to decrease glutathione level, affect DNA repair, activate signal transduction pathways leading to cell death and increase cisplatin accumulation, have been used.<sup>5,17,23,25,43-46</sup> The predominant mechanism of cisplatin resistance in TBLCl2Pt cells was suggested as the membrane restriction of cisplatin uptake.<sup>25</sup> Thus, electroporation could be used to overcome the resistance to cisplatin and potentiate antitumour effectiveness of cisplatin, as previously demonstrated in variable tumour models.<sup>19,25,28,34,37,42</sup> Application of electric pulses to the tumours alone insignificantly delayed tumour growth in all tested tumour models and the data are consistent with previous studies.<sup>25,28,38</sup> However, combined treatment of intratumoural injection either of cisplatin or compound **2** shortly before application of electric pulses, significantly potentiated (up to 3-fold) antitumour effectiveness in all tumour models, but less prominent

effects were observed with compound **2**. As expected, most pronounced antitumour effectiveness after single electrochemotherapy treatment was obtained in cisplatin-sensitive TBLCl2 tumours, resulting in 67% tumour cures after cisplatin electrochemotherapy and 11% tumour cures after compound **2** electrochemotherapy. Notably, cisplatin or compound **2** alone did not delay growth of cisplatin-resistant TBLCl2Pt tumours, but electroporation potentiated antitumour effectiveness of either of the drugs used, resulting in prolonged tumour 2.2-fold and 1.6-fold growth delay, respectively (Table 2, Figure 2). These data suggest that compound **2** electrochemotherapy as an appropriate alternative therapy in cisplatin-resistant tumours or tumours with acquired cisplatin-resistance. Studies using electroporation to improve the antitumour effectiveness of newly synthesized chemotherapeutic are scarce. Among the reported studies, two ruthenium (III) compounds, KP418 ((imH)[*trans*-RuCl<sub>4</sub>(im)<sub>2</sub>], im=imidazole) and KP1339 (Na[*trans*-RuCl<sub>4</sub>(in)<sub>2</sub>], in=indazole), administered intravenously, were used in combination with electroporation.<sup>47-48</sup> However, significant antitumour effectiveness was only obtained with KP1339 electrochemotherapy in SA-1 tumours,

while electrochemotherapy with KP418 has no significant effect on tumour growth delay in SA-1 and in B16F1 melanoma tumours. Although, the type of administration of KP1339 was different (intravenously), at equimolar doses, its antitumour effectiveness was comparable to the effect of compound 2. To our knowledge, only one synthesized platinum (II) compound with 3-Hmpy ligands, 3P-SK, was used in combination with electroporation in recent study of our research group.<sup>19</sup> In that study, similar to the results of the present study, the antitumour effectiveness of local application of electric pulses after intratumoural administration of 3P-SK was less pronounced compared to cisplatin. Still, 3P-SK electrochemotherapy significantly reduced growth of mouse MCA mammary carcinoma tumours and cured 14% of tumours.<sup>19</sup> Overall, considering the 3-fold potentiation in antitumour effectiveness of compound 2 electrochemotherapy compared to the 2-fold potentiation obtained after 3P-SK electrochemotherapy<sup>19</sup>, compound 2 may potentially be more biologically active. Moreover, the potentiation level in antitumour effectiveness of compound 2 electrochemotherapy compared to cisplatin electrochemotherapy, varied between 1.6- and 3-fold, suggesting that different transport mechanisms and intracellular mechanisms of action between compound 2 and cisplatin could be involved in tumour responses (Table 2, Figure 2).

In addition, animal body weight, behaviour and locomotion as indicators of animal wellbeing were monitored after cisplatin or compound 2 electrochemotherapy. Single treatment with intratumoural administration of compound 2 and application of electric pulses induced significantly less body weight loss compared to cisplatin. The animals showed a loss of body weight up to 6 days after treatment (approximately 6%) and recovered thereafter (Figure 2). These results are consistent with those of a previous study, showing that animals bearing SA-1 sarcoma lost significantly less body weight after triple intravenous administration of compound 2 compared to cisplatin.<sup>21</sup> However, the body weight loss obtained after single intratumoural administration of compound 2 compared to triple intravenous administration of compound 2 was less pronounced, indicating that the intratumoural administration of compound 2 was less toxic. Since electrochemotherapy with compound 2 demonstrates fewer side effects on animal wellbeing and despite less pronounced antitumour effectiveness compared to cisplatin, further studies are warranted, particularly for testing the repetitive treatment of tumours with electrochemotherapy.

### Electrochemotherapy with cisplatin or compound 2 increases platinum uptake in tumour and amount of platinum bound to DNA

To clarify whether the antitumour effectiveness of electrochemotherapy either with compound 2 or cisplatin was consistent with increased uptake of the drug in the cells and partially clarify the pharmacology of the drugs used, the amount of platinum was measured in tumours, serum and bound to the DNA. Previous studies have determined an increase in platinum accumulation after application of electric pulses in various mouse tumours (sarcoma (SA-1, LPB) and carcinoma (EAT) tumours), which consequently improve the antitumour effectiveness of cisplatin.<sup>27,29,34</sup> To prevent the washout of drug from the tumour and ensure the highest concentration in SA-1 tumours, electric pulses were delivered at 1 minute after intratumoural injection, as previously optimized in an EAT tumour model.<sup>34</sup> Measurement of platinum amount using ICP-MS in the present study demonstrated electroporation as an effective delivery method for compound 2, transplatin analogue, and cisplatin. An approximately significant 2-fold increase of platinum in tumours was achieved, resulting in pronounced antitumour effectiveness (Figure 3). Initial level of platinum amount in tumours treated with compound 2 alone or compound 2 electrochemotherapy was 1.3-fold higher compared to cisplatin. In addition, the wash out of platinum from the tumours treated with cisplatin or compound 2 alone was up to 1.5-fold quicker compared to tumours treated with electrochemotherapy using either of the drugs. The initial platinum amount in the tumours at one hour after the treatment with drug alone or with electrochemotherapy was reduced up to 48% and up to 18%, respectively, indicating the binding of tested drug to the proteins in serum, in extracellular tumour matrix and transport into the cell. In fact, the aromatic ring of pyridine and hydroxyl groups participates in non-covalent interactions between platinum compound and DNA.<sup>9, 11, 14, 18-20</sup> Furthermore, triple intravenous administration of compound 2 compared to cisplatin resulted in significant higher platinum amount in tumours and serum, 4-fold and 40-fold, respectively.<sup>21</sup> Similarly, significantly higher concentration (up to 39-fold) of platinum concentration in serum of animals treated either with compound 2 alone or compound 2 electrochemotherapy compared to cisplatin correlated with more platinum in tumours (Figure 3). Altogether, compound 2 exhibits a different phar-

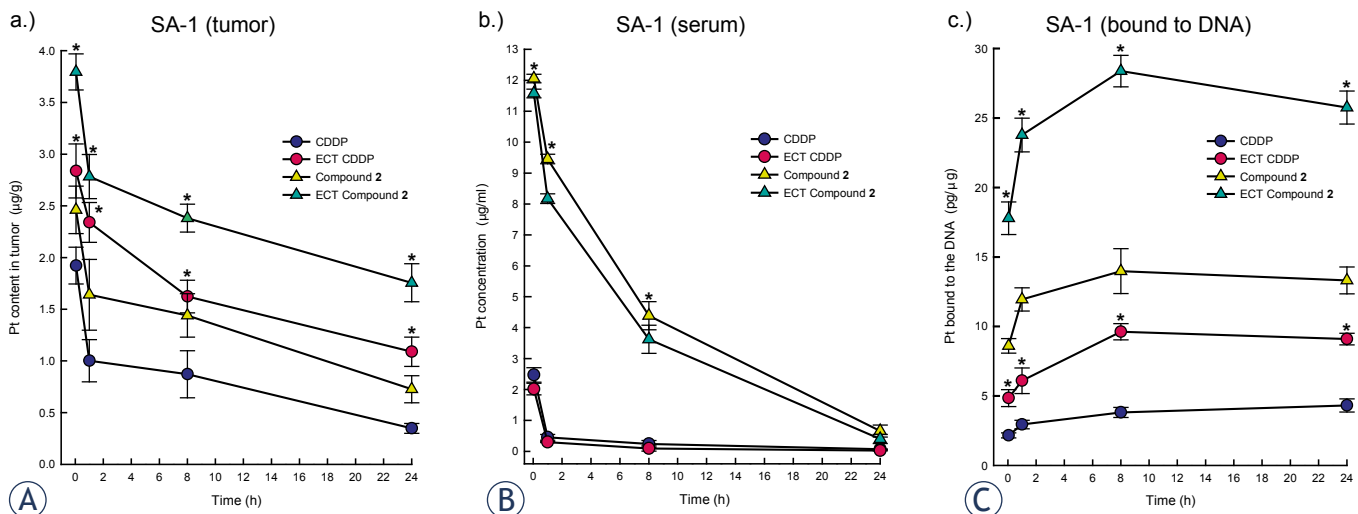


**FIGURE 3.** Platinum amount in sarcoma SA-1 tumours (A), platinum amount in the serum (B) and platinum amount bound to DNA in the cells isolated from SA-1 tumours (C). Animals (8 per group) were treated with intratumoural injection of cisplatin (CDDP, 13.3 mM) alone or compound 2 (13.3 mM) alone or with local application of electric pulses 1 minute after intratumoural drug injection (ECT CDDP; ECT Compound 2; 8 pulses, 1300 V/cm, 100 µs, 1 Hz). The data are presented as the arithmetic mean and standard error of the mean (AM±SE) obtained from 8 samples. \*p (< 0.05) under (A) and (C) statistically significant difference compared to corresponding drug treatment only; \*p (< 0.05) under (B) statistically significant difference compared to cisplatin or cisplatin electrochemotherapy.

macology compared to cisplatin, which could affect tumour responses. Compared to the pharmacology of cisplatin, other mechanisms could be involved in tumour responses to electrochemotherapy. In particular, the drug distribution in tumours depends on tumour vascularization and the content of tumour extracellular matrix, which plays an important role before application of electric pulses. Vascular disruption, reduced oxygenation and induced immune responses greatly contribute to tumour responses.<sup>35-36,49-50</sup>

DNA is considered the main intracellular target of cisplatin and its analogues. Hence, to clarify that antitumour effectiveness of electrochemotherapy primarily depends on increased drug uptake, the amount of platinum bound to DNA was evaluated as an indicator that compound 2 escaped binding to intracellular thiol proteins and reached DNA (Figure 3). Indeed, in tumours treated with electrochemotherapy compared to the drug administration only, approximately 2-fold higher platinum binding to DNA was achieved, correlated with pronounced antitumour effectiveness (Figure 3). Similarly, the higher level of platinum in tumours and serum in animals treated with compound 2 electrochemotherapy compared to cisplatin was reflected in a significantly (approximately 3-fold) higher amount of platinum bound to DNA. However, the antitumour effectiveness was less evident. Overall, a 4-fold increase of platinum bound to DNA was obtained in tumours

treated with compound 2 compared to cisplatin. *In vitro*, despite the enhanced accumulation of a trans-platinum (II) compounds, either with amine, oxine or piperidine ligand, in tumour cells, the cytotoxicity remained comparable or lower than that of cisplatin.<sup>51-53</sup> Thus, the increased accumulation and binding capacity to DNA obviously are not crucial for cytotoxic potential of compounds, suggesting the importance of the mode DNA interaction and DNA repair. Thus, depending on the ligand in *trans* platinum compound a monofunctional and bifunctional adducts can be formed with DNA.<sup>9-10,54-56</sup> Recently, we demonstrated the formation of severe conformational changes in plasmid DNA after treatment with compound 2, and consistent with the findings using other transplatinum analogues<sup>9,54,56</sup>, the formation of bifunctional DNA crosslinks was suggested. Additionally, the effectiveness of DNA repair mechanisms may also render compound 2 less cytotoxic compared to cisplatin. Moreover, the route of drug administration to some extent affected the level of platinum bound to the DNA. Approximately 14% more platinum bound to DNA was obtained after intratumoural compared to the intravenous administration of either compound 2 or cisplatin.<sup>21</sup> Thus, as 80% of cisplatin in blood circulation is bound to proteins, primarily albumin, this difference could be expected, suggesting less free cisplatin molecules reached tumour nodule.<sup>57-58</sup> Taken altogether, the pharmacology of compound 2 seems to differ from cisplatin,

involving binding to the proteins in blood circulation, in tumour extracellular matrix and accumulation in cells. The accumulation of cisplatin in the cell is not fully understood. Cisplatin could enter in cells through passive diffusion and facilitated or active transport mediated through membrane transporters (the Copper transporter 1 (CTR1) and 2 (CTR2); the P-type copper-transporting ATPases ATP7A and ATP7B, multidrug and toxin extrusion transporters).<sup>7</sup> Currently, little is known about the accumulation of transplatin or its analogues. Active transport was demonstrated to play an important role in accumulation, independent of transporter CTR1 and ATP, depending on protein ATP7B and CTR2.<sup>6,8</sup> The details of compound 2 transport mechanisms and its interaction with biological molecules and antitumour effectiveness need further investigation.

## Conclusions

In summary, compound 2, a *trans*-Pt(II) analogue with two 3-Hmpy ligands, shows potential for electrochemotherapy treatment *in vitro* and *in vivo*. Electroporation increased compound 2 cytotoxicity up to 6-fold *in vitro* and antitumour effectiveness up to 3-fold *in vivo*, but it had less evident effects compared to cisplatin. The underlying mechanism of antitumour effectiveness of electrochemotherapy could be increased drug uptake, and an approximately 2 times higher amount of platinum in the tumours was reflected to the same extent in higher amount of Pt bound on its target of action to the DNA. Based on the compound 2 electrochemotherapy cytotoxicity and antitumour effectiveness in cisplatin-resistant tumour model TBLC12Pt, this molecule could potentially be used in the treatment of tumours with intrinsic or acquired resistance to cisplatin. To improve the antitumour effectiveness of compound 2 electrochemotherapy, multiple treatments should be tested in the future. Furthermore, compound 2 could be used in combination with other chemotherapeutics, affecting different targets, immunotherapy, vascular-targeted therapy or irradiation; however, further studies are warranted.

## Acknowledgements

The authors gratefully acknowledge the research grants from the Slovenian Research Agency (P3-0003 and P1-0134).

## References

- Emens LA, Middleton G. The interplay of immunotherapy and chemotherapy: harnessing potential synergies. *Cancer Immunol Res* 2015; **3**: 436-443. doi:10.1158/2326-6066.CIR-15-0064
- Riaz N, Sherman E, Koutcher L, Shapiro L, Katabi N, Zhang ZG, et al. Concurrent chemoradiotherapy with cisplatin versus cetuximab for squamous cell carcinoma of the head and neck. *Am J Clin Oncol-Canc* 2016; **39**: 27-31. doi:10.1097/COC.000000000000006
- Izgi K, Iskender B, Sakalar C, Arslanhan A, Yuksek EH, Hizar E, et al. Effects of epirubicin and cisplatin against 4T1 breast cancer cells are enhanced by myrtoicommulone-A. *Anticancer Agents Med Chem* 2016. [Epub ahead of print]. doi:10.2174/1871520616666160404110543
- Amable L. Cisplatin resistance and opportunities for precision medicine. *Pharmacol Res* 2016; **106**: 27-36. doi:10.1016/j.phrs.2016.01.001
- Galluzzi L, Vitale I, Michels J, Brenner C, Szabadkai G, Harel-Bellan A, et al. Systems biology of cisplatin resistance: past, present and future. *Cell Death Dis* 2014; **5**: e1257. doi:10.1038/cddis.2013.428
- Burger H, Zoumaro-Djyoon A, Boersma AWM, Helleman J, Berns EMJJ, Mathijssen RHJ, et al. Differential transport of platinum compounds by the human organic cation transporter hOCT2 (hSLC22A2). *Brit J Pharmacol* 2010; **159**: 898-908. doi:10.1111/j.1476-5381.2009.00569.
- Ciarimboli G. Membrane transporters as mediators of cisplatin side-effects. *Anticancer Res* 2014; **34**: 547-50.
- Larson CA, Blair BG, Safaei R, Howell SB. The role of the mammalian copper transporter 1 in the cellular accumulation of platinum-based drugs. *Mol Pharmacol* 2009; **75**: 324-30. doi:10.1124/mol.108.052381
- Icel S, Yilmaz VT, Ari F, Ulukaya E, Harrison WTA. *trans*-Dichloridopalladium (II) and platinum (II) complexes with 2-(hydroxymethyl)pyridine and 2-(2-hydroxyethyl)pyridine: synthesis, structural characterization, DNA binding and *in vitro* cytotoxicity studies. *Eur J Med Chem* 2013; **60**: 386-94. doi:10.1016/j.ejmech.2012.12.002
- Kasparkova J, Marini V, Najajreh Y, Gibson D, Brabec V. DNA binding mode of the *cis* and *trans* geometries of new antitumor nonclassical platinum complexes containing piperidine, piperazine, or 4-picoline ligand in cell-free media. Relations to their activity in cancer cell lines. *Biochemistry* 2003; **42**: 6321-32. doi:10.1021/bi0342315
- Martinez A, Lorenzo J, Prieto MJ, Font-Bardia M, Solans X, Aviles FX, et al. Influence of the position of substituents in the cytotoxic activity of *trans* platinum complexes with hydroxymethyl pyridines. *Bioorg Med Chem* 2007; **15**: 969-79. doi:10.1016/j.bmc.2006.10.031
- Najajreh Y, Perez JM, Navarro-Ranninger C, Gibson D. Novel soluble cationic *trans*-diaminedichloroplatinum (II) complexes that are active against cisplatin resistant ovarian cancer cell lines. *J Med Chem* 2002; **45**: 5189-95.
- Quiroga AG. Understanding *trans* platinum complexes as potential anti-tumor drugs beyond targeting DNA. *J Inorg Biochem* 2012; **114**: 106-12. doi:10.1016/j.jinorgbio.2012.06.002
- Ramos-Lima FJ, Moneo V, Quiroga AG, Carnero A, Navarro-Ranninger C. The role of p53 in the cellular toxicity by active *trans*-platinum complexes containing isopropylamine and hydroxymethylpyridine. *Eur J Med Chem* 2010; **45**: 134-41. doi:10.1016/j.ejmech.2009.09.035
- Coluccia M, Natile G. *Trans*-platinum complexes in cancer therapy. *Anticancer Agents Med Chem* 2007; **7**: 111-23.
- Johnstone TC, Suntharalingam K, Lippard SJ. The next generation of platinum drugs: targeted Pt (II) agents, nanoparticle delivery, and Pt (IV) prodrugs. *Chem Rev* 2016; **116**: 3436-86. doi:10.1021/acs.chemrev.5b0059
- Shahsavari F, Bozorgmehr M, Mirzadegan E, Abedi A, Lighvan ZM, Mohammadi F, et al. A novel platinum-based compound with preferential cytotoxic activity against a panel of cancer cell lines. *Anticancer Agents Med Chem* 2016; **16**: 393-403.
- Ari F, Aztatol N, Icel S, Yilmaz VT, Guney E, Buyukgungor O, et al. Synthesis, structural characterization and cell death-inducing effect of novel palladium (II) and platinum (II) saccharinate complexes with 2-(hydroxymethyl)pyridine and 2-(2-hydroxyethyl)pyridine on cancer cells *in vitro*. *Bioorg Med Chem* 2013; **21**: 6427-34. doi:10.1016/j.bmc.2013.08.050
- Cemazar M, Pipan Z, Grabner S, Bukovec N, Sersa G. Cytotoxicity of different platinum (II) analogues to human tumour cell lines *in vitro* and murine tumour *in vivo* alone or combined with electroporation. *Anticancer Res* 2006; **26**: 1997-2002.

20. Grabner S, Cemazar M, Bukovec N, Sersa G. Syntheses and cytotoxicity of Pt (II) complexes with acyclovir. *Acta Chim Slov* 2006; **53**: 153-8.
21. Grabner S, Modec B, Bukovec N, Bukovec P, Cemazar M, Kranjc S, et al. Cytotoxic trans-platinum (II) complex with 3-hydroxymethylpyridine: synthesis, X-ray structure and biological activity evaluation. *J Inorg Biochem* 2016; **161**: 40-51. doi:10.1016/j.jinorgbio.2016.04.031
22. Tiwari G, Tiwari R, Sriwastawa B, Bhati L, Pandey S, Pandey P, et al. Drug delivery systems: an updated review. *Int J Pharm Investig* 2012; **2**: 2-11. doi:10.4103/2230-973X.96920
23. Kaur H, Desai SD, Kumar V, Rathi P, Singh J. Heterocyclic drug-polymer conjugates for cancer targeted drug delivery. *Anticancer Agents Med Chem* 2016; **16**: 1355-77.
24. Neumann E, Schaeferferridder M, Wang Y, Hofschneider PH. Gene-transfer into mouse lymphoma cells by electroporation in high electric-fields. *EMBO J* 1982; **1**: 841-5.
25. Cemazar M, Miklavcic D, Mir LM, Belchradek J, Bonnay M, Fourcault D, et al. Electrochemotherapy of tumours resistant to cisplatin: a study in a murine tumour model. *Eur J Cancer* 2001; **37**: 1166-72. doi:10.1016/S0959-8049(01)00091-0
26. Kranjc S, Cemazar M, Grosel A, Pipan Z, Sersa G. Effect of electroporation on radiosensitization with cisplatin in two cell lines with different chemo- and radiosensitivity. *Radiol Oncol* 2003; **37**: 101-7.
27. Kranjc S; Cemazar M, Grosel A, Scancar J, Sersa G. Electroporation of LPB sarcoma cells *in vitro* and tumors *in vivo* increases the radiosensitizing effect of cisplatin. *Anticancer Res* 2003; **23**: 275-81.
28. Sersa G, Cemazar M, Miklavcic D. Antitumor effectiveness of electrochemotherapy with cis-diamminedichloroplatinum (II) in mice. *Cancer Res* 1995; **55**: 3450-5.
29. Cemazar M, Miklavcic D, Scancar J, Dolzan V, Golouh R, Sersa G. Increased platinum accumulation in SA-1 tumour cells after *in vivo* electrochemotherapy with cisplatin. *Brit J Cancer* 1999; **79**: 1386-91.
30. Cemazar M, Tamzali Y, Sersa G, Tozon N, Mir LM, Miklavcic D, et al. Electrochemotherapy in veterinary oncology. *J Vet Intern Med* 2008; **22**: 826-31. doi:10.1111/j.1939-1676.2008.0117.x
31. Maglietti F, Tellado M, Olai N, Michinski S, Marshal, G. Combined local and systemic bleomycin administration in electrochemotherapy to reduce the number of treatment sessions. *Radiol Oncol* 2016; **50**: 58-63. doi:10.1515/raon-2016-0015
32. Mali B, Jarm T, Snoj M, Sersa G, Miklavcic D. Antitumor effectiveness of electrochemotherapy: a systematic review and meta-analysis. *Eur J Surg Oncol* 2013; **39**: 4-16. doi:10.1016/j.ejso.2012.08.016
33. Yarmush ML, Golberg A, Sersa G, Kotnik T, Miklavcic D. Electroporation-based technologies for medicine: principles, applications, and challenges. *Annu Rev Biomed Eng* 2014; **16**: 295-320. doi:10.1146/annurev-bieng-071813-104622
34. Cemazar M, Milacic R, Miklavcic D, Dolzan V, Sersa G. Intratumoral cisplatin administration in electrochemotherapy: antitumor effectiveness, sequence dependence and platinum content. *Anticancer Drugs* 1998; **9**: 525-30.
35. Sersa G, Teissie J, Cemazar M, Signori E, Kamensek U, Marshall Get al. Electrochemotherapy of tumors as *in situ* vaccination boosted by immunogene electrotransfer. *Cancer Immunol Immunother* 2015; **64**: 1315-27. doi:10.1007/s00262-015-1724-2
36. Markelc B, Sersa G, Cemazar M. Differential mechanisms associated with vascular disrupting action of electrochemotherapy: intravital microscopy on the level of single normal and tumor blood vessels. *PLoS One*, 2013; **8**: e59557. doi:10.1371/journal.pone.0059557
37. Belchradek JJ, Barski G, Thonier M. Evolution of cell-mediated antitumor immunity in mice bearing a syngeneic chemically induced tumor. Influence of tumor growth, surgical removal and treatment with irradiated tumor cells. *Int J Cancer* 1972; **9**: 461-9.
38. Sedlar A, Dolinsek T, Markelc B, Prosen L, Kranjc S, Bosnjak M, et al. Potentiation of electrochemotherapy by intramuscular *IL-12* gene electrotransfer in murine sarcoma and carcinoma with different immunogenicity. *Radiol Oncol* 2012; **46**: 302-11. doi:10.2478/v10019-012-0044-9
39. Hollis LS, Amundsen AR, Stern EW. Chemical and biological properties of a new series of cis-diammineplatinum (II) antitumor agents containing three nitrogen donors: *cis*-[Pt(NH<sub>2</sub>)<sub>2</sub>(N-donor)Cl]<sup>+</sup>. *J Med Chem* 1989; **32**: 128-36.
40. Leng M, Locker D, Giraud-Panis MJ, Schwartz A, Intini FP, Natlie G, et al. Replacement of an NH<sub>2</sub> by an iminoether in transplatin makes an antitumor drug from an inactive compound. *Mol Pharmacol* 2000; **58**: 1525-35.
41. Perez JM, Kelland LR, Montero EI, Boxall FE, Fuertes MA, Alonso C, et al. Antitumor and cellular pharmacological properties of a novel platinum (IV) complex: *trans*-[PtCl<sub>2</sub>(OH)<sub>2</sub>](dimethylamine) (isopropylamine)]. *Mol Pharmacol* 2003; **63**: 933-44.
42. Cemazar M, Miklavcic D, Vodovnik L, Jarm T, Rudolf Z, Stabuc B, et al. Improved therapeutic effect of electrochemotherapy with cisplatin by intratumoral drug administration and changing of electrode orientation for electroporation on EAT tumor model in mice. *Radiol Oncol* 1995; **29**: 121-7.
43. Baharuddin P, Satar, N, Fakiruddin KS, Zakaria N, Lim MN, Yusoff NM, et al. Curcumin improves the efficacy of cisplatin by targeting cancer stem-like cells through p21 and cyclin D1-mediated tumour cell inhibition in non-small cell lung cancer cell lines. *Oncol Rep* 2016; **35**: 13-25. doi:10.3892/or.2015.4371
44. Lee JH, Chae JW, Kim JK, Kim HJ, Chung JY, Kim YH. Inhibition of cisplatin-resistance by RNA interference targeting metallothionein using reducible oligo-peptoplex. *J Control Release* 2015; **215**: 82-90. doi:10.1016/j.jconrel.2015.07.015
45. Chong SX, Au-Yeung SC, To KK. Monofunctional platinum (PtII) compounds - shifting the paradigm in designing new Pt-based anticancer agents. *Curr Med Chem* 2016; **23**: 1268-85. doi:10.2174/092986732366616031114509
46. Igarashi K, Yamamoto N, Hayashi K, Takeuchi A, Miwa S, Odani A, et al. Effectiveness of two novel anionic and cationic platinum complexes in the treatment of osteosarcoma. *Anticancer Agents Med Chem* 2015; **15**: 390-9.
47. Hudej R, Miklavcic D, Cemazar M, Todorovic V, Sersa G, Bergamo A, et al. Modulation of activity of known cytotoxic ruthenium (III) compound (KP418) with hampered transmembrane transport in electrochemotherapy *in vitro* and *in vivo*. *J Membrane Biol* 2014; **247**: 1239-51. doi:10.1007/s00232-014-9696-2
48. Hudej R, Turel I, Kanduser M, Scancar J, Kranjc S, Sersa G, et al. The Influence of electroporation on cytotoxicity of anticancer ruthenium (III) complex KP1339 *in vitro* and *in vivo*. *Anticancer Res* 2010; **30**: 2055-63.
49. Calvet CY, Famin D, Andre FM, Mir LM. Electrochemotherapy with bleomycin induces hallmarks of immunogenic cell death in murine colon cancer cells. *Oncoimmunology* 2014; **3**: e28131. doi:10.4161/onci.28131
50. Cemazar M, Golzio M, Sersa G, Ecoffre JM, Coer A, Vidic S, et al. Hyaluronidase and collagenase increase the transfection efficiency of gene electrotransfer in various murine tumors. *Hum Gene Ther* 2012; **23**: 128-37. doi:10.1089/hum.2011.073
51. Bartel C, Bytsek AK, Scaffidi-Domianello YY, Grabmann G, Jakupec MA, Hartinger CG, et al. Cellular accumulation and DNA interaction studies of cytotoxic trans-platinum anticancer compounds. *J Biol Inorg Chem* 2012; **17**: 465-74. doi:10.1007/s00775-011-0869-5
52. Khazanov E, Barenholz Y, Gibson D, Najjeh Y. Novel apoptosis-inducing trans-platinum piperidine derivatives: synthesis and biological characterization. *J Med Chem* 2002; **45**: 5196-204.
53. Halamikova A, Heringova P, Kasparkova J, Intini FP, Natlie G, Nemirovski A, et al. Cytotoxicity, mutagenicity, cellular uptake, DNA and glutathione interactions of lipophilic trans-platinum complexes tethered to 1-adamantylamine. *J Inorg Biochem* 2008; **102**: 1077-89. doi:10.1016/j.jinorgbio.2007.12.015
54. Chowdhury MA, Huq F, Abdullah A, Beale P, Fisher K. Synthesis, characterization and binding with DNA of four planar platinum (II) complexes of the forms: *trans*-PtL<sub>2</sub>Cl<sub>2</sub> and [PtL<sub>3</sub>Cl]Cl, where L = 3-hydroxypyridine, 4-hydroxypyridine and imidazo(1,2- $\alpha$ )pyridine. *J Inorg Biochem* 2005; **99**: 1098-112.
55. Novakova O, Kasparkova J, Malina J, Natlie G, Brabec V. DNA-protein cross-linking by *trans*-[PtCl<sub>2</sub>(E-iminoether)<sub>2</sub>]. A concept for activation of the trans geometry in platinum antitumor complexes. *Nucleic Acids Res* 2003; **31**: 6450-60.
56. Richards AD, Rodger A. Synthetic metallomolecules as agents for the control of DNA structure. *Chem Soc Rev* 2007; **36**: 471-83.
57. Martincic A, Cemazar M, Sersa G, Kovac V, Milacic R, Scancar J. A novel method for speciation of Pt in human serum incubated with cisplatin, oxaliplatin and carboplatin by conjoint liquid chromatography on monolithic disks with UV and ICP-MS detection. *Talanta* 2013; **116**: 141-8. doi:10.1016/j.talanta.2013.05.01
58. Martincic A, Milacic R, Cemazar M, Sersa G, Scancar J. The use of CIM-DEAE monolithic chromatography coupled to ICP-MS to study the distribution of cisplatin in human serum. *Anal Methods* 2012; **4**: 780-90. doi:10.1016/j.chroma.2014.10.054

# Protective/restorative role of the adipose tissue-derived mesenchymal stem cells on the radioiodine-induced salivary gland damage in rats

Güleser Saylam<sup>1</sup>, Ömer Bayır<sup>1</sup>, Salih Sinan Gültekin<sup>2</sup>, Ferda Alparslan Pınarlı<sup>3</sup>, Ünsal Han<sup>4</sup>, Mehmet Hakan Korkmaz<sup>5</sup>, Mehmet Eser Sancaktar<sup>6</sup>, İlkan Tatar<sup>7</sup>, Mustafa Fevzi Sargon<sup>7</sup>, Emel Çadallı Tatar<sup>1</sup>

<sup>1</sup> University of Health Sciences, Dışkapı Yıldırım Beyazıt Training and Research Hospital, Department of Otolaryngology, Head and Neck Surgery, Ankara, Turkey

<sup>2</sup> University of Health Sciences, Dışkapı Yıldırım Beyazıt Training and Research Hospital, Department of Nuclear Medicine, Ankara, Turkey

<sup>3</sup> University of Health Sciences, Dışkapı Yıldırım Beyazıt Training and Research Hospital, Department of Stem Cell and Genetic Diagnostic Center, Ankara, Turkey

<sup>4</sup> University of Health Sciences, Dışkapı Yıldırım Beyazıt Training and Research Hospital, Department of Pathology, Ankara, Turkey

<sup>5</sup> Yıldırım Beyazıt University, Faculty of Medicine, Department of Otolaryngology, Head and Neck Surgery, Ankara, Turkey

<sup>6</sup> Ministry of Health, Samsun Training and Research Hospital, Department of Otolaryngology, Head and Neck Surgery, Samsun, Turkey

<sup>7</sup> Hacettepe University, Faculty of Medicine, Department of Anatomy, Ankara, Turkey

Radiol Oncol 2017; 51(3): 307-316.

Received 21 December 2016

Accepted 7 April 2017

Correspondence to: Salih Sinan Gültekin, M.D., Department of Nuclear Medicine Dışkapı Yıldırım Beyazıt Training and Research Hospital, Ankara, Turkey. Phone: + 90 312 596 20 00; E-mail: gultekinsinan@gmail.com

Disclosure: No potential conflicts of interest were disclosed.

**Background.** To analyze protective/regenerative effects of adipose tissue-derived mesenchymal stem cells (ADMSC) on <sup>131</sup>I-Radioiodine (RAI)-induced salivary gland damage in rats.

**Materials and Methods.** Study population consisted of controls (n:6) and study groups (n:54): RAI (Group 1), ADMSC (Group 2), amifostine (Group 3), RAI+amifostine (Group 4), concomitant RAI+ADMSC (Group 5) and RAI+ADMSC after 48 h (Group 6). We used light microscopy (LM), transmission electron microscopy (TEM), and salivary gland scintigraphy (SGS), and analyzed data statistically.

**Results.** We observed the homing of ADMSC in salivary glands at 1<sup>st</sup> month on LM. RAI exposure affected necrosis, periductal fibrosis, periductal sclerosis, vascular sclerosis and the total sum score were in a statistically significant manner ( $P < 0.05$ ). Intragroup comparisons with LM at 1<sup>st</sup> and 6<sup>th</sup> months revealed statistically significant improvements in Group 6 ( $P < 0.05$ ) but not in Groups 4 and 5. Intergroup comparisons of the total score showed that Groups 4 and 5 in 1<sup>st</sup> month and Group 6 in 6<sup>th</sup> month had the lowest values. TEM showed vacuolization, edema, and fibrosis at 1<sup>st</sup> month, and an improvement in damage in 6<sup>th</sup> month in Groups 5 and 6. SGSs revealed significant differences for the maximum secretion ratio (Smax) ( $P = 0.01$ ) and the gland-to-background ratio at a maximum count (G/BGmax) ( $P = 0.01$ ) at 1<sup>st</sup> month, for G/BGmax ( $P = 0.01$ ), Smax ( $P = 0.01$ ) and the time to reach the maximum count ratio over the time to reach the minimum count (Tmax/Tmin) ( $P = 0.03$ ) at 6<sup>th</sup> month. 1<sup>st</sup> and 6<sup>th</sup> month scans showed differences for Smax and G/BGmax ( $P = 0.04$ ), but not for Tmax/Tmin ( $p > 0.05$ ). We observed a significant deterioration in gland function in group 1, whereas, mild to moderate deteriorations were seen in protective treatment groups.

**Conclusions.** Our results indicated that ADMSC might play a promising role as a protective/regenerative agent against RAI-induced salivary gland dysfunction.

Key words: salivary gland; radioiodine treatment; radiation damage; radiation protection; stem cell transplantation; adipose tissue-derived mesenchymal stem cells

## Introduction

<sup>131</sup>I-Radioiodine (RAI) is used as an effective and common therapy option in hyperthyroidism and thyroid carcinoma; however, it is frequently associated with salivary gland dysfunction.<sup>1</sup> Several types of deterministic side effects may occur immediately after administration (short term, first 96 h), in the next few months (intermediate, until 3 months), or later (long term: >3 months).<sup>2</sup> RAI-induced sialadenitis remains a major clinical problem with a rising incidence of thyroid carcinoma due to early detection of small tumors.<sup>3</sup> Jeong *et al.*<sup>4</sup> investigated long-term effects of RAI ablation, and reported that 20% of patients had salivary gland dysfunction on scintigraphy.

Salivary glands consist of several cell types, but the glands are mainly differentiated according to serous and mucinous components. Parotid glands are most susceptible to RAI damage because of the dominance of serous glandular tissue. Xerostomia is rare but an important problem that is mainly due to submandibular gland damage after medical irradiation. Xerostomia, or reduced secretion of saliva, compromises a patient's quality of life by corrupting oral and dental health, leading to oral infections, dental caries, taste alterations, nocturnal discomfort, and even difficulties of speaking and swallowing.<sup>1,4</sup> Therefore, prevention or repair of the salivary gland damage is important.

Salivary gland damage is irreversible after development of radiation necrosis, and available treatments can only increase secretion from the remaining surviving tissue.<sup>2</sup> Amifostine is one of the most studied agents used to overcome radiation-related hyposalivation, and its active metabolite (WR-1065) decreases levels of free oxygen radicals. Even though it seems to be a cytoprotective agent, amifostine has many adverse effects, limiting its widespread use. Pilocarpine is used for symptom relief, but none of the medications mentioned above have been advocated for prevention or symptomatic treatment of salivary gland damage.<sup>5-10</sup> However, to improve the patients' quality of life and decrease the associated morbidities; new regenerative solutions are needed to obtain functional restoration and repair in affected tissues.

Mesenchymal stem cells (MSCs) isolated from the umbilical cord, adipose tissue, lung tissue, and bone marrow have been used as treatment agents for several diseases due to their capacity of tissue regeneration, trophic support, and modulation of the innate immune response.<sup>11,12</sup> Homing and en-

graftment of stem cells have been observed in damaged organs, such as the myocardium and kidney; those stem cells may increase function by reducing the levels of proinflammatory cytokines.<sup>13,14</sup>

External radiation-induced salivary gland damage has been investigated in some studies. Lombaert *et al.* showed bone marrow MSCs could travel to damaged salivary glands following mobilization, subsequently inducing the repair processes, which improved gland function and morphology.<sup>15</sup> Jeong *et al.* investigated the effects of transplantation of human submandibular gland stem cells (hSGSCs) to radiation-damaged rat salivary glands.<sup>16</sup> Their data suggested that mesenchymal-like stem cells could be used for treatment of RAI-induced salivary gland damage.

In this controlled animal study, we investigated the protective/regenerative effects of adipose tissue-derived MSCs (ADMSC) on the RAI-exposed rat salivary glands using structural and functional examinations.

## Materials and methods

### Study population and design

Sixty female Wistar albino rats weighed 230 – 250 g were used in this study. The animals were kept under standard conditions (temperature: 24 – 26°C; relative humidity: 65 – 70%) in 12-h light/12-h dark cycles, with access to water and seeds ad libitum. RAI was administered at a dose of 74 MBq (2 mCi) by oral route to induce salivary gland damage. ADMSC (i.p; 2×10<sup>6</sup>) and amifostine (i.v; 200 mg/m<sup>2</sup>) were used as cytoprotective/regenerative agents against the effects of radiation. Our main goal was to determine whether ADMSC had a regenerative effect besides its cytoprotective effect.

The study protocol was approved by Dışkapı Yıldırım Beyazıt Education and Research Hospital's Animal Ethics Board (2013/38), and instructions of local/international animal research were followed. The national/international regulations of radiation safety and waste disposal for contaminated secretion and materials of radio-exposed rats were also followed.

The study groups were designed as follows:

1. Control group: n = 6,
2. RAI alone group (Group 1, n = 9),
3. ADMSC alone group (Group 2, n = 9),
3. Amifostine alone group (Group 3, n = 9),
4. Simultaneous RAI plus amifostine group (Group 4, n = 9): RAI and amifostine were given at the same time.

5. Simultaneous RAI plus ADMSC group (Group 5, n = 9): RAI and ADMSC were given at the same time.
6. RAI and late ADMSC administration group (Group 6, n = 9). This group was named as "late administration group" since ADMSC was administered 48 h after RAI.

Salivary gland scintigraphy was performed at baseline, and after 1 and 6 months. Three animals in each group were sacrificed at the end of 1<sup>st</sup> month, and the rest were sacrificed at the end of 6<sup>th</sup> month of the study. The specimens were examined under the light microscope (LM) and transmission electron microscope (TEM). The study and the control groups were compared in terms of RAI-induced tissue damage. Intergroup comparisons were also done among the study groups.

### Preparation of adipose-derived mesenchymal stem cells

Fried and Moustaid-Moussused's protocol was used to culture adipose tissue.<sup>17</sup> Adipose tissue explants at a volume of 0.5 cm<sup>3</sup> were extracted from the inguinal fat pad of the rats. The tissues were transported from the operating room to the laboratory in a transport buffer (phosphate buffered solution [PBS], 5.5 mM glucose, and 50 g/mL gentamicin), at room temperature. The following procedures were carried out under a laminar flow hood, using sterile equipment. The tissues were transferred to a Petri dish containing 3 mL of PBS, and minced into 10 – 15 mg pieces. The pieces were extensively washed with 10 mL of PBS over a filter containing sterile cotton bandage fabric. Thereafter, they were gently shaken for a short period following transferred to a 25 cm<sup>2</sup> culture flask, containing 1 mL of PBS. Adipose tissue pieces were cultured within MSC medium (Dulbecco's Modified Eagle's Medium – low glucose; Invitrogen; Thermo Fisher Scientific, Waltham, MA, USA), 20% fetal bovine serum (Biological Industries Israel Beit-Haemek Ltd., Kibbutz Beit-Haemek, Israel), 100 U/mL of penicillin, 100 mg/mL of streptomycin (Biological Industries Israel Beit-Haemek Ltd., Kibbutz Beit-Haemek, Israel), and 20 mL/L of L-glutamine. They were incubated at 37°C and in 5% CO<sub>2</sub>. Culture medium was changed every three days, and colony-forming unit-fibroblasts were observed at 14 – 16 days with a 70% confluency of the culture plate. The detached cells were subcultured on a standard culture dish, using 0.25% trypsin in 0.02% ethylenediaminetetraacetic acid. After three passages, the

cell suspensions were defined with MSC markers including CD11b/c (-), CD45(-), CD90(+), CD44(+), and CD49(+) with the FACS Aria III cell sorter, and stored at -80°C DMEM-LG medium included 10% DMSO and 10% FBS.

To label ADMSC *in vitro*, 10 µL of BrdU solution (1 mM BrdU in 1 × Dulbecco's PBS, BD Pharmingen, San Diego, CA, USA) was added for each milliliter of tissue culture medium, and incubated for 2 hours. Cell culture density was 2 × 10<sup>6</sup> cells/mL.

To demonstrate the labeled ADMSC, BrdU staining was performed on 6 mm thick slides those were prepared from formalin-fixed, paraffin-embedded tissues, after deparaffinization in xylene to detect BrdU ion. The slides were transferred into 100% and 95% alcohol, then endogenous peroxidase activity was blocked with 3% hydrogen peroxide, and the slides were subsequently rinsed with PBS. Finally, the sections were immunohistochemically stained with a BrdU detection kit (BD Pharmingen) to show the presence of BrdU+ cells.

### Light microscopy

The excised salivary gland samples were harvested and fixed in 10% formaldehyde solution. After the paraffinization procedure, tissue sections were stained with hematoxylin and eosin, and a blinded pathologist examined all specimens under the light microscope (Olympus BX-50; Olympus Corporation, Tokyo, Japan). Salivary gland damage was categorized into three stages (0: no damage; 1: mild damage; 2: moderate damage; and 3: severe damage) for each of the following findings: acinar epithelial cells (edema, vacuolization, periacinar inflammation, and necrosis), interstitial space (periductal sclerosis, fibrosis, and mucus leakage), ductal system (ductal ectasia), and vascular system (sclerosis). A total score of histological findings reflected the sum of RAI-induced damage in tissues.

### Transmission electron microscopy

Tissue samples were put into 2.5% gluteraldehyde for 24 hours for primary fixation, and they were post-fixed in 1% osmium tetroxide after washing with Sorenson's phosphate buffer solution (pH: 7.4). In the next step, washing with the same buffer and dehydration in increasing concentrations of alcohol series were done. After dehydration, the tissues were washed with propylene oxide, and embedded in epoxy resin embedding media. Semi-thin (2 µm) and ultra-thin (60 nm) sections of the

TABLE 1. Histological findings in the salivary glands of the rats. Mean values of salivary gland damage parameters are given. \*Details of groups are given below the table

Site of damage	Investigated parameters	Control			Group 1			Group 2			Group 3			Group 4			Group 5			Group 6		
		1 <sup>st</sup> m	6 <sup>th</sup> m	p	1 <sup>st</sup> m	6 <sup>th</sup> m	p	1 <sup>st</sup> m	6 <sup>th</sup> m	p	1 <sup>st</sup> m	6 <sup>th</sup> m	p	1 <sup>st</sup> m	6 <sup>th</sup> m	p	1 <sup>st</sup> m	6 <sup>th</sup> m	p	1 <sup>st</sup> m	6 <sup>th</sup> m	p
	Edema	3.67	5.5	ns	6	7.17	ns	5.67	7.67	<b>0.05</b>	5	5.5	ns	4.33	7	<b>0.02</b>	4.33	4.83	ns	5.67	3	<b>0.02</b>
Acinar epithelial cell damage	Vacuolization	4.33	3.5	ns	6.67	6.33	ns	5	7	<b>0.04</b>	4.67	4.17	ns	4	5.33	ns	5	3.67	ns	5.33	2	<b>0.02</b>
	Peri acinar inflammation	0	0	ns	0.67	0.17	ns	1.33	0.17	ns	0.67	0.17	ns	0	0.17	ns	0	0.17	ns	2	0	<b>0.02</b>
	Necrosis	0.67	2.33	ns	0	1.33	<b>0.04</b>	2	0.5	ns	1.67	1	ns	0	1	ns	0.33	0	ns	0.67	0.17	ns
Ductal system damage	Ectasia	3	3.33	ns	6.33	5.83	ns	4.33	6	ns	3.67	2.5	ns	2.67	4.67	<b>0.01</b>	3.67	3.5	ns	3.33	0.83	<b>0.04</b>
	Periductal fibrosis	0	0	ns	1	3.33	<b>0.02</b>	2.33	3.33	ns	1	0.33	ns	0	2.33	<b>0.02</b>	0	1.33	<b>0.01</b>	0	0.67	ns
Interstitial space damage	Periduktal sclerosis	0	0.17	ns	0	2.17	<b>0.02</b>	1.33	1.83	ns	1	0	<b>0.03</b>	0	0.33	ns	0	0.67	ns	0	0	ns
	Periductal mucus leakage	1	0.5	ns	1	1	ns	0.67	1.33	ns	1.33	1	ns	0.33	0.83	ns	0.33	0.33	ns	3	0.5	<b>0.02</b>
Vascular system damage	Sclerosis	0	0.17	ns	1	4.5	<b>0.01</b>	1.67	3.5	ns	1.33	0.5	ns	0.67	1.17	ns	0	1.17	<b>0.01</b>	1.67	0.5	ns
	Total	12.67	15.5	ns	22.67	31.83	<b>0.02</b>	24.33	31.33	ns	20.34	15.17	0.05	12	22.83	<b>0.02</b>	13.66	15.67	ns	21.67	7.67	<b>0.02</b>

Control = healthy subjects; Group 1 = radioiodine; Group 2 = adipose tissue-derived mesenchymal stem cells; Group 3 = amifostine; Group 4 = radioiodine plus amifostine; Group 5 = radioiodine plus adipose tissue-derived mesenchymal stem cells concomitant; Group 6 = radioiodine plus adipose tissue-derived mesenchymal stem cells after 48 h; ns = not significant.

obtained from the tissue blocks were cut with an ultramicrotome (LKB Nova, Sweden). Semi-thin sections were stained with methylene blue, and ultra-thin sections were stained with uranyl acetate and lead citrate. Those sections were examined under a light microscope (Nikon Corporation, Tokyo, Japan), and a transmission electron microscope (Jeol JEM 1200 EX (JEOL Ltd., Tokyo, Japan), respectively. The same microscopes were used to photograph the specimens.

### Salivary gland scintigraphy

A double-headed large-field gamma camera (ECAM, Siemens, IL, USA), equipped with a low-energy, high-resolution collimator was used. After 0.2 – 0.3 ml bolus intravenous injection of <sup>99m</sup>Tc-pertechnetate (74 MBq) through the tail veins of the rats under anesthesia, dynamic images were collected (120 frames at a rate of 1 frame/20 sec) for 40 min with a magnification of 1.23 in a

128 × 128-pixel matrix. For image analysis, oval-shaped regions of interest (ROIs) drawn on the right and left salivary gland regions were used. A ROI on the left supraclavicular area was used for background activity. All ROIs had the same size. The image data were processed, and a time-activity curve (TAC) was generated for each subject using a summarization method including background subtraction and three-point smoothing. Functional assessments of TACs were made for following quantitative parameters: The gland-to-background ratio at a maximum count (G/BG<sub>max</sub>) defined the degree of gland parenchymal damage when compared with the background activity since this ratio dropped off due to the parenchymal injury and destruction in a direct manner. The time to reach the maximum count ratio over the time to reach the minimum count (T<sub>max</sub>/T<sub>min</sub>) showed whether the gland activity slowed down due to mostly ductal system damage. It is dependent on the processes of transit in tissue and trans-

port out of the gland. The maximum secretion ratio ( $S_{max}$ ; maximum count - minimum count / maximum count  $\times$  100) highlighted secretion capacity of the gland as a percentage.

### Statistical analysis

We used SPSS software (version 18.0 for Windows, SPSS Inc., Chicago, USA) for statistical analysis. Kruskal–Wallis test was employed to compare the groups, Mann–Whitney U test was used to analyze the intergroup differences, and Friedman's test was used to assess the differences in continuous variables.

## Results

### Light microscopy findings

Table 1 and Figure 1 show the histological findings of the salivary glands in the study groups. Normal salivary gland histology was shown in upper horizontal line from control samples (Figure 1A–C). Homing of ADMSC to RAI-damaged salivary glands and their trans-differentiation into salivary gland cells are seen in Figure 1D–F.

Intragroup comparison of the parameters in the control group showed that none of parameters had statistically significant difference between 1<sup>st</sup> and 6<sup>th</sup> months ( $P > 0.05$ ).

In Group 1, destructive effects of RAI on acinar cells, interstitial space and vascular system over time were demonstrated with presence of necrosis ( $P = 0.04$ ), periductal fibrosis ( $P = 0.02$ ), periductal sclerosis ( $P = 0.02$ ), vascular sclerosis ( $P = 0.01$ ), and total sum score ( $P = 0.02$ ). However, the effect of RAI on the ductal system was not significant ( $P > 0.05$ ). RAI-induced necrosis and increased vacuolization (Figure 1G), periductal fibrosis and inflammation (Figure 1H–I) were shown in Figure 1.

In Group 2, we observed statistically significant differences on acinar epithelial cells with an increase in edema ( $P = 0.05$ ), vacuolization ( $P = 0.04$ ) and periductal sclerosis ( $P = 0.03$ ).

In Group 3, the findings were not related to RAI, and we assumed those findings as insignificant.

In, Amifostine plus RAI (Group 4), Amifostine did not exhibit a sufficient protective effect in intragroup comparison; and yet the damage increased in a statistically significant manner in terms of edema ( $P = 0.02$ ), ductal ectasia ( $P = 0.01$ ), periductal fibrosis ( $P = 0.02$ ) and total sum score ( $P = 0.02$ ).

Similarly, in the concomitant administration of stem cells plus RAI (Group 5), we determined a

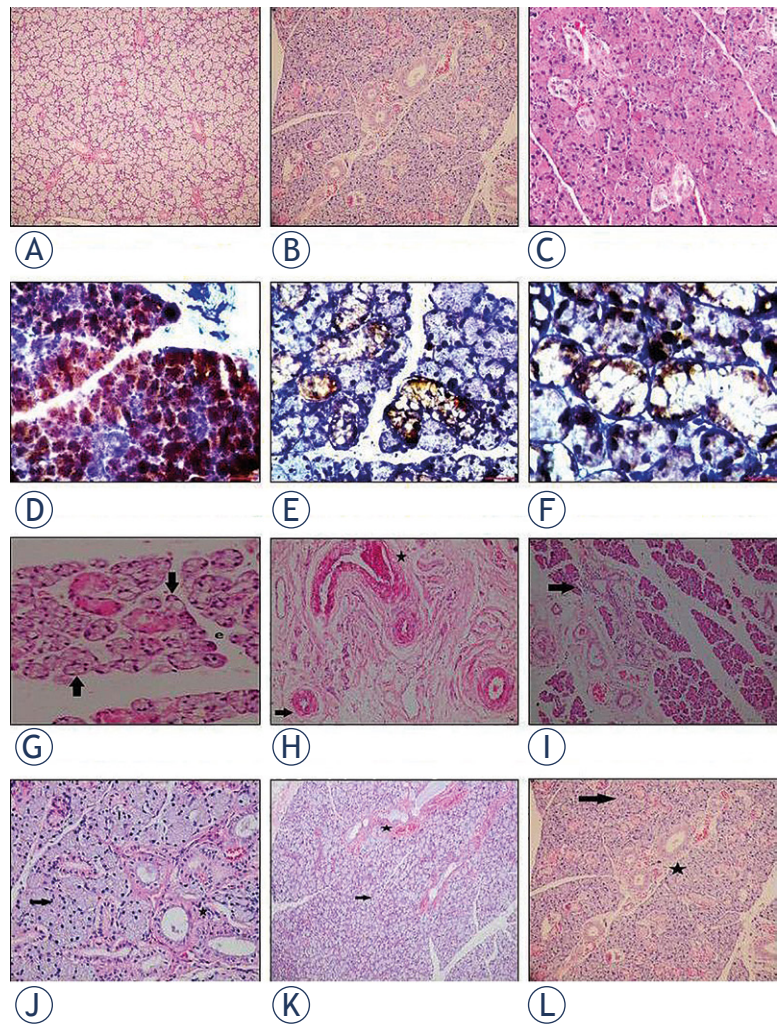


**FIGURE 1.** Histological photographs of salivary gland tissue samples. Pictures on the upper horizontal line show control groups at 1<sup>st</sup> month evaluation (A; haematoxylin and eosin (H&E)X40), and at 6<sup>th</sup> month evaluation in different magnifications (B; H&EX200, C; H&EX400). Pictures on the second horizontal line (D to F; x200 Leica DM 1000) shows the localization of BrdU(+) Adipose Derived Mesenchymal Stem Cells (ADMSC) in the salivary gland (brown stained cells) at 1<sup>st</sup> month after its intraperitoneal injection in different magnifications. Radioiodine-induced damage in Group 1 is seen in pictures on the third horizontal line (G to I; H&Ex400, H&Ex400 and H&Ex100). Massive vacuolization, necrosis (black arrow) and edema were shown in G minimal vacuolization (black arrow) and periductal fibrosis (black star) in H and lenfosit infiltration (black arrow) in I. Pictures on the lower horizontal line (J to L H&Ex400, H&Ex200 and H&Ex40) indicates the improvements in the histological findings (including vacuolization, fibrosis and edema: black arrow; nearly normal mucous acini, black star; nearly normal ductal system) at 6<sup>th</sup> month evaluation after the late ADMSC administration in Group 6.

statistically significant increase in periductal fibrosis ( $P = 0.01$ ) and sclerosis ( $P = 0.01$ ).

ADMSC seemed the most effective in Group 6. There was a statistically significant decrease on 6<sup>th</sup> month for edema, vacuolisation, periaciner inflammation, periductal mucus leakage ( $P = 0.02$ ) and ectasia ( $P = 0.04$ ) compared to the findings obtained

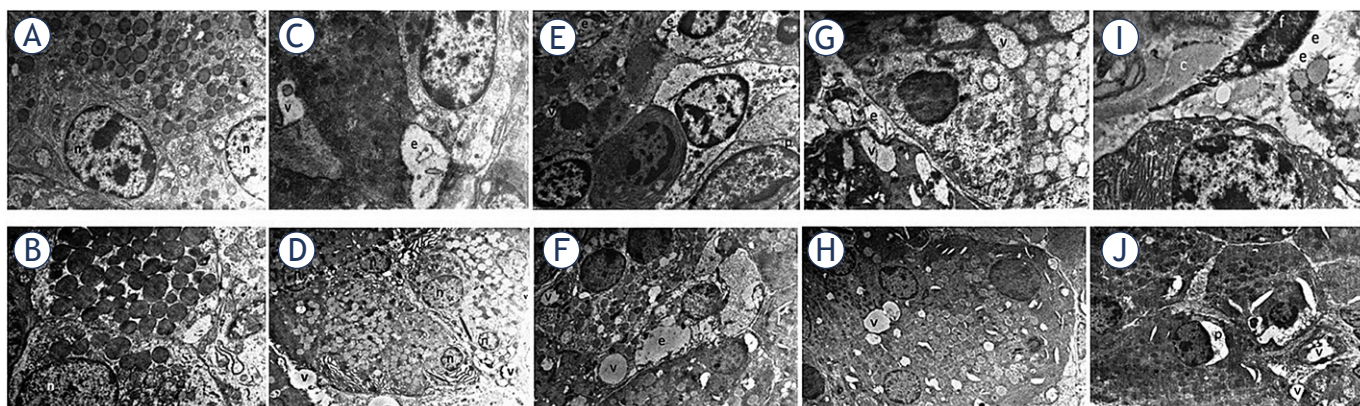


**FIGURE 2.** The figure (magnification x 5000) demonstrates the findings of electron microscopy at months 1 and 6. (A and B). Normal salivary gland samples of the control group. A and D. Intracellular vacuoles and intercellular edema related to radioiodine in Group 1. E and F. We observed intracellular vacuoles, intercellular edema, nucleus of fibroblast and collagen fibers (fibrosis) at 1<sup>st</sup> month evaluation in the treatment groups (Groups 5 and 6); G to J. Improvement in cellular damage at 6<sup>th</sup> month in the stem cell-administered groups (Groups 5 and 6). On the images; c: collagen fibers; e: intercellular edema; f: nucleus of fibroblast; n: nucleus, p: dilated perinuclear cistern; v: intracellular vacuoles.

on month 1. In addition, the sum of all histologic parameters decreased only in Group 6, with late stem cell administration. This improvement in histologic findings were demonstrated in Figure 1J–L.

At 1<sup>st</sup> month, we found a statistically significantly difference among the groups for periductal fibrosis, sclerosis and the total sum score were ( $P < 0.05$ ). The differences among the groups were statistically significant for the changes in edema, vacuolisation, necrosis, ectasia, sclerosis, periductal fibrosis, periductal sclerosis, and the total sum score ( $P < 0.05$ ) at 6<sup>th</sup> month. We supposed that interstitial space damage and total sum score were good indicators of RAI-induced damage. Total sum scores indicated that histologic improvements were statistically significant in all preservative treatment groups (Groups 4, 5, and 6 *vs.* Group 1). Total sum score was the smallest in Groups 4 and 5 at 1<sup>st</sup> month, and in Group 6 at 6<sup>th</sup> month. We concluded that, although concomitant administrations could be effective in the early phase of RAI-induced damage, late stem cell administration (Group 6) was better for recovery of the functional damage over time when compared to the other administration methods.

### Electron microscopy findings

TEM demonstrated cellular damage and fibrosis (Figure 2C–D). Intercellular edema and intracellular vacuolization showed cellular damage.

TEM examinations were normal in the control group at 1<sup>st</sup> and 6<sup>th</sup> months. We observed large intracellular vacuoles and intense intercellular ede-

ma in Group 1. RAI-induced damage was more distinct in samples obtained at 6<sup>th</sup> month, since the samples exhibited smaller intracellular vacuoles and minimal intercellular edema (Figure 2). The findings of ADMSC-administered group (Group 2) were identical to the findings of the control group. Minimal vacuolization and fibrosis were seen in Group 3, which was administered amifostine alone, but this was reversible, since the 6<sup>th</sup> month evaluation was normal. We observed vacuolization, edema, and fibrosis due to RAI damage at 1<sup>st</sup> month in the treatment groups (Groups 4, 5, and 6). The cellular damage and fibrosis improved in both the stem cell plus RAI-administered groups (Groups 5 and 6) at 6<sup>th</sup> month (Figure 2). However, the RAI damage was not partially reversible with amifostine administration in-group 4. The TEM findings demonstrated the regenerative/restorative effect of ADMSC on RAI-induced salivary gland dysfunction.

### Scintigraphy findings

The baseline findings were similar for all parameters in all study groups ( $P > 0.05$ ). RAI groups (Groups 1, 4, 5 and 6) and others (Groups 2 and 3) showed statistically significant differences for Smax ( $P = 0.01$ ) and G/BGmax ( $P = 0.01$ ), but not for Tmax/Tmin ( $P > 0.05$ ) at 1<sup>st</sup> month. On the other hand, 6<sup>th</sup> month scans revealed statistically significantly differences between RAI and non-RAI groups for Smax ( $P = 0.01$ ), G/BGmax ( $P = 0.01$ ) and Tmax/Tmin ( $P = 0.03$ ). Combined treatment groups showed significant differences for 1<sup>st</sup> and

**TABLE 2.** The mean values (the counts from left and right salivary glands) of the Smax, Tmax/Tmin and G/BGmax, and their statistical significance. Baseline and follow-up salivary gland scintigraphies were performed on the subjects who had single treatment (Group 1; radioiodine, Group 2; adipose tissue-derived mesenchymal stem cells, Group 3; amifostine) and combined treatments (Group 4; radioiodine plus amifostine, Group 5; radioiodine plus adipose tissue-derived mesenchymal stem cells concomitant, Group 6; radioiodine plus adipose tissue-derived mesenchymal stem cells after 48 h)

Groups	Smax (%)				Tmax/Tmin				G/BGmax			
	Baseline	1 <sup>st</sup> m	6 <sup>th</sup> m	p	Baseline	1 <sup>st</sup> m	6 <sup>th</sup> m	p	Baseline	1 <sup>st</sup> m	6 <sup>th</sup> m	p
Group 1	34.80	29.58	19.72	<b>0.04</b>	0.07	0.08	0.14	<b>0.05</b>	1.63	1.38	1.30	<b>0.04</b>
Group 2	34.74	34.31	34.62	ns	0.06	0.06	0.07	ns	1.59	1.57	1.58	ns
Group 3	34.72	34.38	33.83	ns	0.08	0.08	0.09	ns	1.59	1.56	1.57	ns
Group 4	33.07	30.30	28.88	<b>0.04</b>	0.08	0.08	0.09	ns	1.57	1.49	1.44	<b>0.04</b>
Group 5	33.51	32.91	28.89	<b>0.04</b>	0.08	0.08	0.09	ns	1.58	1.52	1.49	<b>0.04</b>
Group 6	35.55	31.60	26.07	<b>0.04</b>	0.07	0.07	0.09	ns	1.60	1.51	1.36	<b>0.04</b>
p	ns	<b>0.01</b>	<b>0.01</b>		ns	ns	<b>0.03</b>		ns	<b>0.01</b>	<b>0.01</b>	

G/BGmax = Gland-to-background ratio at a maximum count; ns = Not significant; Smax = Maximum secretion ratio; Tmax/Tmin = Ratio of the time to reach the maximum counts to the time to reach the minimum counts.

6<sup>th</sup> month findings for Smax and G/BGmax values ( $P = 0.04$ ), but not for Tmax/Tmin ( $p > 0.05$ ). This might be due to preservation of ductal secretion. RAI-dependent impairment in function at 6<sup>th</sup> month was the most prominent in Group 1. The measurements for Smax and G/BGmax seemed to be better in concomitant protective administrations with RAI (Groups 4 and 5), but the difference was not statistically significant. Tmax/Tmin ratio was similar among treatment groups with RAI (Groups 4 – 6). These findings suggested that protective agents could partially overcome functional damage related to RAI (Table 2).

The functional status on a salivary gland scintigraphy can be evaluated easily by a TAC generated from dynamic scintigraphic data. We compared pre- and post-treatment TACs generated from the sequential salivary gland scintigraphies of rats at baseline and at 6<sup>th</sup> month to observe time-related healing or worsening in the study groups, and to determine protective/regenerative effects of amifostine and ADMSC. Figure 3 depicts the functional change in activity of rat salivary glands over time in RAI and combined treatment groups. A review of the time-sequential findings in Group 1 showed a significant deterioration in function over time with decreased gland uptake and secretion capability (Figure 3A–B). As expected, TACs of two consecutive scans were not different from the baseline in the groups not treated with RAI (Groups

2 and 3). In the analysis of TAC patterns for RAI plus concomitant amifostine and ADMSC groups (Groups 4 and 5) as well as the late ADMSC-administered group (Group 6) mild to moderate deteriorations were seen in function over time in terms of slope of TAC and secretion capability of the gland (Figure 3C–H).

## Discussion

Well-differentiated thyroid cancer treated with RAI ablation results in high survival rates; however, xerostomia associated with RAI, which is seen in approximately 40–50% of cases, has a severe impact on the quality of life of patients.<sup>18,19</sup> Various methods have been used to avoid radiation-induced damage to the salivary glands.<sup>5–9</sup> Amifostine is the only agent approved by United States Food and Drug Administration for salivary gland protection, and its evidence-based protective effects on salivary glands have been shown. However, treatment-associated side effects of this cytoprotective agent including excessive chills, sweating, excessive tearing, dizziness, flushing, voice changes, tremor, nervousness, and diarrhea have limited its use.<sup>5–10</sup> To our knowledge, this is the first study that showed the favorable effects of ADMSC on RAI-induced salivary gland damage. We administered amifostine in Groups 2 and 3 to compare its effects

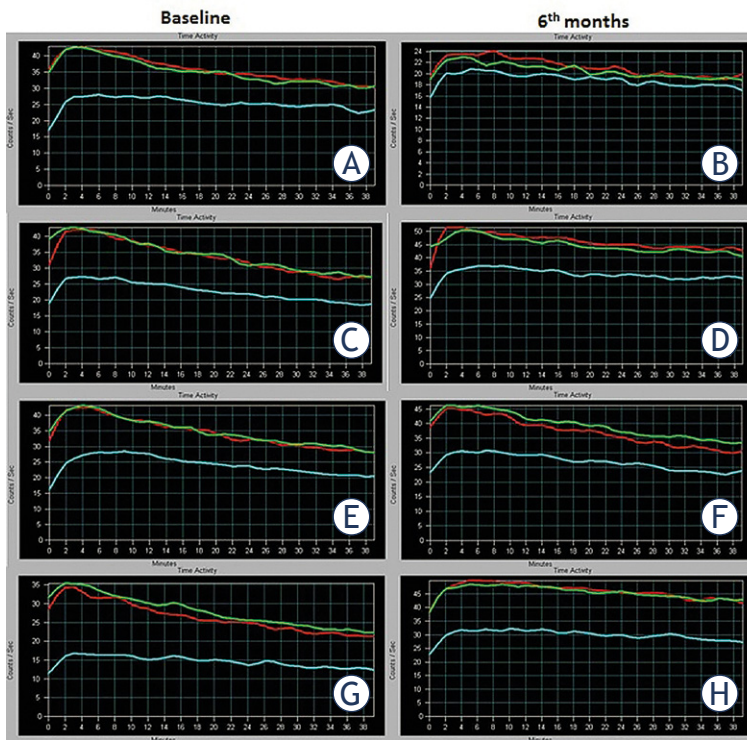


**FIGURE 3.** The figure represents functional data obtained from the time-activity curves of rats. A time-activity curve generated from dynamic scintigraphic data depicts the functional changing in activity of rat salivary glands over time. A baseline study (left side; **A, C, E, G**) and a six-month follow-up study (right side; **B, D, F, H**) on the rats was performed by  $^{99m}\text{Tc}$ -pertechnetate salivary gland scintigraphy (2 mCi, 120 frames, 20 second per frame, 40 min). The functional differences between baseline and post-treatment status can be easily seen, and compared by time-activity curves. Definitions on a time-activity curve in this figure are as follows: x axis; examination time (minutes), y axis; count data (counts/second), purple line; left salivary gland activity curve, blue line; right salivary gland activity curve and red line; background tissue activity curve. (**A and B**). A significant deterioration in function over time with decreased gland uptake and secretion capability with only radioiodine administration (Group 1) is seen. (**C to H**). Radioiodine plus concomitant amifostine (Group 4; **C and D**), radioiodine plus concomitant (Groups 5; **E and F**) and after 48 h (Group 6; **G and H**) adipose tissue-derived mesenchymal stem cells administrations show mild to moderate deteriorations in function over time in terms of slope of the curve and secretion capability of the gland.

with the protective effect of the stem cells. We also administered cytoprotective agents alone to rule out their unexpected effects. We compared amifostine and stem cells for their protective effects. We found stem cell administration superior to amifostine, and our findings may provide an alternative option, in absence of frequent side effects.

Stem cells can transform into different cells due to their regenerative capacity.<sup>20</sup> They have recently drawn attraction in regenerative medicine.<sup>21</sup> MSCs are present in mature tissues as multipotent cells, and can differentiate into specific cells that originate from the mesoderm. Mesenchymal cells have self-renewable properties; they can be easily cultured *in vitro*, and accepted by target tissues. MSCs can be isolated from different tissues such as bone marrow stromal cells, adipose tissue-derived stem cells, and adult skin stromal cells. Some studies on ADMSCs yielded promising results showing that they could be multilineage precursor cells, particularly in regenerative therapies. These cells can be easily obtained from donor tissues with minimal morbidity.<sup>22,23</sup> Although ADMSCs share similar differentiation capabilities with other MSCs, they have higher isolation yield and proliferation ratios in culture when compared to bone marrow stromal stem cells.<sup>24</sup> ADMSC are not the only precursor of adipocytes; they may also be the progenitor of my-

ocytes, osteoblasts, neuronal cells, chondrocytes, and epithelial cells.<sup>25,26</sup>

The first effect of stem cell infiltration is the induction of cytokines. Other healing-related benefits of ADMSC administration are anti-inflammatory activity, an ability to accelerate neovascularization, and the capacity to promote restoration of epithelial integrity.<sup>24</sup> Our results indicated that ADMSC administration resulted in a structural/functional recovery, as this preventive effect was associated with its ability to foster cytokine release and anti-inflammatory effects. Stem cells migrate to salivary glands and promote restoration and neovascularization, which results in functional restoration. Histological improvement following ADMSC administration, particularly in the late period may be associated with neovascularization and regeneration capacity of the cells. Our microscopic and scintigraphic findings demonstrated that ADMSCs were homing to salivary glands, and they could protect from permanent tissue damage and irreversible function loss.

Lombaert *et al.*<sup>15</sup> were first to show the potential use of stem cell transplantation for functional rescue of the salivary glands. They concluded that granulocyte-colony stimulating factor with mobilized bone marrow-derived stem cells might be effective for regenerating and functionally

restoring externally irradiated salivary glands. Jeong *et al.*<sup>16</sup> isolated and amplified tissue-specific hSGSCs. They developed a culture system (lasting 4–5 weeks) without any selection. The researchers found that transplantation of hSGSCs to radiation-damaged rat salivary glands rescued the function of the submandibular gland, and improved morphological damage. In another study, the authors systematically administered human ADMSC to mice immediately after local irradiation, and this was repeated once a week for three times.<sup>27</sup> They used salivary flow rates for functional assessment, and immunofluorescence histochemistry for morphological evaluation. The authors suggested that intravenous human ADMSC administration was a candidate therapy for the treatment of radiation-induced salivary gland damage. In light of all those studies, one may say that adult stem cell transplantation may be useful for functional and morphological regeneration of radiation damage in human salivary glands.

Our study differs from the others methodologically, and in terms of its findings in various aspects.<sup>8,10,15,16</sup> Internal instead of external radiation exposure was used to induce salivary gland damage. Salivary gland scintigraphy with <sup>99m</sup>Tc-pertechnetate was employed for functional evaluation instead of saliva collection or salivary flow rate. In addition, we used TEM to show the healing of damage on ultrastructural level. According to LM findings, initial damage occurs in the interstitial space and vascular system, which results in fibrosis and functional impairment. Sequential scintigraphy findings showed that the parenchyma damage was more than ductal damage. We may conclude that RAI-induced tissue damage is progressive. We observed a decrease in RAI-induced salivary gland damage by administration of amifostine and ADMSC. Concomitant stem cell infiltration had a protective effect; however, the late stem cell administration was restorative. This finding represents evidence of the protective and regenerative effects of ADMSC. Ultrastructural improvements were seen in the stem cell-administered groups in the vascular system damage demonstrated by TEM as vacuole formation and fibrosis. Our scintigraphic findings demonstrated the functional damage of RAI administration, which was prevented with amifostine and stem cell administration.

In this study, we found that the stem cell administration might be more effective than amifostine in rats, concomitant stem cell infiltration could reduce damage, and the late stem cell infiltration could restore tissue more than the other treatments. Our

TEM findings indicated that vacuolization, edema, and fibrosis were present at the 1<sup>st</sup> month evaluation of the preventive treatment groups. One promising result of this study was the improvements seen at 6<sup>th</sup> month. The ultrastructural healing was better in the stem cell plus RAI-administered groups compared to the amifostine plus RAI groups.

In fact, the patients are administered RAI in hypothyroid state, after thyroidectomy. They have a high concentration of RAI in the body due to especially its slow clearance.<sup>28</sup> In our study, we did not perform thyroidectomy. We administered a higher dose of RAI as given dose per gram of tissue compared to that used in a standard clinical setting. Thus, we may say that we could safely test the effect of protective agents against damage caused by RAI in nonthyroidectomized rats.

Our findings demonstrated that late stem cell administration was more effective than other treatments tested, and all stem cell administrations provided a mild to moderate protection against RAI damage in salivary gland scintigraphy. Therefore, we may suggest a combination of both applications for prevention/restoration of RAI-induced salivary gland damage, with minimal side effects. Further studies are needed to enlighten the effect of stem cell therapy in humans.

We did not investigate releasing factors after stem cell administration; we accepted this as a limitation of our study. We know that stem cells could migrate to all tissues.<sup>11,12</sup> However, we focused on only salivary gland damage.

In conclusion, radiation-induced hyposalivation remains as a major problem following external radiation or RAI. Since permanent dysfunction decreases the patients' quality of life, prevention of salivary gland damage and/or restoration of gland functions are important. In the current study, we showed the preventive and restorative capacity of stem cells, with histologic and functional improvements. The underlying key point of histologic and functional restoration could be the ultrastructural improvement of cellular damage. Stem cell infiltration may be a novel and promising method to prevent of xerostomia after radiation. We believe that this valuable approach has a potential to be a standard treatment option in near future after further studies are conducted in humans.

## Acknowledgements

This study was financially supported by a grant from Dışkapı Yıldırım Beyazıt Training and

Research Hospital Scientific Research Support Committee.

## References

- Jensen SB, Pedersen AM, Vissink A, Andersen E, Brown CG, Davies AN, et al. Salivary Gland Hypofunction/Xerostomia Section, Oral Care Study Group, Multinational Association of Supportive Care in Cancer (MASCC)/International Society of Oral Oncology (ISOO). A systematic review of salivary gland hypofunction and xerostomia induced by cancer therapies: prevalence, severity and impact on quality of life. *Support Care Cancer* 2010; **18**: 1039-60. doi:10.1007/s00520-010-0827-8
- Mandel SJ, Mandel L. Radioactive iodine and the salivary glands. *Thyroid* 2003; **13**: 265-71. doi:10.1089/105072503321582060
- Fard-Esfahani A, Emami-Ardekani A, Fallahi B, Fard-Esfahani P, Beiki D, Hassanzadeh-Rad A, et al. Adverse effects of radioactive iodine-131 treatment for differentiated thyroid carcinoma. *Nucl Med Commun* 2014; **35**: 808-17. doi:10.1097/MNM.0000000000000132
- Jeong SY, Kim HW, Lee SW, Ahn BC, Lee J. Salivary gland function 5 years after radioactive iodine ablation in patients with differentiated thyroid cancer: direct comparison of pre- and postablation scintigraphies and their relation to xerostomia symptoms. *Thyroid* 2013; **23**: 609-16. doi:10.1089/thy.2012.0106
- Bohuslavizki KH, Klutmann S, Jenicke L, Kröger S, Buchert R, Mester J, et al. Salivary gland protection by S-2-(3-aminopropylamino)-ethylphosphorothioic acid (amifostine) in high-dose radioiodine treatment: results obtained in a rabbit animal model and in a double-blind multi-arm trial. *Cancer Biother Radiopharm* 1999; **14**: 337-47. doi:10.1089/cbr.1999.14.337
- Joseph LJ, Bhartiya US, Raut YS, Hawaldar RW, Nayak Y, Pawar YP, et al. Radioprotective effect of Ocimum sanctum and amifostine on the salivary gland of rats after therapeutic radioiodine exposure. *Cancer Biother Radiopharm* 2011; **26**: 737-43. doi:10.1089/cbr.2011.1014
- Sagowski C, Wenzel S, Metternich FU, Kehrl W. Studies on the radioprotective potency of amifostine on salivary glands of rats during fractionated irradiation: acute and late effects. *Eur Arch Otorhinolaryngol* 2003; **260**: 42-7. doi:10.1007/s00405-002-0496-4
- Pimentel MJ, Filho MM, Araújo M, Gomes DQ, DA Costa LJ. Evaluation of radioprotective effect of pilocarpine ingestion on salivary glands. *Anticancer Res* 2014; **34**: 1993-9.
- Koca G, Gültekin SS, Han U, Kuru S, Demirel K, Korkmaz M. The efficacy of montelukast as a protective agent against 131I-induced salivary gland damage in rats: scintigraphic and histopathological findings. *Nucl Med Commun* 2013; **34**: 507-17. doi:10.1097/MNM.0b013e32835ffecf
- Hamlar DD, Schuller DE, Gahbauer RA, Buerki RA, Staubus AE, Hall J, et al. Determination of the efficacy of topical oral pilocarpine for postirradiation xerostomia in patients with head and neck carcinoma. *Laryngoscope* 1996; **106**: 972-6.
- Ding DC, Chang YH, Shyu WC, Lin SZ. Human umbilical cord mesenchymal stem cells: a new era for stem cell therapy. *Cell Transplant* 2015; **24**: 339-47. doi:10.3727/096368915X686841
- Ramdasi S, Sarang S, Viswanathan C. Potential of mesenchymal stem cell based application in cancer. *Int J Hematol Oncol Stem Cell Res* 2015; **9**: 95-103.
- Luo CJ, Zhang FJ, Zhang L, Geng YQ, Li QG, Hong Q, et al. Mesenchymal stem cells ameliorate sepsis-associated acute kidney injury in mice. *Shock* 2014; **41**: 123-129. doi:10.1097/SHK.0000000000000080
- Weil BR, Manukyan MC, Herrmann JL, Wang Y, Abarbanell AM, Poynter JA, et al. Mesenchymal stem cells attenuate myocardial functional depression and reduce systemic and myocardial inflammation during endotoxemia. *Surgery* 2010; **148**: 444-52. doi:10.1016/j.surg.2010.03.010
- Lombaert IM, Wierenga PK, Kok T, Kampinga HH, deHaan G, Coppes RP. Mobilization of bone marrow stem cells by granulocyte colony-stimulating factor ameliorates radiation-induced damage to salivary glands. *Clin Cancer Res* 2006; **12**: 1804-12. doi:10.1158/1078-0432.CCR-05-2381
- Jeong J, Baek H, Kim YJ, Choi Y, Lee H, Lee E, et al. Human salivary gland stem cells ameliorate hyposalivation of radiation-damaged rat salivary glands. *Exp Mol Med* 2013; **45**: e58. doi:10.1038/emm.2013.121
- Fried SK, Moustaid-Moussa N. Culture of adipose tissue and isolated adipocytes. *Methods Mol Biol* 2001; **155**: 197-212. doi:10.1385/1-59259-231-7:197
- Alexander C, Bader JB, Schaefer A, Finke C, Kirsch CM. Intermediate and long-term side effects of high-dose radioiodine therapy for thyroid carcinoma. *J Nucl Med* 1998; **39**: 1551-4.
- Solans R, Bosch JA, Galofré P, Porta F, Roselló J, Selva-O'Callagan A, et al. Salivary and lacrimal gland dysfunction (sicca syndrome) after radioiodine therapy. *J Nucl Med* 2001; **42**: 738-43.
- Wei X, Yang X, Han ZP, Qu FF, Shao L, Shi YF. Mesenchymal stem cells: a new trend for cell therapy. *Acta Pharmacol Sin* 2013; **34**: 747-54. doi:10.1038/aps.2013.50
- Horwitz EM, Le Blanc K, Dominici M, Mueller I, Slaper-Cortenbach I, Marini FC, et al. International Society for Cellular Therapy. Clarification of the nomenclature for MSC: The International Society for Cellular Therapy position statement. *Cytotherapy* 2005; **7**: 393-5. doi:10.1080/14653240500319234
- Mayshar Y, Ben-David U, Lavon N, Biancotti JC, Yakir B, Clark AT, et al. Identification and classification of chromosomal aberrations in human induced pluripotent stem cells. *Cell Stem Cell* 2010; **7**: 521-31. doi:10.1016/j.stem.2010.07.017
- Zuk PA, Zhu M, Ashjian P, De Ugarte DA, Huang JI, Mizuno H, et al. Human adipose tissue is a source of multipotent stem cells. *Mol Biol Cell* 2002; **13**: 4279-95. doi:10.1091/mbc.E02-02-0105
- Salibian AA, Widgerow AD, Abrouk M, Evans GR. Stem cells in plastic surgery: a review of current clinical and translational applications. *Arch Plast Surg* 2013; **40**: 666-75. doi:10.5999/aps.2013.40.6.666
- Zuk PA, Zhu M, Mizuno H, Huang J, Futrell JW, Katz AJ, et al. Multilineage cells from human adipose tissue: implications for cell-based therapies. *Tissue Eng* 2001; **7**: 211-28. doi:10.1089/107632701300062859
- Brayfield C, Marra K, Rubin JP. Adipose stem cells for soft tissue regeneration. *Handchir Mikrochir Plast Chir* 2010; **42**: 124-8. doi:10.1055/s-0030-1248269
- Lim JY, Ra JC, Shin IS, Jang YH, An HY, Choi JS, et al. Systemic transplantation of human adipose tissue-derived mesenchymal stem cells for the regeneration of irradiation-induced salivary gland damage. *PLoS One* 2013; **8**: e71167. doi:10.1371/journal.pone.0071167
- Gültekin SS, Sahmaran T. The efficacy of patient-dependent practices on exposure rate in patients undergoing iodine-131 ablation. *Health Phys* 2013; **104**: 454-8. doi:10.1097/HP.0b013e318283f853

# Electrochemotherapy - supplementary treatment for loco-regional metastasized breast carcinoma administered to concomitant systemic therapy

Eva-Maria Grischke, Carmen Röhm, Eva Stauß, Florin-Andrei Taran, Sara Y. Brucker, Diethelm Wallwiener

Department of Gynecology, University Hospital of Tübingen, Tübingen, Germany

Radiol Oncol 2017; 51(3): 317-323.

Received 29 March 2017  
Accepted 18 June 2017

Correspondence to: Prof. Eva-Maria Grischke, M.D., Department of Gynecology, University Hospital Tübingen, Tübingen, Germany.  
E-mail: eva-maria.grischke@med.uni-tuebingen.de

Disclosure: No potential conflicts of interest were disclosed.

**Background.** Electrochemotherapy (ECT) is an established procedure for treating breast cancer loco-regional recurrences following surgical intervention and/or radiotherapy. Limited information is available on ECT application as a concomitant procedure to systemic therapy in recurrent breast cancer. The primary objective of this study was to determine if the application of ECT in close temporal relation to systemic chemotherapy could lead to increased local and/or systemic side effects. For this purpose we evaluated the safety of ECT as a supplemental local therapy to systemic therapy. ECT local and systemic toxicity and side effects were recorded and whether the anticipated local therapeutic effect of ECT would be influenced by the concomitant use of systemic therapies was investigated.

**Patients and methods.** This is an observational study. Thirty three patients with loco-regional metastasized breast carcinoma were treated and observed over a period of three years with 46 ECT applications for local tumour control in addition to established systemic therapy. A specific timeline for ECT administration was not fixed up, but was generally performed one week before the following chemotherapy administration with the aim to avoid the so called nadir, this means the peak period with risk of neutropenia.

**Results.** Data was collected over a period of three years on a population of 33 metastatic patients. Fifteen patients, received neo-adjuvant therapy as part of their primary treatment, but still had an advanced stage tumour. Some patients received repeated ECT applications. Objective tumour response was observed in 90% of the treated patients. Patients showed no increased local toxicity, especially no higher dermal toxicity, e.g. formation of local necrosis.

**Conclusions.** ECT proved to be an effective supplement to a cytotoxic systemic therapy, especially for high-risk patients who did not respond well to systemic therapy of loco-regional metastases, without creating any greater systemic or loco-regional toxicities.

Key words: electroporation; loco-regional metastases; local control; local toxicity; supplement systemic therapy; concomitant systemic therapy

## Introduction

About 2–20% of the time, breast carcinoma recurrences are loco-regional.<sup>1</sup> In most cases, the recidivism is not exclusively an isolated local problem, but rather one associated with other distant metastases, in particular for long courses of the disease.<sup>2,3</sup>

In spite of operative intervention and radiotherapy, loco-regional relapses can occur repeatedly, persist, or exhibit therapy-resistance, often in a highly disseminated form. Currently, in such situations, systemic therapy is the only available approach following usual ones, like local radiation and operative intervention. In these cases, other therapies

come into consideration, which may be applied concomitantly to systemic therapy.<sup>4</sup> In such situations, the high probability of recurrence arising from the local manifestation of disease demands further local treatments to achieve rapid therapeutic response.

Furthermore, a proportion of patients show progression of the cutaneous loco-regional recurrences despite good clinical responses of visceral metastases, *e.g.* lung or liver metastases, to systemic therapy. Although patients often do not perceive organ manifestations as restraining, in most cases they see loco-regional cutaneous recurrences as negatively affecting their quality of life to a greater extent. The reasons for this are often weeping ulcerations with an odour and secretion, or possibly unpleasant and itchy lymphangitic changes. Hence, it is crucial to effectively control the loco-regional manifestation of the disease while managing the overall disease progression.

Electrochemotherapy (ECT) is a proven procedure for treating loco-regional metastases following surgical intervention and/or radiotherapy; having shown higher efficacy and limited toxicity it compares favourably with other skin treatments. Its potential for expansion from its current rather limited use to first line, widespread treatment is supported by recent publications.<sup>5,6</sup> Available data suggests that the effectiveness of ECT would be higher, in terms of response rate and duration of local response, if used early in the treatment pathway, in conjunction with multimodality regimens.<sup>7,8</sup> There is significant amounts of data on the outcome of ECT as the sole procedure, but limited information is available on ECT feasibility, safety and activity in combination or as a concomitant procedure to established cytotoxic systemic therapy in recurrent breast cancer.

ECT combines the antitumor activity of non-permeant (*e.g.* bleomycin) anticancer drugs with short electrical pulses that enhance the drug uptake into tumour cells, thus increasing the intracellular concentration and local toxicity of the cytostatic agent.<sup>9</sup> The electric field is applied precisely and directly with needle electrodes to the tumour, and the appropriate cytotoxic effect is achieved locally on the diseased tissue.

In the past decade, clinical use of ECT gained acceptance and its effectiveness has been widely demonstrated in several cutaneous pathologies such as metastatic melanoma, cutaneous recurrences from breast cancer, basal cell carcinoma, squamous cell carcinoma, Kaposi sarcoma, and head and neck cancers.<sup>10</sup> The publication of validated standard

operating procedures<sup>9,11</sup> allowed the dissemination of ECT across Europe and improved the clinical outcome of the therapy.<sup>10</sup>

Although adequate experience has been gained on this method for loco-regional procedures involving breast carcinoma, and for other kinds of tumours, there is scarce clinical data to definitively answer the question of whether ECT can safely supplement cytotoxic systemic therapy. Therefore, the main objective of this study was to determine if the application of ECT in close temporal relation to systemic chemotherapy could lead to increased local and/or systemic side effects, when compared to historical toxicity profile of ECT and systemic therapies. Furthermore, this study investigated whether it is feasible and safe to apply ECT as a concomitant local therapy to established systemic therapy in patients with metastasized breast carcinoma who previously did not respond adequately to systemic therapy to treat loco-regional metastases.

## Patients and methods

### Study design

This observational study was approved by the Institutional Review Board of our Institute and was conducted according to the declaration of Helsinki. Informed consent has been obtained from all patients included in the trial.

The primary objective was to determine local and systemic toxicity and evaluate if the application of ECT in close temporal relation (*e.g.* in between consecutive chemotherapy administrations) to systemic chemotherapy could lead to increased local and/or systemic side effects. Whether the anticipated local therapeutic effect of ECT is influenced by the concomitant use of systemic therapies was also considered as a secondary endpoint.

### Patients

The study included treatment and analysis of data on 33 patients over a period of three years (December 2012, December 2015) with loco-regional breast carcinoma, for whom other operative intervention or radiotherapy was neither possible nor appropriate because of highly extended local findings and/or disseminated tumours.

These 33 patients were subjected to a total of 46 individual ECT sessions. The indications were extended lymphangitic changes, ulcerations, or nodular skin metastases, disseminated over a very wide area or in several regions of the body.

Inclusion criteria were written informed consent, presence of symptomatic local metastasis without response to usual therapy like surgery, radiotherapy or other systemic anticancer therapy. Patients were offered ECT as a therapeutic option based on poor general condition, age, cardiac deficit not related to electrical malfunction, comorbidities, or that whether surgical procedure was not possible.

Exclusion criteria were reduced WHO performance (WHO score > 2) status clinically manifested arrhythmia, interstitial lung fibrosis, epilepsy, an active infection, a known allergy to bleomycin, kidney failure, and previous treatment with bleomycin at the maximum cumulative dosage. In case of clinical symptoms of impaired pulmonary function a lung capacity test was performed.

The patients underwent routine follow-up visits. In case of pulmonary metastases or pleural effusion, a CT of the thoracic area was performed. If necessary, a thoracic drainage was carried out.

Local response to the therapy was evaluated, along with the current systemic therapy, the tumour biology, and the tumour stage upon initial diagnosis. In addition to local response of the tumour, the study observed possible local toxicities and additional systemic reactions during the ongoing systemic therapy.

## Treatment procedure

ECT has been performed according to the established ESOPE SOPs.<sup>9</sup> Briefly, bleomycin was administered intravenously (15,000 IU/m<sup>2</sup> in a bolus in 30–60 s). Within 8–28 min after intravenous administration of bleomycin, electroporation of the tumour nodules was completed. Electric pulses were applied using sterile, single use hexagonal needles N-10-HG and N-20-HG, 10 or 20 mm long needle electrodes respectively, using the clinical electroporation device Cliniporator™ (Igea S.p.a., Italy). The type of electrode to be used was selected according to the physical characteristic of the lesion, *i.e.* lesion area and thickness.

In order to minimize the pain associated with the delivery of electric pulses, the procedure was performed under general anaesthesia. In most of the cases, the procedure was performed in 1 or 2 days hospitalization.

## Results

Twenty four patients underwent a single ECT procedure. Nine patients received repeated ECT ap-

TABLE 1. Data on 33 patients at time of the first electrochemotherapy

Metastasis localization	N. of patients (%)
Loco-regional – exclusively	12 (36.3)
Loco-regional + distal	21 (63.6)
<b>Distant metastasis</b>	
1 organ affected	15 (45.4)
2 organs affected	3 (9)
> 2 organs affected	3 (9)
<b>Distant metastasis and organs affected</b>	
Metastases → pulmonary/pleural	11 (33)
Metastases → bone	10 (30.3)
Metastases → cerebral	3 (9)
Metastases → hepatic	3 (9)

lications: seven patients underwent 2 ECT procedures, one patient had ECT 3 times and one patient underwent ECT 5 times. Intervals between applications ranged from 6 weeks to a maximum of 11 months.

Twelve (36.3%) of the patients exhibited only extended loco-regional metastases, with at minimum area of 10 × 8 cm. The cutaneous metastases in most cases were confluent, only in 3 cases disseminated. Further specificities were ulceration or lymphangiogenesis. Twenty-one (63.3%) patients also had distant metastases; additional metastatic localizations are summarized in Table 1.

In most cases, systemic monotherapies were used: 8 patients received eribulin, 4 received taxane, 3 received vinorelbine, 3 patients were treated with capecitabine, 1 with mitomycin, and 1 with pegylated liposomal doxorubicin. Four patients received combi - chemotherapy; 3 of them a combination of carboplatin and gemcitabine, and 1 was given vinorelbine and capecitabine. Four patients were treated with bevacizumab and 6 with trastuzumab as an antibody therapy. Patients given endocrine treatment received an aromatase inhibitor, antiestrogen in the form of fulvestrant, and in 1 case exemestane in combination with everolimus. Thus, 5 patients were treated solely with endocrine therapy (Table 2). The sequence of metastasis treatments ranged from first line (because of distant metastases) to fifth line. Systemic treatment was given for distant metastasis and/or repeated local recurrent tumour (characterizing can be seen Table 1).

In all cases, loco-regional recidivism concerned the thoracic wall and/or cutaneous area of the contra-lateral thoracic wall or mammary gland. In 23



**FIGURE 1.** Patient with triple negative breast cancer under chemotherapy before ECT. The patient was previously under treatment with taxanes, carboplatin and eribulin. In contrast to response in liver and lung metastasis, skin metastasis showed progression.



**FIGURE 2.** Two month after ECT. Good tumour control in the pretreated area was obtained but progression in the border is visible and partially with tumour-free area. Typical hyperpigmentation following ECT treatment is visible.

cases (69.7%), the tumour occurred on one side, and in 7 (21.2%) cases on two sides. The axillary region was also affected in 5 patients, the dorsal thoracic wall in 5, and the upper arm in 3. One patient had an extended supra/ infraclavicular tumour (Table 3). In all cases, the changes covered large areas, partly lymphangitic, partly with ulcerations and large nodular areas. Especially the tumours in the axilla exhibited large nodules.

Local tumours, especially with lymphangitic changes, showed good response 3 months after

**TABLE 2.** Systemic therapy at the time of electrochemotherapy

Monochemotherapy	N. of patients
Eribulin	8
Taxane	4
Vinorelbine	3
Capecitabine	3
Mitomycin	1
Pegylated liposomal doxorubicin	1
<b>Combo-chemotherapy</b>	
Carboplatin & gemcitabine	3
Vinorelbine & capecitabine	1
<b>Antibody therapy</b>	
Trastuzumab	6
Bevacizumab	4
<b>Endocrine monotherapy</b>	
AI with everolimus & fulvestrant	5

**TABLE 3.** Findings of locoregional recidivism prior to electrochemotherapy

Areas of treated thorax wall	N. of patients (%)
On one side	23 (69.7)
On two sides	7 (21.2)
+ axilla	5
+ upper arm	3
+ dorsal	5
+ supra/infraclavicular	1

ECT. The redness improved rapidly or disappeared completely, and exudation of weeping areas either declined significantly or stopped fully. In terms of complete or partial remission, tumour response was observed in 90% of the treated patients. Necrosis occurred exclusively in large nodules, with consecutive healing of the changes. The hyperpigmentation of the treated area is a common skin toxicity following ECT treatment but the extent and intensity is variable.<sup>6,16</sup> In almost a third of the patients, new lesions appeared primarily in peripheral areas, depending on the remaining disease dynamics (Figures 1, 2).

Analysis of the primary tumour stages and primary tumour biology showed that the patients treated were part of a high-risk group (Table 4). Almost half of the patients, namely 15 of the 33 (45.5%), received neo-adjuvant therapy (as first-

TABLE 4. Findings on patient characterization at initial diagnosis and after systemic therapy

	N. of patients (%)	N. of patients (%)	N. of patients (%)
Tumour stage	pT1	pT2	pT3/4
Total 18 patients	7 (38.9)	7 (38.9)	4 (22.2)
Post-PST	ypT1	ypT2	ypT3/4
Total of 15 patients	2 (13.3)	8 (53.3)	5 (33.3)
Nodal stage	pNo	pN1	pN2/3
Total of 22 patients	8 (36.3)	6 (27.2)	8 (36.3)
Post-PST	Nodal stage not determined		ypN2/3
Total of 11 patients	4 (36.3)		7 (63.6)

PST = primary systemic therapy

line systemic therapy) as part of their primary treatment. In spite of responsive chemotherapy, 13 of the 15 (86.7%) patients still had an advanced stage tumour in the form of ypT2 and/or ypT3 and ypT4. Eight of the 33 patients (24.2%) exhibited a triple negative breast carcinoma. The HER2 status was positive for 6 of the 33 patients (18.2%), while a positive receptor status was seen in over half of the patients (20 of 33, 55.2%). Since 21 (63.6%) patients had a distant metastases along with several other affected organ systems, it was ensured that the systemic therapy interval could be freely set as short as possible, ECT could be conducted on all patients without procedure related complications. For follow up the patient came 2 weeks after ECT therapy for local control. If patients were under treatment in our department they were seen regularly. In case of treatment of patients referred to our institution by other hospitals, disease progression was reported to us by the referring centre and the patients evaluated for further treatment proposal including additional ECT if appropriate. In case of local tumour progression, generally in the border area of the original recurrence, additional ECT took place within the following 6 months, but was in dependency of tumour biology and aggressiveness. For patients under chemotherapy, the best time for planning ECT was one week before the next chemotherapy administration, but a specific timeline was not determined *a priori*. The primary aim was to avoid the so-called nadir, this means the peak period with risk of neutropenia. In rare cases of extended ECT, the following chemotherapy was delayed for one to two weeks until patient's performance status was considered adequate. Since all except 4 patients generally received fractionated monochemotherapy treatments, the appointment for treatment could be easily selected without any major shift in the interval, at which point it was ensured there was no grade 3 or 4 neutropenia.

## Discussion

Despite operative intervention and radiotherapy, loco-regional relapses can occur repeatedly, persist, or exhibit therapy-resistance, often in a highly disseminated form. In these cases, additional local treatments can be proposed, and may be applied simultaneously or parallel to systemic therapy. In our study, ECT was offered as an additional treatment to systemic anticancer therapy with the objective of preventing local (skin) disease progression in patients with a highly extended local finding and/or disseminated tumours and to treat the symptoms of ulceration or lymphangitic tumour areas. Repeated therapy (ECT) was deemed necessary if the lesion was too extensive for complete treatment in one session or if the tumour progression was observed at follow-up.

In our institution, breast cancer metastases to the skin and subcutaneous tissue are the most frequent lesions treated with ECT. In the past clinical experiences, ECT has been applied to patients in different disease stages, *i.e.* locoregional disease such as chest wall recurrence after mastectomy or visceral disease with concomitant skin tumour involvement.<sup>9,12</sup> In most cases, the treatment has been reserved to very advanced cases with large ulcerated bleeding metastatic nodules.<sup>13</sup> It has been observed that early patient treatment would not require multiple treatment session, save the patient discomfort and improve quality of life, while achieving higher local tumour control rates and longer local progression-free survivals.<sup>8,13-17</sup> ECT represents an attractive locoregional therapy for unresectable chest wall recurrence (CWR) from breast cancer. In the study of Campana *et al.*<sup>8</sup> thirty-five consecutive patients with refractory CWR were enrolled from December 2006 through September 2011 and were administered with bleomycin-based ECT. Although only approximately

one third of patients (12 out of 35) achieved an effective chest wall control, the authors observed that if ECT would be applied earlier in the clinical course of chest wall recurrence, patients with fewer and less scattered skin metastases are less likely to develop new lesions. In a multicentre retrospective cohort study, 125 patients with breast cancer skin metastases underwent ECT between 2010 and 2013. The overall response rate after 2 months was 90.2%, while the complete response (CR) rate was 58.4%. Small tumour size, absence of visceral metastases, estrogen receptor positivity, and low Ki-67 index were predictors of CR after ECT. Patients who experienced CR had durable local control.<sup>16</sup> In a prospective observational study performed by Benevento *et al.*<sup>18</sup>, twelve consecutive elderly (median age of 76 years) with regional or distant skin or subcutaneous metastases from breast cancer, with or without visceral disease, were treated with ECT. A CR was observed in 75.3%, partial response in 17% no change in 7.7% patients. No serious ECT-related adverse events were reported. According to the authors, ECT could be suggested as a primary local therapy in patients not suitable for surgical removal of the primary tumour, and clinicians should not hesitate to use it even in the elderly.<sup>18</sup> Campana *et al.* confirmed that elderly breast cancer patients are highly responsive to ECT and achieved durable local tumour control.<sup>19</sup>

In our study, the data were collected over a period of three years. Of the 33 patients, 21 also had distant metastases and underwent appropriate cytotoxic systemic therapy. An indication for ECT followed either none or limited response of the loco-regional tumour to previous or current systemic therapy. Patients enrolled in this study not only received treatment for the systemic character of the disease, but also received ECT to control the tumour locally. In considering the risk factors arising from each additional intervention during ongoing chemotherapy, the patients showed no increased local toxicity, especially no higher dermal toxicity with formation of local necrosis. Patients with pulmonary metastases were given a preoperative pulmonary function test, depending on the extent of the metastases and clinical limitations. The extra bleomycin dosage of 15 mg/m<sup>2</sup> of body surface area did not result in any higher dermal or non-dermal toxicity, compared with prior toxicities.

The literature research showed that none of the studies noted the clinical response of primary systemic chemotherapy (neo-adjuvant chemotherapy) applied as a part of primary treatment of the breast carcinoma. In our study, almost half of the patients,

*i.e.* 15 of 33, underwent primary systemic therapy, whereby 13 of these patients still had a ypT2 to ypT4 stage tumour after successful application of the systemic therapy. These characteristics mean that the group included exclusively high-risk patients. Moreover, 25% of the patients, or 8 of 33, had a triple negative tumour. In comparison, the literature listed a maximum of 5 from 35 such patients or 14.3% that fell into this category.<sup>16,17</sup>

In our experience, ECT proved to be an effective supplement to a cytotoxic systemic therapy, especially for high-risk patients who did not respond well to systemic therapy of loco-regional metastases, without creating any greater systemic or loco-regional toxicities (grades 3 & 4 dermal toxicity). Tolerance and response of ECT did not differ between patients undergoing any systemic therapy and those receiving only endocrinal treatments, especially from the standpoint of the most common known side effects such as pain, muscle soreness, and local paraesthesia.

Furthermore, even the presence of distant metastases was not contraindicative for ECT, and did not hamper the local therapeutic effect. It is important to select the proper time for application and to monitor it. No evidence was seen of any possible occurrence of myelotoxicity resulting from the cytotoxic systemic therapy.

An analysis of the primary tumour data (prognosis factors) and the phenomenon of an overly high rate of failure of primary chemotherapy of large remaining tumours showed that this study treated a group of patients with an extremely high-risk of recurrence, especially at the loco-regional level. Particularly in these cases, ECT was found to be a key supplementary therapy that should be applied as early as possible during the course of the disease. The data clearly rule out any higher levels of local or systemic toxicity.

## References

1. Gerber B, Freund M, Reimer T. Recurrent breast cancer: treatment strategies for maintaining and prolonging good quality of life. [German]. *Dtsch Arztl Int* 2010; **107**: 85-91. doi:10.3238/arztebl.2010.0085
2. Bruce J, Carter DC, Fraser J. Patterns of recurrent disease in breast cancer. *Lancet* 1970; **1**: 433-5. doi:http://dx.doi.org/10.1016/S0140-6736(70)90829-9
3. Kurtz JM, Amalric R, Brandone H., Aymes Y, Jacquemier J, Pietra JC et al. Local recurrence after breast-conserving surgery and radiotherapy. Frequency, time course, and prognosis. *Cancer* 1989; **63**: 1912-7. doi:10.1016/j.ijrobp.2014.04.039
4. Grischke, E-M. Wallwiener D, Souchon R, Fehm T, Loehberg CR, Jud SM, et al. Isolated loco-regional recurrence of breast cancer – established and innovative therapy concepts. *Geburtsh Frauenheilk* 2013; **73**: 1-12. doi:10.1055/s-0032-1328660

5. Spratt D, Spratt E A, Wu S, DeRosa A, Lee NY, Lacouture ME, Barker CA. Efficacy of skin-directed therapy for cutaneous metastases from advanced cancer: A meta-analysis. *J Clin Oncol* 2014; **55**, 4634. doi:10.1200/JCO.2014.55.4634
6. Banerjee SM, Keshtgar MRS. Electrochemotherapy for treatment of cutaneous breast cancer metastases: A Review *Arch Breast Cancer* 2016; **3**: 108-17. doi:http://dx.doi.org/10.19187/abc.201634108-117
7. Bourke MG, Salwa SP, Sadacharam M, Whelan MC, Forde PF, Larkin JO, et al: Effective treatment of intractable cutaneous metastases of breast cancer with electrochemotherapy: Ten-year audit of single centre experience. *Breast Cancer Res Treat* 2017; **161**: 289-97. doi:10.1007/s10549-016-4046-y
8. Campana L, Valpione S, Falci C, Mocellin S, Basso M, Corti L, et al. The activity and safety of electrochemotherapy in persistent chest wall recurrence from breast cancer after mastectomy: a phase-II study. *Breast Cancer Res Treat* 2012; **7**: e39484. doi:10.1007/s10549-012-2095-4
9. Marty M, Sersa G, Garbay JR Gehl J, Christopher G, Collins CG, Snoj M, et al. Electrochemotherapy – an easy, highly effective and safe treatment of cutaneous and subcutaneous metastases: results of ESOPe (European Standard Operating Procedures of Electrochemotherapy) study. *Eur J Cancer Suppl* 2006; **4**: 3-13. doi:http://dx.doi.org/10.1016/j.ejcsup.2006.08.002
10. Mali B, Jarm T, Snoj M, Sersa G, Miklavcic D. Antitumor effectiveness of electrochemotherapy: a systematic review and meta-analysis. *Eur J Surg Oncol* 2012; **39**: 4-16. doi:http://dx.doi.org/10.1016/j.ejcsup.2006.08.002
11. Mir, L, Gehl, J, Sersa G, Collins CG Garbay JR, Billard V, et al. Standard operating procedures of the electrochemotherapy: Instructions for the use of bleomycin or cisplatin administered either systemically or locally and electric pulses delivered by the Cliniporator by means of invasive or non-invasive electrodes. *Eur J Cancer Suppl* 2006; **4**: 14-25. doi:http://dx.doi.org/10.1016/j.ejcsup.2006.08.003
12. Larkin JO, Collins CG, Aarons S, Tangney M, Whelan M, O'Reily S, et al: Electrochemotherapy aspects of preclinical development and early clinical experience. *Ann Surg* 2007; **3**: 469-79. doi:10.1097/01.sla.0000250419.36053.33
13. Matthiessen LW, Chalmers RL, Sainsbury DC, Veeramani S, Kessel G, Humphreys AC, et al. Management of cutaneous metastases using electrochemotherapy. *Acta Oncol* 2011; **50**: 621-5. doi:10.3109/0284186X.2011.573626
14. Sersa G, Cufer T, Paulin SM, Cemazar M, Snoj M. Electrochemotherapy of chest wall breast cancer recurrence. *Cancer Treat Rev* 2012; **38**: 379-86. doi:10.1016/j.ctrv.2011.07.006
15. Quaglino P, Matthiessen L, Curatolo P, Muir T, Bertino G, Kunte C, et al. Predicting patients at risk for pain associated with electrochemotherapy. *Acta Oncol* 2015; **54**: 298-306. doi:10.3109/0284186X.2014.992546
16. Cabula C, Campana LG, Grilz G, Galuppo S, Bussone R, De Meo L, et al. Electrochemotherapy in the treatment of cutaneous metastases from breast cancer: A multicenter cohort analysis. *Ann Surg Oncol*, 2015; **22**: S442-50. doi:10.1245/s10434-015-4779-6
17. Matthiessen L, Johannesen HH, Skougaard K, Gehl J, Hendel HW, et al. Dual time point imaging fluorine-18 flourodeoxyglucose positron emission tomography for evaluation of large loco-regional recurrences of breast cancer treated with electrochemotherapy. *Radiol Oncol* 2013; **47**: 358-65. doi:10.2478/raon-2013-0054
18. Benevento R, Santoriello A, Perna, G, Canonico S. Electrochemotherapy of cutaneous metastases from breast cancer in elderly patients: a preliminary report. *BMC Surgery* 2012; **12**: S6. doi:10.1186/1471-2482-12-S1-S6
19. Campana L, Galuppo S, Valpione S, Brunello A, Ghiotto C, Ongaro A, Rossi CR. Bleomycin electrochemotherapy in elderly metastatic breast cancer patients: clinical outcome and management considerations. *J Cancer Res Clin Oncol* 2014; **140**: 1557-65. doi:10.1007/s00432-014-1691-6

# High dose hypofractionated proton beam therapy is a safe and feasible treatment for central lung cancer

Takashi Ono<sup>1</sup>, Tomonori Yabuuchi<sup>2</sup>, Tatsuya Nakamura<sup>1</sup>, Kanako Kimura<sup>1</sup>, Yusuke Azami<sup>1</sup>, Katsumi Hirose<sup>1</sup>, Motohisa Suzuki<sup>1</sup>, Hitoshi Wada<sup>1</sup>, Yasuhiro Kikuchi<sup>1</sup>, Kenji Nemoto<sup>3</sup>

<sup>1</sup> Department of Radiation Oncology, Southern Tohoku Proton Therapy Center, 7-172, Yatsuyamada, Koriyama, Fukushima, Japan

<sup>2</sup> Department of Radiation Oncology, Ninohe Hospital, 38 - 2, Okawarage, Aza, Horino, Ninohe, Iwate, Japan

<sup>3</sup> Department of Radiation Oncology, Yamagata University Faculty of Medicine, 2-2-2, Iida-Nishi, Yamagata, Japan

Radiol Oncol 2017; 51(3): 324-330.

Received 17 January 2017

Accepted 14 May 2017

Correspondence to: Takashi Ono, M.D., Department of Radiation Oncology, Southern Tohoku Proton Therapy Center, 7-172, Yatsuyamada, Koriyama, Fukushima, 963-8052, Japan. Phone: +81-24-934-3888; Fax: +81-24-934-5393; E-mail: abc1123513@gmail.com

Disclosure: No potential conflicts of interest were disclosed.

**Background.** There have been few reports about high total dose hypofractionated proton beam therapy for central lung cancer. The aim of this study was to examine retrospectively the safety and efficacy of high total dose hypofractionated proton beam therapy for central lung cancer.

**Patients and methods.** Patients treated by proton beam therapy for central lung cancer located less than 2 cm from the trachea, mainstem bronchus, or lobe bronchus were included in this study. All patients received 80 Gy of relative biological dose effectiveness (RBE) in 25 fractions with proton beam therapy over 5 weeks between January 2009 and February 2015. The toxicities were evaluated using the Radiation Therapy Oncology Group and European Organization for Research and Treatment of Cancer criteria.

**Results.** Twenty patients, including 14 clinically inoperable patients (70%), received proton beam therapy for central lung cancer. The median patient age was 75 years (range: 63–90 years), the median follow up time was 27.5 months (range: 12–72 months), and the median tumor diameter was 39.5 mm (range: 24–81 mm). All patients were followed for at least 20 months or until death. The 2-year overall survival rate was 73.8% (100% in operable patients, and 62.5% in inoperable patients), and the 2-year local control rate was 78.5%. There was no Grade 3 or higher toxicities, including bronchial stricture, obstruction, and fistula.

**Conclusions.** The present study suggests that a high total dose hypofractionated proton beam therapy for central lung cancer was safe and feasible.

Key words: central; lung cancer; hypofractionated; proton beam therapy

## Introduction

Lung cancer accounted for approximately 13% of total cancer diagnoses and was the most frequently diagnosed cancer worldwide in 2012.<sup>1</sup> In 2013, the number of lung cancer deaths was estimated to be 1.6 million, while 34.7 million disability-adjusted life-years were also caused. Specifically, it was the most common cause of cancer death globally, including both developing and developed countries.<sup>2</sup>

Early-stage lung cancer is treated via lung resection. However, an increasing number of people are now receiving radiotherapy, including stereotactic body radiotherapy (SBRT).<sup>3-5</sup> SBRT can also be used for inoperable patients, and several studies have also demonstrated that SBRT is as effective for stage I lung cancer as lung resection.<sup>5,6</sup> However, SBRT for centrally located lung cancer has been reported to cause more toxicity than for peripheral lung cancer.<sup>7</sup>

An increasing number of patients with lung cancer, including those with locally advanced lung cancer, have been treated using proton beam therapy (PBT) with or without chemotherapy.<sup>8-12</sup> The advantage of PBT is that it can shape the dose more conformally to the target volume than conventional radiotherapy or SBRT using X-ray irradiation, thus reducing the dose distributed to surrounding healthy structures.<sup>13-15</sup> However, few reports have been published regarding the use of PBT in the treatment of patients with central lung cancer.

The purpose of the present study was to evaluate retrospectively the efficacy and safety of PBT for central lung cancer.

## Patients and methods

### Ethics statement

The treatment methods and procedures were approved by the Ethics committee of our institution. The study was conducted in accordance with the Declaration of Helsinki. Patients signed informed consent.

### Patients

The present study enrolled patients who were diagnosed with central lung cancer and were treated with PBT between January 2009 and February 2015 at the Southern Tohoku Proton Therapy Center. Central lung cancer was defined as tumors located less than 2 cm from the trachea, mainstem bronchus, or lobe bronchus.<sup>7</sup> Patients were retrospectively recruited from our database.

Whether or not the pathology of the lung tumor was histologically confirmed did not matter. If the pathology was not confirmed, an increase in the size of the lung tumor or high positron emission tomography (PET) uptake was regarded as a clinical malignancy. The clinical stage of the lung cancer was determined using computed tomography (CT) and PET-CT. Written informed consent was obtained from all of patients.

The inclusion criteria were as follows: (1) a solitary lung tumor without any previous treatment for it, (2) a World Health Organization performance status of 0-2, (3) no lymph node metastasis, and (4) the absence of distant other-organ metastasis or other sites of uncontrolled cancer. Patients with interstitial pneumonia were excluded from this study.

### Proton beam therapy

Treatment planning for PBT was based on 3-dimensional CT images taken at 2 mm intervals in the

exhalation phase while using a respiratory gating system (Anzai Medical, Tokyo, Japan). A custom-indexed vacuum-lock bag (Engineering System Co, Nagano, Japan) was used to immobilize the patients. A Xio-M treatment planning system (CMS Japan, Tokyo, Japan; and Mitsubishi Electric) was used to calculate the dose distributions for PBT. The gross tumor volume (GTV) included the lung tumor, the clinical target volume (CTV) was defined as the GTV plus 0.5 cm, and the planning target volume (PTV) was the CTV plus a 0.5 cm margin. The proton energy levels of 150 MeV and 210 MeV for 1-3 portals and a spread-out Bragg peak were tuned as much as possible until the PTV was exposed to a 90% isodose of the prescribed dose, and was not exposed to 110% isodose (upper limit) (Figure 1). The PBT system at our institute (Proton Beam System; Mitsubishi, Tokyo, Japan) uses a synchrotron and a passive scattering method in which a proton beam passes a bar ridge filter, a range shifter, and a customized compensator before entering the patient. The treatment was administered during the exhalation phase using a respiratory gating system. A multileaf collimator, which consisted of 40 iron plates with a width of 3.75 mm, and could be formed into an irregular shape, was used. Daily front and lateral X-ray imaging was used for positioning. The PBT for central lung tumors was set at 80 Gy of relative biological dose effectiveness (RBE) in 25 fractions over 5 weeks in our institution (isocenter prescription); the biological equivalent dose was 105.6 Gy when tumor alpha/beta ratio was regarded 10. The dose constraints were set for the esophagus ( $\leq 55$  Gy [RBE]), spinal cord ( $\leq 40$



**FIGURE 1.** Dose distribution map of proton beam therapy for central lung cancer. The red line represents the gross tumor volume and the purple line around the tumor represents the 90% dose line. The region outside the outermost blue line is allocated to < 10% radiation.

TABLE 1. The patient characteristics (n = 20)

Characteristics	Patients
Age (years)	
Median (range)	75 (63–90)
Gender	
Male	17 (85%)
Female	3 (15%)
Performance status	
0	8 (40%)
1	8 (40%)
2	4 (20%)
Charlson Index	
0	5 (25%)
1	6 (30%)
2	7 (35%)
3	2 (10%)
Follow-up time (months)	
Median (range)	27.5 (12–72)
Chronic obstructive pulmonary disease	
Yes	9 (45%)
No	11 (55%)
T category*	
T1	4 (20%)
T2	11 (55%)
T3	4 (20%)
T4	1 (5%)
Stage*	
I	15 (75%)
II	4 (20%)
III	1 (5%)
Tumor location	
Right upper lobe	7 (35%)
Right middle lobe	2 (10%)
Right lower lobe	6 (30%)
Left upper lobe	3 (15%)
Left lower lobe	2 (10%)
Histopathology	
Squamous cell carcinoma	8 (40%)
Adenocarcinoma	5 (25%)
Clinical malignancy	7 (35%)
Diameter of lung tumor (mm)	
Median (range)	39.5 (24–81)

\* Numbers correspond to the tumor-node-metastasis system of classification (International Union Against Cancer criteria)

Gy [RBE]), and heart ( $\leq 40$  Gy [RBE]) in principle. However, we did not reduce prescribed dose and irradiated over 40 Gy (RBE) to the heart when the lung tumor was too close to it.

## Evaluation and follow-up

All patients underwent either CT or PET-CT to evaluate the initial tumor response within 3 months after the completion of treatment. The initial treatment response was evaluated based on the Response Evaluation Criteria in Solid Tumors version 1.1.<sup>16</sup> A complete response was defined as the complete disappearance of all detectable tumors. In this study, a complete metabolic response (extinction of PET uptake) was also defined as a complete response.<sup>17</sup> A partial response was defined as  $\geq 30\%$  reduction in the maximal diameter of the tumor. Stable disease was defined as neither a partial response nor progressive disease. Progressive disease was defined as  $\geq 20\%$  enlargement of the primary tumor or the appearance of new lesions, including lymph node metastases and distant metastases. The evaluation of comorbidities was performed in accordance with Charlson *et al.* previously reported.<sup>18</sup> The follow-up interval was every 1–3 months for the first year and every 3–6 months thereafter. Imaging performed every 3–6 months after evaluating the initial tumor response. The cause of death was determined as lung cancer when patients had local recurrence or metastases and no other causes of death except for cancer, were presented. Toxicities were evaluated using the Radiation Therapy Oncology Group and European Organization for Research and Treatment of Cancer criteria.<sup>19</sup> The following dosimetric factors were examined with the use of a dose volume histogram of the lung minus the GTV and heart: mean lung dose, lung V5 (lung irradiated 5 Gy [RBE]), lung V10, lung V15, lung V20, and mean heart dose.

## Statistical analysis

All statistical analyses were performed using the IBM SPSS Statistics software program (version 22; SPSS Inc., Chicago, IL, USA). The overall survival (OS) time was defined as the time between the start of PBT and the time of the last follow-up examination or death. The Kaplan-Meier method and a log rank test were used to estimate the survival probability and compare the survival, respectively. The relationships between the occurrence of lung or heart toxicities and the dose volume histogram

factors were examined using the Mann-Whitney *U* test. All *p*-values were two-sided, and *p*-values of < 0.05 were considered to indicate statistical significance.

## Results

### Patients

The initial study population included 86 patients who received 80 Gy (RBE) for lung cancer. Patients were excluded from the analysis for the following reasons: lymph node metastasis, *n* = 13; distant other-organ metastasis, *n* = 13; treatment for lung cancer before PBT *n* = 7; other sites of uncontrolled cancer *n* = 5; interstitial pneumonia *n* = 9; and failure to satisfy the criteria of central lung cancer, *n* = 19. Thus, the characteristics of 20 patients, including 14 (70%) with clinically inoperable cancer due to poor respiratory function (*n* = 9), elderly (90 years old, *n* = 1), comorbidities (*n* = 4), as well as 9 (45%) with chronic obstructive pulmonary disease, were analyzed (Table 1). The median age was 75 years (range: 63–90 years), the median follow up time was 27.5 months (range: 12–72 months), the median tumor diameter was 39.5 mm (range: 24–81 mm), the median tumor volume 35.7 cc (range: 6.1–151.2 cc), and the median dose of mean PTV coverage was 79.5 Gy (RBE) (range: 75–81 Gy [RBE]).

### Survival and local control

All patients were followed for at least 20 months (living patients) or until death. The 1- and 2-year overall survival (OS) rates were 95.0% (95% confidence interval [CI]: 87.7–100%), and 73.8% (95% CI: 53.9–93.7%), respectively (Figure 2A). The 2-year OS rates of stage I and II/III were 80% and 53.3%, respectively. Six patients died of lung cancer, due to local recurrence (*n* = 3) and distant failure (*n* = 3) and 2 of other disease, due to heart failure (*n* = 1) and sepsis (*n* = 1). The 2-year OS rates for operable and inoperable patients were 100%, and 62.5%, respectively (Figure 2B), although the 2-year OS between the two groups was not significantly different (*p* = 0.109). Thirteen patients (65%) achieved a complete response, 5 (25%) achieved a partial response, and 2 (10%) achieved stable disease. The 2-year local control rate was 78.5% (95% CI: 59.5–97.5%); all local recurrences were in-field recurrence) (Figure 3A). The 2-year local control rates of lung cancers with diameters of ≤ 39.5 mm and > 39.5 mm (39.5 mm was the median tumor diameter) were 90% and 68.6%, respectively (Figure 3B), although the 2-year

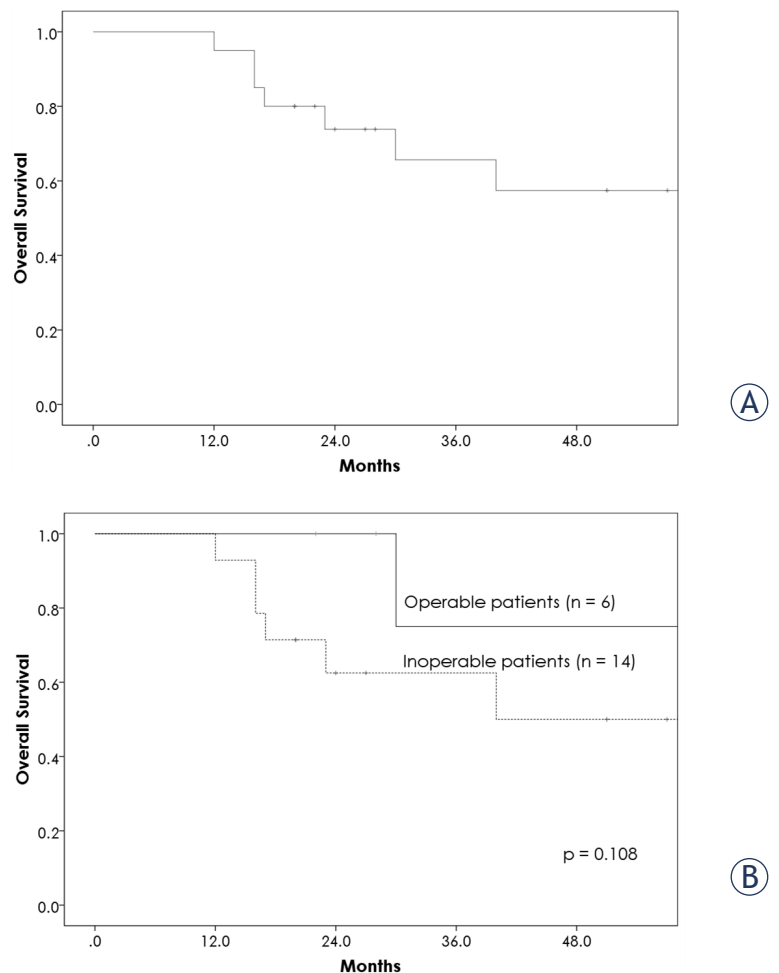


**FIGURE 2.** (A) The overall survival rate of the patients treated for central lung cancer. The 1- and 2-year overall survival rates were 95.0% and 73.8%, respectively. (B) The 2-year overall survival rates of operable and inoperable patients were 100% and 62.5%, respectively.

**TABLE 2.** Toxicities

Toxicities	Grade 0	Grade 1	Grade 2	Grade 3 - 5
Lung	0	18 (90%)	2 (10%)	0
Esophagus	20 (100%)	0	0	0
Heart	16 (80%)	4 (20%)	0	0
Bone	15 (75%)	3 (15%)	2 (10%)	0

local control rate between the two groups was not significantly different (*p* = 0.348).

### Toxicities

Table 2 shows the toxicities after PBT. The median dose of mean lung dose and mean heart dose were

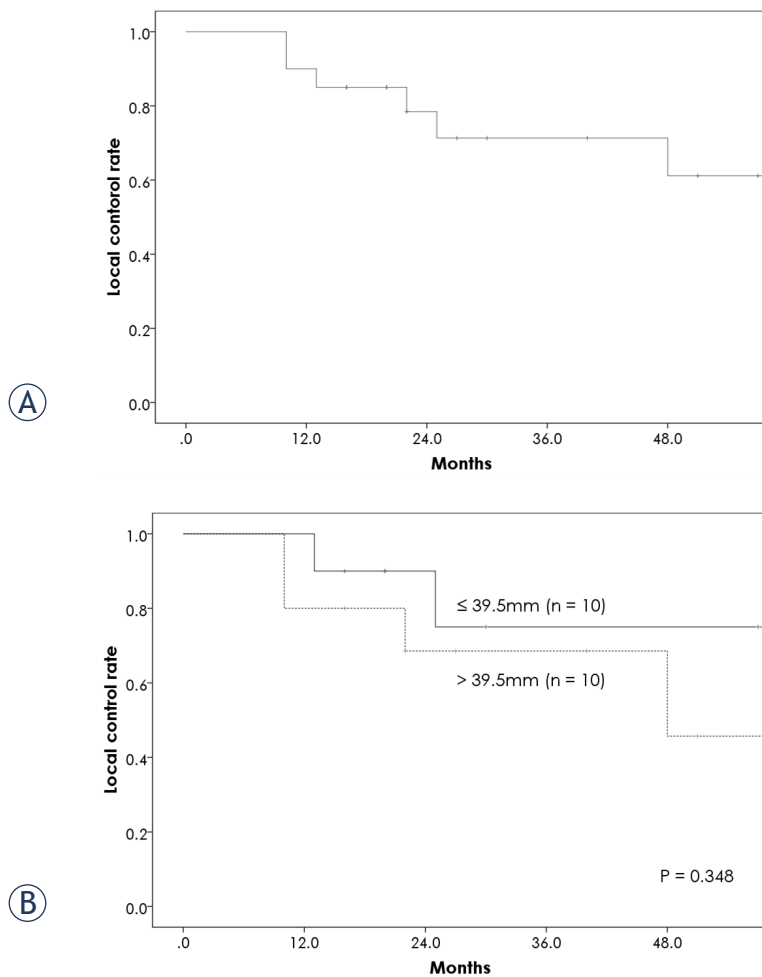


**FIGURE 3.** (A) The local control rate for patients with central lung cancer after proton beam therapy. The 2-year local control rate was 78.5%. (B) The 2-year local control rates of lung cancers with a diameter  $\leq 39.5$  mm and  $> 39.5$  mm were 90% and 68.6%, respectively ( $p = 0.348$ ).

7.2 Gy (RBE) and 0.5 Gy (RBE), respectively. There were 2 patients (10%) with Grade 2 lung toxicities (both pneumonitis) and no patients with Grade 3

or higher lung toxicities, including bronchial stricture, obstruction, and fistula. Moreover, there were 2 patients (10%) with Grade 2 bone toxicities (both rib fracture). No Grade 2 or higher heart toxicities were observed, although 4 patients had Grade 1 toxicities (all of them pericardial effusion). Lastly, there were no esophageal toxicities, as no tumor included in the study was close enough to the esophagus. There were no statistically significant differences with regard to the dosimetric factors of mean lung dose (7.4 Gy [RBE] vs 7.0 Gy [RBE],  $p = 0.830$ ), lung V5 (18.2% vs 16.6%,  $p = 0.677$ ), lung V10 (16.1% vs 14.5%,  $p = 0.647$ ), lung V15 (14.8% vs 13.1%,  $p = 0.625$ ), and lung V20 (13.5% vs 12.0%,  $p = 0.629$ ) between patients with Grade 2 pneumonitis and those without it. Furthermore the dosimetric factors of mean heart dose (1.3 Gy [RBE] vs 1.9 Gy [RBE],  $p = 0.667$ ) between patients with Grade 1 pericardial effusion and those without it demonstrated no statistically significant differences.

## Discussion

Table 3 shows the OS of the present study and previous reports.<sup>20-23</sup> According to that, the 2-year OS of the present study was not inferior to that in previous studies. At our institution, PBT for central lung cancer delivered 3.2 Gy (RBE) per fraction, because a high dose per fraction using SBRT for central lung cancer was reported to be associated with a high risk of morbidity.<sup>7</sup> However, by comparing the outcomes between the present and previous studies, it was demonstrated that a high OS was achieved in our patients with high total dose, comparable with other series that used SBRT with a higher dose per fraction, although the ratio of T1 stage in the present study (20%) was less than that reported in previous studies (35–63%).<sup>20-23</sup> Nagata *et al.* reported on the outcomes of SBRT for opera-

**TABLE 3.** Overall survival of central lung cancer

	Number of patients	Median follow up time	treatment	Overall survival rate	All grade 3-5 toxicities
Song et al. (20)	9	26.5 months	SBRT	50% (2-year)	33%
Modh et al. (21)	125	17.4 months	SBRT	64% (2-year)	8%
Chaudhuri et al. (22)	34	18.4 months	SBRT	63.2% (2-year)	3%
Tekatli et al. (23)	80	47 months	SBRT	53% (3-year)	6.4%
Bush et al. (8)	33	48 months	PBT	Not applicable	0
present study	20	27.5 months	PBT	73.8% (2-year)	0

Abbreviations: SBRT = stereotactic body radiotherapy

ble and inoperable patients with lung cancer.<sup>5</sup> They reported that the 3-year OS of operable patients was superior to that of inoperable patients (76.5% vs 59.9%). In the present study, the OS of operable patients was also superior to that of inoperable patients, but not to a significant degree. Therefore, a better OS may be achieved if PBT for central lung cancer is only administered in medically operable patients who refused surgery.

Grade 3 or higher lung toxicities of SBRT for central lung tumor were reported at rates of 1.5–4.8%.<sup>21,22,24,25</sup> However, Bush *et al.* reported no Grade 3 or higher toxicities including lung toxicities after PBT for central lung cancer (table 3).<sup>8</sup> These results were consistent with the results the present study, even though the tumors irradiated were larger than those subjected to SBRT. These findings suggest that high total dose PBT may result in lower rates of lung toxicities than SBRT, although the relatively low dose per fraction may also have been involved. This finding may be because PBT can reduce the irradiated lung dose compared with SBRT.<sup>13</sup> Indeed, there have been some reports suggesting that reducing the lung dose leads to a low rate of lung toxicities. Matsuo *et al.* reported that the lung volume, which was irradiated with 25 Gy, was significantly associated with radiation pneumonitis.<sup>26</sup> Barriger *et al.* also reported that the mean lung dose and lung volume irradiated with 20 Gy was significantly associated with Grade 2–4 radiation pneumonitis.<sup>27</sup> PBT has the advantage of a dose fall-off associated with particle beams and as such offers the possibility of sparing healthy lung tissue, and the low rate of toxicities makes it an attractive potential treatment choice.

Regarding the impact of the total dose for the treatment lung cancer, Bush *et al.* reported that a high dose level PBT for lung cancer, including central lung cancer, significantly improved the 4-year OS compared with lower doses.<sup>8</sup> Nakayama *et al.* also reported good OS with high total dose for stage I peripheral and central lung cancer; specifically, patients with central lung cancer received 72.6 Gy (RBE) in 22 fractions.<sup>28</sup> These suggest that a higher total dose for lung cancer can improve the OS of patients with lung cancer. Paul *et al.* reported that SBRT resulted in an equivalent OS to surgery in patients with tumors sized  $\leq 2$  cm, but in an inferior OS in patients with tumors sized  $\leq 5$  cm.<sup>29</sup> Indeed, larger lung tumor resulted in a lower local control rate in the present study, but no statistically significance difference was observed. Therefore, a high dose may be needed to control the disease and prolong the OS in patients with lung tumors,

especially large tumors. PBT can increase the dose to tumors without increasing the lung dose compared with SBRT. PBT may therefore be useful for increasing the dose to lung tumors in order to achieve better control and prolong the OS.

Several limitations associated with the present study warrant mention. First, the number of patients was small. However, there have been few reports about PBT for central lung cancer, so we feel that the present study is still meaningful. Second, the present study was retrospective. Third, we did not examine the trachea with endoscopy, mainstem bronchus, or main bronchi. Therefore, bronchial stenosis and obstruction might have been more prevalent than we assumed. However, there were no problems clinically, as there was no Grade 3 or higher lung toxicities in the present study.

The present study suggests that high-dose hypofractionated PBT for central lung cancer is safe and feasible.

## Acknowledgements

We thank all staff of the Radiation Oncology section.

## References

1. Torre LA, Bray F, Siegel RL, Ferlay J, Lortet-Tieulent J, Jemal A. Global cancer statistics, 2012. *CA Cancer J Clin* 2015; **65**: 87-108. doi:10.3322/caac.21262
2. Fitzmaurice C, Dicker D, Pain A. The global burden of cancer 2013. *JAMA Oncol* 2015; **1**: 505-27. doi:10.1001/jamaoncol.2015.0735
3. Li Q, Swanick CW, Allen PK, Gomez DR, Welsh JW, Liao Z, et al. Stereotactic ablative radiotherapy (SABR) using 70 Gy in 10 fractions for non-small cell lung cancer: exploration of clinical indications. *Radiother Oncol* 2014; **112**: 256-61. doi:10.1016/j.radonc.2014.07.010
4. Nagata Y, Takayama K, Matsuo Y, Norihisa Y, Mizowaki T, Sakamoto T, et al. Clinical outcomes of a phase I/II study of 48 Gy of stereotactic body radiotherapy in 4 fractions for primary lung cancer using a stereotactic body frame. *Int J Radiat Oncol Biol Phys* 2005; **63**: 1427-31. doi:10.1016/j.ijrobp.2005.05.034
5. Nagata Y, Hiraoka M, Shibata T, Onishi H, Kokubo M, Karasawa K, et al. Prospective trial of stereotactic body radiation therapy for both operable and inoperable T1N0M0 non-small cell lung cancer: Japan Clinical Oncology Group Study JCOG0403. *Int J Radiat Oncol Biol Phys* 2015; **93**: 989-96. doi:10.1016/j.ijrobp.2015.07.2278
6. Chang JY, Senan S, Paul MA, Mehran RJ, Louie AV, Balter P, et al. Stereotactic ablative radiotherapy versus lobectomy for operable stage I non-small-cell lung cancer: a pooled analysis of two randomised trials. *Lancet Oncol* 2015; **16**: 630-37. doi:10.1016/S1470-2045(15)70168-3
7. Timmerman R, McGarry R, Yiannoutsos C, Papiez L, Tudor K, DeLuca J, et al. Excessive toxicity when treating central tumors in a phase II study of stereotactic body radiation therapy for medically inoperable early-stage lung cancer. *J Clin Oncol* 2006; **24**: 4833-9. doi:10.1200/JCO.2006.07.5937
8. Bush DA, Cheek G, Zaheer S, Wallen J, Mirshahidi H, Katerelos A, et al. High-dose hypofractionated proton beam radiation therapy is safe and effective for central and periphPheral early-stage non-small cell lung cancer: results of a 12-year experience at Loma Linda University Medical Center. *Int J Radiat Oncol Biol Phys* 2013; **86**: 964-8. doi:10.1016/j.ijrobp.2013.05.002

9. Register SP, Zhang X, Mohan R, Chang JY. Proton stereotactic body radiation therapy for clinically challenging cases of centrally and superiorly located stage I non-small-cell lung cancer. *Int J Radiat Oncol Biol Phys* 2011; **80**: 1015-22. doi:10.1016/j.ijrobp.2010.03.012
10. Chang JY, Komaki R, Wen HY, De Gracia B, Bluett JB, McAleer MF, et al. Toxicity and patterns of failure of adaptive/ablative proton therapy for early-stage, medically inoperable non-small cell lung cancer. *Int J Radiat Oncol Biol Phys* 2011; **80**: 1350-7. doi:10.1016/j.ijrobp.2010.04.049
11. Nihei K, Ogino T, Ishikura S, Nishimura H. High-dose proton beam therapy for Stage I non-small-cell lung cancer. *Int J Radiat Oncol Biol Phys* 2006; **65**: 107-111. doi:10.1016/j.ijrobp.2005.10.031
12. Chang JY, Komaki R, Lu C, Wen HY, Allen PK, Tsao A, et al. Phase 2 study of high-dose proton therapy with concurrent chemotherapy for unresectable stage III nonsmall cell lung cancer. *Cancer* 2011; **117**: 4707-13. doi:10.1002/cncr.26080
13. Kadoya N, Obata Y, Kato T, Kagiya M, Nakamura T, Tomoda T, et al. Dose-volume comparison of proton radiotherapy and stereotactic body radiotherapy for non-small-cell lung cancer. *Int J Radiat Oncol Biol Phys* 2011; **79**: 1225-31. doi:10.1016/j.ijrobp.2010.05.016
14. Lee CH, Tait D, Nahum AE, Webb S. Comparison of proton therapy and conformal X-ray therapy in non-small cell lung cancer (NSCLC). *Br J Radiol* 1999; **72**: 1078-84. doi:10.1259/bjr.72.863.10700825
15. Suit H, Goldberg S, Niemierko A, Trofimov A, Adams J, Paganetti H. Proton beams to replace photon beams in radical dose treatments. *Acta Oncol* 2003; **42**: 800-8. doi:10.1080/02841860310017676
16. Eisenhauer EA, Therasse P, Bogaerts J, Schwartz LH, Sargent D, Ford R, et al. New response evaluation criteria in solid tumours: revised RECIST guideline (version 1.1). *Eur J Cancer* 2009; **45**: 228-47. doi:10.1016/j.ejca.2008.10.026
17. Young H, Baum R, Cremerius U, Herholz K, Hoekstra O, Lammertsma AA, et al. Measurement of clinical and subclinical tumour response using [18F]-fluorodeoxyglucose and positron emission tomography: review and 1999 EORTC recommendations. European Organization for Research and Treatment of Cancer (EORTC) PET Study Group. *Eur J Cancer* 1999; **35**: 1773-82. doi:10.1016/S0959-8049(99)00229-4
18. Charlson ME, Pompei P, Ales KL, MacKenzie CR. A new method of classifying prognostic comorbidity in longitudinal studies: development and validation. *J Chronic Dis* 1987; **40**: 373-83. doi:10.1016/0021-9681(87)90171-8
19. Cox JD, Stetz J, Pajak TF. Toxicity criteria of the Radiation Therapy Oncology Group (RTOG) and the European Organization for Research and Treatment of Cancer (EORTC). *Int J Radiat Oncol Biol Phys* 1995; **31**: 1341-6. doi:10.1016/0360-3016(95)00060-C
20. Song SY, Choi W, Shin SS, Lee SW, Ahn SD, Kim JH, et al. Fractionated stereotactic body radiation therapy for medically inoperable stage I lung cancer adjacent to central large bronchus. *Lung Cancer* 2009; **66**: 89-93. doi:10.1016/j.lungcan.2008.12.016
21. Modh A, Rimner A, Williams E, Foster A, Shah M, Shi W, et al. Local control and toxicity in a large cohort of central lung tumors treated with stereotactic body radiation therapy. *Int J Radiat Oncol Biol Phys* 2014; **90**: 1168-76. doi:10.1016/j.ijrobp.2014.08.008
22. Chaudhuri AA, Tang C, Binkley MS, Jin M, Wynne JF, von Eyben R, et al. Stereotactic ablative radiotherapy (SABR) for treatment of central and ultra-central lung tumors. *Lung Cancer* 2015; **89**: 50-6. doi:10.1016/j.lungcan.2015.04.014
23. Tekatli H, Senan S, Dahele M, Slotman BJ, Verbakel WF. Stereotactic ablative radiotherapy (SABR) for central lung tumors: Plan quality and long-term clinical outcomes. *Radiother Oncol* 2015; **117**: 64-70. doi:10.1016/j.radonc.2015.09.028
24. Mangona VS, Aneese AM, Marina O, Hymas RV, Ionascu D, Robertson JM, et al. Toxicity after central versus peripheral lung stereotactic body radiation therapy: a propensity score matched-pair analysis. *Int J Radiat Oncol Biol Phys* 2015; **91**: 124-32. doi:10.1016/j.ijrobp.2014.08.345
25. Lischak JW, Malik RM, Collins SP, Collins BT, Matus IA, Anderson ED, et al. Stereotactic body radiotherapy (SBRT) for high-risk central pulmonary metastases. *Radiat Oncol* 2016; **11**: 28. doi:10.1186/s13014-016-0608-8
26. Matsuo Y, Shibuya K, Nakamura M, Narabayashi M, Sakanaka K, Ueki N, et al. Dose-volume metrics associated with radiation pneumonitis after stereotactic body radiation therapy for lung cancer. *Int J Radiat Oncol Biol Phys* 2012; **83**: e545-9. doi:10.1016/j.ijrobp.2012.01.018
27. Barriger RB, Forquer JA, Brabham JG, Andolino DL, Shapiro RH, Henderson MA, et al. A dose-volume analysis of radiation pneumonitis in non-small cell lung cancer patients treated with stereotactic body radiation therapy. *Int J Radiat Oncol Biol Phys* 2012; **82**: 457-62. doi:10.1016/j.ijrobp.2010.08.056
28. Nakayama H, Sugahara S, Tokita M, Satoh H, Tsuboi K, Ishikawa S, et al. Proton beam therapy for patients with medically inoperable stage I non-small-cell lung cancer at the university of tsukuba. *Int J Radiat Oncol Biol Phys* 2010; **78**: 467-71. doi:10.1016/j.ijrobp.2009.07.1707
29. Paul S, Lee PC, Mao J, Isaacs AJ, Sedrakyan A. Long term survival with stereotactic ablative radiotherapy (SABR) versus thoracoscopic sublobar lung resection in elderly people: national population based study with propensity matched comparative analysis. *BMJ* 2016; **354**: i3570. doi:10.1136/bmj.i3570

# Expression of LOC285758, a potential long non-coding biomarker, is methylation-dependent and correlates with glioma malignancy grade

Alenka Matjasic<sup>1</sup>, Mara Popovic<sup>2</sup>, Bostjan Matos<sup>3</sup> and Damjan Glavac<sup>1</sup>

<sup>1</sup> Department of Molecular Genetics, Institute of Pathology, Faculty of Medicine, University of Ljubljana, Slovenia

<sup>2</sup> Institute of Pathology, Faculty of Medicine, University of Ljubljana, Slovenia

<sup>3</sup> Department of Neurosurgery, University Medical Center, Ljubljana, Slovenia

Radiol Oncol 2017; 51(3):331-341.

Received 24 October 2016

Accepted 22 November 2016

Correspondence to: Prof. Dr. Damjan Glavač, Department of Molecular Genetics, Institute of Pathology, Faculty of Medicine, University of Ljubljana, Korytkova 2, SI-1000 Ljubljana, Slovenia. E-mail: damjan.glavac@mf.uni-lj.si, Tel.: +386-1-543-7180

Disclosure: No potential conflicts of interest were disclosed.

**Background.** Identifying the early genetic drivers can help diagnose glioma tumours in their early stages, before becoming malignant. However, there is emerging evidence that disturbance of epigenetic mechanisms also contributes to cell's malignant transformation and cancer progression. Long non-coding RNAs are one of key epigenetic modulators of signalling pathways, since gene expression regulation is one of their canonical mechanisms. The aim of our study was to search new gliomagenesis-specific candidate lncRNAs involved in epigenetic regulation.

**Patients and methods.** We used a microarray approach to detect expression profiles of epigenetically involved lncRNAs on a set of 12 glioma samples, and selected LOC285758 for further qPCR expression validation on 157 glioma samples of different subtypes. To establish if change in expression is a consequence of epigenetic alterations we determined methylation status of lncRNA's promoter using MS-HRM. Additionally, we used the MLPA analysis for determining the status of known glioma biomarkers and used them for association analyses.

**Results.** In all glioma subtypes levels of LOC285758 were significantly higher in comparison to normal brain reference RNA, and expression was inversely associated with promoter methylation. Expression substantially differs between astrocytoma and oligodendroglioma, and is elevated in higher WHO grades, which also showed loss of methylation.

**Conclusions.** Our study revealed that lncRNA LOC285758 changed expression in glioma is methylation-dependent and methylation correlates with WHO malignancy grade. Methylation is also distinctive between astrocytoma I-III and other glioma subtypes and may thus serve as an additional biomarker in glioma diagnosis.

Key words: glioma; lncRNA; LOC285758; over-expression; epigenetics; DNA methylation; MS-HRM; MLPA; IDH1; 1p/19q

## Introduction

Glioma are the commonest primary brain tumours in adults and also the most aggressive, with overall poor survival.<sup>1,2</sup> Clinically, they are extremely heterogeneous primary brain tumours that are presenting a great challenge in clinical oncology. This heterogeneity is reflected in the lack of knowledge about the exact mechanisms of tumour formation and progression, subsequently leading to less ac-

curate classification and choosing the appropriate treatment. It is why numerous researchers have focused to find new genetic factors and molecular mechanisms involved in gliomagenesis, which may also contribute to developing new therapeutic approaches and improving the prognosis for glioma patients.

lncRNAs are widely expressed in mammalian nervous system<sup>3</sup> and several were identified to be specifically linked with neuro-oncological

TABLE 1. Patients' demographics and glioma histopathological classification

Patients demographic		
Number of patients	157	
Gender (female/male)	67/90 (1 : 1.34)	
Mean age at diagnosis (years)	43.8 (SD ±18,89)	
# < 45 years	86	
# > 45 years	71	
Glioma classification	Glioma subtype	WHO grade
Astrocytoma (AC)	15 pilocytic	WHO I
	9 diffuse	WHO II
	11 diffuse with signs of anaplasia	WHO II-III
	9 anaplastic	WHO III
	23 secondary GBM	WHO IV
Oligodendroglioma (ODG)	31 primary GBM	WHO IV
	4 diffuse	WHO II
	5 diffuse with signs of anaplasia	WHO II-III
Oligoastrocytoma (OAC)	28 anaplastic	WHO III
	2 diffuse	WHO II
	3 diffuse with signs of anaplasia	WHO II-III
	17 anaplastic	WHO III

disorders<sup>4,5</sup>, and as such they could help explain the mechanisms of glioma malignant transformation.<sup>6,7</sup> LncRNAs are a class of non-coding RNAs that share many features with protein-coding RNAs (mRNAs), but lack the open reading frame, have lower sequence conservation and lower level of expression.<sup>8,9</sup> However, they are more cell- and tissue-type specific than mRNAs.<sup>10</sup> For many of them functional analyses showed to have key roles in numerous fundamental biological processes, such as cell cycle regulation, epigenetic regulation, imprinting, cell differentiation and apoptosis, and diseases, including tumorigenesis.<sup>11-17</sup> The involvement of lncRNAs in disease processes as one of the most important factors controlling gene expression creates an urgency to understand the mechanisms by which these RNAs seek their targets and impact signalling pathways<sup>16</sup>, and how much their disturbance might contribute to disease development.

Gene expression regulation by lncRNAs appears to be mediated largely through epigenetic mechanisms, which play a crucial role in regulating gene expression and are closely associated with disease onset. A number of studies show that as much as 20-30% of lncRNAs have been able to physically interact with specific epigenetic enzymes and driving them to specific genomic loci.<sup>18</sup> By binding to the chromatin-modifying proteins, such as PRC2,

G9a, hnRNPK, and SWI/SNF, they modulate the chromatin states and thus impact gene expression of cell cycle, cell differentiation, apoptosis, DNA repair, and cell adhesion.<sup>3,17,19</sup> Moreover, they can directly modulate the transcription of proximally-located genes by interacting with promoters and transcription factors.<sup>3</sup>

In glioma, epigenetic alterations and mechanisms, including methylation of gene promoters, histone modifications and chromatin modifiers are relatively unexplored, although DNA methylation of *O6-methylguanin-DNA methyltransferase (MGMT)* expression was associated with the prognosis of glioma patients.<sup>20,21</sup> DNA methylation is one of the primary epigenetic mechanisms in regulating gene expression, and disturbance of this process may cause various diseases, including cancer. It is also the most common epigenetic modification found in tumour cells.<sup>22</sup> Moreover, DNA methylation is an important regulator of expression of not only the mRNAs but also of the lncRNAs, and it seems that DNA demethylation of silent lncRNAs results in their activation.<sup>23</sup> Methylation patterns differ among various tissue-types and cell-types<sup>24</sup>, which means the cell-/tissue-specific methylation status, similarly to expression pattern, could be a useful biomarker.

In this study, we performed an expressional profiling of lncRNAs potentially involved in epigenetic levels of regulation in glioma samples of different histological subtypes compared to normal brain reference RNA. We used the microarray approach (LncPath™ Human Epigenetic Pathway) to search for novel lncRNA biomarkers potentially involved in glioma development. To validate microarray profiling results we used the qPCR method on a set of 125 glioma samples of different subtype and malignancy grade. In addition, we wanted to investigate if the change in gene's expression is due to changed methylation pattern of its promoter, and if there is any association with the hallmark markers, such as *IDH1/2* and *TP53* mutation, copy number variation of genes *CDKN2A* and *CDKN2B*, and 1p/19q co-deletion.

## Patients and methods

### Patients

Hundred and fifty-seven tumours that were surgically removed from patients between the years 2007 and 2015 were chosen for the study. Immediately after surgical biopsy tumours were stabilized in *RNAlater* (Applied Biosystems, USA), incubated at

4°C for at least 24 hours and subsequently stored at -20°C until needed. All tumours were evaluated by neuro-pathologist in order to assess glioma subtype and tumour grade (see Table 1), according to the WHO 2007 guidelines.<sup>25</sup> We collected patient's demographic data and results of immunohistochemical analyses, if they were performed, from our institutional database. The tumour biopsies used in the study belonged to 67 female and 90 male patients (mean age at diagnosis: 43.8 years). For reference RNA we used commercially available FirstChoice Human Brain Reference Total RNA (Cat.no. 6050, Ambion; Invitrogen, USA) (further referred to as brain reference RNA) obtained from the healthy brain tissue of 23 individuals without any signs of neurodegeneration. The study was approved by the National Medical Ethics Committee of the Republic of Slovenia (115/5/14). As DNA control samples we used nine samples of freshly frozen brain tissue that were collected at the autopsy of five patients (5 cerebrum and 4 cerebellum tissue samples). Samples were evaluated as a normal brain tissue, without any visible signs of neurodegeneration.

### Nucleic acid extraction

For extraction and purification of nucleic acids we used the AllPrep DNA/RNA/miRNA Universal Kit (Qiagen, Germany). Total DNA and RNA were simultaneously extracted from the same piece of tissue (up to 20 mg) that was homogenized with TissueLyser LT (Qiagen, Germany) for 5 min at 50 Hz, and further processed according to manufacturer's instructions. The yield of both RNA and DNA was measured spectrophotometrically using the NanoDrop ND-1000 (Thermo Scientific, USA). The quality and fragmentation of the extracted RNA (RNA integrity) was determined by agarose gel electrophoresis on Bioanalyzer 2100 (Agilent Technologies, USA), using the RNA 6000 Nano kit (Agilent Technologies, USA) according to manufacturer's instructions. Only the samples with appropriate yield and quality were considered for further analyses; thus, not all samples were used for all analyses performed.

### Expressional profiling of epigenetically involved lncRNA

We performed expressional profiling on 12 RNA samples of different glioma subtype and a brain reference RNA. Samples were chosen from a sample set of our previous glioma study (unpublished

study), and selected upon histopathologically determined glioma subtypes so that each of the four subgroups, *i.e.* astrocytoma (WHO grade II or III), primary GBM, secondary GBM and oligodendroglioma (WHO grade III), included 3 samples of sufficient RNA concentration and high quality. Samples were sent to ArrayStar Inc, USA, where sample preparation and microarray hybridization were performed, based on the manufacturer's standard protocols (Arraystar Inc.). One µg of RNA for individual sample was hybridized to the LncPath Human Epigenetic Pathway microarray (6x7K). Scanned slide images were processed by GenePix Pro 6.0 software (Axon) for raw data extraction, which were further normalized and processed using the R language. After filtering, only the probes for which at least 2 out of 13 samples had raw intensity above 32 were retained for further differential analyses. LncRNAs that showed significant change in expression between tumour group and brain reference RNA were identified through volcano plot filtering. After identifying groups' candidate genes, each group was compared to others. The »fold change« cut-off value for lncRNA to be considered as differentially expressed was set to < - 1.5 (expression is decreased) and > 1.5 (expression is increased), and p-value cut-off was set at 0.05.

### Quantitative real-time PCR (qPCR) validation of LOC285758 expression

LOC285758 expression levels were validated with the quantitative real-time PCR method, based on the intercalating dye (SYBR Green) technology. Only the samples with total RNA concentration higher than 50 ng/µL and RIN above 5.5 were used for qPCR analysis. The first strand cDNA was generated with One Taq RT-PCR kit according to manufacturer's instructions (New England Biolabs, UK) and using random primer mix. The reverse transcription reaction was prepared in a 10 µL reaction mixture with 300 ng of total input RNA. cDNA was properly diluted and amplified in a 10 µL reaction volume, using the SYBR Select Master Mix (Thermo Fisher Scientific, USA). We used *GAPDH* and *U6* as reference genes (endogenous controls) and brain reference RNA (mentioned in section 2.1) as the control RNA. All qPCR reactions were performed in duplicate using the Rotor Gene-Q system (Qiagen, Germany) following the primer manufacturer's standard cycling protocol for pre-designed primers for LOC285758 (PrimeTime qPCR Assay primer, IDT – Integrated

**TABLE 2.** Primers used for validation of *LOC285758* expression profiling results, reference genes and determining methylation status of lncRNA's promoter

Quantitative real-time PCR			
Gene	Assay ID	Amplicon length (bp)	Annealing temperature (°C)
<i>LOC285758</i>	Hs.PT.58.26012748	129	60
<i>GAPDH</i>	QT00079247	95	55
Gene	Primer sequence (5' - 3')	Amplicon length (bp)	Annealing temperature (°C)
<i>U6</i>	CTCGCTTCGGCAGCACA AACGCTTCACGAATTGCGT	94	60
Methylation sensitive HRM			
Gene	Oligonucleotide sequence (5' - 3')	Amplicon length (bp)	Annealing temperature (°C)
<i>LOC285758 F</i>	TTGTTTTTGAAAAGTTTTTGA	118	55
<i>LOC285758 R</i>	AAACACAAAAAACCTAACAAAA		

DNA Technology, USA) and *GAPDH* (QuantiTect qPCR Primer Assay, Qiagen, Germany). The cycling protocol for designed *U6* primers was similar to that of Qiagen with optimized  $T_A$  (see Table 2). The signal was collected on the Green channel at the end point of every cycle, and following amplification melt curve analysis was performed to verify specificity of qPCR amplicon.

Relative quantification levels of the target gene were calculated following the  $\Delta\Delta C_T$  method;  $\Delta\Delta C_T$  represents the difference between the quantity of target transcript in brain reference RNA (control RNA) ( $\Delta C_T$  control) and in tumour ( $\Delta C_T$  sample), after each sample and control were normalized to geometric mean expression of reference genes (*GAPDH* and *U6*).<sup>26</sup> A positive  $\Delta\Delta C_T$  value in our calculations means higher expression level in tumour samples.

### Methylation-sensitive HRM

For determining lncRNA's promoter methylation status we used the methylation sensitive high resolution melt (MS-HRM) analysis. Primers for amplifying *LOC285758* promoter's target region were designed with a freely available software tool Methyl Primer Express software v1.0 (Applied Biosystems, USA) in such a manner that they amplify both methylated and unmethylated DNA. Primers were designed to target CpG specific region at 5'UTR end (flanking sequence/exon1). Prior to MS-HRM analysis, 500 ng of input amount of sample DNA were bisulphite converted (bsDNA) using innu-CONVERT Bisulfite Basic Kit (Analytik Jena AG,

Germany) according to manufacturer's protocol. We created two DNA control pools by mixing 5 control samples of cerebrum and 4 control samples of cerebellum, treated them with bisulphite and used them for comparing the methylation status between normal brain tissue and tumour samples. For fully methylated/unmethylated (positive/negative) controls we used commercially available EpiTect Control DNA (Qiagen, Germany). All MS-HRM reactions were prepared with EpiTect HRM PCR Kit (Qiagen, Germany) in a 10  $\mu$ L reaction mixture by manufacturer's recommendations and adjustments according to primer optimization analysis (1.5  $\mu$ L of each primer, 1  $\mu$ L bsDNA (10 ng/ $\mu$ L)). We included the negative and positive control, both control pools and no-template control in each MS-HRM experiment, which were carried out on Rotor Gene Q (Qiagen, Germany). Amplification conditions were set based on manufacturer's recommendations as follows: 5 minutes of initial denaturation at 95°C, 45 cycles: denaturation at 95°C for 10 seconds, annealing at optimized temperature ( $T_A$  in Table 2) for 30 seconds, and elongation at 72°C for 20 seconds. After amplification, the HRM analysis was conducted by increasing the temperature from 65°C to 95°C by 0.1°C per 2 seconds. Fluorescence signal was collected from the green channel in elongation step and from the HRM channel during HRM analysis. For analysing MS-HRM results, we used the Rotor-Gene Q Series Software 2.3.1 (Qiagen, Germany). For determining methylation status of individual sample, samples HRM melting plots were normalized and further compared to controls.

## Multiplex ligation-dependent probe amplification

We used the P088-C1 Oligodendroglioma SALSA MLPA probe mix (MRC-Holland, the Netherlands) to detect loss of chromosome arms 1p and 19q, copy number variations in *CDKN2A* and *CDKN2B* genes, and to determine the status of the most common mutations of *IDH1* (R132H and R132C) and *IDH2* (R172K and R172M) genes in different glioma subtypes. The results of MLPA analysis have been further considered as the criteria for sample sub-classification for additional comparison, and determining possible differences in gene expression and promoter methylation. The MLPA experiment was prepared according to manufacturer's protocol and recommendations with 100 ng of input DNA amount. Capillary gel electrophoresis was performed using ABI Prism 310 Genetic Analyser (Applied Biosystems, USA), and we used Coffalyser software (MRC-Holland, the Netherlands) for fragment analysis.

## Data analysis

All statistical tests were performed using IBM SPSS Statistics 20. software (IBM Corporation, New York, USA). We used the one-way ANOVA analysis for comparing differences in expression between all glioma subtypes, and Mann-Whitney 2-independent test to cross test differences between two subtypes. Pearson's correlation coefficient was used to establish association of expression with promoter's methylation status, status of known biomarkers, and glioma subtype. Differences were considered statistically significant when they reached or were below  $p \leq 0.05$ .

## Results

### Expression profiling of epigenetically involved lncRNAs

Expression profiling of 12 glioma tumour samples of four different subtypes was performed with an ArrayStar microarray technology. Differential analysis of tumour samples compared to brain reference RNA, with absolute fold change (FC) cut-off value at 1.5, showed 351 lncRNAs with altered expression levels in at least one subtype (Figure 1A,B). Among these, 60 lncRNAs were differentially expressed in all four subtypes (Figure 1B). A more stringent analysis with absolute FC cut-off set at 2 showed 187 lncRNAs with altered expression

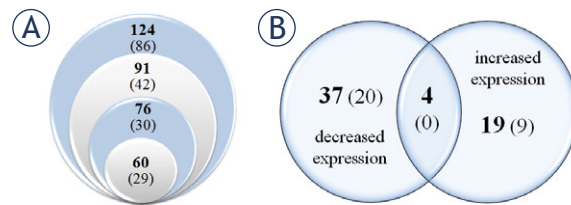


**FIGURE 1.** Venn's diagram of lncRNAs that were significantly differentially expressed using microarray screening of lncRNAs involved in epigenetic mechanisms and/or pathways. **(A)** Number of lncRNAs in regard to the number of subtypes in which they were found differentially expressed (the number of subtypes rises from the outer circle (one subtype) towards the inner one (four subtypes)). **(B)** The number of lncRNAs found differentially expressed in all four analysed subtypes (using two levels of stringency – absolute fold change cut-off value of 1.5 and (2)).

in at least one subtype and only 29 lncRNAs in all four subtypes (Figure 1A,B; numbers of lncRNAs matching this criteria are in parentheses). In Table 3 are listed top 10 over-expressed and top 10 under-expressed lncRNAs in each glioma subtype.

With the purpose to identify new potential biomarker candidates we searched through public databases, such as PubMed (<https://www.ncbi.nlm.nih.gov/pubmed/>), Ensembl (<http://www.ensembl.org/index.html>), HGNC (<http://www.genenames.org/>), and lncRNADB (<http://lncrnadb.com/>), for information about gene's location in the genome, its known function or involvement in cellular pathways, and previous mention in the literature. Among the most differentially changed was lncRNA *LOC285758*, which showed increased expression in all four glioma subtypes, but lower expression in GBMs in comparison to astrocytoma and oligodendroglioma (Table 3). Also, it was significantly changed between the two GBM subtypes.

### Validation of LOC285758 expression

To validate the microarray expression results of *LOC285758* we used the quantitative real-time PCR method on a subset of 125 samples that met both the concentration and quality criteria. Expression levels were significantly increased in 105/125 samples (84%) compared to brain reference RNA (Figure 2A), and all glioma subtypes showed positive  $\Delta\Delta C_T$  average values (Figure 2B). Data obtained by qPCR validation analysis were in concordance with results of microarray profiling that showed increased levels in all four subtypes (Figure 2B). However, the expression in GBMs did not significantly differ, as observed on microar-

**TABLE 3.** Top 10 lncRNAs that showed significantly increased/decreased expression in four glioma subtypes, using the LncPath Human Epigenetic Pathway microarray (ArrayStar, USA)

Astrocytoma II+III*		Secondary GBM		Primary GBM		Oligodendroglioma	
FC(abs)	Gene Name	FC(abs)	Gene Name	FC(abs)	Gene Name	FC(abs)	Gene Name
<b>TOP 10 OVER-EXPRESSED</b>							
9.775	RP11-434O22.1	9.840	APOC2	11.343	AK024556	10.085	RP6-201G10.2
7.863	LOC285758	9.105	AK024556	9.761	FJ209302	7.233	LOC285758
6.203	LOC100129034	7.971	LOC100129034	9.402	AK055628	6.241	GASS
5.247	RP11-264F23.3	7.578	AK055628	9.267	H19	5.454	RP11-264F23.3
5.211	RP6-201G10.2	4.509	RP11-145M9.3	7.012	RP11-434O22.1	5.360	LOC100216546
5.107	APOC2	4.243	RP11-73E17.2	6.720	APOC2	5.043	SNRPE
4.374	RP11-770J1.3	3.657	KB-1836B5.1	5.527	LOC285758	4.991	AK024556
4.211	HOXA11-AS	3.394	H19	4.851	LOC100216546	4.930	AC009506.1
3.861	RP3-405J24.1	2.878	BANCR	4.770	LOC100129034	4.351	RP11-73E17.2
3.795	AK055628	2.695	AB447886	4.525	HOXA11-AS	3.846	LOC286059
<b>TOP 10 UNDER-EXPRESSED</b>							
9.638	RP11-678P16.1	24.555	MEG3	22.494	MEG3	43.328	RP11-678P16.1
7.026	XLOC_013368	11.341	AK054921	16.532	AK054921	23.879	FABP5P3
6.797	AK054921	8.050	AF520792	11.157	RP11-678P16.1	18.840	DGCR5
6.148	MEG3	6.845	DGCR5	8.208	DGCR5	8.073	MEG3
6.003	RP11-18F14.2	6.623	XLOC_013368	8.207	XLOC_013368	7.092	AK054921
5.820	HAR1A	6.470	AK054970	7.979	HAR1B	6.887	XLOC_013368
5.052	SNAR-A2	6.243	HAR1A	6.325	HAR1A	6.318	NEAT1
4.216	FABP5P3	6.114	XIST	6.218	SNAR-A2	6.205	SEPT7P6
4.082	RP11-325F22.4	5.799	MIAT	6.066	RP11-208G20.2	6.090	CASC2
3.887	SEPT7P6	5.712	SNAR-A2	5.652	XLOC_008014	5.873	TMSB10P2

\* = II+III – tumours of WHO grade II and III; (abs) = absolute value; FC = fold change

ray. We observed the highest average expression in oligoastrocytoma and oligodendroglioma, and statistical analysis of ANOVA showed significant differences comparing all groups ( $p = 0.004$ ). Cross comparison of two subtypes using Mann-Whitney test showed significantly increased expression between oligodendroglioma and astrocytoma I-III ( $p = 0.007$ ), secondary GBM ( $p = 0.021$ ), and primary GBM ( $p = 0.014$ ), respectively. Comparing astrocytoma to oligoastrocytoma showed lower expression and borderline value of significance ( $p = 0.051$ ), and similar was observed in comparison of secondary GBM and oligoastrocytoma ( $p = 0.052$ ) (Figure 2).

### Methylation status of LOC285758 promoter

After we quantified and analysed the lncRNA expression, we wanted to see if this change could be

a consequence of changed DNA methylation pattern. Methylation status of LOC285758 promoter was determined for individual sample from a subset of 125 samples with sufficient DNA concentration and quality. We compared sample's normalized and melting curve compared to fully methylated and fully unmethylated control. Fifty-one percent (64/125) of samples were methylated and we found methylation status to be inversely associated with LOC285758 expression (Figure 3A) ( $r_s = -0.455$ ,  $p < 0.001$ ). We also compared normalized curves of tumour samples and control pools. LOC285758 promoter was shown as methylated in control pools (normal brain), but hypo-methylated against positive control, and 87% (109/125) of tumour samples were hypo-methylated or unmethylated in regard to normal brain. Further analysis, regarding the glioma subtype (Figure 3C), showed astrocytoma of WHO grades I-III are methylated in 96% of samples, whereas astrocytoma of grade

IV, *i.e.* GBM showed high percent of unmethylated cases (57% of secondary GBM (12/21) and 77% of primary GBM (20/26)). Cases of oligodendroglioma were unmethylated in 75% (21/28), whereas oligoastrocytoma were unmethylated in 44% (8/18) (Figure 3C). Also, classifying samples upon WHO grade showed tumours of lower grades are largely methylated (Figure 3B).

### Association of LOC285758 expression and methylation with glioma hallmark markers

We wanted to search for a possible association of expression with already established glioma biomarkers. For determining mutation status of *IDH1* and *IDH2* gene, variation in copy number of *CDKN2A* and *CDKN2B* gene, and deletion of chromosome arm 1p and 19q we conducted the MLPA analysis. Additionally, results of routine immunohistochemical analyses were collected from our database. *TP53* was mutated in 38% of samples (59 mutations (MUT), 36 wild type (WT), and 62 not acquired (NA)). *IDH1* mutation R132H was found in 34% (54 MUT, 64 WT, and 38 NA) of samples, and R132C in one case (< 1%). In *IDH2* we did not find any mutations. *CDKN2A/CDKN2B* were deleted in 23% (37/37 deletions (DEL), 44/45 WT, 2/1 duplications (DUPL), and 74 NA). Chromosome arm 1p was lost completely in 17% (27 DEL, 7 partial DEL, 3 DUPL, 69 WT and 51 NA) and 19q in 19% (30 DEL, 14 partial DEL, 11 DUPL, 49 WT, and 53 NA). Duplication of 19q was found mainly in GBM tumours. Co-deletion of 1p and 19q arm was detected in 15% of samples (24 cases) and majority of them were oligodendroglioma. For correlation analysis we excluded partial deletions and duplications of *CDKN2A/B*, 1p and 19q.

We compared both *LOC285758* expression and promoter methylation status to above biomarkers. Pearson's correlation coefficient test showed both expression and methylation to be significantly associated with WHO malignancy grade (Figure 3B). Expression was also positively associated with the *IDH1* mutation – samples with *IDH1* mutation had higher expression, but independently from promoter's methylation. A more detailed analysis, regarding the subtype, showed expression of *LOC285758* does not differ between *IDH1* mutated and wildtype astrocytoma of lower grades. But significantly does in secondary GBM, oligoastrocytoma and oligodendroglioma. We found methylation to be in weak relation to age at diagnosis and loss of *CDKN2A* and *CDKN2B*, but in an inverse

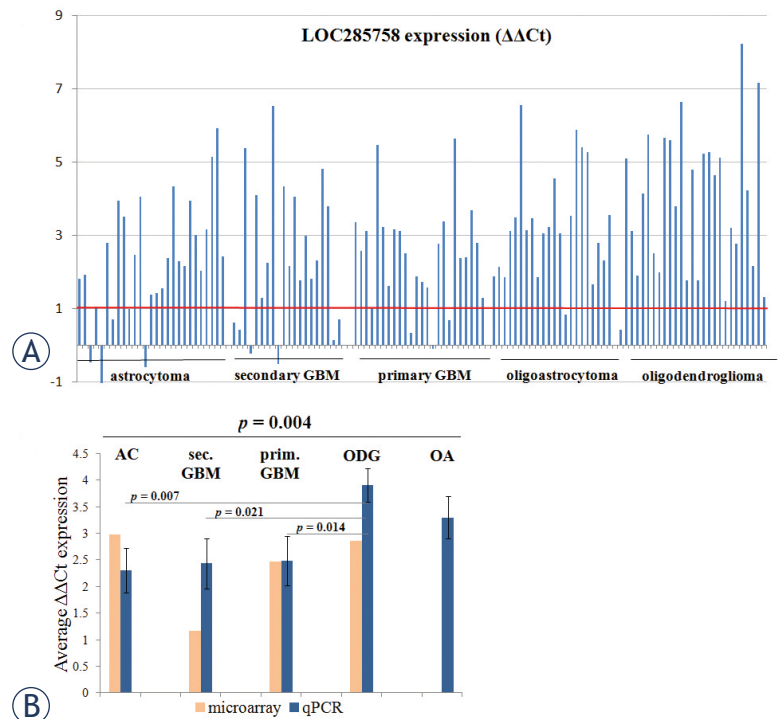


**FIGURE 2.** (A) Differential expression of *LOC285758* in individual samples (y-axis presents  $\Delta\Delta C_t$  values). (B) Comparison of average  $\Delta\Delta C_t$  values for individual glioma subtype, determined by microarray and qPCR. Oligoastrocytoma samples were not included in microarray analysis.  $\Delta\Delta C_t$  represents difference of gene's expression in comparison to brain reference RNA, and the positive values mean that gene's levels are increased. p-values were determined for qPCR data (ANOVA for comparing all five subtypes and Mann-Whitney U-test for comparing two subtypes).

**TABLE 4.** Association of *LOC285758* expression with patients demographic data and glioma hallmark biomarkers: mutations of *IDH1* and *TP53*, copy number variations of *CDKN2A* and *CDKN2B*, and loss of chromosome arm 1p and 19q (1p/19q co-deletion)

	LOC285758 expression		LOC285758 promoter methylation	
	$r_s$	p-value	$r_s$	p-value
Gender	-0.044	0.634	0.009	0.920
Age at diagnosis (< 45y >)	0.065	0.475	<b>-0.313</b>	<b>&lt; 0.001</b>
WHO grade (low/high)	<b>0.213</b>	<b>0.019</b>	<b>-0.433</b>	<b>&lt; 0.001</b>
<i>IDH1</i> (wt/mut)	<b>0.375</b>	<b>&lt; 0.001</b>	0.096	0.331
<i>TP53</i> (wt/mut)	-0.083	0.483	0.153	0.178
1p loss (wt/del)	<b>0.310</b>	<b>0.005</b>	<b>-0.396</b>	<b>&lt; 0.001</b>
19q loss (wt/del)	<b>0.267</b>	<b>0.032</b>	<b>-0.360</b>	<b>0.002</b>
1p/19q loss (wt/del)	<b>0.262</b>	<b>0.014</b>	<b>-0.373</b>	<b>&lt; 0.001</b>
<i>CDKN2A</i> (wt/del)	0.085	0.477	<b>-0.231</b>	<b>0.042</b>
<i>CDKN2B</i> (wt/del)	0.093	0.435	<b>-0.240</b>	<b>0.033</b>

$r_s$  = Pearson's correlation/association coefficient (0.2–0.4 – weak, 0.4–0.5 – moderate, > 0.6 strong correlation); p-value cut-off is set at 0.05 (95% confidence interval)

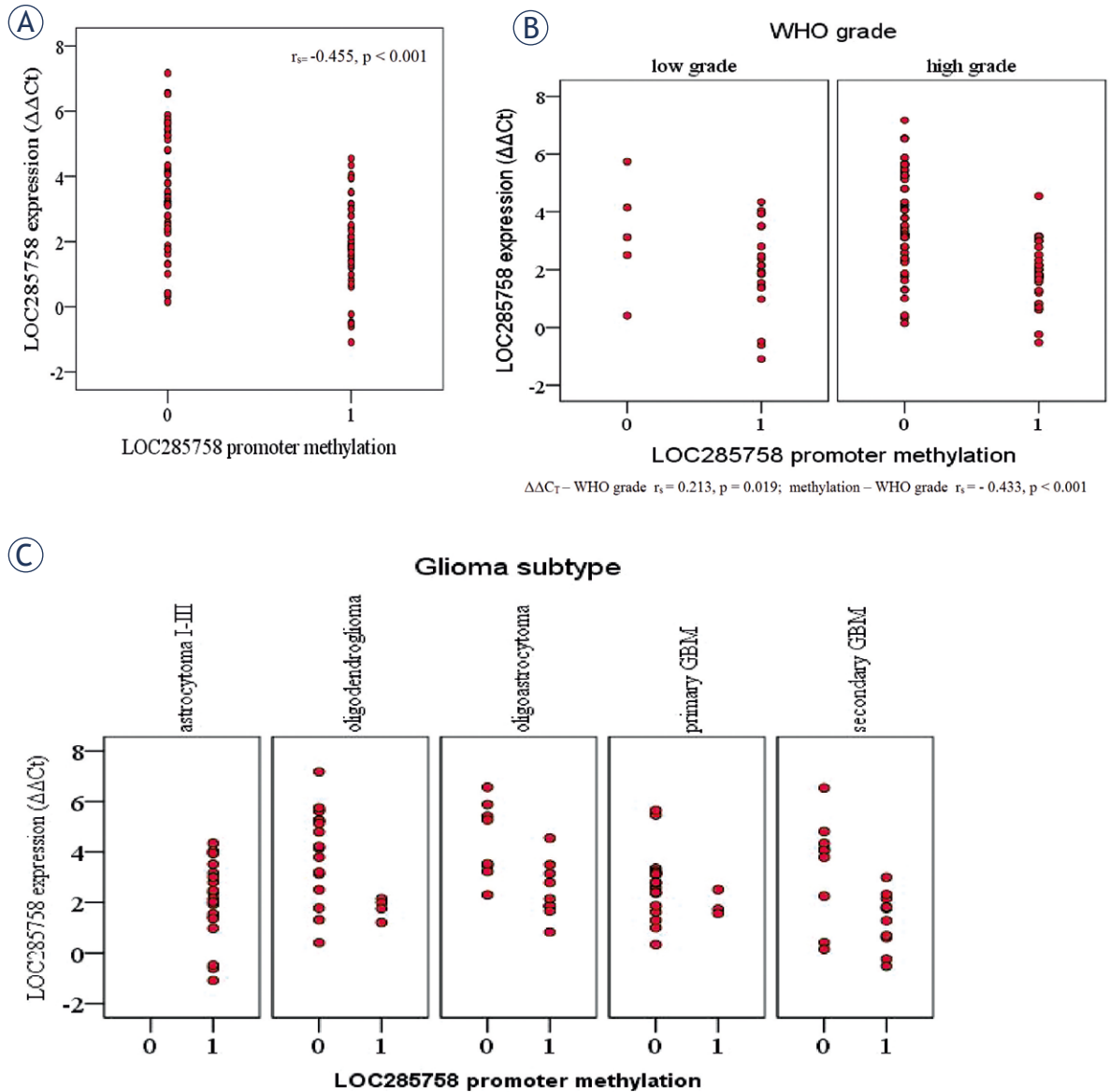


**FIGURE 3.** Scatter plots showing (A) LOC285758 expression (qPCR) in association to methylation status. Unmethylated samples showed higher expression levels compared to methylated ones. (B) LOC285758 expression and promoter methylation status significantly differ regarding the WHO malignancy grade and (C) glioma subtype, especially comparing astrocytoma grade I-III (all samples were methylated) to grade IV (GBMs were largely unmethylated).

Promoter methylation: 0 = unmethylated, 1 = methylated

manner. The loss of chromosome arm 1p, 19q and both arms concurrently was associated with both expression and methylation (Table 4); however, as mentioned above, co-deletion was found mainly in oligodendroglioma.

## Discussion

Due to the aggressive nature of glioma, poor prognosis and especially the resistance of tumour cells

against established and/or even modern treatments there is a need for more precise definition of glioma molecular background and finding new biomarkers. The simplest way to screen through high number of genes potentially involved in tumour development is expression profiling using microarray technology. We analysed the differences in expression of lncRNAs, potentially involved in epigenetic regulatory mechanisms. Among 879 lncRNA microarray probes we identified 351 lncRNAs with significantly changed expression (with absolute

fold change cut-off of 1.5) in at least one glioma subtype, which once again confirms molecularly heterogeneous nature of glioma tumours.<sup>1</sup> We determined 60 lncRNAs with changed expression in all four analyzed subtypes and selected few lncRNAs due to their significantly changed expression either in or between all four subtypes either regarding a specific subtype. For many lncRNAs we did not find any previous reports; however, expression of few lncRNAs, such as *MEG3*<sup>27,28</sup>, *H19*<sup>29</sup>, *Xist*<sup>30</sup>, and just recently *NEAT1*<sup>31</sup> and *HOXA11-AS*<sup>32</sup>, was already shown to be significantly changed in glioma. Moreover, they were associated with disturbance of key cellular pathways and patient's prognosis.

To the best of our knowledge, one of the unknown cancer-related lncRNAs is *LOC285758*, or long intergenic non-protein coding RNA 1268 (LINC01268), that lies in close proximity of the *MARCKS* (myristoylated alanine-rich C-kinase substrate) gene, which encodes a cell cycle and motility promoting protein. As *LOC285758* expression on microarray appeared to be significantly lower in secondary GBM in comparison to primary GBM it represented a candidate biomarker for potentially distinguish these two entities, especially since many cases are morphologically alike and thus misclassified.<sup>6</sup> However, validation results showed expression does not significantly differ between astrocytic tumours, but methylation status does as almost all primary GBM were un-methylated versus variable status in secondary GBM. This variation in DNA methylation might be associated with secondary GBM developing through low-grade astrocytic precursors<sup>33</sup>, since we found almost all astrocytic tumours of lower grades methylated. It could also indicate that methylation pattern of lncRNA's promoter changes as the tumour progresses.

Nevertheless, *LOC285758* expression levels do significantly differ between astrocytoma, oligoastrocytoma and oligodendroglioma, respectively, which could also be a helpful discriminating feature of oligoastrocytoma from astrocytic tumours of grade I-III, since these neoplasms are somewhat a mix of genetic changes characteristic for astrocytic (*IDH1* mutations) and oligodendroglial tumours (1p/19q co-deletion).<sup>1</sup> Expression levels and methylation status of *LOC285758* found in oligoastrocytoma, compared to both subtypes, even more corroborate their mixed genetic background. Additionally, *LOC285758* could be an additional feature to distinguish oligodendroglioma and astrocytoma, since these entities might arise from the same cells of origin, but develop through different molecular pathways.<sup>1</sup>

Results of different methylation further highlight epigenetic alterations of lncRNAs. We chose the MS-HRM method for determining methylation status of gene's promoter as it is simple, fast and highly sensitive; even one single base substitution can be observed as a significant fluorescence drop and melting peak shift.<sup>34,35</sup>

As lncRNAs principal mechanism is regulation of coding genes and many bind to chromatin-modifying genes<sup>17</sup>, the potential targets of *LOC285758* could be addressed by its genome location, with *MARCKS* and *HDAC2* as neighbouring genes. In contrast to the anonymity of *LOC585758*, there are numerous reports of *MARCKS* being involved in various cancers, including glioma.<sup>36-39</sup> It has the ability to regulate various signalling pathways; by sequestering the phosphatidylinositol 4,5-bisphosphate (PIP2) molecules, a PI3K target, *MARCKS* functions as a tumour suppressor of PI3K/Akt signalling pathway.<sup>40,41</sup> On contrary, it can also function as tumour enhancer as its overexpression was associated with metastasis and poorer prognosis in patients with lung squamous cell carcinoma<sup>42</sup>, and promoting EGFRvIII-mediated GBM tumorigenesis.<sup>39</sup> There is only one report showing association of *LOC285758* expression with expression of its antisense mRNA, and changed methylation of intragenic CpG island; however, it was not cancer related.<sup>43</sup> *HDAC2* is an enzyme of histone deacetylase family, the key players in epigenetic silencing of gene expression and one of the regulators of major cellular functions, such as cell cycle, apoptosis, DNA damage repair, and senescence.<sup>44,45</sup> Like *MARCKS*, *HDAC2* is already extensively studied, largely due to its crucial biological function, and was found significantly deregulated in broad spectrum of diseases.<sup>46-50</sup> *HDAC2* was overexpressed in astrocytoma, like *HDAC1*, and expression increases during tumour recurrence and progression, but it is not WHO-grade-related.<sup>50</sup> Whether the functional association of *LOC285758* and its neighbouring genes exist is yet to be investigated.

Some limitations of our study are related to collecting patient's data as no complete clinical data were available at the time of the study. Another limitation is the lack of knowledge about exact functions and roles of lncRNA *LOC285758* in normal brain and cancer tissue, but such studies are beyond our research timeframe.

We can conclude the microarray expression profiling of glioma tumours proved useful for identification of novel lncRNAs involved in epigenetic pathways of glioma development as we determined several potential lncRNAs with sig-

nificantly changed expression, including lncRNA *LOC285758*. Our study is, to the best of our knowledge, the first to report disturbed expression of *LOC285758* in glioma tumours. Elevated expression of *LOC285758* and its association to loss of cytosine methylation and higher malignancy grade suggest to an oncogenic function of this lncRNA in glioma biogenesis. Furthermore, significantly different expression between astrocytoma and oligodendroglioma, and oligoastrocytoma, respectively, might suggest *LOC285758* as a new biomarker candidate of glioma development with added diagnostic value, but its exact function is yet to be revealed.

## Acknowledgment

This research is a part of Alenka Matjašič doctoral thesis. This study was supported by the Slovenian Research Agency (P3-054).

## References

- Louis DN, Molecular pathology of malignant gliomas. *Annu Rev Pathol* 2006; **1**: 97-117. doi:10.1146/annurev.pathol.1.110304.100043
- Mesti T, Moltara ME, Boc M, Rebersek M, Ocvirk J, Bevacizumab and irinotecan in recurrent malignant glioma, a single institution experience. *Radiol Oncol* 2015; **49**: 80-5. doi:10.2478/raon-2014-0021
- Qureshi IA, Mattick JS, Mehler MF, Long non-coding RNAs in nervous system function and disease. *Brain Res* 2010; **1338**: 20-35. doi:10.1016/j.brainres.2010.03.110
- Gibb EA, Vucic EA, Enfield KS, Stewart GL, Lonergan KM, Kennett JY, et al., Human cancer long non-coding RNA transcriptomes. *PLoS One* 2011; **6**: e25915. doi:10.1371/journal.pone.0025915
- Qureshi IA, Mehler MF, Emerging roles of non-coding RNAs in brain evolution, development, plasticity and disease. *Nat Rev Neurosci* 2012; **13**: 528-41. doi:10.1038/nrn3234
- Zhang X, Sun S, Pu JK, Tsang AC, Lee D, Man VO, et al., Long non-coding RNA expression profiles predict clinical phenotypes in glioma. *Neurobiol Dis* 2012; **48**: 1-8. doi:10.1016/j.nbd.2012.06.004
- Gibb EA, Brown CJ, Lam WL, The functional role of long non-coding RNA in human carcinomas. *Mol Cancer* 2011; **10**: 38. doi:10.1186/1476-4598-10-38
- Guttman M, Amit I, Garber M, French C, Lin MF, Feldser D, et al., Chromatin signature reveals over a thousand highly conserved large non-coding RNAs in mammals. *Nature* 2009; **458**: 223-7. doi:10.1038/nature07672
- Djebali S, Davis CA, Merkel A, Dobin A, Lassmann T, Mortazavi A, et al., Landscape of transcription in human cells. *Nature* 2012; **489**: 101-8. doi:10.1038/nature11233
- Weichenhan D, Plass C, The evolving epigenome. *Hum Mol Genet* 2013; **22**: R1-6. doi:10.1093/hmg/ddt348
- Hassler MR, Egger G, Epigenomics of cancer - emerging new concepts. *Biochimie* 2012; **94**: 2219-30. doi:10.1016/j.biochi.2012.05.007
- Tripathi V, Shen Z, Chakraborty A, Giri S, Freier SM, Wu X, et al., Long noncoding RNA MALAT1 controls cell cycle progression by regulating the expression of oncogenic transcription factor B-MYB. *PLoS Genet* 2013; **9**: e1003368. doi:10.1371/journal.pgen.1003368
- Tian D, Sun S, Lee JT, The long noncoding RNA, *Xist*, is a molecular switch for X chromosome inactivation. *Cell* 2010; **143**: 390-403. doi:10.1016/j.cell.2010.09.049
- Lee C, Kikyo N, Strategies to identify long noncoding RNAs involved in gene regulation. *Cell Biosci* 2012; **2**: 37. doi:10.1186/2045-3701-2-37.
- Kitagawa M, Kitagawa K, Kotake Y, Niida H, Ohhata T, Cell cycle regulation by long non-coding RNAs. *Cell Mol Life Sci* 2013; **70**: 4785-94. doi:10.1007/s00018-013-1423-0
- Han L, Zhang K, Shi Z, Zhang J, Zhu J, Zhu S, et al., LncRNA profile of glioblastoma reveals the potential role of lncRNAs in contributing to glioblastoma pathogenesis. *Int J Oncol* 2012; **40**: 2004-12. doi:10.3892/ijo.2012.1413
- Mercer TR, Mattick JS, Structure and function of long noncoding RNAs in epigenetic regulation. *Nat Struct Mol Biol* 2013; **20**: 300-7. doi:10.1038/nsmb.2480
- Karapetyan AR, Buiting C, Kuiper RA, Coolen MW, Regulatory roles for long ncRNA and mRNA. *Cancers (Basel)* 2013; **5**: 462-90. doi:10.3390/cancers5020462
- Kanduri C, Long noncoding RNAs: Lessons from genomic imprinting. *Biochim Biophys Acta* 2016; **1859**: 102-11. doi:10.1016/j.bbagr.2015.05.006
- Fietkau R, Putz F, Lahmer G, Semrau S, Buslei R, Can MGMT promoter methylation status be used as a prognostic and predictive marker for glioblastoma multiforme at the present time? A word of caution. *Strahlenther Onkol* 2013; **189**: 993-5. doi:10.1007/s00066-013-0459-2
- Smrdel U, Popovic M, Zwitter M, Bostjancic E, Zupan A, Kovac V, et al., Long-term survival in glioblastoma: methyl guanine methyl transferase (MGMT) promoter methylation as independent favourable prognostic factor. *Radiol Oncol* 2016; **50**: 394-401. doi:10.1515/raon-2015-0041
- Shi X, Sun M, Liu H, Yao Y, Song Y, Long non-coding RNAs: a new frontier in the study of human diseases. *Cancer Lett* 2013; **339**: 159-66. doi:10.1016/j.canlet.2013.06.013
- Bian EB, Li J, Xie YS, Zong G, Zhao B, LncRNAs: New players in gliomas, with special emphasis on the interaction of lncRNAs with EZH2. *J Cell Physiol* 2015; **230**: 496-503. doi:10.1002/jcp.24549
- Alelu-Paz R, Ashour N, Gonzalez-Corpas A, Ropero S, DNA methylation, histone modifications, and signal transduction pathways: a close relationship in malignant gliomas pathophysiology. *J Signal Transduct* 2012; **2012**: 956958. doi:10.1155/2012/956958
- Louis DN, Ohgaki H, Wiestler OD, Cavenee WK, Burger PC, Jouvet A, et al., The 2007 WHO classification of tumours of the central nervous system. *Acta Neuropathol* 2007; **114**: 97-109. doi:10.1007/s00401-007-0243-4
- Livak KJ, Schmittgen TD, Analysis of relative gene expression data using real-time quantitative PCR and the 2<sup>-</sup>(Delta Delta C(T)) Method. *Methods* 2001; **25**: 402-8. doi:10.1006/meth.2001.1262
- Li J, Bian EB, He XJ, Ma CC, Zong G, Wang HL, et al., Epigenetic repression of long non-coding RNA MEG3 mediated by DNMT1 represses the p53 pathway in gliomas. *Int J Oncol* 2016; **48**: 723-33. doi:10.3892/ijo.2015.3285
- Wang P, Ren Z, Sun P, Overexpression of the long non-coding RNA MEG3 impairs in vitro glioma cell proliferation. *J Cell Biochem* 2012; **113**: 1868-74. doi:10.1002/jcb.24055
- Park JY, Lee JE, Park JB, Yoo H, Lee SH, Kim JH, Roles of long non-coding RNAs on tumorigenesis and glioma development. *Brain Tumor Res Treat* 2014; **2**: 1-6. doi:10.14791/btrt.2014.2.1.1
- Yao Y, Ma J, Xue Y, Wang P, Li Z, Liu J, et al., Knockdown of long non-coding RNA XIST exerts tumor-suppressive functions in human glioblastoma stem cells by up-regulating miR-152. *Cancer Lett* 2015; **359**: 75-86. doi:10.1016/j.canlet.2014.12.051
- He C, Jiang B, Ma J, Li Q, Aberrant NEAT1 expression is associated with clinical outcome in high grade glioma patients. *Apmis* 2016; **124**: 169-74. doi:10.1111/apm.12480
- Wang Q, Zhang J, Liu Y, Zhang W, Zhou J, Duan R, et al., A novel cell cycle-associated lncRNA, HOXA11-AS, is transcribed from the 5-prime end of the HOXA transcript and is a biomarker of progression in glioma. *Cancer Lett* 2016; **373**: 251-9. doi:10.1016/j.canlet.2016.01.039
- Ohgaki H, Kleihues P, The definition of primary and secondary glioblastoma. *Clin Cancer Res* 2013; **19**: 764-72. doi:10.1158/1078-0432.ccr-12-3002

34. Wojdacz TK, Dobrovic A, Methylation-sensitive high resolution melting (MS-HRM): a new approach for sensitive and high-throughput assessment of methylation. *Nucleic Acids Res* 2007; **35**: e41. doi:10.1093/nar/gkm013
35. Switzeny OJ, Christmann M, Renovanz M, Giese A, Sommer C, Kaina B, MGMT promoter methylation determined by HRM in comparison to MSP and pyrosequencing for predicting high-grade glioma response. *Clin Epigenetics* 2016; **8**: 49. doi:10.1186/s13148-016-0204-7
36. Hagedorn M, Siegfried G, Hooks KB, Khatib AM, Integration of zebrafish fin regeneration genes with expression data of human tumors in silico uncovers potential novel melanoma markers. *Oncotarget* 2016; **7**: 71567-79. doi:10.18632/oncotarget.12257
37. Legendre CR, Demeure MJ, Whitsett TG, Gooden GC, Bussey KJ, Jung S, et al., Pathway implications of aberrant global methylation in adrenocortical cancer. *PLoS One* 2016; **11**: e0150629. doi:10.1371/journal.pone.0150629
38. Yang Z, Xu S, Jin P, Yang X, Li X, Wan D, et al., MARCKS contributes to stromal cancer-associated fibroblast activation and facilitates ovarian cancer metastasis. *Oncotarget* 2016; **7**: 37649-63. doi:10.18632/oncotarget.8726
39. Micallef J, Taccone M, Mukherjee J, Croul S, Busby J, Moran MF, et al., Epidermal growth factor receptor variant III-induced glioma invasion is mediated through myristoylated alanine-rich protein kinase C substrate overexpression. *Cancer Res* 2009; **69**: 7548-56. doi:10.1158/0008-5472.can-08-4783
40. Rohrbach TD, Shah N, Jackson WP, Feeney EV, Scanlon S, Gish R, et al., The effector domain of MARCKS is a nuclear localization signal that regulates cellular PIP2 levels and nuclear PIP2 localization. *PLoS One* 2015; **10**: e0140870. doi:10.1371/journal.pone.0140870
41. Rohrbach TD, Jarboe JS, Anderson JC, Trummell HQ, Hicks PH, Weaver AN, et al., Targeting the effector domain of the myristoylated alanine rich C-kinase substrate enhances lung cancer radiation sensitivity. *Int J Oncol* 2015; **46**: 1079-88. doi:10.3892/ijo.2014.2799
42. Hanada S, Kakehashi A, Nishiyama N, Wei M, Yamano S, Chung K, et al., Myristoylated alanine-rich C-kinase substrate as a prognostic biomarker in human primary lung squamous cell carcinoma. *Cancer Biomark* 2013; **13**: 289-98. doi:10.3233/cbm-130354
43. Punzi G, Ursini G, Shin JH, Kleinman JE, Hyde TM, Weinberger DR, Increased expression of MARCKS in post-mortem brain of violent suicide completers is related to transcription of a long, noncoding, antisense RNA. *Mol Psychiatry* 2014; **19**: 1057-9. doi:10.1038/mp.2014.41
44. Ropero S, Esteller M, The role of histone deacetylases (HDACs) in human cancer. *Mol Oncol* 2007; **1**: 19-25. doi:10.1016/j.molonc.2007.01.001
45. Li Z, Zhu WG, Targeting histone deacetylases for cancer therapy: from molecular mechanisms to clinical implications. *Int J Biol Sci* 2014; **10**: 757-70. doi:10.7150/ijbs.9067
46. Conte M, Dell'Aversana C, Benedetti R, Petraglia F, Carissimo A, Petrizzi VB, et al., HDAC2 deregulation in tumorigenesis is causally connected to repression of immune modulation and defense escape. *Oncotarget* 2015; **6**: 886-901. doi:10.18632/oncotarget.2816
47. Alzoubi S, Brody L, Rahman S, Mahul-Mellier AL, Mercado N, Ito K, et al., Synergy between histone deacetylase inhibitors and DNA-damaging agents is mediated by histone deacetylase 2 in colorectal cancer. *Oncotarget* 2016; **7**: 44505-21. doi:10.18632/oncotarget.9887
48. Qu X, Yu H, Jia B, Yu X, Cui Q, Liu Z, et al., Association of downregulated HDAC 2 with the impaired mitochondrial function and cytokine secretion in the monocytes/macrophages from gestational diabetes mellitus patients. *Cell Biol Int* 2016; **40**: 642-51. doi:10.1002/cbin.10598
49. Stojanovic N, Hassan Z, Wirth M, Wenzel P, Beyer M, Schafer C, et al., HDAC1 and HDAC2 integrate the expression of p53 mutants in pancreatic cancer. *Oncogene* 2016. doi:10.1038/onc.2016.344
50. Campos B, Bermejo JL, Han L, Felsberg J, Ahmadi R, Grabe N, et al., Expression of nuclear receptor corepressors and class I histone deacetylases in astrocytic gliomas. *Cancer Sci* 2011; **102**: 387-92. doi:10.1111/j.1349-7006.2010.01792.x

# Health-related quality of life assessed by the EORTC QLQ-C30 questionnaire in the general Slovenian population

Vaneja Velenik<sup>1</sup>, Ajra Secerov-Ermenc<sup>1</sup>, Jasna But-Hadzic<sup>1</sup>, Vesna Zadnik<sup>2</sup>

<sup>1</sup> Institute of Oncology Ljubljana, Division of Radiotherapy, Ljubljana, Slovenia

<sup>2</sup> Institute of Oncology Ljubljana, Epidemiology and Cancer Registry, Ljubljana, Slovenia

Radiol Oncol 2017; 51(3): 342-350.

Received 15 January 2017

Accepted 17 March 2017

Correspondence to: Assoc. Prof. Vesna Zadnik, M.D., Ph.D., Zaloska 2, Institute of Oncology Ljubljana, Epidemiology and Cancer Registry, SI-1000 Ljubljana, Slovenia. Phone: +386 1 5879 451; Fax: +386 1 5879 400; E-mail: vzadnik@onko-i.si

Disclosure: No potential conflicts of interest were disclosed.

**Background.** The aim of our study was to obtain reference data of the EORTC QLQ-C30 quality of life dimensions for the general Slovenian population. We intend to provide the researchers and clinicians in our country with the expected mean health-related quality of life (HRQL) scores for distinctive socio-demographic population groups.

**Methods.** The EORTC QLQ-C30 questionnaire supplemented by a socio-demographic inquiry was mailed or distributed to 1,685 randomly selected individuals in the Slovenian population aged 18 – 90. Answers from 1,231 subjects representing socio-demographic diversity of the Slovenian population were collected and transformed into EORTC dimensions and symptoms. The impact of socio-demographic features on HRQL scores was assessed by multiple linear regression models.

**Results.** Gender, age and self-rated social class are the important confounders in the quality of life scores in our population. Men reported better quality of life on the majority of the specific scales and, at the same time, reported fewer symptoms. There was no gender-specific difference in cognitive functioning. The mean scores were consistently lower with age in both sexes.

**Conclusions.** This is the first study to report the normative EORTC QLQ-C30 scores for one of the south-eastern European populations. The reported expected mean scores allow Slovenian oncologists to estimate what the quality of life in cancer patients would be, had they not been ill. As they are derived by common methodology, our results can easily be included in any further international comparisons or in the calculation of European summarized HRQL scores.

Key words: health-related quality of life; EORTC QLQ-C30; normative values; socio-demographic determinants; reference data

## Introduction

Cancer burden in Slovenia is increasing. There are approximately 14,000 new cancer patients annually (age standardized incidence rate (world) = 335/100,000), the life-time prevalence is almost 100,000. More than 10,000 patients are currently in the process of primary cancer treatment; almost 30,000 have recently completed a specific oncological treatment but have still been followed by oncologists.<sup>1</sup> Because of improvements in diagnostics

and treatment we are observing a constant increase in cancer patients' survival. Five-year relative survival is approaching 60%.<sup>2</sup> However, despite being widely recognised as a central endpoint in cancer research<sup>3</sup>, the health-related quality of life (HRQL) has not been used systematically as an outcome measure in clinical trials or oncological practice in our country so far.

Evaluation of quality of life is conducted by using the standardized questionnaires.<sup>4</sup> The most widely used and generally accepted tool

for assessing HRQL in oncology is the questionnaire launched by the European Organization for Research and Treatment of Cancer (EORTC).<sup>5</sup> The core questionnaire, which consists of 30 questions (EORTC QLQ-C30), is supplemented by disease-specific modules and is translated into 81 languages, including Slovene.<sup>6</sup> To assist the overall interpretation of results from clinical research of HRQL the population-based reference values are used; the scores of the general population can be used as guidelines in the interpretation of HRQL scores from different patients' populations.

The normative (reference) values of the QLQ-C30 questionnaire for a generally healthy population are already available for some countries: Denmark – women<sup>7</sup>, Norway – both men and women<sup>8</sup>, Sweden<sup>9,10</sup>, Germany<sup>11,12</sup>, the Netherlands<sup>13</sup> and again Denmark – both men and women.<sup>3</sup> Outside Europe, they have obtained reference data for the EORTC QLQ-C30 in Columbia<sup>14</sup> and South Korea.<sup>15,16</sup> Recently, Hinz *et al.*<sup>17</sup> published the European reference values of the EORTC QLQ-C30 by summarizing six European general population normative studies from four countries (Sweden, Norway, the Netherlands and Germany). Fayers compared reference data from Germany and the Scandinavian countries and noticed some differences, which can be attributable to differences in health status between these countries or to cultural differences.<sup>18</sup> Similar conclusions were made by Scott *et al.* where they analysed the results of 106 clinical studies in order to assess international differences in response to the questionnaire EORTC QLQ-C30. Most response patterns were similar, but the largest variations were found in the results for Eastern Europe and East Asia.<sup>19</sup>

The aim of our study was to obtain reference data of the EORTC QLQ-C30 quality of life dimensions for the general Slovenian population. We intend to provide the researchers and clinicians in our country with the expected mean HRQL scores for distinctive socio-demographic population groups, which will allow them to estimate what the HRQL in cancer patients would be, had they not been ill.

## Patients and methods

### Population sample

The study was conducted in the year 2011 and the first half of the year 2012. The healthy individuals were sampled from the Slovenian adult population, aged between 18 and 90 years. All the participants have provided an informed consent for participa-

tion in the study. All procedures performed in our study were in accordance with, and with the approval of, the National Medical Ethics Committee (No. 134/09/09, from 5.11.2009) and with the 1964 Helsinki declaration and its later amendments or comparable ethical standards.

The random sample from the target population of 1,650,000 was collected from two data sources: (1) the copy of the Central Population Registry for the age groups 50 – 69 kept by the Registry of the National colorectal screening program SVIT (the questionnaire was sent by ordinary mail together with the screening invitation) and (2) the list of visitors to the outpatient clinic at the Institute of Oncology in Ljubljana (the questionnaires were distributed to the relatives or companions of the cancer patients).

The response rate in the first data source was 63%; 566 subjects returned the questionnaire out of 898 selected. By the second approach, 787 questionnaires had been distributed to the relatives or companions of the cancer patients, of which 731 answered questionnaires were returned (response rate 93%). In total we collected 1,297 questionnaires, of which 66 were not included in the study because some answers were missing or were not clear. The final sample consists of 1,231 subjects. The comparison with the national data provided by the Statistical Office of the Republic of Slovenia<sup>20</sup> shows that the collected sample is representative for the general Slovenian population in respect of age ( $p = 0.140$ ) and gender ( $p = 0.582$ ) (Table 1). To check the representativeness by socio-demographic variables our sample was compared with the population-based socio-economic variables obtained in the Countrywide Integrated Noncommunicable Diseases Intervention (CINDI) research, which was conducted in Slovenia investigating the socio-economic and geographic determinants in correlation with the incidence of chronic non-infectious disease or unhealthy lifestyle.<sup>21</sup> Our sample is representative for the general population in respect of education ( $p = 0.054$ ), employment ( $p = 0.100$ ), living environment ( $p = 0.103$ ) and geographical area ( $p = 0.260$ ), but it is not comparable for marital status ( $p < 0.000$ ) or social class ( $p < 0.000$ ) (Table 1).

### Questionnaires

The EORTC QLQ-C30 is a questionnaire assessing individual HRQL during the previous week. The EORTC QLQ-C30 has 30 items arranged into nine scales (dimensions) and six single items. The scales are divided into five function scales (physi-

TABLE 1. Socio-demographic characteristics of the sample by gender and its comparisons with national averages<sup>21,20</sup>

	Men Number (%)	Women Number (%)	Total Number (%)	National reference (S,C)* (%)	p (chi square)
<b>Gender</b>					0.582
Men	619 (50.3)			49.51 <sup>s</sup>	
Women		612 (49.7)		50.5 <sup>s</sup>	
<b>Age category</b>					0.140
18-39 years	224 (36.2)	188 (30.7)	412 (33.5)	35.7 <sup>s</sup>	
40-59 years	230 (37.2)	262 (42.8)	492 (40.0)	37.4 <sup>s</sup>	
60-90 years	165 (26.7)	162 (26.5)	327 (26.6)	26.9 <sup>s</sup>	
<b>Marital status</b>					<0.000
With a partner	441 (71.2)	439 (71.2)	880 (71.5)	76.7 <sup>c</sup>	
Single	178 (28.8)	173 (28.3)	351 (28.5)	23.3 <sup>c</sup>	
<b>Education</b>					0.054
Elementary or less	107 (17.3)	101 (16.5)	208 (16.9)	16.7 <sup>c</sup>	
Secondary school	346 (55.9)	298 (48.7)	644 (52.3)	55.4 <sup>c</sup>	
More than secondary school	166 (26.8)	213 (34.8)	379 (30.8)	27.9 <sup>c</sup>	
<b>Employment</b>					0.100
Employed	338 (54.6)	325 (53.1)	663 (53.9)	53.5 <sup>c</sup>	
Unemployed	39 (6.3)	45 (7.4)	84 (6.8)	8.5 <sup>c</sup>	
Not active	242 (39.1)	242 (39.5)	484 (39.3)	38.1 <sup>c</sup>	
<b>Living environment</b>					0.103
Urban	187 (30.2)	235 (28.4)	422 (34.3)	31.5 <sup>c</sup>	
Suburban	119 (19.2)	150 (24.5)	269 (21.9)	23.2 <sup>c</sup>	
Rural	313 (50.6)	227 (37.1)	540 (43.9)	45.3 <sup>c</sup>	
<b>Geographical area</b>					0.230
West	125 (20.2)	170 (27.8)	295 (24.0)	22.3 <sup>c</sup>	
Central	179 (28.9)	194 (28.9)	373 (30.3)	29.9 <sup>c</sup>	
East	315 (50.9)	248 (40.5)	563 (45.7)	47.8 <sup>c</sup>	
<b>Social class</b>					<0.000
Lower	214 (34.6)	189 (30.9)	403 (32.7)	42.2 <sup>c</sup>	
Middle	340 (54.9)	351 (57.4)	691 (56.1)	47.9 <sup>c</sup>	
Upper	65 (10.5)	72 (11.8)	137 (11.1)	9.9 <sup>c</sup>	

\*As a national reference the data from Statistical Office of the Republic Slovenia (S) and Countrywide Integrated Noncommunicable Diseases Intervention in Slovenia (C) is applied.

cal, role, cognitive, emotional and social functions); three symptom scales (fatigue, pain, nausea or vomiting) and one global health-status/quality of life dimension. The six single items address specific symptoms: dyspnoea, appetite loss, insomnia, constipation, diarrhoea and a question addressing the financial impact of the disease. Each item has four response alternatives: 1) "not at all", 2) "a little" 3) "quite a bit" 4) "very much" except for the global health-status/quality of life scale, which has response options ranging from 1) "very poor" to 7)

"excellent". The questionnaire was officially translated into the Slovenian language.<sup>5,6,22</sup>

The subjects in our research also received a questionnaire on their socio-demographic data, including gender, age, marital status, education, employment, social class, living environment and geographical area. The categories of socio-demographic variables were adapted from the Slovenian CINDI research.<sup>21</sup> To facilitate the analysis some of the categories were merged – the applied response categories are presented in Table 1.

TABLE 2. Mean scores (MS) with standard deviations (SD) for all scales and items by gender

	Total		Men		Women		p (t-test)
	MS	SD	MS	SD	MS	SD	
Global health status/quality of life	71.1	21.4	72.5	21.4	69.7	21.3	0.882
Physical functioning	91.8	14.0	93.3	12.6	90.3	15.1	<0.000
Role functioning	88.7	20.1	90.0	19.3	87.5	20.9	0.056
Emotional functioning	82.0	18.5	83.6	18.4	80.4	18.5	0.686
Cognitive functioning	90.2	16.0	90.2	16.3	90.2	15.7	0.760
Social functioning	90.9	17.3	91.6	16.9	90.2	17.8	0.094
Fatigue	19.8	19.8	17.4	19.3	22.2	20.0	0.769
Nausea/vomiting	3.3	10.6	3.0	10.2	3.5	11.0	0.116
Pain	14.5	20.2	13.1	19.6	16.0	20.8	0.134
Dispnea	5.3	15.3	5.0	14.7	5.7	15.8	0.087
Insomnia	19.8	25.1	16.8	23.9	22.8	25.9	0.056
Appetite loss	5.3	15.5	5.3	16.0	5.2	15.1	0.795
Constipation	6.9	16.9	4.6	13.8	9.2	19.3	<0.000
Diarrhoea	4.2	13.6	4.4	14.1	4.0	13.0	0.247
Financial problems	6.6	17.5	6.4	17.2	6.9	17.9	0.385

## Statistical analysis

The answers recorded by the EORTC QLQ-C30 questionnaire were transformed into dimensions ranged 0 – 100 according to the EORTC scoring instructions.<sup>22</sup> In all dimensions, where the linear transformation includes multiple answers, internal consistency was proved adequate by a high Cronbach alpha coefficient of reliability. The coefficients for the scales were as follows: global health-status / quality of life 0.89, social functioning 0.86, emotional functioning 0.83, physical functioning 0.80, role functioning 0.80, cognitive functioning 0.64, fatigue 0.80, nausea/vomiting 0.69 and pain 0.70.

The dimensions were considered as numerical variables and presented by mean and standard deviations. Socio-demographic characteristics were analysed as categorical variables. The differences between genders in all scales were tested by Student's t test. The chi-square test was applied to check if the collected sample is representative for the general Slovenian population. The impact of socio-demographic features on HRQL was assessed by multiple linear regression models as suggested by Hjermstadt.<sup>23</sup> A separate model has been constructed for each dimension. The model constants and the regression coefficients have been applied in the calculation of the expected mean scores for

each socio-demographic population group using equation 1:

$$\text{Dimension score} = n + \sum_{i=1}^I b_i X_i, \quad [\text{Equation 1}]$$

where  $X_i$  ( $i = 1, \dots, I$ ) represents a particular socio-demographic feature (expressed as dummy variables),  $b_i$  represents the regression coefficient for the  $i$ -th socio-demographic feature and  $n$  is the model constant.

The values of  $p < 0.05$  were considered as statistically significant. All statistical analyses were performed using SPSS (IBM SPSS Statistics, Version 21).

## Results

There were 1,231 questionnaires eligible for analysis. The subjects were made up of 50.3% men (619 persons) and 49.7% women (612 persons). Table 1 shows the socio-demographic data of the sample divided by gender. The mean age was 48 (range 19 to 90 years). As in the general Slovenian population, the majority of the subjects in the sample were employed, had a secondary school education and were living in the rural environment of Eastern Slovenia. In comparison with the general population in our sample, the individuals, on average, reported a higher social class and there were significantly more single living persons in our sample in comparison with the national averages.

**TABLE 3.** Regression coefficients with constants for all scales and items applied in the calculation of the expected mean scores according to gender, age and social class in Slovenian population

	Men	18-39 years	40-59 years	Lower social class	Middle social class	Constant
Global health status/quality of life	-0.07	0.30	0.21	0.30	-0.12	71.5
Physical functioning	-0.11	0.42	0.29	-0.25	-0.08	89.6
Role functioning	-0.07	0.10	0.06	0.20	-0.05	91.6
Emotional functioning	-0.09	0.04	0.06	-0.11	0.00	83.7
Cognitive functioning	0.00	0.21	0.16	-0.15	-0.06	88.6
Social functioning	-0.04	0.17	0.12	-0.17	-0.03	90.6
Fatigue	0.13	-0.10	-0.12	0.19	0.05	16.8
Nausea/vomiting	0.03	0.03	-0.06	0.02	-0.08	4.5
Pain	0.07	-0.26	-0.17	0.19	0.05	15.7
Dispnea	0.02	-0.22	-0.15	0.09	-0.01	8.4
Insomnia	0.12	-0.18	-0.16	0.08	-0.01	21.9
Appetite loss	0.01	0.05	-0.04	0.09	-0.07	5.3
Constipation	0.13	-0.10	-0.05	0.08	0.05	4.8
Diarrhoea	-0.02	-0.05	-0.02	0.00	-0.04	5.8
Financial problems	0.02	-0.08	-0.02	0.23	0.03	4.3

### Scale and item scores

Table 2 shows mean values of EORTC QLQ-C30 scores for all scales and items. The distribution of means is highly skewed since most subjects reported no symptoms and the best functioning. Men reported better global quality of life as well as better physical, role, emotional and social functioning. On the cognitive functioning scale there is no difference between genders. Men also reported less fatigue, nausea or vomiting, pain, dyspnoea, insomnia, constipation and financial impact. Women reported less diarrhoea and loss of appetite. The described differences are not statistically significant except for physical functioning, which is significantly higher in men and obstipation, which is significantly more prevalent in women. However, as presented graphically in Figure 1, the differences between genders are more prominent in older age groups. The mean scores of the global health-status/quality of life and specific functional scales are consistently lower with age in both sexes. However the decrease of mean scores with age, is the highest in women evaluating physical and role functioning. The mean scores of symptom scales and single items increase with age. We observed the highest increase in the mean score for women when evaluating fatigue and pain. The mean score

of nausea/vomiting, appetite loss and diarrhoea did not change much with age.

### The impact of socio-demographic features

The impact of socio-demographic features on all scales of HRQL was assessed by multiple linear regression models. In our population gender, age and social class have a critical impact on HRQL. A separate model has been constructed for each dimension; gender had an impact on 8 scales of HRQL, age on 9 scales, education on 3 scales, employment on 2 scales, living environment on 1 scale, marital status and geographical area on no scale and social class on 10 scales.

Table 3 shows the regression coefficients with model constants for all scales in relation to gender, age and social class. These statistics are the inputs in the calculation of the expected mean score of each scale according to gender, age and social class. The universal model fitted is described by equation 1. As an empirical example for the calculation of expected mean scores for a particular socio-demographic population group we apply the case of women, aged 65 from the middle social class. Their expected score for the scale physical functioning is 89.52:

$$\text{Physical functioning score} = -0.11 \times 0 + 0.42 \times 0 + 0.29 \times 0 - 0.25 \times 0 - 0.08 \times 1 + 89.60 = 89.52$$

Values for dummies included in the model are as follows: gender: men = 1, age1: 18 – 39 years = 1, age2: 40 – 59 years = 1, social class 1: lower class = 1, social class 2: middle class = 1.

## Discussion

In this study we present the reference data of the EORTC QLQ-C30 quality of life dimensions for the general Slovenian population. The collected raw questionnaire data are transformed into expected mean HRQL scores for distinctive socio-demographic population groups. In the results we reveal the expected mean score of only one single empirical example (women, 65, middle social class: 89.52) - the complete table of all expected mean HRQL scores for all significant socio-demographic population groups is too complex and was, in order to keep the focus on the primary aim of the study, deliberately not added to the paper. Still, as a part of our entire research project, all the expected mean HRQL scores for any significant socio-demographic population group were prepared and are freely available to Slovenian oncologists in a suitable format to be used in everyday practice.

The suggested comparison of scores measured in cancer patients and the obtained Slovenian average values will enable better clinical interpretation of disease progress and treatment effects. The quality of life in Slovenian cancer patients could be monitored objectively, excluding the impact of important socio-demographic factors. As established in several papers so far<sup>18,19</sup>, to avoid over- or underestimation of the mean score difference it is essential to use the population-specific norms incorporating each country's socio-economic characteristics. Alternatively, the expected mean scores could be used in a clinical practice as baseline individual HRQL scores, since newly diagnosed patients can already have disease symptoms and psychological problems affecting the results of the questionnaire.<sup>12</sup>

The expected mean scores have been calculated by identical multiple linear regression models as described in equation 1 and as already proposed by Hjermstad.<sup>23</sup> The relationship between the variables and scale or item scores in our data was generally linear. There were some non-linear components in the age/fatigue and age/pain association which could be expressed in an additional Age<sup>2</sup> component in the regression models as suggested

by Schwartz.<sup>11</sup> For simplicity and clarity reasons we decided to omit this quadratic term and further on to assume equal independent variables (the socio-demographic feature) for all scales, even though some of the factors do not contribute to some of the scales at all. However, for the final linear model, only the three most influential variables were selected: gender, age and social class.

The results of our study considering age and gender distribution were similar to the results conducted in the other European countries and elsewhere in the world.<sup>3,7-16</sup> Some important but mostly statistically insignificant gender differences were identified in Slovenian population: men reported better quality of life on the majority of the specific scales and, at the same time, reported fewer symptoms. On the other hand, women reported less appetite loss and diarrhoea. We didn't observe any gender-specific difference on cognitive functioning. In the Norwegian study, which was the first to be conducted on a sample of the general population, men reported better quality of life on all scales and fewer symptoms.<sup>8</sup> Similar results were observed in the German study – men reported better quality of life on all scales and fewer symptoms in comparison to women.<sup>11</sup> In the last study from Denmark, which was published in 2014, the better quality of life assessed by men was not so obvious. Men reported better physical functioning, less insomnia and constipation, whereas women reported better social functioning and less dyspnoea.<sup>3</sup>

In our study we observed that all scales deteriorated with age. Older subjects also reported more symptoms. The only exception is emotional functioning where there was no age-dependent fall. Similarly, emotional functioning was not age-dependent also in three Scandinavian studies<sup>3,9,8</sup>, but in the German population there was a slight decrease of emotional functioning in the older age groups.<sup>11</sup> In the comparison of the German, Norwegian and Sweden HRQL scores Fayers<sup>18</sup> noticed that in Germany there is a steeper age-dependent decline in the mean score for the global quality of life, ending at far lower scores in older patients, compared to the Scandinavian results. A similar difference was noticed with the fatigue scale. In the Slovenian population we noticed a similar fall in the mean score of the global health-status/quality of life scale and a similar increase of the mean score of the fatigue scale as in the German study. As the Slovenian scores of most scales are more similar to the German results, we can assume

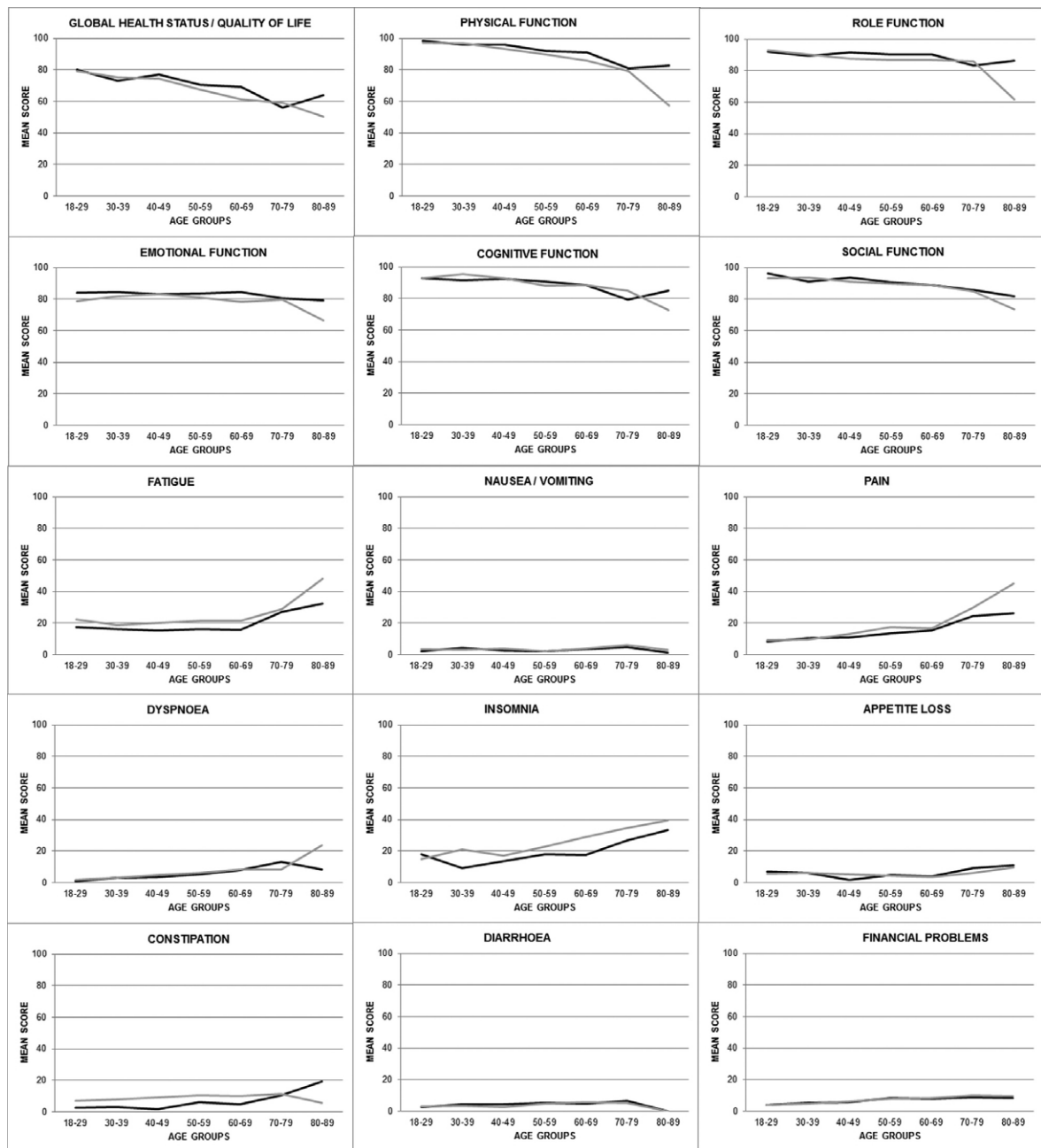


FIGURE 1. Mean scores of all scales divided by sex (grey – women, black – men).

our cultural environment and health status is more similar to the Germans than to the Scandinavians.

In Slovenia we have been following the impact of demographic, socio-economic and geographic features on the incidence of chronic non-infectious diseases and health-related lifestyle for more than a decade.<sup>21</sup> Furthermore we have investigated the

impact of the socio-demographic determinants on the cancer incidence in Slovenia – in the socio-economically more deprived regions in the eastern part of the country there is higher incidence of head and neck tumours but less female skin melanoma and breast cancer.<sup>24</sup> Yet another study in Slovenia confirmed the higher prevalence of poor self-rated

health in individuals from lower self-assessed social class.<sup>25</sup> As, when resuming all this research, the socio-demographic determinants have an impact on the incidence of non-infectious disease, cancer and on self-rated health in Slovenia, we assumed that determinants could also affect the HRQL. Besides gender and age we have tested the influence of six additional socio-demographic variables on HRQL in the general Slovenian population – it turned out that only self-assessed social class has a significant impact on HRQL in our population. On the contrary, Hjermstad and Juul showed that education, employment status, marital status and living environment have a significant influence on at least some HRQL scores in the Norwegian and Danish populations respectively.<sup>3,8</sup>

Although gender, age and other socio-demographic features are important confounders in normative as well as in clinical quality of life scores it seems that morbidity has a distinct impact on all functional scales and should be considered as a strong confounder in all quality of life evaluations.<sup>3</sup> The impact of associated health problems on HRQL can sometimes be higher than late treatment effect in cancer patients.<sup>26</sup> In this study we have not investigated whether HRQL in the general Slovenian population depends on morbidity. However we believe that worsening of HRQL with age should be explained by the fact that physical strength and vital function deteriorate with age as the elderly have more pain, insomnia and dispnea which all are a consequence of more morbidity. Surely the impact of morbidity on HRQL in our population will be the field of our further surveys.

In conclusion, in this study we have derived, by common methodology, the Slovenian HRQL normative values. Gender, age and self-rated social class are the important confounders in the quality of life scores in our population. The expected mean scores reported could be used as a reference in the clinical interpretation of disease progress and treatment effects. Finally, our study is the first to report the normative EORTC QLQ-C30 scores for one of the south-eastern European populations and can easily be included in any further international comparisons or in the calculation of European summarized scores.

## References

- Zadnik V, Primic Zakelj M, Lokar K, Jarm K, Ivanus U, Zagar T. Cancer burden in Slovenia with the time trends analysis. *Radiol Oncol* 2017; 51(3): 342-350.; 51: 47-55. doi:10.1515/raon-2017-0008
- Primic Žakelj M, Zadnik V, Zagar T, Zakotnik B. *Survival of Cancer Patients in Slovenia 1991-2005*. Ljubljana: Institute of Oncology Ljubljana; 2009.
- Juul T, Petersen MA, Holzner B, Laurberg S, Christensen P, Gronvold M. Danish population-based reference data for the EORTC QLQ-C30: associations with gender, age and morbidity. *Qual Life Res* 2014; 23: 2183-93. doi:10.1007/s11136-014-0675-y
- Luckett T, King MT, Butow PN, Oguchi M, Rankin N, Price MA, et al. Choosing between the EORTC QLQ-C30 and FACT-G for measuring health-related quality of life in cancer clinical research: issues, evidence and recommendations. *Ann Oncol* 2011; 22: 2179-90. doi:10.1093/annonc/mdq721
- Aaronson NK, Ahmedzai S, Bergman B, Bullinger M, Cull A, Duez N J, et al. The European Organization for Research and Treatment of Cancer QLQ-C30: a quality-of-life instrument for use in international clinical trials in oncology. *J Natl Cancer Inst* 1993; 85: 365-76.
- Life ESG oQo. *EORTC QLQ-C30 (version 3.0.) Slovenian*. Brussels: EORTC; 1996.
- Klee M, Groenvold M, Machin D. Quality of life of Danish women: population-based norms of the EORTC QLQ-C30. *Qual Life Res* 1997; 6: 27-34.
- Hjermstad MJ, Fayers PM, Bjordal K, Kaasa S. Health-related quality of life in the general Norwegian population assessed by the European Organization for Research and Treatment of Cancer Core Quality-of-Life Questionnaire: the QLQ=C30 (+ 3). *J Clin Oncol* 1998; 16: 1188-96.
- Derogar M, van der Schaaf M, Lagergren P. Reference values for the EORTC QLQ-C30 quality of life questionnaire in a random sample of the Swedish population. *Acta Oncol* 2012; 51: 10-6. doi:10.3109/02841816X.2011.614636
- Michelson H, Bolund C, Nilsson B, Brandberg Y. Health-related quality of life measured by the EORTC QLQ-C30—reference values from a large sample of Swedish population. *Acta Oncol* 2000; 39: 477-84.
- Schwarz R, Hinz A. Reference data for the quality of life questionnaire EORTC QLQ-C30 in the general German population. *Eur J Cancer* 2001; 37: 1345-51.
- Waldmann A, Schubert D, Katalinic A. Normative data of the EORTC QLQ-C30 for the German population: a population-based survey. *PLoS One* 2013; 8: e74149. doi:10.1371/journal.pone.0074149
- van de Poll-Franse LV, Mols F, Gundy CM, Creutzberg CL, Nout RA, Verdonck-de Leeuw IM, et al. Normative data for the EORTC QLQ-C30 and EORTC-sexuality items in the general Dutch population. *Eur J Cancer* 2011; 47: 667-75. doi:10.1016/j.ejca.2010.11.004
- Finck C, Barradas S, Singer S, Zenger M, Hinz A. Health-related quality of life in Colombia: reference values of the EORTC QLQ-C30. *Eur J Cancer Care (Engl)* 2012; 21: 829-36. doi:10.1111/ecc.12000
- Park SY, Bae DS, Nam JH, Park CT, Cho CH, Lee JM, et al. Quality of life and sexual problems in disease-free survivors of cervical cancer compared with the general population. *Cancer* 2007; 110: 2716-25.
- Yun YH, Kim YA, Min YH, Chang YJ, Lee J, Kim M S, et al. Health-related quality of life in disease-free survivors of surgically treated lung cancer compared with the general population. *Ann Surg* 2012; 255: 1000-7. doi:10.1097/SLA.0b013e31824f1e9e
- Hinz A, Singer S, Brahler E. European reference values for the quality of life questionnaire EORTC QLQ-C30: Results of a German investigation and a summarizing analysis of six European general population normative studies. *Acta Oncol* 2014; 53: 958-65. doi:10.3109/0284186X.2013.879998
- Fayers PM. Interpreting quality of life data: population-based reference data for the EORTC QLQ-C30. *Eur J Cancer* 2001; 37: 1331-4.
- Scott NW, Fayers PM, Aaronson NK, Bottomley A, de Graeff A, Groenvold M, et al. The use of differential item functioning analyses to identify cultural differences in responses to the EORTC QLQ-C30. *Qual Life Res* 2007; 16: 115-29.
- SI-Stat Data Portal. SURS. [cited 2016 Aug 31]. Available at: <http://pxweb.stat.si/pxweb/dialog/statfile1.asp>
- Maucer Zakotnik J, Tomsic S, Kofol-Bric T, Korosec A. *Health and lif style in Slovenian population. Trends from CINDI researches 2001-2004-2008; in Slovene. [Slovenian]*. Ljubljana: IVZ; 2012.
- Fayers P, Aaronson N, Bjordal K, Groenvold M, Curran D, Bottomley A. *EORTC QLQ-C30 Scoring Manual (Third edition)*. Brussels: EORTC; 2001.
- Hjermstad MJ, Fayers PM, Bjordal K, Kaasa S. Using reference data on quality of life—the importance of adjusting for age and gender, exemplified by the EORTC QLQ-C30 (+3). *Eur J Cancer* 1998; 34: 1381-9.
- Zadnik V. *Geografska analiza vpliva socialno-ekonomskih dejavnikov na incidenco raka v Sloveniji v obdobju 1995-2002 [Geographical analysis of the association of socioeconomic status and cancer incidence in Slovenia in the period 1995-2002; in Slovene]*. [PhD thesis]. Ljubljana: University of Ljubljana; 2006.

25. Farkaš J, Pahor M, Zaletel-Kragelj L. Self-rated health in different social classes of Slovenian adult population: nationwide cross-sectional study. *Int J Public Health* 2011; **56**: 45-54. doi:10.1007/s00038-009-0103-1
26. Fossa SD, Hess SL, Dahl AA, Hjermstad MJ, Veenstra M. Stability of health-related quality of life in the Norwegian general population and impact of chronic morbidity in individuals with and without a cancer diagnosis. *Acta Oncol* 2007; **46**: 452-61.

# The outcome of the first 100 nasopharyngeal cancer patients in Thailand treated by helical tomotherapy

Imjai Chitapanarux<sup>1,2</sup>, Wannapha Nobnop<sup>1,2</sup>, Patumrat Sripan<sup>1,2</sup>, Ausareeya Chumachote<sup>1</sup>, Ekkasit Tharavichitkul<sup>1,2</sup>, Somvilai Chakrabandhu<sup>1,2</sup>, Pitchayaponne Klunklin<sup>1,2</sup>, Wimrak Onchan<sup>1,2</sup>, Bongkot Jia-Mahasap<sup>1,2</sup>, Suwapim Janlaor<sup>1</sup>, Patcharawadee Kayan<sup>1</sup>, Patrinee Traisathit<sup>3</sup>, Dirk Van Gestel<sup>4</sup>

<sup>1</sup> Division of Radiation Oncology, Faculty of Medicine, Chiang Mai University, Chiang Mai, Thailand

<sup>2</sup> Northern Thai Research Group of Radiation Oncology (NTRG-RO), Faculty of Medicine, Chiang Mai University, Chiang Mai, Thailand

<sup>3</sup> Department of Statistics, Faculty of Science, Chiang Mai University, Chiang Mai, Thailand

<sup>4</sup> Department of Radiation Oncology, Institut Jules Bordet, Université libre de Bruxelles, Brussels, Belgium.

Radiol Oncol 2017; 51(3): 351-356.

Received 10 January 2017

Accepted 18 February 2017

Correspondence to: Imjai Chitapanarux, M.D., Division of Radiation Oncology, Faculty of Medicine, Chiang Mai University, Chiang Mai, Thailand, 110 Intawarorose Road, Chiang Mai, 50200, Thailand. E-mail: imjai@hotmail.com ; imjai.chitapanarux@cmu.ac.th

Disclosure: No potential conflicts of interest were disclosed.

**Background.** The aim of the study was to analyse of two-year loco-regional failure free survival (LRFFS), distant metastasis free survival (DMFS), overall survival (OS), and toxicity outcomes of the first 100 nasopharyngeal carcinoma patients in Thailand treated by helical tomotherapy.

**Patients and methods.** Between March 2012 and December 2015, 100 patients with non-metastatic nasopharyngeal carcinoma were treated by helical tomotherapy. All patients were treated by platinum-based concurrent chemoradiotherapy and adjuvant or neo-adjuvant chemotherapy.

**Results.** The median age was 51 years (interquartile ranges [IQR]: 42.5–57.0). The mean  $\pm$  SD of D95% of planning target volume (PTV) 70, 59.4 and 54 were 70.2  $\pm$  0.5, 59.8  $\pm$  0.6, and 54.3  $\pm$  0.8 Gy, respectively. The mean  $\pm$  SD of conformity index, and homogeneity index were 0.89  $\pm$  0.13 and 0.06  $\pm$  0.07. Mean  $\pm$  SD of D2 % of spinal cord and brainstem were 34.1  $\pm$  4.4 and 53.3  $\pm$  6.3 Gy. Mean  $\pm$  SD of D50 of contralateral and ipsilateral parotid gland were 28.4  $\pm$  6.7 and 38.5  $\pm$  11.2 Gy. At a median follow-up of 33 months (IQR: 25–41), the 2-year LRFFS, DMFS, OS were 94% (95%CI: 87–98%), 96% (95% CI: 89–98%), and 99% (95% CI: 93–100%), respectively. Acute grade 3 dermatitis, pharyngoesophagitis, and mucositis occurred in 5%, 51%, and 37%, respectively. Late pharyngoesophagitis grade 0 and 1 were found in 98% and 2% of patients. Late xerostomia grade 0, 1 and 2 were found in 17%, 78% and 5%, respectively.

**Conclusions.** Helical tomotherapy offers good dosimetric performance and achieves excellent treatment outcome in nasopharyngeal carcinoma patients.

Key words: nasopharynx; cancer; helical tomotherapy

## Introduction

Helical tomotherapy is an intensity-modulated radiotherapy (IMRT) dedicated system with an integrated megavoltage computed tomography (MVCT) scanner for patient position verification. The helical IMRT is able to produce highly confor-

mal dose distribution to large and complex target volumes such as in nasopharyngeal carcinoma and other head and neck cancers. Helical tomotherapy can lower the mean dose to the salivary glands, with improved dose homogeneity and conformity compared to other IMRT techniques.<sup>1-5</sup> In our centre, step and shoot IMRT was the standard radiother-

apy technique in most nasopharyngeal carcinoma patients with curative intent treated since 2000. The helical tomotherapy unit, Hi-ART II (TomoTherapy Inc., Madison, WI) has been installed in March 2012. The aim of this study was to assess the treatment outcome in terms of loco-regional failure free survival (LRFFS), distant metastasis free survival (DMFS), overall survival (OS), and treatment toxicities of the first 100 non-metastatic nasopharyngeal carcinoma patients treated by this technique. Dosimetric details were also reported.

## Patients and methods

We reviewed the first 100 patients with newly-diagnosed non-metastatic nasopharyngeal carcinoma patients treated with curative intent by helical tomotherapy between April 2012 and December 2015. Pretreatment evaluations consisted of physical examination, pre-treatment dental evaluations, and laboratory studies. Good bone marrow, renal, and liver function tests were required. Contrast enhanced computer tomography (CT) scan or magnetic resonance imaging (MRI) of the nasopharynx and the neck region, chest x-ray, and bone scan were performed. The diseases were staged according to the American Joint Committee on Cancer Staging 2010, 7<sup>th</sup> edition.<sup>6</sup>

Target delineation was done according to RTOG 0225.<sup>7</sup> The gross target volume (GTV) included the primary tumour and nodes larger than 1 cm in diameter or nodes with necrotic centres. Clinical target volume 70 (CTV 70) was equivalent to the GTV plus 5 mm margin. CTV 59.4 was defined as CTV 70 plus entire nasopharynx with retropharyngeal lymph nodes, pterygoid fossa, parapharyngeal space, inferior sphenoid sinus, posterior third of the nasal cavity and maxillary sinuses, skull base, and high risk nodal groups (upper deep jugular, subdiaphragic, midjugular, posterior cervical, and retropharyngeal lymph nodes). CTV 54 included the lower jugular and supraclavicular lymph nodes. Planning target volume (PTV) was created by adding a circumferential margin of 5 mm to each CTV. We also contoured the critical organs at risk such as bilateral parotid glands, brainstem, spinal cord, optic nerves and chiasm. For planning, the helical tomotherapy Planning Station (Hi-Art Version 4.2.3.9 TomoTherapy Inc., Madison, WI) was used with a Field Width (FW) of 5.02 cm, a Pitch Factor (PF) of 0.287, and a Modulation Factor (MF) of 3.0. ICRU83 recommendations were implemented for the optimization procedure. The dose prescriptions in our

simultaneous integrated boost technique (SIB) were 70 Gy for PTV 70 at 2.12 Gy/fraction, 59.4 Gy for PTV 59.4 at 1.8 Gy/fraction, and 54 Gy for PTV 54 at 1.64 Gy/fraction. Treatment was delivered in five fractions per week for a total of 33 fractions.

Acute adverse events of concurrent chemoradiotherapy were evaluated at weekly visits using version 3.0 of the National Cancer Institute Common Terminology Criteria for Adverse Events (NCI-CTCAE).<sup>8</sup> Patients were evaluated for disease control, survival, and late toxicities of radiotherapy at 2–3 month intervals for the first 2 years, at 3–6 month intervals between the third and fifth year. Late toxicities were assessed by the RTOG/EORTC late radiation morbidity scoring system.<sup>9</sup> At every visit fiber-optic endoscopy by an otolaryngologists has been done. CT scan of the neck was performed every 6 months in the first 2 years and annually thereafter.

OS and LRFFS were estimated using the Kaplan-Meier method. OS was defined as the time from beginning of treatment to the date of death of any cause. LRFFS was defined as the time between beginning of treatment and local or regional recurrence/progression, or death due to nasopharyngeal cancer or due to unknown causes with undocumented site of failure. DMFS was defined from beginning of treatment to the date of diagnosis of distant metastases. *P*-values < 0.05 were considered statistically significant, and all *P* values reported in this article are two-sided values, determined using Stata version 11 (StataCorp LP, College Station, TX, USA).

The results presented herein resulted from a retrospective study based on the analysis of medical records. This study was approved by the Ethics committee of Faculty of Medicine, Chiang Mai University.

## Results

A hundred non-metastatic nasopharyngeal carcinoma patients have been treated with curative intent by helical tomotherapy. Baseline characteristics are shown in Table 1. The median age was 51 years (interquartile ranges [IQR]: 42.5–57.0). Most patients (66%) had undifferentiated non-keratinizing nasopharyngeal carcinoma.

Treatment protocols for nasopharyngeal carcinoma in our centre include concurrent chemoradiotherapy plus either 3 cycles of induction chemotherapy (IC) or 3 cycles of adjuvant chemotherapy (AC). Of the 100 patients, all of them received

TABLE 1. Patient and treatment characteristics

Characteristics	Values N=100 N (%)
Gender	
Female	38 (38%)
Male	62 (62%)
Histological subtype	
Keratinizing	2 (2%)
Non-keratinizing; differentiated	32 (32%)
Non-keratinizing; undifferentiated	66 (66%)
Stage	
II	23 (23%)
III	45 (45%)
IVA	21 (21%)
IVB	11 (11%)
T stage	
T1	28 (28%)
T2	30 (30%)
T3	20 (20%)
T4	22 (22%)
N stage	
N0	5 (5%)
N1	30 (30%)
N2	54 (54%)
N3a	7 (7%)
N3b	4 (4%)
Dose statistic	
D95% of PTV70, mean (SD)	70.2 (0.5)
D95% of PTV59.4, mean (SD)	59.8 (0.6)
D95% of PTV54, mean (SD)	54.3 (0.8)
Conformity index (CI), mean (SD)	0.89 (0.13)
Homogeneity index (HI), mean (SD)	0.06 (0.07)
D2% of spinal cord, median (SD)	34.1 (4.4)
D2 cc of brainstem, mean (SD)	53.3 (6.3)
D50 of ipsilateral parotid gland, mean (SD)	38.5 (11.2)
D50 of contralateral parotid gland, mean (SD)	28.4 (6.7)

platinum-based concurrent chemoradiotherapy, either weekly cisplatin 40 mg/m<sup>2</sup> × 6 cycles (53%), cisplatin 70 mg/m<sup>2</sup> every 21 days × 3 cycles (11%), or weekly carboplatin 100 mg/m<sup>2</sup> × 6 cycles (36%). Forty-one patients (41%) received 3 cycles of IC, because of N2 and N3a disease in 29% and because of a waiting time for radiotherapy of more than 6 weeks in 15% of patients. Thirty patients (30%) received IC with PF regimen (cisplatin 100 mg/m<sup>2</sup> on day 1 or carboplatin with area under curve (AUC) 5 on day 1 plus 5-FU 1000 mg/m<sup>2</sup>/d in day 1–4 every 21 days). Eleven patients (11%) received IC with TPF regimen (cisplatin 75 mg/m<sup>2</sup> on day 1, docetaxel 75 mg/m<sup>2</sup> on day 1, 5-FU 750 mg/m<sup>2</sup>/d in day 1–4 every 21 days). We performed CT scan after 3 cycles of IC for response evaluation and planning radiotherapy. Fifty-nine patients (59%) received AC with PF regimen (cisplatin 100 mg/m<sup>2</sup> on day 1 plus 5-FU 1000 mg/m<sup>2</sup>/d in day 1–4 every 21 days in 23 patients and carboplatin with area under curve (AUC) 5 on day 1 plus 5-FU 1000 mg/m<sup>2</sup>/d in day 1–4 every 21 days in 36 patients).

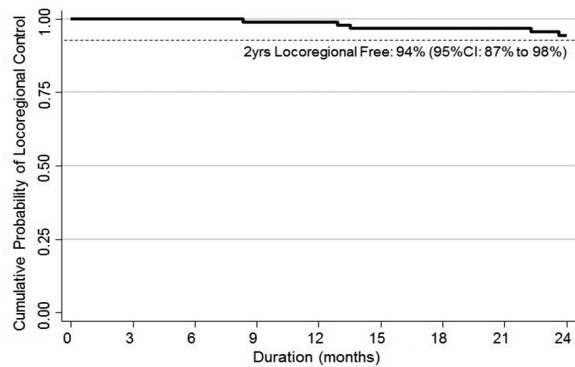


FIGURE 1. Kaplan-Meier estimate of loco-regional failure free survival (LRFFS).

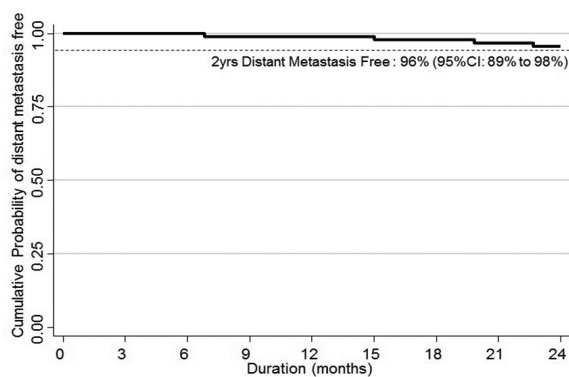


FIGURE 2. Kaplan-Meier estimate of distant metastasis free survival (DMFS).

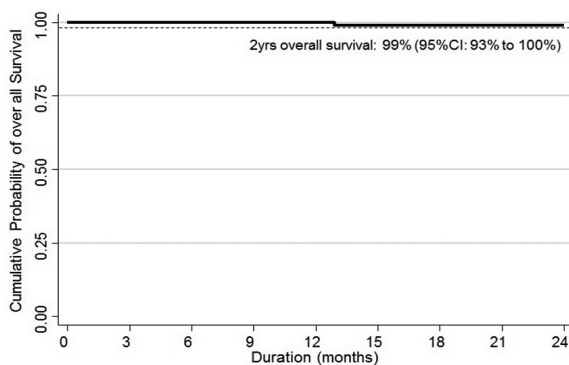


FIGURE 3. Kaplan-Meier estimate of overall survival (OS).

With a median follow up time of 33 months (inter-quartile range, IQR: 25–41 months), the 2-year LRFFS, DMFS and OS rates were 94%, 96%, and 99% respectively (Figures 1–3). Ninety-nine patients were alive at the last follow up of whom 84 patients without any evidence of disease. No patients developed second primary cancer.

TABLE 2. Comparative studies of outcome and toxicities in NPC treated by HT concurrent with chemotherapy

Study	Median Follow up (Range) (month)	No. of CCRT (%)	LRFFS (%)	DMFS (%)	OS (%)	Severe toxicity (grade > 2)				
						Acute Dermatitis (%)	Acute Mucositis (%)	Acute Pharyngitis (%)	Acute Xerostomia (%)	Late Xerostomia (%)
Wong et al. 22	34 (9-50)	70	93.6 (3 yr)	86.6 (3 yr)	87.2 (3 yr)	-	67.4	-	-	2.3
Wolden et al. 23	35 (3-74)	93	91 (3 yr)	78 (3 yr)	-	-	-	-	-	-
Kam et al. 24	29 (8-45)	30	92 (3 yr)	79 (3 yr)	90 (3 yr)	-	92	-	75	23 (2 yr)
Lee et al. 7	31 (6-55)	65	89.3 (2 yr)	84.7 (2 yr)	80.2 (2 yr)	-	4.4 (grade4)	-	-	3.1
Tham et al. 25	36.5	100	93.1 (3 yr)	-	-	-	29	-	3	-
Lee et al. 26	31 (7-22)	75	98 (4 yr)	66 (4 yr)	88 (4 yr)	-	94	-	-	2.5 (2 yr)
Liu et al. 27	13 (8/18)	58	100 (13 M)	-	-	5	79	-	5	-
Wang et al. 28	47.1 (11-68)	83	94 (4 yr)	85 (4 yr)	86.1 (4 yr)	-	33.3	-	4.7	12.3 (2 yr)
Sultanem et al. 27	21.8 (5-49)	91	100 (4 yr)	57 (4 yr)	94 (4 yr)	-	51 (grade3)	-	-	-
Du et al. 20	32 (3-38)	64	96.1 (3 yr)	92 (3 yr)	86.3 (3 yr)	4.7	3.2	-	0	-
Leung et al. 17	41 (0.2-67)	62.5	97 (5 yr)	84.6 (5 yr)	-	0	4	-	-	0
Du et al. 21	23.7 (12-38)	100	92.2 (2 yr)	92.7 (2 yr)	93.2 (2 yr)	5.3	9.1	0.5 (grade 3)	0	-
Zhang et al. 30	48 (41.7-58)	100 (cetuximab)	95.2 (2 yr)	88.1 (2 yr)	93 (2 yr)	7 (grade3)	81.4 (grade3)	-	-	-
Our Study	33 (25-41)	100	94 (2 yr)	96 (2 yr)	99 (2 yr)	5	37 (grade3)	51 (grade 3)	-	5 (grade 3)

CCRT = concurrent chemoradiotherapy; DMFS = distant metastasis free survival; LRFFS = locoregional failure free survival; M = month; OS = overall survival; Yr = year

Acute and late toxicities of our study are shown in the bottom of Table 2. Acute grade 3 Pharyngoesophagitis and mucositis occurred in 51% and 37% respectively, responsible for a weight loss of more than 15% from baseline in 42 patients (42%) and with a nasogastric (NG) tube insertion in 10 patients (10%, in all during concurrent chemoradiotherapy). Five patients (5%) had grade 3 acute radiation dermatitis. No patient died during concurrent chemoradiotherapy. Late pharyngoesophagitis was of grade 1 and was registered in only 2% of the patients. We also found grade 1, 2 and 3 late xerostomia in 17%, 78% and 5% of the patients, respectively.

Dosimetric parameters related to conformity, homogeneity and organ at risk (OAR) sparing are presented in Table 1. All helical tomotherapy plans showed satisfactory conformity index and homogeneity index, being  $0.89 \pm 0.13$  and  $0.06 \pm 0.07$ , respectively. Mean  $\pm$  SD of D2% of spinal cord and brainstem were  $34.1 \pm 4.4$  and  $53.3 \pm 6.3$  Gy. Mean  $\pm$  SD of D50 of contralateral and ipsilateral parotid gland

were  $28.4 \pm 6.7$  and  $38.5 \pm 11.2$  Gy. The mean beam on time was 3.91 minutes (range = 3.53–4.21 minutes).

## Discussion

Several studies have shown the benefits of IMRT, which can reduce dose to the surrounding organs at risk, mainly the parotids, and also allows for dose escalation to the tumour.<sup>10-14</sup> The use of daily image-guided radiotherapy (IGRT) is necessary in locally advanced nasopharyngeal carcinoma patients in order to reduce marginal miss due to the very steep dose gradients towards the critical structures.<sup>15</sup>

Helical tomotherapy integrates both techniques, IMRT and IGRT, in one machine. Although randomized studies<sup>16-20</sup> found level 1 evidence of superiority of static beam IMRT over classical 2- and 3-dimensional RT in terms of xerostomia, such evidence is missing for the rotational IMRT techniques, Helical tomotherapy being one of them.

So clinical evidence is warranted. The study from Leung *et al.*<sup>21</sup> demonstrated outstanding 5 year disease control with acceptable toxicity for nasopharyngeal carcinoma treated by helical tomotherapy. Du *et al.* also reported excellent 3-year LRC, DMFS, and OS with minor acute and late toxicities with helical tomotherapy.<sup>22</sup> The present data investigated the first 100 nasopharyngeal carcinoma patients treated by helical tomotherapy in Thailand. Our short term 2-year results are excellent with a LRRFS, DMFS, and OS of 94%, 96%, and 99%, respectively. This is comparable to the results reported from IGRT studies<sup>21-23</sup> and other IMRT studies<sup>7,21-32</sup> as shown in Table 2. Moreover, we have excellent results although more than three thirds (77%) of our patients had stage III to IVB disease.

We considered the parotid glands as the most important OARs in regard to quality of life of our patients. We followed RTOG 0225 protocol<sup>7</sup> in that the mean dose less than or equal to 26 Gy should be achieved in at least 1 gland. This could reduce the degree of xerostomia and therefore we tried to keep the Dmean under 26 Gy whenever possible. Helical tomotherapy offered very good preservation of this organ as also shown by Van Gestel *et al.* who reported a parotid Dmean with helical tomotherapy of 21.7–24.1 Gy in an oropharyngeal cancer planning study<sup>4</sup> and of 24.7 Gy as found by Broggi *et al.*<sup>5</sup> Specific for nasopharyngeal carcinoma treated by helical tomotherapy, Yao *et al.*<sup>33</sup> reported parotid glands Dmean of 30 Gy, whereas Du *et al.*<sup>23</sup> used simultaneous modulated accelerated radiation therapy via helical tomotherapy and found that parotid gland Dmean of left and right side were 31.2 Gy and 31.0 Gy, respectively. Finally, Leung *et al.* reported a very low 22.1 Gy and 20.7 Gy of Dmean of the ipsilateral and contralateral parotid gland, respectively.<sup>21</sup> Our study had slightly higher D50 of ipsilateral and contralateral parotid glands than the previous studies with 38.5 Gy and 28.4 Gy, respectively. This could be explained by the fact that 95% of patients in our study were node positive, of whom 60% had  $\geq$  N2 disease. Despite the higher mean dose to both parotid glands, 2 year late grade 2 xerostomia only occurred in 5% of our patients, with no grade 3 or 4 reported. This 5% is consistent with the studies by Wong *et al.*<sup>24</sup>, Lee *et al.*<sup>7</sup>, and Lee *et al.*<sup>28</sup> but is lower than the severe late xerostomia reported by Wang *et al.*<sup>30</sup> and Kam *et al.*<sup>26</sup>, as shown in Table 2. In our study, acute radiation related side effects were mainly pharyngoesophagitis and mucositis. Grade 3 acute pharyngoesophagitis was the most common toxicity, higher than in the study of Du *et al.*<sup>23</sup> However the patients in their

study received concurrent treatment in 87% with different chemotherapy regimen and some of them received concurrent anti-EGFR therapy, whereas 100% of our patients received concurrent treatment with chemotherapy. Moreover, we found that our chemotherapy schedule had higher dose intensity compared to their study. However late pharyngoesophagitis was found in only 2% of our patients, and was only grade 1. Grade 3 acute mucositis was less severe and of lower incidence than in other studies as shown in Table 2.<sup>24,26,29,31,32</sup> Grade 3 acute radiation dermatitis was found in 5% of our patient, these numbers are comparable to those from other series.<sup>22,23,29,32</sup> Other OARs such as brainstem and spinal cord, could be treated within the dose constraint limits.

It has been reported that helical tomotherapy provided excellent conformity and homogeneity index in the treatment of nasopharyngeal carcinoma and other head and neck cancers.<sup>21-23</sup> We achieved excellent dose coverage of the three PTVs with homogeneity index and conformity index comparable to the other studies.

We conclude that helical tomotherapy achieved good target coverage in nasopharyngeal cancer patients with favorable dose profile to most of OARs. As such helical tomotherapy achieved favorable 2-year locoregional failure free survival, distant metastasis free survival, and overall survival, with an acceptable rate of moderate and severe acute toxicities, but minimal rate of late toxicities.

## Authors' contributions

IC conceived and coordinated the study, analysed the data, and drafted the manuscript. SC, WN, SJ coordinated and analysed the study. ET, PK, WO, BS, PK, AC participated in acquisition of data. PT, PS performed the statistical analysis. DVG helped to draft the manuscript. All authors read and approved the final manuscript.

## References

1. Kodaira T, Tomita N, Tachibana H, Nakamura T, Nakahara R, Inokuchi H, et al. Aichi cancer center initial experience of intensity modulated radiation therapy for nasopharyngeal cancer using helical tomotherapy. *Int J Radiat Oncol Biol Phys* 2009; **73**: 1129-34. doi:10.1016/j.ijrobp.2008.06.1936
2. Chen AM, Jennelle RLS, Sreeraman R, Yang CC, Liu T, Vijayakumar S, et al. Initial clinical experience with helical tomotherapy for head and neck cancer. *Head Neck* 2009; **31**: 1571-8. doi:10.1002/hed.21123
3. Ren G, Du L, Ma L, Feng L-C, Zhou G-X, Qu B-L, et al. Clinical observation of 73 nasopharyngeal carcinoma patients treated by helical tomotherapy: the China experience. *Technol Cancer Res Treat* 2011; **10**: 259-66. doi:10.7785/tcr.2012.500201

4. Van Gestel D, van Vliet-Vroegindeweij C, Van den Heuvel F, Crijns W, Coelmont A, De Ost B, et al. RapidArc, SmartArc and TomoHD compared with classical step and shoot and sliding window intensity modulated radiotherapy in an oropharyngeal cancer treatment plan comparison. *Radiat Oncol* 2013; **8**: 37. doi:10.1186/1748-717X-8-37
5. Broggi S, Perna L, Bonsignore F, Rinaldin G, Fiorino C, Chiara A, et al. Static and rotational intensity modulated techniques for head-neck cancer radiotherapy: a planning comparison. *Phys Med* 2014; **30**: 973-9. doi:10.1016/j.ejmp.2014.07.001
6. *AJCC cancer staging manual*. 7<sup>th</sup> edition. Philadelphia: Lippincott-Raven; 2009.
7. Lee N, Harris J, Garden AS, Straube W, Glisson B, Xia P, et al. Intensity-modulated radiation therapy with or without chemotherapy for nasopharyngeal carcinoma: radiation therapy oncology group phase II trial 0225. *J Clin Oncol* 2009; **27**: 3684-90. doi:10.1200/JCO.2008.19.9109
8. US National Institute of Health. Cancer Therapy Evaluation Program. Common terminology criteria for adverse events v3.0 (CTCAE). [cited 2017 Aug 9]. Available at [https://ctep.cancer.gov/protocoldevelopment/electronic\\_applications/docs/ctcae3.pdf](https://ctep.cancer.gov/protocoldevelopment/electronic_applications/docs/ctcae3.pdf)
9. Cox JD, Stetz J, Pajak TF. Toxicity criteria of the Radiation Therapy Oncology Group (RTOG) and the European Organization for Research and Treatment of Cancer (EORTC). *Int J Radiat Oncol Biol Phys* 1995; **31**: 1341-6. doi:10.1016/0360-3016(95)00060-C
10. Nutting C, Dearnaley DP, Webb S. Intensity modulated radiation therapy: a clinical review. *Br J Radiol* 2000; **73**: 459-69.
11. Eisbruch A, Ship JA, Martel MK, Ten Haken RK, Marsh LH, Wolf GT, et al. Parotid gland sparing in patients undergoing bilateral head and neck irradiation: techniques and early results. *Int J Radiat Oncol Biol Phys* 1996; **36**: 469-80. doi:10.1259/bjr.73.869.10884741
12. Eisbruch A, Ten Haken RK, Kim HM, Marsh LH, Ship JA. Dose, volume, and function relationships in parotid salivary glands following conformal and intensity-modulated irradiation of head and neck cancer. *Int J Radiat Oncol Biol Phys* 1999; **45**: 577-87.
13. Kreps S, Berges O, Belin L, Zefkili S, Petras S, Giraud P. Salivary gland-sparing helical tomotherapy for head and neck cancer: Preserved salivary function on quantitative salivary gland scintigraphy after tomotherapy. *Eur Ann Otorhinolaryngol Head Neck Dis* 2016; **133**: 257-62. doi:10.1016/j.anorl.2016.05.003
14. Voordeckers M, Farrag A, Everaert H, Tournel K, Storme G, Verellen D, et al. Parotid gland sparing with helical tomotherapy in head-and-neck cancer. *Int J Radiat Oncol Biol Phys* 2012; **84**: 443-8. doi:10.1016/j.ijrobp.2011.11.070
15. Jiang F, Jin T, Feng X-L, Jin Q-F, Chen X-Z. Long-term outcomes and failure patterns of patients with nasopharyngeal carcinoma staged by magnetic resonance imaging in intensity-modulated radiotherapy era: The Zhejiang Cancer Hospital's experience. *J Cancer Res Ther* 2015; **11**(Suppl 2): C179-84. doi:10.4103/0973-1482.168181
16. Pow EH, Kwong DL, McMillan AS et al. Xerostomia and quality of life after intensity-modulated radiotherapy versus conventional radiotherapy for early-stage nasopharyngeal carcinoma: initial report on a randomized controlled clinical trial. *Int J Radiat Oncol Biol Phys* 2006; **66**: 981-91.
17. Kam MK, Leung SF, Zee B, Chau RM, Suen JJ, Mo F et al. Prospective randomized study of intensity-modulated radiotherapy on salivary gland function in early-stage nasopharyngeal carcinoma patients. *J Clin Oncol* 2007; **25**(31): 4873-9.
18. Nutting C, Morden J, Harrington K, Urbano TG, Bhide SA, Clark C et al. Parotid-sparing intensity modulated versus conventional radiotherapy in head and neck cancer (PARSPORT): a phase 3 multicentre randomised controlled trial. *Lancet Oncol* 2011; **12**: 127-36.
19. Gupta T, Agarwal J, Jain S et al. Three-dimensional conformal radiotherapy (3D-CRT) versus intensity modulated radiation therapy (IMRT) in squamous cell carcinoma of the head and neck: A randomized controlled trial. *Radiother Oncol*. 2012; **104**: 343-48.
20. Peng G, Wang T, Yang KY et al. A prospective, randomized study comparing outcomes and toxicities of intensity-modulated radiotherapy vs. conventional two-dimensional radiotherapy for the treatment of nasopharyngeal carcinoma. *Radiother Oncol*. 2012; **104**: 286-93.
21. Leung SW, Lee T-F. Treatment of nasopharyngeal carcinoma by tomotherapy: five-year experience. *Radiat Oncol* 2013; **8**: 107. doi:10.1186/1748-717X-8-107
22. Du L, Zhang X-X, Ma L, Feng L-C, Li F, Zhou G-X, et al. Clinical study of nasopharyngeal carcinoma treated by helical tomotherapy in China: 5-year outcomes. *Biomed Res Int* 2014; e980767. doi:10.1155/2014/980767
23. Du L, Zhang XX, Feng LC, Chen J, Yang J, Liu HX, et al. Treatment of nasopharyngeal carcinoma using simultaneous modulated accelerated radiation therapy via helical tomotherapy: a phase II study. *Radiat Oncol* 2016; **50**: 218-25. doi:10.1515/raon-2016-0001
24. Wong FCS, Ng AWY, Lee VHF, Lui CMM, Yuen K-K, Sze W-K, et al. Whole-field simultaneous integrated-boost intensity-modulated radiotherapy for patients with nasopharyngeal carcinoma. *Int J Radiat Oncol Biol Phys* 2010; **76**: 138-45. doi:10.1016/j.ijrobp.2009.01.084
25. Wolden SL, Chen WC, Pfister DG, Kraus DH, Berry SL, Zelefsky MJ. Intensity-modulated radiation therapy (IMRT) for nasopharynx cancer: update of the Memorial Sloan-Kettering experience. *Int J Radiat Oncol Biol Phys* 2006; **64**: 57-62. doi:10.1016/j.ijrobp.2005.03.057
26. Kam MKM, Teo PML, Chau RMC, Cheung KY, Choi PHK, Kwan WH, et al. Treatment of nasopharyngeal carcinoma with intensity-modulated radiotherapy: the Hong Kong experience. *Int J Radiat Oncol Biol Phys* 2004; **60**: 1440-50. doi:10.1016/j.ijrobp.2004.05.022
27. Tham IW-K, Hee SW, Yeo RM-C, Salleh PB, Lee J, Tan TW-K, et al. Treatment of nasopharyngeal carcinoma using intensity-modulated radiotherapy-the national cancer centre singapore experience. *Int J Radiat Oncol Biol Phys* 2009; **75**: 1481-6. doi:10.1016/j.ijrobp.2009.01.018
28. Lee N, Xia P, Quivey JM, Sultanem K, Poon I, Akazawa C, et al. Intensity-modulated radiotherapy in the treatment of nasopharyngeal carcinoma: an update of the UCSF experience. *Int J Radiat Oncol Biol Phys* 2002; **53**: 12-22.
29. Liu W-S, Su M-C, Wu M-F, Tseng H-C, Kuo H-C. Nasopharyngeal carcinoma treated with precision-oriented radiation therapy techniques including intensity-modulated radiotherapy: preliminary results. *Kaohsiung J Med Sci* 2004; **20**: 49-55. doi:10.1016/S1607-551X(09)70084-1
30. Wang R, Wu F, Lu H, Wei B, Feng G, Li G, et al. Definitive intensity-modulated radiation therapy for nasopharyngeal carcinoma: long-term outcome of a multicenter prospective study. *J Cancer Res Clin Oncol* 2013; **139**: 139-45. doi:10.1007/s00432-012-1313-0
31. Sultanem K, Shu HK, Xia P, Akazawa C, Quivey JM, Verhey LJ, et al. Three-dimensional intensity-modulated radiotherapy in the treatment of nasopharyngeal carcinoma: the University of California-San Francisco experience. *Int J Radiat Oncol Biol Phys* 2000; **48**: 711-22.
32. Zhang X, Du L, Zhao F, Wang Q, Yang S, Ma L. A Phase II clinical trial of concurrent helical tomotherapy plus cetuximab followed by adjuvant chemotherapy with cisplatin and docetaxel for locally advanced nasopharyngeal carcinoma. *Int J Biol Sci* 2016; **12**: 446-53. doi:10.7150/ijbs.12937
33. Yao W, Du L, Ma L, Feng L, Cai B, Xu S, et al. Effect of adaptive replanning on adverse reactions and clinical outcome in nasopharyngeal carcinoma treated by helical tomotherapy. *Zhong Nan Da Xue Xue Bao Yi Xue Ban* 2013; **38**: 468-75. doi:10.3969/j.issn.1672-7347.2013.05.005

# PD-L1 expression in squamous-cell carcinoma and adenocarcinoma of the lung

Urska Janzic<sup>1</sup>, Izidor Kern<sup>2</sup>, Andrej Janzic<sup>3</sup>, Luka Cavka<sup>4</sup>, Tanja Cufer<sup>1</sup>

<sup>1</sup> Department of Medical Oncology, University Clinic Golnik, Golnik, Slovenia

<sup>2</sup> Department of Pathology, University Clinic Golnik, Golnik, Slovenia

<sup>3</sup> University of Ljubljana, Faculty of Pharmacy, Ljubljana, Slovenia

<sup>4</sup> Department of Medical Oncology, Institute of Oncology, Ljubljana, Slovenia

Radiol Oncol 2017; 51(3): 357-362.

Received 27 April 2017

Accepted 9 August 2017

Correspondence to: Urska Janzic, M.D., Department of Medical Oncology, University Clinic Golnik, Golnik 36, 4204 Golnik, Slovenia. Phone: +386 4 1240 266; Fax: +386 4 256 9174; E-mail: urska.janzic@klinika-golnik.si

Disclosure: No potential conflicts of interest were disclosed.

**Background.** With introduction of immunotherapy (IT) into the treatment of advanced non-small-cell lung cancer (NSCLC), a need for predictive biomarker became apparent. Programmed death ligand 1 (PD-L1) protein expression is most widely explored predictive marker for response to IT. We assessed PD-L1 expression in tumor cells (TC) and immune cells (IC) of squamous-cell carcinoma (SCC) and adenocarcinoma (AC) patients.

**Patients and methods.** We obtained 54 surgically resected tumor specimens and assessed PD-L1 expression by immunohistochemistry after staining them with antibody SP142 (Ventana, USA). Clinicopathological characteristics were acquired from the hospital registry database. Results were analyzed according to cut-off values of  $\geq 5\%$  and  $\geq 10\%$  of PD-L1 expression on either TC or IC.

**Results.** 29 (54%) samples were AC and 25 (46%) were SCC. PD-L1 expression was significantly higher in TC of SCC compared to AC at both cut-off values (52% vs. 17%,  $p = 0.016$  and 52% vs. 14%,  $p = 0.007$ , respectively) no difference in PD-L1 expression in IC of SCC and AC was found. In AC alone, PD-L1 expression was significantly higher in IC compared to TC at both cut-off values (72% vs. 17%,  $p < 0.001$  and 41% vs. 14%,  $p = 0.008$ , respectively), while no significant difference between IC and TC PD-L1 expression was revealed in SCC.

**Conclusions.** Our results suggest a significantly higher PD-L1 expression in TC of SCC compared to AC, regardless of the cut-off value. PD-L1 expression in IC is high in both histological subtypes of NSCLC, and adds significantly to the overall positivity of AC but not SCC.

Key words: lung cancer; squamous-cell lung cancer; adenocarcinoma; tumor cells; immune cells; PD-L1 expression

## Introduction

Immunotherapy with checkpoint inhibitors (CPIs) is becoming a new standard of treatment for metastatic non-small cell lung cancer (NSCLC) patients. Thus far, three agents, two anti-PD-1 inhibitors and one PD-L1 inhibitor, have proven antitumor efficacy in terms of improved response rates and overall survival compared to standard chemotherapy in the second-line setting, namely nivolumab, pembrolizumab and atezolizumab.<sup>1-6</sup> Moreover, pembrolizumab also showed survival advantage over standard chemotherapy in the first-line setting, while

nivolumab failed to deliver the same, the main difference probably being patient selection criteria in the clinical trials.<sup>7,8</sup> Patients that benefit from immune checkpoint inhibitors have durable responses with mild toxicities that are mostly immune-related. However, only about 20% of unselected NSCLC patients actually respond to these therapies.<sup>9,10</sup>

Until now, PD-L1 (programmed death ligand 1) protein expression determined by immunohistochemistry (IHC) has been most widely explored as a putative predictive biomarker for response to CPIs in cancer, also in NSCLC. The PD-L1 expression can be explored on tumor cells (TC) and or tu-

mor-infiltrating immune cells (IC).<sup>10-12</sup> In NSCLC, PD-L1 expression was mainly evaluated on TC, while data on PD-L1 expression on IC is scarce and its importance is yet to be validated.<sup>10,13-16</sup> In general, higher PD-L1 expression correlated with higher overall response rates (ORRs) and consequently better overall survival (OS) across majority of clinical trials. This was demonstrated in clinical trials assessing activity of pembrolizumab and atezolizumab in histologically unselected NSCLC and nivolumab in non-squamous lung carcinoma (non-SCC).<sup>2-6</sup> On the contrary, in the trial studying nivolumab activity exclusively in squamous-cell lung carcinoma (SCC) no major differences in efficacy were observed regarding PD-L1 expression.<sup>1</sup> So there seems to be a vital difference between PD-L1 expressions in major subtypes of NSCLC, which makes them react differently to CPIs. One possible reason is that mutational burden is probably higher in patients with SCC, which might be related to their smoking status.<sup>17,18</sup>

PD-L1 expression determination is also subjected to antibody clone, assay platform and cut-off values used in a particular study. In drug development programs, specific diagnostic tests, including antibody clone and staining platform have been used and validated for each particular PD-L1/PD-1 inhibitor.<sup>10-12</sup> Substitutability of these tests and antibodies is still uncertain. Harmonization trials addressing the question of interchangeability between them showed no major differences considering certain antibodies with only outlying of SP142 antibody being less sensitive for TC, but not for IC staining, compared to other antibodies.<sup>13-16</sup> The importance of tissue specimen selection seems to be vital, since data suggest that PD-L1 expression in tumor tissue is indeed heterogeneous and small biopsy specimens showed lower PD-L1 positivity compared to surgical resection specimens.<sup>19</sup>

Within this research, we studied PD-L1 expression in tumor resection specimens, in TC and IC, of two most common NSCLC histology subtypes - adenocarcinoma (AC) and SCC.

## Patients and methods

### Patient selection

This prospective study was conducted on surgical specimens from patients with primary operable NSCLC, diagnosed and treated at the University Clinic Golnik from 2006–2015. The specimens were collected and stored at the Laboratory of pathology at the same clinic. Tumor specimens of consecutive

patients diagnosed with squamous-cell carcinoma and adenocarcinoma were included.

### Patient characteristics

Baseline clinicopathological characteristics, such as age at diagnosis, sex and smoking status were obtained from the University Clinic Golnik hospital lung cancer registry database.

Smoking status categories were divided into current smoker, never smoker and former smoker, the latter defined as a person that quit smoking more than a year before the initial diagnosis of lung cancer.

This study was conducted according to the Declaration of Helsinki and was approved by National Ethics Committee (approval number 40/04/12).

### Tumor tissue

The specimens were formalin-fixed, paraffin embedded (FFPE), sliced into 4  $\mu$ m sections and stained for PD-L1 with a rabbit monoclonal antibody SP142 (Ventana/Roche, USA) on an automated platform (Benchmark, Ventana/Roche, USA). Three independent investigators (I.K., U.J. and L.C.) examined whole slices without prior knowledge of the clinicopathological features of the patients. The presence of IC (yes/no) was evaluated for each individual specimen. Percentage of PD-L1 positive immunohistochemical reaction was evaluated in TC and IC, ranging from 0–100%, regardless of staining intensity. The staining of TC on the cell membrane was regarded as positive, whereas IC showed PD-L1 positive reaction in the cytoplasm. Human placenta was also immunostained as a control tissue for PD-L1 expression. The results were then statistically analyzed for two preplanned cut-off values, namely 5% or higher and 10% or higher PD-L1 expression in either TC or IC.

### Statistical considerations

Statistical analyses were performed using SPSS v22 software. Inter-rater agreement of PD-L1 expression in TC and IC was evaluated using Fleiss kappa. PD-L1 expression in either TC or IC was evaluated for unconditional association with the dependent variables using a Chi-square test for categorical data and t-test for continuous data. Association between expression in TC and IC was evaluated with McNemar test. In all analyses the p value of < 0.05 was considered statistically significant.

## Results

A total of 54 tumor samples were examined, 29 of them (54%) were AC and 25 (46%) were SCC. The majority of samples were retrieved from male patients 34 (63%) and 20 (37%) from female. The mean (SD) age at diagnosis was 62.4 (8.6) years. Most of the patients were smokers (46%) or ex-smokers (39%). Patient characteristics are listed in Table 1.

PD-L1 positive reaction in either TC or IC is shown in Figure 1. In TC, the expression of PD-L1 was equal or higher than 10% in 17 samples, between 5% and 10% in only 1 sample, lower than 5% in 14 samples and completely absent in 22 samples. The inter-rater agreement in this case was almost perfect ( $\kappa = 0.89$ ;  $p < 0.001$  at 5% cut-off value). Significantly higher rates of TC PD-L1 positivity were determined in SCC than in AC, at both 5% and 10% cut-off values (52% vs. 17%;  $p = 0.016$  and 52% vs. 14%;  $p = 0.007$ , respectively). The proportion of PD-L1 positivity in TC of AC and SCC is depicted in Figure 2.

Compared to the expression in TC, PD-L1 was more often present in IC. PD-L1 expression in IC was equal or higher than 10% in 28 samples, between 5% and 10% in 12 samples, lower than 5% in

TABLE 1. Clinicopathological patient characteristics

Total	N = 54
Histology	
Squamous-cell carcinoma	25 (46%)
Adenocarcinoma	29 (54%)
Sex	
Male	34 (63%)
Female	20 (37%)
Age (years)	
Mean (SD)	62.4 (8.6)
Smoking status	
Current smoker	25 (46%)
Former-smoker (>1 year)	21 (39%)
Non-smoker	0 (0%)
Unknown	8 (15%)

6 samples and completely absent in 8 samples. In this case the inter-rater agreement was lower as in the determination of TC ( $\kappa = 0.12$ ;  $p = 0.119$  at 5% or higher cut-off value). There were no significant differences observed in IC PD-L1 positivity rates be-

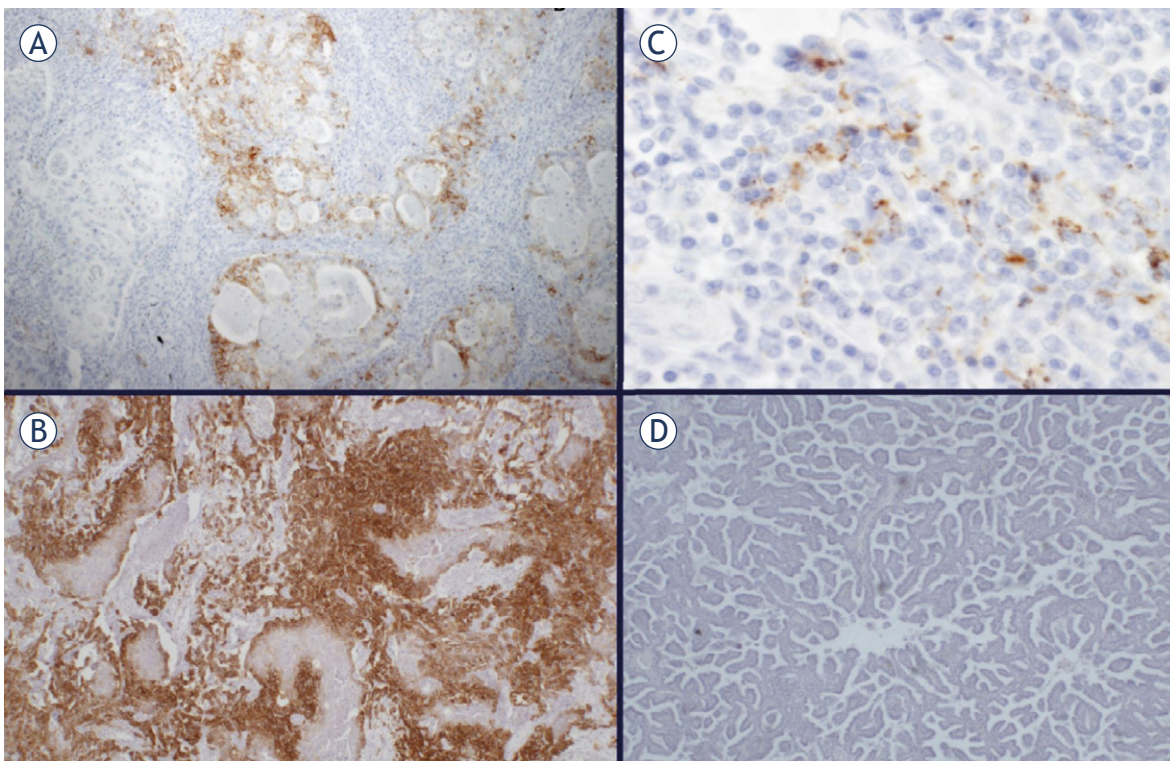


FIGURE 1. PD-L1 expression in NSCLC. Positive membranous reaction in tumor cells in adenocarcinoma (A), and squamous-cell carcinoma (B), positive cytoplasmic reaction in immune cells (C), negative reaction in adenocarcinoma (D).

TABLE 2. PD-L1 positivity according to histology for cut-off value of 5% and higher and 10% and higher

	Tumor specimens N	PD-L1 positivity (cut-off $\geq$ 5%)				PD-L1 positivity (cut-off $\geq$ 10%)			
		TC or IC	TC	IC	p value	TC or IC	TC	IC	p value
		N (%)	N (%)	N (%)	TC vs. IC	N (%)	N (%)	N (%)	TC vs. IC
Total	54	43 (80)	18 (33)	40 (74)		31 (57)	17 (31)	28 (52)	
Adenocarcinoma	29	21 (72)	5 (17)	21 (72)	<b>&lt; 0.001</b>	12 (41)	4 (14)	12 (41)	<b>0.008</b>
Squamous-cell carcinoma	25	22 (88)	13 (52)	19 (76)	0.146	19 (76)	13 (52)	16 (64)	0.508

IC = immune cells; TC = tumor cells. Statistically significant results are in bold.

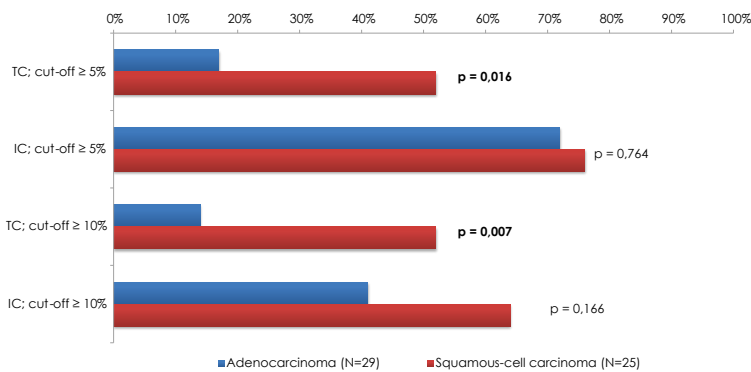


FIGURE 2. Proportions of PD-L1 positive samples of adenocarcinoma and squamous-cell carcinoma in tumor cells (TC) and immune cells (IC) at pre-defined cut-off values ( $\geq$  5% and  $\geq$  10%) with corresponding p values.

tween SCC in AC samples at both 5% and 10% cut-off values (76% vs. 72%;  $p = 0.764$  and 64% vs. 41%;  $p = 0.166$ , respectively) (Figure 2). However, while at the lower cut-off level of 5% the PD-L1 expression in IC was similar in AC and SCC samples, the numerically higher, but not statistically significant, higher PD-L1 positivity rate was observed in SCC. At the same time, this PD-L1 expression in IC was the only noticed difference in PD-L1 expression by predefined cut-off values. (Figure 2)

Higher levels of expression of PD-L1 were observed in IC than in TC. Approximately one third of samples were PD-L1 positive in TC irrespective of the cut off level, compared to more than half of the samples that were positive in IC at 10% cut-off and three quarters at 5% cut-off. The difference in expression between IC and TC reached the level of significance in AC, but not in SCC at both cut-off values (Table 2).

The total PD-L1 positivity rate (either in TC or IC) was the same as determined for IC in AC, irrespective of the cut-off value, since all of the positive TC samples were also IC positive. In SCC the total positivity rate was slightly higher than the rates observed in IC, since three samples that were TC

positive, were IC negative, irrespective of the cut-off value (Table 2).

Histology was associated with different PD-L1 expression in our 54 samples. In total, the samples obtained from SCC patients were more frequently determined as PD-L1 positive compared to the samples from AC patients, mainly due to a significantly higher rate of PD-L1 positivity of TC in SCC compared to AC histology (Table 2 and Figure 2).

## Discussion

In the present study, we showed that PD-L1 expression in lung cancer might differ according to histology and that the selection of TC and/or IC for the evaluation influences the PD-L1 positivity rate in adenocarcinomas. Based on our results, we observed a significantly higher proportion of PD-L1 positivity among SCC than AC, when considering staining in the TC, whereas PD-L1 positivity in IC is quite high in both histological subtypes of NSCLC.

According to our knowledge, only few studies reported PD-L1 expression separately in SCC and AC. Among them, two studies by Yang *et al.*<sup>20,21</sup> mirror our results in terms of higher positivity in SCC. In these studies, the PD-L1 positivity in TC was 56.2% and 39.9% in SCC and AC, respectively. They used another PD-L1 antibody to stain the tissue (Proteintech Group Inc., USA), but similar cut-off point of 5%.

There are also studies with different results in the literature. For example, D'Incecco *et al.*<sup>22</sup> analyzed PD-L1 expression in NSCLC tumor specimens separately for SCC and non-SCC, and reported on TC positivity rate of 30% and 63%, respectively. The reason for different results compared to ours could be the use of different antibody (Ab58810 by Ventana) in this particular study and the fact that they used both whole tissue specimens and small biopsies, which may not reflect the actual PD-L1

expression of the tumor. Since NSCLC tumor specimens are obviously quite heterogeneous, we firmly believe that it is important to have a large tissue specimen for PD-L1 determination, as small specimens are unreliable and might not represent the whole image of PD-L1 positivity in the tumor.<sup>19</sup>

The clinical trials with immune checkpoint inhibitors put the clinical outcomes in perspective according to PD-L1 expression. Most of these trials used only biopsy specimens, while whole tissue specimens were in minority, since the population included patients with advanced NSCLC.<sup>1-6</sup> Two phase 3 trials with NSCLC patients evaluating nivolumab, namely CheckMate 017 and CheckMate 057, were the only two that performed separate clinical trials on SCC and non-SCC subpopulations of advanced NSCLC patients. Results showed similar response rates in the overall population of around 20%, but differences emerged when responses were examined according to PD-L1 expression. While SCC population has a stable response to therapy no matter the cut-off value, ranging from 17–21% in the PD-L1 positive and negative population of patients, responses of non-SCC population are higher with increasing PD-L1 expression, ranging from 31–37% for PD-L1 positive patients and less than 10% in PD-L1 negative population of patients.<sup>1,2</sup> The same applies to undivided advanced NSCLC patient population, treated with pembrolizumab and atezolizumab. It should be noted that these trials recruited substantially more non-SCC than SCC patients and showed that the higher the positivity rate of PD-L1 expression, the better the clinical outcomes.<sup>3-6</sup>

Based on our data as well as data published and described above, SCC seems to be distinct from non-SCC. That reflects both in high PD-L1 positivity and in steady responses to immune checkpoint therapy across SCC subgroup of patients. One of the possible explanations could be high levels of acquired somatic mutations in SCC patients caused with carcinogens such as cigarette smoke, especially because most of the patients with SCC are smokers. Rizvi *et al.* analyzed the responses to pembrolizumab with respect to the mutational burden of NSCLC patients and discovered that patients with a high rate of somatic mutational burden had a much higher rate of responses to pembrolizumab and that those responses were durable.<sup>17,18</sup>

So far, data on the importance of IC in tumor microenvironment are scarce and even less data exist on PD-L1 positivity of these cells and what is their clinical significance. Our study showed high levels of PD-L1 positive IC across all histological

subtypes of NSCLC no matter the cut-off value applied. Only one paper reported PD-L1 expression on IC separately, but used different methodology for their determination, so these data are hardly comparable with ours.<sup>23</sup> Most of the clinical trials with immune checkpoint inhibitors used PD-L1 expression on TC as enrichment predictive biomarker.<sup>1-3</sup> The trials with atezolizumab were the only ones that considered PD-L1 expression on both, TC and IC.<sup>6-8</sup> The antibody used in these trials was the same as in our study (Ventana SP142), but their cut-off values were determined a bit different. Since they reported the results of PD-L1 expression on TC and IC together, it cannot be established if one type of cells are more prominent than the other or which cells prevail concerning PD-L1 expression.<sup>4,6</sup>

PD-L1 assays poses major challenges and barriers in comparing results obtained by different IHC assays. When dealing with different antibodies, cut-off values, platforms, tissue specimens, tumor heterogeneity and different types of cells being evaluated, a uniform way of determining PD-L1 expression comes to mind.<sup>11,12</sup> Three trials of harmonization and standardization for quantitative assessment of PD-L1 positivity were already published<sup>13-15</sup> and one was presented in form of an abstract.<sup>16</sup> The major finding of The Blueprint project<sup>13</sup> and of the German study<sup>14</sup>, which compared four assays (with corresponding platforms and antibodies Ventana SP142, Ventana SP263, Dako 22C3 and Dako 28-8) was that the Ventana SP142 assay stains less TC than the other three. Staining of the IC was observed across different assays, but with greater variability compared to TC staining, which they clarify by the lack of criteria for scoring of the PD-L1 positive IC component in tumors. This is a viable explanation for our results as well, since we showed IC to be highly positive across both histological subtypes. Whether using Ventana SP142 assay influenced the differences in TC staining between AC and SCC samples observed in our study cannot be ruled out completely.

In addition to the use of specific Ventana SP142 assay, which obviously stains less TC, the limitation of our study is also a relatively small number of patients, which makes results barely comparable to other trials.

In conclusion, we have shown significantly higher levels of PD-L1 expression in TC of SCC compared to AC samples, while no difference in PD-L1 expression on IC was observed. Even though PD-L1 positivity is far from being an optimal predictive marker, higher PD-L1 expression in SCC might reflect a high mutational load in this

smoking related lung cancer. Ongoing research is already oriented at mutational load and smoking gene signatures in addition to other immune markers that might offer a more accurate prediction of response to CPIs in future. Until then, we might feel comfortable to use some of the CPIs in lung cancer without PD-L1 determination, at least in patients with squamous-cell carcinoma.

## Acknowledgement

The research was publicly funded by Slovenian Research Agency (ARRS), grant number J3-4076.

## References

- Brahmer J, Reckamp KL, Baas P, Crino L, Eberhardt WE, Poddubskaaya E, et al. Nivolumab versus docetaxel in advanced squamous-cell non-small-cell lung cancer. *N Engl J Med* 2015; **373**: 123-35. doi:10.1056/NEJMoa1504627
- Borghaei H, Paz-Ares L, Horn L, Spigel DR, Steins M, Ready NE, et al. Nivolumab versus docetaxel in advanced nonsquamous non-small-cell lung cancer. *N Engl J Med* 2015; **373**: 1627-39. doi:10.1056/NEJMoa1507643
- Herbst RS, Baas P, Kim DW, Felip E, Perez-Gracia JL, Han JY, et al. Pembrolizumab versus docetaxel for previously treated, PD-L1-positive, advanced non-small-cell lung cancer (KEYNOTE-010): a randomised controlled trial. *Lancet* 2016; **387**: 1540-50. doi:10.1016/S0140-6736(15)01281-7
- Fehrenbacher L, Spira A, Ballinger M, Kowanzet M, Vansteenkiste J, Mazieres J, et al. Atezolizumab versus docetaxel for patients with previously treated non-small-cell lung cancer (POPLAR): a multicentre, open-label, phase 2 randomised controlled trial. *Lancet* 2016; **387**: 1837-46. doi:10.1016/S0140-6736(16)00587-0
- Rittmeyer A, Barlesi F, Waterkamp D, Park K, Ciardiello F, von Pawel J, et al. Atezolizumab versus docetaxel in patients with previously treated non-small-cell lung cancer (OAK): a phase 3, open-label, multicentre randomised controlled trial. *Lancet* 2017; **389**: 255-65. doi:10.1016/S0140-6736(16)32517-X
- Besse B, Johnson M, Janne PA, Garassino M, Eberhardt WEE, Peters S, et al. Phase II, single-arm trial (BIRCH) of atezolizumab as first-line or subsequent therapy for locally advanced or metastatic PD-L1-selected non-small cell lung cancer (NSCLC). [abstract]. *Eur J Cancer* 2015; **51(Suppl 3)**: abstr 16LBA, S717-18. doi:10.1016/S0959-8049(16)31938-4
- Reck M, Rodriguez-Abreu D, Robinson AG, Hui RN, Csozsi T, Fulop A, et al. Pembrolizumab versus chemotherapy for PD-L1-positive non-small-cell lung cancer. *New Engl J Med* 2016; **375**: 1823-33. doi:10.1056/NEJMoa1606774
- Socinski M, Creelan B, Horn L, Reck M, Paz-Ares L, Steins M, et al. CheckMate 026: A phase 3 trial of nivolumab vs investigator's choice (IC) of platinum-based doublet chemotherapy (PT-DC) as first-line therapy for stage IV/recurrent programmed death ligand 1 (PD-L1)-positive NSCLC. [abstract]. *Ann Oncol* 2016; **27(Suppl)**: abstr LBA7. doi:10.1093/annonc/mdw435.39
- Kumar R, Collins D, Dolly S, McDonald F, O'Brien ME, Yap TA. Targeting the PD-1/PD-L1 axis in non-small cell lung cancer. *Curr Probl Cancer* 2017; **41**: 111-24. doi:10.1016/j.cuprprobcancer.2016.12.002
- Califano R, Kerr K, Morgan RD, Lo Russo G, Garassino M, Morgillo F, et al. Immune checkpoint blockade: a new era for non-small cell lung cancer. *Curr Oncol Rep* 2016; **18**: 59. doi:10.1007/s11912-016-0544-7
- Kerr KM, Tsao MS, Nicholson AG, Yatabe Y, Wistuba II, Hirsch FR. Programmed death-ligand 1 immunohistochemistry in lung cancer: In what state is this art? *J Thorac Oncol* 2015; **10**: 985-9. doi:10.1097/JTO.0000000000000526
- Herbst RS, Soria JC, Kowanetz M, Fine GD, Hamid O, Gordon MS, et al. Predictive correlates of response to the anti-PD-L1 antibody MPDL3280A in cancer patients. *Nature* 2014; **515**: 563-7. doi:10.1038/nature14011
- Hirsch FR, McElhinny A, Stanforth D, Ranger-Moore J, Jansson M, Kulangara K, et al. PD-L1 immunohistochemistry assays for lung cancer: results from phase 1 of the blueprint PD-L1 IHC assay comparison project. *J Thorac Oncol* 2017; **12**: 208-22. doi:10.1016/j.jtho.2016.11.2228
- Scheel AH, Dietel M, Heukamp LC, Johrens K, Kirchner T, Reu S, et al. Harmonized PD-L1 immunohistochemistry for pulmonary squamous-cell and adenocarcinomas. *Modern Pathol* 2016; **29**: 1165-72. doi:10.1038/modpathol.2016.117
- McLaughlin J, Han G, Schalper K, Carvajal-Hausdorf D, Pelekanou V, Rehman J et al. Quantitative assessment of the heterogeneity of PD-L1 expression in non-small-cell lung cancer. *Jama Oncol* 2016; **2**: 46-54. doi:10.1001/jamaoncol.2015.3638
- Ratcliffe MJ, Sharpe A, Midha A, Barker C, Scorer P, Walker J. A comparative study of PD-L1 diagnostic assays and the classification of patients as PD-L1 positive and PD-L1 negative. [abstract]. *Cancer Res* 2016; **76(Suppl)**: abstr LB-094. doi:10.1158/1538-7445.AM2016-LB-094
- Rizvi NA, Hellmann MD, Snyder A, Kvistborg P, Makarov V, Havel JJ, et al. Mutational landscape determines sensitivity to PD-1 blockade in non-small cell lung cancer. *Science* 2015; **348**: 124-8. doi:10.1126/science.aaa1348
- Hellmann M, Rizvi N, Wolchok JD, Chan TA. Genomic profile, smoking, and response to anti-PD-1 therapy in non-small cell lung carcinoma. *Mol Cell Oncol* 2016; **3**: e1048929. doi:10.1080/23723556.2015.1048929
- Ilie M, Long-Mira E, Bence C, Butori C, Lassalle S, Bouhlel L, et al. Comparative study of the PD-L1 status between surgically resected specimens and matched biopsies of NSCLC patients reveal major discordances: a potential issue for anti-PD-L1 therapeutic strategies. *Ann Oncol* 2016; **27**: 147-53. doi:10.1093/annonc/mdv489
- Yang CY, Lin MW, Chang YL, Wu CT, Yang PC. Programmed cell death-ligand 1 expression in surgically resected stage I pulmonary adenocarcinoma and its correlation with driver mutations and clinical outcomes. *Eur J Cancer* 2014; **50**: 1361-9. doi:10.1016/j.ejca.2014.01.018
- Yang CY, Lin MW, Chang YL, Wu CT, Yang PC. Programmed cell death-ligand 1 expression is associated with a favourable immune microenvironment and better overall survival in stage I pulmonary squamous cell carcinoma. *Eur J Cancer* 2016; **57**: 91-103. doi:10.1016/j.ejca.2015.12.033
- D'Incecco A, Andreozzi M, Ludovini V, Rossi E, Capodanno A, Landi L, et al. PD-1 and PD-L1 expression in molecularly selected non-small-cell lung cancer patients. *Br J Cancer* 2015; **112**: 95-102. doi:10.1038/bjc.2014.555
- Schmidt LH, Kummel A, Gorlich D, Mohr M, Brockling S, Mikesch JH, et al. PD-1 and PD-L1 expression in NSCLC indicate a favorable prognosis in defined subgroups. *PLoS One* 2015; **10**: e0136023. doi: 10.1371/journal.pone.0136023

# A novel mutation in the FOXC2 gene: a heterozygous insertion of adenosine (c.867insA) in a family with lymphoedema of lower limbs without distichiasis

Tanja Planinsek Rucigaj<sup>1,3</sup>, Matija Rijavec<sup>2</sup>, Jovan Miljkovic<sup>3</sup>, Julij Selb<sup>2</sup>, Peter Korosec<sup>2</sup>

<sup>1</sup> Dermatovenereological Clinic, University Medical Centre Ljubljana, Ljubljana, Slovenia

<sup>2</sup> University Clinic of Respiratory and Allergic Diseases Golnik, Golnik, Slovenia

<sup>3</sup> Faculty of Medicine, University of Maribor, Maribor, Slovenia

Radiol Oncol 2017; 51(3): 363-368.

Received 26 December 2016

Accepted 23 May 2017

Correspondence to: Tanja Planinšek Ručigaj, M.D., Dermatovenereological Clinic, University Medical Center Ljubljana, Zaloška cesta 2, 1000 Ljubljana, Slovenia. E-mail: t.rucigaj@gmail.com

Disclosure: No potential conflicts of interest were disclosed.

**Background.** Primary lymphoedema is a rare genetic disorder characterized by swelling of different parts of the body and highly heterogenic clinical presentation. Mutations in several causative genes characterize specific forms of the disease. FOXC2 mutations are associated with lymphoedema of lower extremities, usually distichiasis and late onset.

**Patients and methods.** Subjects from three generations of a family with lymphoedema of lower limbs without distichiasis were searched for mutations in the FOXC2 gene.

**Results.** All affected family members with lymphoedema of lower limbs without distichiasis, and still asymptomatic six years old girl from the same family, carried the same previously unreported insertion of adenosine (c.867insA) in FOXC2.

**Conclusions.** Identification of a novel mutation in the FOXC2 gene in affected family members of three generations with lymphoedema of lower limbs without distichiasis, highlights the high phenotypic variability caused by FOXC2 mutations.

Key words: primary lymphoedema; FOXC2 mutation; distichiasis; lower limbs lymphoedema

## Introduction

Lymphoedema, swelling due to excess accumulation of the protein-rich lymph in the tissues, is caused by inadequate lymph reabsorption or when the lymphatic vessels are absent or function defectively.<sup>1</sup> Primary lymphoedema is affecting approximately 1.15/100,000 of less than 20 years of age population.<sup>2</sup> Affected individuals suffer from chronic lymphoedema and are at greater risk for developing infections, including bacterial infection of the skin and underlying tissue (cellulitis) or infection of the lymphatic vessels (lymphangitis).<sup>3</sup> They are also at a greater risk than the general population

for developing a malignancy, at the affected site. The most common malignancy associated with the affected area is the angiosarcoma<sup>4-6</sup> (the condition called the Stewart-Treves syndrome), however, also other malignancies, the basal cell carcinoma, squamous cell carcinoma, melanoma, Kaposi sarcoma, Merkel cell carcinoma, and several cutaneous lymphomas<sup>6</sup> can occur, and are probably due to the immunocompromised district of the affected area or because of the environment rich in growth factors due to the formation of collateral lymphatic vessels.<sup>6</sup> Therefore, identification (also with the aid of genetic testing) and monitoring of patients with chronic lymphoedema (no matter the etiology)

should be performed periodically to identify and treat malignant changes that can develop in the affected areas.<sup>6</sup>

The clinical presentation of primary lymphoedema is very variable and varies in the age of onset, the edematous part of the body affected, associated anomalies and different inheritance patterns.<sup>7</sup> The most recent classification of primary lymphoedema has been developed as a diagnostic algorithm, proposed by Connell in 2010<sup>7</sup> and 2013<sup>8</sup>, and is based first on different clinical presentations and second on the genetic findings.

The genetic basis of primary lymphoedema are mutations in five causative genes that also underlie specific forms of the disease<sup>9,10</sup> namely: *FLT4* (fms-related tyrosine kinase 4 encoding VEGFR-3 (vascular endothelial growth factor receptor 3)) mutations, that cause Milroy disease<sup>11-15</sup>; *CCBE1* (collagen and calcium binding EGF domain containing protein 1) mutations that are responsible for autosomal-recessive generalized lymphatic dysplasia<sup>16-18</sup>; *SOX18* (sex determining region Y-box 18) mutations that account for the hypotrichosis-lymphoedema-telangiectasia syndrome<sup>19</sup>; *GJC2* (gap junction protein gamma 2, encoding (CX47) connexin-47) mutations which were identified in patients with four-limb lymphoedema<sup>20,21</sup> and *FOXC2* (fork head box protein C2) mutations that are responsible for autosomal dominant lymphoedema distichiasis syndrome (LDS).<sup>22,23</sup> With the advent of the next generation sequencing technology, muta-

tions in the number of new candidate genes (*NRP2* (neuropilin 2), *SOX17* (sex determining region Y-box 17), *FABP4* (fatty acid binding protein 4), *VCAM1* (vascular cell adhesion molecule 1) have been also linked to primary lymphoedema.<sup>10,24</sup>

In patients with LDS, lymphoedema of both lower limbs, that typically starts in late childhood or during puberty<sup>10,15</sup>, and varicose veins are accompanied by extra eyelashes (known as distichiasis) and also other comorbidities, such as ptosis (35% of patients), congenital heart disease (8%) and cleft palate (3%).<sup>7,8,15</sup> In the majority (95%) of patients with LDS, mutations in the *FOXC2* gene, on chromosome 16q24, are responsible for the disease (15). *FOXC2* encodes a transcription factor for the signal transduction pathway ensuring normal development of the lymphatic collecting vessels and valves.<sup>25</sup>

Besides causing LDS, *FOXC2* mutations have also been identified in lymphoedema without distichiasis.<sup>26</sup> Therefore, the aim of our study was to search for causative mutations in the *FOXC2* gene in three generations of a family with lymphoedema of lower limbs without distichiasis.

## Patients and methods

### Patients

Three family members, a 39-year-old woman, her 74-year-old father and 14-year-old son, have been

**TABLE 1.** Clinical findings of family members with primary lymphoedema

	Patients				
	M	F	M	F	F
Gender	M	F	M	F	F
Age (years)	74	39	14	9	6
Lymphoedema	Yes	Yes	Yes	No	No
Lower limbs	Yes <sup>a</sup>	Yes <sup>a</sup>	Yes <sup>b</sup>	No	No
Genital	Yes	No	No	No	No
Distichiasis	No	No	No	No	No
Onset (years)	11	9	13	/	/
Varicose veins	Yes	Yes	No	No	No
Ptosis	No	No	No	No	No
Cleft palate	No	No	No	No	No
Congenital heart disease	No	No	No	No	No
<i>FOXC2</i> mutation	c.867insA	c.867insA	c.867insA	No	c.867insA
Cellulitis	Yes	Yes	No	No	No
Yellow nails	No	No	No	No	No

<sup>a</sup> = whole lower limbs; <sup>b</sup> = calves only; F = female; M = male

diagnosed with primary lymphoedema at the Dermatovenerological Clinic, University Clinical Centre Ljubljana.

The 74-year-old has lymphoedema of both lower limbs stage III with fibrosis and sclerosis with only some small reticular veins present and genital edemas with lymphatic cysts. The disease started when the patient was 11 years old. The patient does not have distichiasis, ptosis, and cleft palate. There is no known history of lymphoedema in the patient's family and his wife, who had died, also did not have any history of lymphoedema. The patient has suffered a myocardial infarction in 2007 and had a mitral and a tricuspid valve replacement. Patient is being treated with short-stretch bandages and manual lymph drainage and in the maintenance phase with compression garments (bermuda shorts, and flat knitted thigh high stocking class III). Before therapy, he had suffered several erysipelas which have not reoccurred after regular therapy for lymphoedema.

The 39-years-old daughter has lymphoedema stage III of both lower limbs without genital involvement, with the disease onset at age 9. The patient, like her father, also does not have distichiasis, ptosis or cleft palate. She has varicose veins present on both of her legs. Her husband does not have lymphoedema. She is being treated with flat

knitted thigh high stocking class III. Again, she had suffered several erysipelas which were stopped after regular therapy for lymphoedema. She has three children.

In her son, lymphoedema stage II of both lower limbs first occurred at the age of 13. He has no other pathological clinical findings. He is being treated with round knitted stockings class II. He has not suffered any erysipelas.

Both her daughters aged 9 and 6 years have no symptoms and signs of lymphoedema. Age, gender, and detailed clinical characteristics of the recruited subject are presented in Table 1.

The study was approved by the Slovenian national ethics committee (number: 157/07/10) and all participants gave their informed written consent.

### Genetics analysis

Genomic DNA was extracted from EDTA-containing whole blood samples using a QIAamp DNA Blood Mini Kit (Qiagen, Hilden, Germany) according to the manufacturer's instructions. The detection of *FOXC2* mutations in the 1506 bp single exon coding region, as well as in the 5' and 3' regions of *FOXC2* gene was performed as previously described.<sup>26,27</sup> The primer sequence and conditions used are presented in Table 2. PCR prod-

**TABLE 2.** Primer sequences and conditions used to amplify and sequence the *FOXC2* gene and its upstream and downstream regions

Name of primer	Sequence (5'-3')	Annealing temp (°C)	Product size (bp)	DMSO %	MgCl <sub>2</sub> mM
FOXC2-1F <sup>a</sup>	TCTGGCTCTCTCGCGCTCT	58	476	6	1.5
FKHL14-2R	AGTAACTGCCCTTGCCGG				
FOXC2-2F <sup>a</sup>	ACCGCTCCCCCTTCTACCGG	60	519	10	1.5
FOXC2-2R	TCATGATGTTCTCCACGCTGAA				
FKHL14-4F <sup>a</sup>	GAAGGTGGTGATCAAGAGCG	60	496	6	1.5
FOXC2-3R	GAGGTTGAGAGCGCTCAGGG				
FOXC2-4F <sup>a</sup>	CTGGACGAGGCCCTCTCGGAC	61	464	10	1.5
FOXC2-4R	GGAGGTCCCGGGACACGTCA				
FOX_5P_1F <sup>b</sup>	GCCGACGGATTCTGCGCTC	61	378	10	1.5
FOX_5P_1R	CCGCTCTCGCTGGCTCCA				
FOX_5P_2F <sup>b</sup>	CCGATTCGCTGGGGGCTGGAG	61	607	6	1.5
FOX_5P_2R	GCGGGCTGGTGGTGGTGGTAGG				
FOX_3P_1F <sup>b</sup>	CAACGTGCGGGAGATGTTCAAC	61	464	10	1.5
FOX_3P_1R	CACAGCACAGCCGCTCCTGGTAG				
FOX_3P_2F <sup>c</sup>	TACTGACGTGTCCCGGGACC	61	468	6	1.5
FOX_3P_2R	CCACACATTGTACAGCACGGTTG				

<sup>a</sup> = Primer pairs from<sup>27</sup>; <sup>b</sup> = Primer pairs from<sup>28</sup>; <sup>c</sup> = Primer pairs from<sup>26</sup>

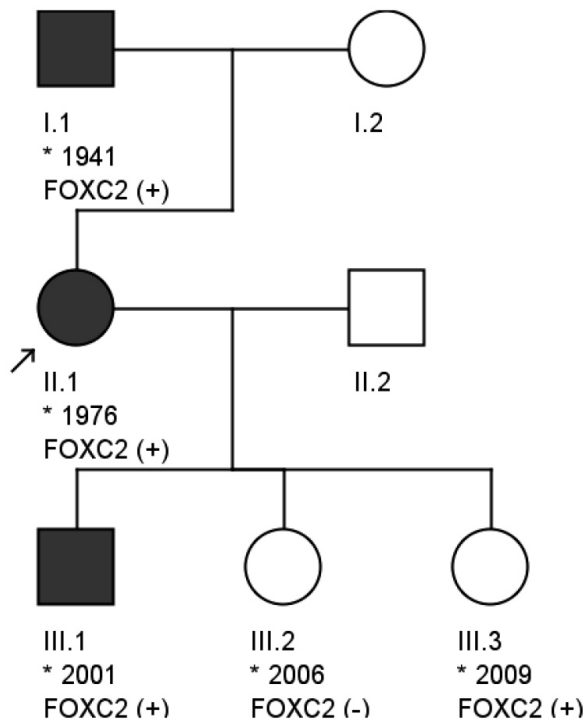


**FIGURE 1.** Pedigree of the family with new mutation in *FOXC2* gene. Full symbols indicate patients with lymphoedema, asterisk (\*) indicate year of birth of the recruited subjects and subjects with c.867insA *FOXC2* mutation are indicated as FOXC2 (+).

ucts were sequenced using Big Dye Terminator kit (Thermo Fisher Scientific) and 3730xl DNA analyzer (Thermo Fisher Scientific). To identify mutations, sequences were compared with the *FOXC2* reference sequence in the GenBank (GenBank accession number NG\_012025.1) using the SeqScape Software v2.6 (Thermo Fisher Scientific). Mutations numbering is based on cDNA sequence, where the first nucleotide (A) of the initiation codon (ATG) is considered nucleotide number one.

## Results

### Clinical details

The clinical detail of all five patients are shown in Table 1.

### Genetics analysis

In all affected members of the described three generation family with lymphoedema of lower limbs without distichiasis the same mutation in *FOXC2* responsible for the disease was identified (Figure 1). The mutation identified in our

patients is a heterozygous insertion of adenosine (c.867insA) and was not previously described. This insertion was present in three family members affected by primary lymphoedema, as well as in a six years old girl without any symptoms and signs of lymphoedema at the time of analysis, while it was absent in a healthy nine years old girl.

Since the discovered mutation was not previously reported we additionally evaluated this mutation in 182 normal controls. None of the controls harbored the mutation, which further supports the causative nature of the mutation.

## Discussion

Up to date only one lymphedema family with *FOXC2* mutation without any individual with distichiasis was found.<sup>26</sup> We report the second family of three generations with *FOXC2* mutation and in which all affected individuals demonstrated lymphedema without distichiasis. Molecular analysis helped to identify the causative heterozygous insertion of adenosine (c.867insA) in the *FOXC2* gene, which was previously not described. This mutation causes frameshift and premature termination of the mature protein since stop codon is inserted behind amino acid 461, leading to a truncation of the mature protein and consequently to the elimination of key alpha-helical domains required for the transcription process.<sup>26</sup> Frameshift mutations are expected to alter the reading frame or lead to a premature termination of the protein, and as a result those unstable mRNA transcripts are removed through the nonsense-mediated mRNA decay pathway.<sup>28,29</sup> The causative nature of the identified variant was further supported by the fact that the mutation was not found in any of the 182 tested normal controls.

In all three patients of our family, lymphoedema developed between the age of 9 and 13. The onset of lymphoedema in literature is typically during puberty or in late childhood.<sup>7,26,30</sup> In the 6 years old girl without clinical manifestations of lymphoedema with mutation in *FOXC2*, lymphoedema will very likely develop within the next few years. She also has no other clinical findings that were described in patients with *FOXC2* mutations. All three patients have lymphoedema of both lower limbs like the patients described in the literature.<sup>14,28</sup> Because of delayed therapy with compression in the female patient and her father, lymphoedema of the legs is in the III<sup>rd</sup> stage. Patient's father also has lymphoedema of genital region with oc-

casional lymphorrhoea. Several papers have mentioned that lymphoscintigraphy, because of valve failure, indicate distal lymph reflux in patients with LDS.<sup>6,29,31</sup> In our two older patients not only early therapy, but also lymphoscintigraphy have been performed in other institutions abroad, and thus unfortunately any information about those findings are not available. Also for the young boy, his mother did not allow to perform early diagnostic procedures, because of known family diagnosis. Both, the patient and her father had suffered many erysipelas before therapy. After regular wearing of compression garments erysipelas were stopped. The son started with compression stockings class II immediately after the onset of edema. He has lymphoedema stage II with morning swelling, without sequelae. Our female patient and her father both have reticular varicose veins without reflux. In the literature lymphoedema and varicose veins are accompanied by distichiasis, which occur in 94.3% of the patients with mutations in the *FOXC2* gene.<sup>15,32</sup> Affected individuals can also have ptosis (in 35% of patients), congenital heart disease (8%), cleft palate (3%) and in some patients yellow nails and cystic hygromas have been described.<sup>26</sup> In our patients there were no distichiasis, no cleft palate, no ptosis or yellow nails, no congenital heart defects or cystic hygromas.

Mutations in the *FOXC2* appear to be the primary cause of LDS. However, not only that some features of the LDS phenotype can be found in patients without *FOXC2* mutations<sup>26</sup> our study and also previous report<sup>26</sup> obviously suggest that mutations in the *FOXC2* gene can be found in lymphoedema patients without distichiasis.

The *FOXC2* gene encodes for a forkhead transcription factor implicated in the development of lymphatic and vascular system, particularly affecting the function of the valves.<sup>25,32</sup> The role has been implicated from animal models where it is expressed in developing mesenchymal cells which develop into blood and lymphatic vessels. Moreover, homozygous null mice (*foxc2*<sup>-/-</sup>) have non-functioning blood vessels.<sup>25,32</sup> In humans *FOXC2* mutations were associated with primary valve failure and venous reflux, indicating its requirement for proper venous function.<sup>15,25,32</sup> Mutations in *FOXC2* most often cause LDS, with lymphoedema of lower extremities, distichiasis, and the disease onset usually after puberty.<sup>7,8,10,15,26,32-35</sup> However, the penetrance and disease expression seems to be highly variable. This was also confirmed by our family in which none of the patients with the novel *FOXC2* mutation had distichiasis.

## Conclusions

In conclusion, we identified a causative previously unreported insertion in *FOXC2* in affected members of three generation family with lymphoedema of lower limbs without distichiasis, highlighting the high heterogeneity of phenotypic variability caused by *FOXC2* mutations.

## References

1. Planinsek Rucigaj T, Tlaker Zunter V. Lymphedema: clinical picture, diagnosis and management. In: Singh N, editor. *Radioisotopes - applications in bio-medical science*. InTech; 2011. Available from: <https://www.intechopen.com/books/radioisotopes-applications-in-bio-medical-science/lymphedema-clinical-picture-diagnosis-and-management>. doi:10.5772/24515
2. Smeltzer DM, Stickler GB, Schirger A. Primary lymphedema in children and adolescents: a follow-up study and review. *Pediatrics* 1985; **76**: 206-18.
3. Al-Niimi F, Cox N. Cellulitis in lymphoedema: a vicious cycle. *J Lymph* 2009; **42**: 38-42.
4. Sharma A, Schwartz RA. Stewart-Treves syndrome: pathogenesis and management. *J Am Acad Dermatol* 2012; **67**: 1342-8. doi:10.1016/j.jaad.2012.04.028
5. Dürr HR, Pellengahr C, Nerlich A, Baur A, Maier M, Jansson V. Stewart-Treves syndrome as a rare complication of a hereditary lymphedema. *Vasa* 2004; **33**: 42-5. doi:10.1024/0301-1526.33.S65.42
6. Lee R, Saardi KM, Schwartz RA. Lymphedema-related angiogenic tumors and other malignancies. *Clin Dermatol* 2014; **32**: 616-20. doi:10.1016/j.clindermatol.2014.04.008
7. Connell F, Brice G, Jeffery S, Keeley V, Mortimer P, Mansour S. A new classification system for primary lymphatic dysplasias based on phenotype. *Clin Genet* 2010; **77**: 438-52. doi:10.1111/cge.12173
8. Connell F, Gordon K, Brice G, Keely V, Jeffrea S, Mortimer P, et al. The classification and diagnostic algorithm for primary lymphatic dysplasia: an update from 2010 to include molecular findings. *Clin Genet* 2013; **84**: 303-14.
9. Ostergaard P, Simpson MA, Jeffery S. Massively parallel sequencing and the identification of genes for primary lymphoedema: a perfect fit. *Clin Genet* 2011; **80**: 110-6. doi:10.1111/j.1399-0004.2011.01706.x
10. Mendola A, Schlögel MJ, Ghalamkarpour A, Irrthum A, Nguyen HL, Fastré E, et al. Mutations in the VEGFR3 signaling pathway explain 36% of familial lymphedema. *Mol Syndromol* 2013; **4**: 257-66. doi:10.1159/000354097
11. Ferrell RE, Levinson KL, Esmen JH, Kimak MA, Lawrence EC, Barmada NM, et al. Hereditary lymphedema: evidence for linkage and genetic heterogeneity. *Hum Mol Genet* 1998; **7**: 2073-8.
12. Evans AL, Brice G, Sotirova V, Mortimer P, Beninson J, Burnard K, et al. Mapping of primary congenital lymphedema to the 5q35.3 region. *Am J Hum Genet* 1999; **64**: 547-55. doi:10.1086/302248
13. Karkkainen MJ, Ferrell RE, Lawrence EC, Kimak MA, Levinson KL, McTigue MA, et al. Missense mutations interfere with VEGFR-3 signalling in primary lymphoedema. *Nat Genet* 2000; **25**: 153-9. doi:10.1038/75997
14. Irrthum A, Karkkainen MJ, Devriendt K, Alitalo K, Vikkula M. Congenital hereditary lymphedema caused by a mutation that inactivates VEGFR3 tyrosine kinase. *Am J Hum Genet* 2000; **67**: 295-301. doi:10.1086/303019
15. Brice G, Mansour S, Bell R, Collin JR, Child AH, Brady AF, et al. Analysis of the phenotypic abnormalities in lymphoedema distichiasis syndrome in 74 patients with *FOXC2* mutations or linkage to 16q24. *J Med Genet* 2002; **39**: 478-83. doi:10.1136/jmg.39.7.478
16. Hennekam RCM, Geerdink RA, Hamel BCI, Hennekam FA, Kraus P, et al. Autosomal recessive intestinal lymphangiectasia and lymphedema, with facial anomalies and mental retardation. *Am J Med Genet* 1989; **34**: 593-600. doi:10.1002/ajmg.1320340429

17. Alders M, Hogan BM, Gjini E, Salehi F, Al-Gazali L, Hennekam EA, et al. Mutations in *CCBE1* cause generalized lymph vessel dysplasia in humans. *Nat Genet* 2009; **41**: 1272-4. doi:10.1038/ng.484
18. Alders M, Mendola A, Ades L, Al Gazali L, Bellini C, Dallapicola B, et al. Evaluation of clinical manifestations in patients with severe lymphedema with and without *CCBE1* mutations. *Mol Syndromol* 2013; **4**: 107-13. doi:10.1159/000342486
19. Irrthum A, Devriendt K, Chitayat D, Matthijs G, Glade C, Steijlen PM, et al. Mutations in the transcription factor gene *SOX18* underlie recessive and dominant forms of hypotrichosis-lymphedema-telangiectasia. *Am J Hum Genet* 2003; **72**: 1470-8. doi:10.1086/375614
20. Ferrell RE, Baty CJ, Kimak Ma, Karlsson JM, Lawrence EC, Franke-Snyder M, et al. GJC2 missense mutations cause human lymphedema. *Am J Hum Genet* 2010; **86**: 943-8. doi:10.1016/j.ajhg.2010.04.010
21. Ostergaard P, Simpson MA, Brice G, Mansour S, Connell FC, Onaoufridaï A, et al. Rapid identification of mutations in *GJC2* in primary lymphoedema using whole exome sequencing combined with linkage analysis with delineation of the phenotype. *J Med Genet* 2011; **48**: 251-5. doi:10.1136/jmg.2010.085563
22. Fang J, Dagenais SL, Erickson RP, Arlt MF, Glynn MW, Gorski JL, et al. Mutations in *FOXC2* (MFH-1), a forkhead family transcription factor, are responsible for the hereditary lymphedema-distichiasis syndrome. *Am J Hum Genet* 2000; **67**: 1382-8. doi:10.1086/316915
23. Shimoda H, Bernas MJ, Witte MH. Dysmorphogenesis of lymph nodes in *Foxc2* haploinsufficient mice. *Histochem Cell Biol* 2011; **135**: 603-13. doi:10.1007/s00418-011-0819-x
24. Ferrell RE, Kimak MA, Lawrence EC, Finegold DN. Candidate gene analysis in primary lymphedema. *Lymphat Res Biol* 2008; **6**: 69-76. doi:10.1089/lrb.2007.1022
25. Bell R, Brice G, Child AH, Murday VA, Mansour S, Sandy CJ, et al. Analysis of lymphoedema-distichiasis families for *FOXC* mutations reveals small insertions and deletions throughout the gene. *Hum Genet* 2001; **108**: 546-51.
26. Finegold DN, Kimak MA, Lawrence EC, Levinson KL, Cherniske EM, Pober BR, et al. Truncating mutations in *FOXC2* cause multiple lymphedema syndromes. *Hum Mol Genet* 2001; **10**: 1185-9.
27. Kovacs P, Lehn-stefan A, Stumvoll M, Bogardus C, Baier LJ. Genetic variation in the human winged helix/forkhead transcription factor gene *FOXC2* in Pima Indians. *Diabetes* 2003; **52**: 1292-5. doi:10.2337/diabetes.52.5.1292
28. Frischmeyer PA, van Hoof A, O'Donnell K, Guerrero AL, Parker R, Dietz HC. An mRNA surveillance mechanism that eliminates transcripts lacking termination codons. *Science* 2002; **295**: 2258-61. doi:10.1126/science.1067338
29. Van Steensel MA, Damstra RJ, Heitink M, Bladergroen RS, Veraart J, Steijlen PM, et al. Novel missense mutations in the *FOXC2* gene alter transcriptional activity. *Hum Mutat* 2009; **30**: E1002-9. doi:10.1002/humu.21127
30. Burnand KG, Mortimer PS. Lymphangiogenesis and genesis of lymphedema. In: Browse N, Burnand KG, Mortimer PS, editors. *Diseases of the lymphatics*. London: Arnold; 2003. p. 102-9.
31. Sholto-Douglas-Vernon C, Bell R, Brice G, Mansur S, Satfarazi M, Child AH, et al. Lymphoedema distichiasis and *FOXC2*: unreported mutations, *de novo* mutation estimate, families without coding mutations. *Hum Genet* 2005; **117**: 238-42. doi:10.1007/s00439-005-1275-2
32. Mellor RH, Brice G, Stanton AW, French J, Fernch J, Smith A, et al. Mutations in *FOXC2* are strongly associated with primary valve failure in veins of the lower limb. *Circulation* 2007; **115**: 1912-20. doi:10.1161/CIRCULATIONAHA.106.675348
33. Sutkowska E, Gil J, Stembalska A, Hill-Bator A, Szuba A. Novel mutation in the *FOXC2* gene in three generations of a family with lymphoedema-distichiasis syndrome. *Gene* 2012; **498**: 96-9. doi:10.1016/j.gene.2012.01.098
34. Rosbotham JL, Brice GW, Child AH, Nunan TO, Mortimer PS, Burnand KG. Distichiasis-lymphoedema: clinical features, venous function and lymphoscintigraphy. *Br J Dermatol* 2000; **142**: 148-52. doi:10.1046/j.1365-2133.2000.03258.x
35. Petrova TV, Karpanen T, Norrm'en C, Mellor R, Tamakoshi T, Finegold D, et al. Defective valves and abnormal mural cell recruitment underlie lymphatic vascular failure in lymphedema distichiasis. *Nat Med* 2004; **10**: 974-81. doi:10.1038/nm1094

## Izbor bolnikov z ne-drobnoceličnim pljučnim rakom za izmenično zdravljenje s kemoterapijo in z inhibitorji tirozinske kinaze

Matjaž Zwitter M, Antonio Rossi, Di Maio M, Pohar Perme M, Lopes G

**Izhodišča.** Pri bolnikih z napredovalim ne-drobnoceličnim pljučnim rakom se s shemo izmeničnega zdravljenja in s časovnim razmikom med kemoterapijo in inhibitorji tirozinske kinaze izognemo medsebojnemu nasprotnemu učinku obeh skupin zdravil. V pregledu objavljenih raziskav se osredotočamo na odnos med vključitvenimi kriteriji in učinkovitostjo izmeničnega zdravljenja.

**Metode.** Pri iskanju objavljenih raziskav smo pregledali pomembnejše medicinske podatkovne zbirke, kongresne zbornike in citate v objavljenih raziskavah. Kot osnovni kazalec uspešnosti zdravljenja smo upoštevali srednji čas do napredovanja bolezni (PFS). S Pearsonovim korelacijskim koeficientom smo ocenjevali korelacijo med značilnostmi bolnikov in srednjim PFS, ločeno za prvi in za drugi red zdravljenja.

**Rezultati.** V pregled smo vključili 11 kliničnih raziskav z eno samo roko zdravljenja ter 18 randomiziranih kliničnih raziskav 2. ali 3. faze s skupaj 2903 bolniki. Šestnajst raziskav je zajelo poprej nezdravljene bolnike, 13 pa bolnike z napredovanjem bolezni po predhodnem zdravljenju. Štirinajst raziskav je vključilo le bolnike z ne-ploščatočeličnim histološkim tipom raka. Analiza je pokazala zmerno ali močno soodvisnost med srednjim PFS in deležem bolnikov z ne-ploščatoceličnim pljučnim rakom (pri prvem redu zdravljenja), deležem nekadilcev (pri prvem in drugem redu zdravljenja) ter deležem bolnikov z mutacijo receptorja epidermnega rastnega faktorja (EGFR, pri prvem in drugem redu zdravljenja). V 6 raziskavah izmeničnega zdravljenja za poprej nezdravljene bolnike s potrjenimi mutacijami EGFR so potrdili objektivni odgovor na zdravljenje pri 83,1 % bolnikov, srednje PFS pa je bilo 18,6 mesecev.

**Zaključki.** Za izmenično zdravljenje so najprimernejši poprej nezdravljeni bolniki z tumorji, ki imajo mutacijo gena za EGFR, kot to določimo z biopsijo tumorja ali s preiskavo periferne krvi. Pri teh bolnikih dosežemo z izmeničnim zdravljenjem zelo spodbudne rezultate, zato bi bila upravičena randomizirana raziskava s primerjavo z najboljšim standardnim zdravljenjem.

Radiol Oncol 2017; 51(3): 252-262.

doi:10.1515/raon-2017-0032

## Ocena neoadjuvantnega zdravljenja z magnetnoresonančnim slikanjem pri bolnikih z lokalno napredujočim rakom danke

Fusco R, Petrillo M, Vincenza G, Salvatore F, Sansone M, Catalano O, Petrillo A

**Izhodišča.** Predstavili smo sodobne slikovne metode, ki jih uporabljamo za diagnozo in oceno predoperativnega zdravljenja pri bolnikih z lokalno napredujočim rakom danke. Obravnavali smo morfološko magnetnoresonančno preiskavo (MR) ter funkcionalni MR kot sta dinamična MR s kontrastom (DMR) in difuzijsko obteženo slikanje (DOS). Primerjali smo njihovo diagnostično natančnost pri oceni predoperativnega odgovora na zdravljenje kot tudi uporabo pozitronske emisijske tomografije z računalniško tomografijo (PET/CT).

**Metode.** Pregledali smo podatkovne zbirke *PubMed*, *Scopus*, *Web of Science* in *Google Scholar*. V analizo smo vključili raziskave, ki so preiskovale odgovor na zdravljenje lokalno napredujočega raka danke z omenjenimi metodami. Predstavili smo diagnostično natančnost, resnično in lažno negativne rezultate ter resnično in lažno pozitivne rezultate preiskovanih metod. Analizo smo predstavili s Forestovim diagramom in krivuljo ROC (*receiver operating characteristic*). Izračunali smo tveganje vplivanja in uporabnosti raziskave.

**Rezultati.** Vključili smo 25 raziskav. S pomočjo krivulj ROC smo ugotovili, da ima kombinirano slikanje z morfološko MR preiskavo in DMR največjo natančnost ocenitve odgovora na predoperativno zdravljenje. DMR in PET/CT imata visoko diagnostično natančnost in njune ocene so prav tako bolj zanesljive kot ocene morfološke MR in DOS.

**Zaključki.** Morfološka MR je metoda izbire za oceno stadija raka danke in nam pomaga načrtovati kirurško zdravljenje. Poda natančno oceno razširjenosti bolezni, vključenosti bezgavk, vključenosti mezorektalne fascije in sfinkterskega kompleksa. Kombinirano slikanje z uporabo DMR nam lahko pomaga pri boljši oceni odgovora na predoperativno zdravljenje in tako tudi pri odločitvi o nadaljnji obravnavi bolnika.

Radiol Oncol 2017; 51(3): 263-269.

doi:10.1515/raon-2017-0028

## Fuzija slikovnih preiskav za oceno terapevtske učinkovitosti radiofrekvenčne ablacije hepatocelularnega raka

Toshikuni N, Matsue Y, Ozaki K, Yamada K, Hayashi N, Tsuchishima M, Tsutsumi M

**Izhodišča.** Med ultrazvočno vodeno radiofrekvenčno ablacijo (RFA) hepatocelularnega carcinoma (HCC), se pojavijo hiperehogeni mehurčki, ki pripomorejo k ovrednotenju učinka zdravljenja. Hkrati ta pojav zakrije tumor, kar ovira oceno, ali smo z RFA zajeli celotni tumor. Z namenom izboljšati oceno zajetosti tumorja z RFA smo preizkusili fuzijski sistem slikovnih preiskav (IFS).

**Bolniki in metode.** V raziskavo smo vključili bolnike, ki smo jih zdravili z enkratno RFA brez ali z uporabo IFS. V skupini IFS smo krožno označili konture zdravljenega tumorja. Označitev je predstavljala referenčno konturo za tarčni volumen pri ultrazvočnem preverjanju med posegom. Ko je hiperehogena pokritost tumorja v celoti zajela označeno konturo, smo ocenili, da je tumor v celoti pokrit. Primerjali smo učinkovitost zdravljenja z in brez uporabe IFS.

**Rezultati.** V raziskavo smo vključili 25 bolnikov z uporabo IFS in 20 brez nje. Izhodišče značilnosti zdravljenih tumorjev so bile primerljive med skupinama. Učinkovitost ablacije tumorjev z RFA je bila značilno večja v skupini z IFS, kot v skupini brez uporabe IFS (88,0 % vs. 60,0 %;  $P = 0,041$ ).

**Zaključki.** Raziskava ugotavlja bolj natančno določanje tarčnega tumorskega volumna za RFA pri HCC, kar pripomore k bolj uspešnemu zdravljenju in zmanjša obremenitev bolnika pri posegu.

Radiol Oncol 2017; 51(3): 270-276.  
doi:10.1515/raon-2017-0025

## Kvantitativni vidiki difuzijsko poudarjenega magnetnoresonančnega slikanja in ocena odgovora na neoadjuvantno zdravljenje pri raku danke

Bassaneze T, Gonçalves JE, Ferreira F, Palma RT, Waisberg J

**Izhodišča.** Namen raziskave je bil oceniti dodano vrednost navideznega difuzijskega koeficienta (ADC), pridobljenega pri difuzijsko poudarjenem magnetnoresonančnem slikanju (DW-MRI) pri bolnikih z rakom danke, ki smo jih zdravili z neoadjuvantno kemoterapijo in radioterapijo (KT-RT). Uporabnost DW-MRI pri oceni odgovora raka danke na zdravljenje danes obsežno raziskujejo, saj je natančna določitev popolnega odgovora na zdravljenje v patoloških preparatih (pPO) ključna za odločanje o nadaljnjem zdravljenju bolnikov.

**Bolniki in metode.** Pri 33 bolnikih z lokalno napredovalim rakom danke smo pred in po neoadjuvantni KT-RT ocenili slike MR hkrati z difuzijsko obteženimi sekvencami in ustreznimi slikami difuzijske konstante (mapami ADC). Bolnike smo nato zdravili operativno z namenom ozdravitve. Zamejitev tumorja, ki smo jo opravili na osnovi konvencionalnih sekvenc MR in s pomočjo meritev vrednosti ADC, smo primerjali s histopatološkimi ugotovitvami v kirurških preparatih.

**Rezultati.** Slikanje MR v kombinaciji z difuzijsko obteženim slikanjem za napoved patomorfološkega popolnega odgovora je imelo občutljivost 96,1 %, specifičnost 71,4 %, pozitivno napovedno vrednost 83,3 % in negativno napovedno vrednost 83,3 %. Vrednost ADC pred KT-RT ni bila zanesljiv napovedni dejavnik za skupino bolnikov s patomorfološkim popolnim odgovorom. Mejna vrednost ADC po KT-RT  $1,49 \times 10^{-3}$  mm<sup>2</sup>/s je bila najbolj natančna za določanje patomorfološkega odgovora in je povečala negativno napovedno vrednost za 16,7 % in občutljivost za 3,9 %. Bolniki z doseženim popolnim patomorfološkim odgovorom ob neoadjuvantnem zdravljenju so se od bolnikov z drugačnim odgovorom na zdravljenje razlikovali glede na absolutne vrednosti ADC po KT-RT ( $p < 0,01$ ).

**Zaključki.** Vrednosti ADC, izmerjene pri bolnikih z rakom danke po zdravljenju z neoadjuvantno KT-RT povečajo diagnostično natančnost difuzijskega slikanja MR pri napovedi končnega patološkega stadija.

Radiol Oncol 2017; 51(3): 277-285.

doi:10.1515/raon-2017-0031

## Dinamična kontrastno dovzetna magnetnoresonančna perfuzija in plazemskih citokinov pri bolnikih po tonično-kloničnih epileptičnih napadih

Filipović T, Šurlan Popović K, Ihan A, Vodušek DB

**Izhodišča.** Vnetno dogajanje v možganskem parenhimu in glialnem tkivu je del procesa epileptogeneze. Koncentracija citokinov v krvi je povečana po tonično-kloničnih epileptičnih napadih. Posledica vnetja je povečana prepustnost krvnožilne možganske pregrade, ki jo lahko ocenjujemo s slikovnimi tehnikami, kot je dinamična kontrastno dovzetna magnetnoresonančna perfuzija (DSC-MRI). Namen raziskave je bila ocena vnetnega dogajanja v možganih po epileptičnem napadu z DSC-MRI in določitev citokinov v plazmi. Ocenjevali smo povezavo med tipom in številom epileptičnih napadov, nivojem citokinov v plazmi po epileptičnem napadu in parametri DSC-MRI. Ocenjevali smo tudi povezavo med naštetimi parametri in enoletnim spremljanjem razvoja bolezni.

**Bolniki in metode.** V raziskavo smo vključili 30 bolnikov. Preiskave smo naredili 8–24 ur po enem ali po ponavljajočih se tonično-kloničnih napadih.

**Rezultati.** 25 bolnikov je imelo normalne parametre perfuzije, pri 5 bolnikih smo našli področja hipoperfuzije. Pri 2 bolnikih je hipoperfuzija vztrajala tudi na kontrolni preiskavi DSC-MRI po 3 mesecih. Število napadov je negativno koreliralo s koncentracijo citokinov IL-10, IFN- $\gamma$  in TNF- $\alpha$  v plazmi pri vseh bolnikih. Pri bolnikih s hipoperfuzijo smo ugotavljali statistično značilne nižje vrednosti protivnetnih citokinov IL-4 in višje vrednosti proinflammatoryh TNF- $\alpha$ .

**Zaključki.** Dolgotrajna prepustnost krvnožilne možganske pregrade je pomembna v procesu epileptogeneze v izbrani skupini bolnikov.

Radiol Oncol 2017; 51(3): 286-294.  
doi:10.1515/raon-2017-0035

# Učinki elektrokemoterapije s cisplatinom in peritumoralnega genskega elektroprenosa interleukina 12 na mastocitome pri psih. Histopatološka in imunološka raziskava

Salvadori C, Švara T, Rocchigiani G, Millanta F, Pavlin D, Čemažar M, Lamprecht Tratar U, Serša G, Tozon N, Poli A

**Izhodišča.** Namen raziskave je bil opredeliti odgovor spontanah mastocitomov pri psih na kombinirano zdravljenje z elektrokemoterapijo in genskim elektroprenosom interleukina 12 (IL-12).

**Materiali in metode.** V raziskavo smo vključili 11 psov z 11 mastocitomi. Histološke spremembe smo določevali na biopsijskih vzorcih, ki smo jih odvzeli pred zdravljenjem (T0), ter 4 (T1) in 8 (T2) tednov kasneje. Celične infiltrate smo opredelili z imunohistokemičnim barvanjem pri tem smo uporabili protitelesa proti CD3, CD20, Foxp3 (Treg), CD68 in MHC-razred II. Proliferacijo in proti-apoptotično aktivnost tumorskih celic smo določili z uporabo protiteles proti Ki67 in protiteles proti proteinu Bcl-2. Angiogenezo smo proučevali z določevanje gostote tumorskega mikrožilja, ki smo ga imunohistokemijsko označili s protitelesi proti faktorju VIII in CD31.

**Rezultati.** S histopatološkim pregledom vzorcev v času T0 smo potrdili diagnozo in zelo redko prisotnost infiltratov imunskih celic, v katerih so bili predvsem T limfociti in makrofagi. Ob času T1 in T2 je bilo število tumorskih celic zelo zmanjšano pri 7/11 vzorcev, pri 3/11 vzorcev so bili vidni manjši skupki tumorskih celic, medtem ko so bile pri enem vzorcu tumorske celice še vedno prisotne. Število proliferajočih tumorskih celic je bilo značilno zmanjšano po zdravljenju v obeh časovnih točkah, medtem, ko je bilo izražanje protiapoptotičnega proteina Bcl2 zmanjšano samo ob času T1. Gostota tumorskega mikrožilja je bila močno zmanjšana pri vseh vzorcih po zdravljenju. Število limfocitov T je bilo povišano po zdravljenju, a ne značilno. Število limfocitov Treg je bilo značilno povišano ob času T1, makrofagov pa ob času T2.

**Zaključki.** Kombinacija elektrokemoterapije in genskega elektroprenosa IL-12 učinkovito izzove celični odgovor proti tumorskim celicah, ki predvsem vključuje infiltracijo limfocitov T in makrofagov. Ugotovili smo tudi proliferacijo fibroblastov in zmanjšano gostoto tumorskega mikrožilja.

Radiol Oncol 2017; 51(3): 295-306.

doi:10.1515/raon-2017-0034

## Elektrokemoterapija s *trans*-platinovim analogom *trans*-[PtCl<sub>2</sub>(3-Hmpy)<sub>2</sub>], raziskava *in vitro* in *in vivo*

Simona Kranjc S, Čemažar M, Serša G, Ščančar J, Grabner S

**Izhodišča.** Cisplatin uporabljamo za zdravljenje raka, pri tem pa ugotavljamo tudi njegove stranske učinke in tvorbo celic, ki so na zdravljenje s cisplatinom odporne. Tako v številnih raziskavah sintetizirajo in vrednotijo protitumorsko delovanje novih platinovih spojin. Nedavno so sintetizirali platinovo spojino *trans*-[PtCl<sub>2</sub>(3-Hmpy)<sub>2</sub>] (3-Hmpy = 3-hidroksimetilpiridin) (spojina **2**) z dobrim citotoksičnim in protitumorskim delovanjem. Z namenom, da bi izboljšali citotoksično delovanje spojine **2** *in vitro* in njeno protitumorsko delovanje *in vivo*, smo uporabili elektroporacijo, ki poveča prepustnost celične membrane, kot dostavni sistem nove spojine v celico (elektrokemoterapija).

**Materiali in metode.** *In vitro* smo preživetje sarkomskih celic z različno občutljivostjo na cisplatin (občutljive TBLCI2, odporne TBLCI2Pt in zmerno občutljive SA-1 celice) po tretiranju z elektrokemoterapijo s spojino **2** določili s testom klonogenosti. *In vivo* smo protitumorsko delovanje elektrokemoterapije s spojino **2** v primerjavi s cisplatinom določili s testom zaostanka rasti tumorjev. V nadaljevanju smo z induktivno sklopljeno plazmo in masno spektrometrijo določili še količino vnešene platine v tumorjih, njeno vezavo na DNK ter količino platinove spojine v serumu po elektrokemoterapiji s spojino **2** ali cisplatinom.

**Rezultati.** Elektrokemoterapija s spojino **2** je preživetje sarkomskih celic z različno občutljivostjo na cisplatin statistično značilno zmanjšala, vendar je bil ta učinek zmanjšanja v primerjavi s cisplatinom manj izrazit. Faktor povečanja (5-krat) citotoksičnega delovanja elektrokemoterapije s spojino **2** je bil enak pri za cisplatin občutljivih TBLCI2 in odpornih TBLCI2Pt celicah. Zaostanek v rasti tumorjev po elektrokemoterapiji s spojino **2**, *in vivo*, je bil manjši kot v primeru zdravljenja z elektrokemoterapijo s cisplatinom. Najboljše protitumorsko delovanje elektrokemoterapije s cisplatinom ali spojino **2** smo dosegli pri tumorjih TBLCI2, kjer je bilo ozdravljenih 67 % oziroma 11 % tumorjev. Izguba telesne teže po zdravljenju tumorjev z elektrokemoterapijo s spojino **2** je bila statistično značilno manjša kot pri zdravljenju s cisplatinom. Nadalje, količine platine v tumorjih po elektrokemoterapiji s spojino **2** ali cisplatinom so bile približno dvakrat višje kot pri zdravljenju s samim zdravilom, kar se je v enaki meri odrazilo tudi v količini platine vezane na DNK.

**Zaključki.** Spodbudni rezultati delovanja spojine **2** na celičnem *in vitro* in protitumorskem *in vivo* nivoju nakazujejo na možno uporabo elektrokemoterapije s spojino **2** za zdravljenje tumorjev.

Radiol Oncol 2017; 51(3): 307-316.  
doi:10.1515/raon-2017-0022

## Zaščitna/regenerativna vloga mezenhimskih matičnih celic, ki izvirajo iz maščobnega tkiva, na z $^{131}\text{I}$ -radiojodom inducirane poškodbe žlez slinavk pri podganah

Saylam G, Bayır Ö, Gültekin SS, Pınarlı FA, Han Ü, Korkmaz MH, Sancaktar ME, Tatar İ, Sargon MF, Tatar EC

**Izhodišča.** Namen raziskave je bil analizirati zaščitne/regenerativne učinke mezenhimskih matičnih celic, ki izvirajo iz maščobnega tkiva (ADMSC) na poškodbe žlez slinavk, inducirane z  $^{131}\text{I}$ -radiojodom (RAI) pri podganah.

**Materiali in metode.** Populacija živali je bila sestavljena iz kontrolne (n: 6) in eksperimentalnih skupin (n: 54): RAI (skupina 1), ADMSC (skupina 2), amifostin (skupina 3), RAI+amifostin (skupina 4), sočasna RAI+ADMSC (skupina 5) in RAI+ADMSC po 48 urah (skupina 6). Uporabili smo svetlobno mikroskopijo (LM), transmisijsko elektronsko mikroskopijo (TEM) in scintigrafijo žlez slinavk (SGS) ter podatke statistično analizirali.

**Rezultati.** Z LM smo opazovali kopičenje ADMSC v žleze slinavke v 1. mesecu. Izpostavljenost RAI je vplivala na nekrozo, periduktalno fibrozo, periduktalno sklerozo in vaskularno sklerozo - skupni rezultat je bil statistično značilen ( $p < 0,05$ ). Primerjava z LM med eksperimentalnimi skupinami v 1. in 6. mesecu je pokazala statistično pomembne izboljšave v skupini 6 ( $P < 0,05$ ), ne pa tudi v skupinah 4 in 5. Rezultati primerjave skupin so pokazali, da so bile najnižje vrednosti v 1. mesecu pri skupinah 4 in 5, v 6. mesecu pa pri skupini 6. TEM je pri skupinah 5 in 6 pokazala vakuolizacijo, edem in fibrozo v 1. mesecu in izboljšanje stanja v 6. mesecu. SGS je pokazala razlike v deležu maksimalnega izločanja (Smax) ( $P = 0,01$ ) in razmerju ozadja proti žlezam pri največjem številu (G/BGmax) ( $P = 0,01$ ) v 1. mesecu, za G/BGmax ( $p = 0,01$ ), Smax ( $p = 0,01$ ) in čas za dosego največjega razmerja števila proti času za dosego minimalnega števila (Tmax/Tmin) ( $P = 0,03$ ) v 6. mesecu. Pregled v 1. in 6. mesecu je pokazal razlike v Smax in G/BGmax ( $p = 0,04$ ), ne pa tudi v Tmax / Tmin ( $p > 0,05$ ). Pri skupini 1 smo opazili znatno poslabšanje v delovanju ščitnice, pri skupinah z zaščitnimi sredstvi pa le blago do zmerno poslabšanje.

**Zaključki.** Naši rezultati kažejo, da bi ADMSC lahko imeli obetavno vlogo kot zaščitno/regeneracijsko sredstvo proti z RAI inducirani disfunkciji žlez slinavk.

Radiol Oncol 2017; 51(3): 317-323.

doi:10.1515/raon-2017-0027

## Elektrokemoterapija - adjuvantno zdravljenje pri lokalno napredovalem raku dojke ob sistemski terapiji

Grischke EM, Röhm C, Stauß E, Taran FA, Brucker SY, Wallwiener D

**Izhodišča.** Elektrokemoterapija (ECT) je že dobro uveljavljena pri zdravljenju lokalno napredovalega raka dojke po kirurgiji ali radioterapiji. Malo podatkov pa je o uporabi ECT kot adjuvantnega zdravljenja ob sistemski terapiji. Zato je bil primarni cilj raziskave ugotoviti, ali lahko uporaba ECT v kratkem časovnem intervalu pred sistemsko terapijo vpliva na lokalne ali sistemske stranske pojave. Beležili smo lokalne in sistemske stranske pojave in vpliv sistemske terapije na učinkovitost ECT.

**Bolniki in metode.** V observacijski raziskavi smo sledili 33 bolnikom z lokalno napredovalim rakom dojke v obdobju treh let po 46 zdravljenjih z ECT. Ugotavljali smo stranske pojave in lokalno kontrolo rasti tumorjev ob pridruženih sistemski terapiji. Specifičen čas ECT ni bil določen, a je bil največkrat en teden pred začetkom sistemske terapije.

**Rezultati.** Zbrali smo podatke v času trajanja raziskave na 33 metastatskih bolnicah raka dojke. Petnajst bolnic je prejelo neo-adjuvantno terapijo kot del primarnega zdravljenja, pri napredovalih stadijih bolezni. Nekatere bolnice so prejele več ciklov ECT. Objektivni odgovor na zdravljenje smo videli pri 90 % bolnic. Nismo zaznali povečane lokalne toksičnosti ECT, posebno ne kožnih sprememb kot je lokalna nekroza in tudi ne povečane sistemske toksičnosti.

**Zaključki.** ECT se je pokazala kot učinkovita metoda za zdravljenje lokalno napredovale bolezni raka dojke, ob sočasni sistemski terapiji, posebno pri bolnicah z visokim tveganjem, ki že predhodno niso dobro odgovorile na sistemsko zdravljenje. Nismo zaznali povečane lokalne ali sistemske toksičnosti.

Radiol Oncol 2017; 51(3): 324-330.

doi:10.1515/raon-2017-0023

## Visokodozno hipofrakcionirano obsevanje s protoni za zdravljenje centralno ležečih pljučni rakov je varno in izvedljivo

Ono T, Yabuuchi T, Nakamura T, Kimura K, Yusuke Azami Y, Hirose K, Suzuki M, Wada H, Kikuchi Y, Nemoto K

**Izhodišča.** Malo je poročil o zdravljenju centralno ležečega pljučnega raka z visoko skupno dozo in hipofrakcionacijo protonskih žarkov. Namen retrospektivne raziskave je bil preučiti varnost in učinkovitost vidokodozne protonske hipofrakcionacije pri centralno ležečih pljučnih tumorjih.

**Bolniki in metode.** V raziskavo smo vključili bolnike, obsevane s protonskimi žarki, ki so imeli centralno ležeče pljučne tumorje lobarnih bronhov ali glavnega bronha, oddaljene manj kot dva centimetra od traheje. Vsi bolniki so prejeli v petih tednih 80 Gy relativne biološke doze (RBE) v 25 protonskih obsevanjih v času od januarja 2009 do februarja 2015. Toksičnost smo ocenjevali s pomočjo meril onkološke skupine za obsevanje - RTOG (*Radiation Therapy Oncology Group*) in evropske organizacije za raziskave in zdravljenje raka - EORTC (*European Organization for Research and Treatment of Cancer*)

**Rezultati.** Dvajset bolnikov, vključno s 14 klinično inoperabilnimi bolniki (70 %), je prejelo protonsko obsevanje pri centralnem pljučnem raku. Srednja starost bolnikov je bila 75 let (razpon: 63-90 let), mediana spremljanja je bila 27,5 mesecev (razpon: 12-72 mesecev), srednji premer tumorja pa je bil 39,5 mm (razpon: 24-81 mm). Vse bolnike smo sledili vsaj 20 mesecev ali do smrti. Skupno dvoletno preživetje je bilo 73,8 % (100 % za operabilne bolnike in 62,5 % za inoperabilne bolnike), 2-letna lokalna kontrola bolezni je bila 78,5 %. Toksičnosti 3. stopnje, vključno z bronhialno zožitvijo, obstrukcijo in fistulo, nismo beležili.

**Zaključki.** Raziskava kaže, da je zdravljenje z visoko skupno dozo hipofrakcioniranega protonskega obsevanja pri centralno ležečih tumorjih varno in izvedljivo.

Radiol Oncol 2017; 51(3):331-341.  
doi:10.1515/raon-2017-0004

## Izražanje dolge nekodirajoče RNA *LOC285758* je odvisno od metiliranosti promotorja in povezano z malignostjo gliomov ter ima potencial novega diagnostičnega tumorskega označevalca

Matjašič A, Popović M, Matos B, Glavač D

**Izhodišča.** Opredelitev zgodnjih genetskih vzrokov je lahko v veliko pomoč pri diagnozi gliomov že v njihovi zgodnji fazi razvoja, torej preden postanejo maligni. Vendar pa vzroki niso le genetski, temveč k napredovanju bolezni prispevajo tudi spremembe na epigenetskem nivoju. Dolge nekodirajoče RNA (lncRNA) so ene ključnih epigenetskih modulatorjev signalnih poti, saj je regulacija izražanja genov njihov temeljni mehanizem. Namen naše študije je bil poiskati nove lncRNA kandidate, ki so vključeni v epigenetske poti regulacije in so specifični za gliome.

**Bolniki in metode.** Na setu 12 tumorskih vzorcev smo z uporabo mikromrež določili profil izražanja epigenetsko povezanih lncRNA in za nadaljnje analize izbrali *LOC285758*. Rezultate izražanja smo validirali z uporabo metode qPCR na naboru 157 vzorcev gliomov različnih histopatoloških podtipov. Zanimalo nas je ali je sprememba v izražanju posledica spremenjene metilacije promotorske regije lncRNA, za kar smo uporabili metodo MS-HRM. Še dodatno pa smo za potrebe asociacijske analize z metodo MLPA določili status že znanih tumorskih označevalcev.

**Rezultati.** Izražanje *LOC285758* je bilo, v primerjavi z referenčno RNA zdravih možganov, značilno povišano v vseh podtipih gliomov in inverzno povezano z metilacijo promotorja. Višji nivo izražanja in izgubo metilacije smo ugotovili v tumorjih večje malignosti, še posebej se je izražanje razlikovalo med astrocitomi in oligodendrogliomi.

**Zaključki.** Spremenjeno izražanje lncRNA *LOC285758* v gliomih je odvisno od metilacijskega statusa njene promotorske regije in v povezavi z malignostjo tumorja. Metilacijski status se prav tako razlikuje med astrocitomi nižjih gradusov (WHO I-III) in ostalimi podtipi gliomov in bi kot tak lahko služil kot dodatni diagnostični tumorski označevalec.

Radiol Oncol 2017; 51(3): 342-350.

doi:10.1515/raon-2017-0021

## Z zdravljenjem povezana kakovost življenja v splošni slovenski populaciji ocenjena z vprašalnikom EORTC QLQ-C30

Velenik V, Šečerov-Ermenc A, But-Hadžić J, Zadnik V

**Izhodišča.** V raziskavi smo želeli pridobiti referenčne podatke za zdravo slovensko populacijo o vseh dimenzijah z zdravjem povezane kakovosti življenja, ki jih merimo z vprašalnikom Evropske organizacije za raziskavo in zdravljenje raka (*angl. European Organisation for Research and Treatment of Cancer quality of life-C30, EORTC QLQ-C30*). Želeli smo pripraviti izhodišča pri raziskovalnem in kliničnem delu za vrednotenje kakovosti življenja skupin bolnikov glede na njihove socialno-demografske značilnosti.

**Metode.** Naključno smo izbrali vzorec 1685 prebivalcev Slovenije, starih najmanj 18 in največ 90 let. 1231 preiskovancev je vrnilo izpolnjene vprašalnike EORTC QLQ-C30 in vprašalnike o socialno-demografskih značilnostih. Odgovore smo pretvorili v dimenzije in simptome EORTC, vpliv socialno-demografskih značilnosti pa ocenili z modeli multiple linearne regresije.

**Rezultati.** Spol, starost in samoocenjen družben sloj so pomembni dejavniki, ki vplivajo na z zdravjem povezano kakovostjo življenja v splošni slovenski populaciji. Moški so navajali boljšo kakovost življenja pri večini dimenzij ter so hkrati navajali manj simptomov. V kognitivnem delovanju med spoloma ni bilo razlik. Pri obeh spolih se je kazal tudi značilen upad kakovosti življenja s starostjo.

**Zaključki.** Raziskava prva predstavlja referenčne populacijske vrednosti vprašalnika EORTC QLQ-C30 za eno od držav jugovzhodne Evrope. Pridobljene povprečne vrednosti za posamezne dimenzije kakovosti življenja glede na socialno-demografske značilnosti omogočajo slovenskim onkologom vpogled v kakovost življenja njihovih bolnikov, če le-ti ne bi zboleli. Ker smo v raziskavi uporabili v EORTC priporočeno metodologijo, so pridobljene vrednosti pripravljene za vključitev v različne Evropske skupinske kazalnike z zdravjem povezane kakovosti življenja.

Radiol Oncol 2017; 51(3): 351-356.

doi:10.1515/raon-2017-0017

## Izid zdravljenja s helično tomoterapijo pri prvih 100 tajskih bolnikih z rakom nosnega žrela

Chitapanarux I, Nobnop W, Sripan P, Chumachote A, Tharavichitkul E, Chakrabandhu S, Klunklin P, Onchan W, Jia-Mahasap B, Janlaor S, Kayan P, Traisathit P, Van Gestel D

**Izhodišča.** Namen raziskave je bil analiza dvoletnega preživetja brez lokoregionalne ponovitve bolezni, preživetja brez oddaljenih zasevkov in celokupnega preživetja ter analiza toksičnosti pri prvih 100 tajskih bolnikih z rakom nosnega žrela, ki smo jih zdravili s helično tomoterapijo.

**Bolniki in metode.** Med marcem 2012 in decembrom 2015 smo s helično tomoterapijo zdravili 100 bolnikov z nemetastatskim rakom nosnega žrela. Vsi bolniki so prejeli sočasno kemoradioterapijo na osnovi platine in adjuvantno ali neoadjuvantno kemoterapijo.

**Rezultati.** Srednja starost je bila 51 let (interkvartilni razpon [IQR] 42,5–57,0). Povprečna  $\pm$  standardna deviacija (SD) doza (D) 95 % za planirne tarčne volumne (PTV) 70; 59,3 in 54 je znašala 70,2  $\pm$  0,5; 59,8  $\pm$  0,6 in 54,3  $\pm$  0,8. Povprečje  $\pm$  SD indeksa konformnosti in indeksa homogenosti je bilo 0,89  $\pm$  0,13 in 0,06  $\pm$  0,07. Povprečna  $\pm$  SD D 2 % za hrbtenjačo in možgansko deblo je znašala 34,1  $\pm$  4,4 in 53,3  $\pm$  6,3 Gy. Povprečna  $\pm$  SD D 50 za kontralateralno in ipsilateralno parotidno žlezo je bila 28,4  $\pm$  6,7 in 38,5  $\pm$  11,2 Gy. Ob srednjem času sledenja 33 mesecev (IQR: 25–41) je bilo 2-letno preživetje brez lokoregionalne ponovitve bolezni 94 % (95 % interval zaupanja [CI]: 87–98 %), preživetja brez oddaljenih zasevkov 96 % (95 % CI: 897–98 %) in celokupno preživetje 99 % (95 % CI: 937–100 %). Akutni dermatitis, faringozofagitis in mukozitis stopnje 3 so se pojavili pri 5 %, 51 % in 37 %. Kasni faringozofagitis stopenj 0 in 1 smo ugotovili pri 98 % in 2 % bolnikov. Kasna kserostomija stopenj 0, 1 in 2 pa pri 17 %, 78 % in 5 % bolnikov.

**Zaključki.** Pri bolnikih z rakom nosnega žrela smo s helično tomoterapijo dosegli dobro dozno razporeditev in dosegli odlične terapevtske rezultate

Radiol Oncol 2017; 51(3): 357-362.  
doi:10.1515/raon-2017-0037

## Izraženost PD-L1 pri pljučnem žleznem raku in ploščatoceličnem raku

Janžič U, Kern I, Janžič A, Čavka L, Čufer T

**Izhodišča.** Ob uvedbi imunoterapije za zdravljenje napredovalega nedrobnoceličnega raka pljuč (NDRP) se je pojavila potreba po biološkem označevalcu, ki bo napovedoval odgovor na zdravljenje (prediktivni tumorski označevalec). Izraženost PD-L1 (*angl. programmed death ligand 1*) v tumorskem tkivu je do sedaj najboljše proučen napovedni dejavnik odgovora na imunoterapijo pri NDRP. V raziskavi smo preučevali izraženost PD-L1 v tumorskih in imunskih celicah ploščatoceličnega in žleznega raka pljuč.

**Bolniki in metode.** Izraženost PD-L1 smo določili na vzorcih kirurško odstranjenih tumorjev, ki smo jih pobarvali po imunohistokemični metodi s protitelesom SP142 (Ventana, ZDA). Klinične in patološke značilnosti bolnikov smo pridobili iz bolnišničnega registra. Izraženost PD-L1 smo analizirali glede na dve predhodno določeni mejni vrednosti,  $\geq 5\%$  in  $\geq 10\%$  pozitivnih tumorskih in/ali imunskih celicah.

**Rezultati.** Od 54 tumorskih vzorcev je bilo 29 (54 %) žleznih rakov in 25 (46 %) ploščatoceličnih rakov. Izraženost PD-L1 je bila statistično višja v tumorskih celicah pri ploščatoceličnih rakih kot pa pri žleznih, pri obeh mejnih vrednostih (52 % proti 17 %,  $p = 0,016$  in 52 % proti 14 %,  $p = 0,007$ ). Razlik v izraženosti PD-L1 v imunskih celicah med ploščatoceličnimi in žleznimi raki nismo ugotovili. Samo v skupini žleznih rakov je bila izraženost PD-L1 v imunskih celicah značilno višja v primerjavi s tumorskimi celicami, ponovno pri obeh mejnih vrednostih (72 % proti 17 %,  $p < 0,001$  in 41 % proti 14 %,  $p = 0,008$ ), medtem ko razlike med izraženostjo PD-L1 v imunskih celicah in tumorskih celicah pri ploščatoceličnem raku nismo ugotovili.

**Zaključki.** V raziskavi je bila izraženost PD-L1 značilno višja v tumorskih celicah ploščatoceličnih rakov v primerjavi z žleznimi raki. Izraženost PD-L1 v imunskih celicah pa je bila enaka ne glede na histoloških podtip, kar je značilno vplivalo na celokupno izraženost PD-L1 pri žleznih rakih, ne pa tudi ploščatoceličnih rakih.

Radiol Oncol 2017; 51(3): 363-368.  
doi:10.1515/raon-2017-0026

## Nova mutacija gena FOXC2. Heterozigotna insercija adenozina (c.867insA) pri družini z limfedemom spodnjih okončin brez distihiaze

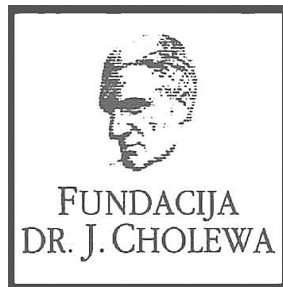
Planinšek Ručigaj T, Rijavec M, Miljkovič J, Selb J, Korošec P

**Izhodišča.** Primarni limfedem je redko genetsko obolenje. Zanj je značilno otekanje posameznih delov telesa z zelo raznoliko pridruženo klinično sliko. Mutacije vzročnih genov imajo za posledico specifične oblike bolezni. Mutacijam FOXC2 so pridruženi limfedem spodnjih okončin in distihiaza, ki se prične kasneje v življenju.

**Bolniki in metode.** Pri bolnikih z limfedemom spodnjih okončin brez distihiaze treh generacij iste družine smo iskali mutacije gena FOXC2.

**Rezultati.** Vsi družinski člani z že razvitim limfedemom spodnjih okončin in asimptomatska šest-letna deklica iste družine so imeli do sedaj neopisano in neobjavljeno mutacijo na genu FOXC2 z insercijo adenozina (c.867insA).

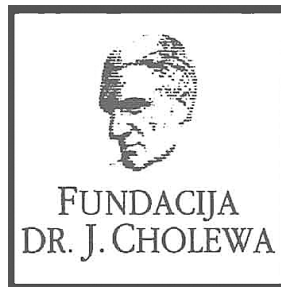
**Zaključki.** Identifikacija nove, do sedaj neopisane mutacije gena FOXC2 pri družini z limfedemom spodnjih okončin v treh generacijah brez distihiaze osvetljuje visoko fenotipsko variabilnost povzročeno z omenjeno mutacijo.



FUNDACIJA "DOCENT DR. J. CHOLEWA"  
JE NEPROFITNO, NEINSTITUCIONALNO IN NESTRANKARSKO  
ZDRUŽENJE POSAMEZNIKOV, USTANOV IN ORGANIZACIJ, KI ŽELIJO  
MATERIALNO SPODBUJATI IN POGLABLJATI RAZISKOVALNO  
DEJAVNOST V ONKOLOGIJI.

DUNAJSKA 106  
1000 LJUBLJANA

IBAN: SI56 0203 3001 7879 431



## Activity of “Dr. J. Cholewa” Foundation for Cancer Research and Education - a report for the third quarter of 2017

Dr. Josip Cholewa Foundation for cancer research and education continues with its planned activities in the second quarter of 2017. Its primary focus remains the provision of grants and scholarships and other forms of financial assistance for basic, clinical and public health research in the field of oncology. In parallel, it also makes efforts to provide financial and other support for the organisation of congresses, symposia and other forms of meetings to spread the knowledge about prevention and treatment of cancer, and finally about rehabilitation for cancer patients. In Foundation’s strategy the spread of knowledge should not be restricted only to the professionals that treat cancer patients, but also to the patients themselves and to the general public.

The Foundation continues to provide support for »Radiology and Oncology«, a quarterly scientific magazine with a respectable impact factor that publishes research and review articles about all aspects of cancer. The magazine is edited and published in Ljubljana, Slovenia. »Radiology and Oncology« is an open access journal available to everyone free of charge. Its long tradition represents a guarantee for the continuity of international exchange of ideas and research results in the field of oncology for all in Slovenia that are interested and involved in helping people affected by many different aspects of cancer.

The Foundation will continue with its activities in the future, especially since the problems associated with cancer affect more and more people in Slovenia and elsewhere. Ever more successful treatment results in longer survival in many patients with previously incurable cancer conditions, thus adding many new dimensions in life of cancer survivors and their families.

Borut Štabuc, M.D., Ph.D.  
Tomaž Benulič, M.D.  
Andrej Plesničar, M.D., M.Sc.  
Viljem Kovač, M.D., Ph.D.

# XGEVA®

# VAŠE BOLNIKE BOLJE ZAŠČITI PRED KOSTNIMI ZAPLETI<sup>1\*</sup>



## AMGEN®

## XGEVA®

(denosumab)

NATANČEN, MOČAN, DOKAZAN.

Podatki integrirane analize preskušanj III. faze, ki so vključevala bolnike z rakom dojke, rakom prostate, ostalimi solidnimi tumorji ali diseminiranim plazmocitomom, ki so imeli zasevke v kosteh.<sup>1</sup>  
<sup>\*</sup>XGEVA® značilno podaljša čas do pojava prvega zapleta kostnih zasevkov (ZKZ) za 8,21 mesec in zmanjša tveganje za pojav prvega ZKZ za 17% (HR: 0,83 [95% CI, 0,76–0,90]; p < 0,001) v primerjavi z zoleđronsko kislino.  
<sup>†</sup>Opredelitev kostnih zapletov: Preprečevanje zapletov kostnih zapletov pri odraslih s kostnimi zasevki solidnih tumorjev.

**XGEVA® 120 mg raztopina za injiciranje (denosumab) – SKRAJŠAN POVZETEK GLAVNIH ZNAČILNOSTI ZDRAVILA.**  
Samo za strokovno javnost. Pred predpisovanjem si preberite celoten Povzetek glavnih značilnosti zdravila. V za to zdravilo se izvaja dodatno spremljanje varnosti. Poročati je potrebno o vseh domnevnih neželenih učinkih zdravila.

**SESTAVA ZDRAVILA:** Ena viala vsebuje 120 mg denosumaba v 1,7 ml raztopine (70 mg/ml). Pomozne snovi z znanim učinkom: 1,7 ml raztopine vsebuje 78 mg sorbitola (E420). **TERAPEVTSKE INDIKACIJE:** Preprečevanje skeletnih dogodkov (patoloških zlomov, obsevanja kosti, kompresije hrbtenjače ali operacije kosti) pri odraslih s kostnimi metastazami solidnih tumorjev. Zdravljenje odraslih bolnikov in skeletno dozorelih mladostnikov z gigantocelularnim kostnim tumorjem, ki ni operabilen, ali pri katerem bi kirurška odstranitev verjetno povzročila hudo bolelost, ki ni operabilen, ali pri katerem bi kirurška odstranitev verjetno povzročila hudo bolelost, je enako kot za odrasle. Za subkutano uporabo. **KONTRAINDIKACIJE:** Preobčutljivost na zdravilno učinkovino ali katero koli pomožno snov. Huda nezdravljena hipokalcemija. Neozdravljena lezija po zobnih ali ustnih kirurških posegih. **POSEBNA OPOZORILO IN PREVIDNOSTNI UKREPI:** Vsi bolniki morajo prejemati dodatek kalcija in vitamina D, razen če ima bolnik hiperkalcemijo. Obstoječa hipokalcemija je treba odpraviti še pred začetkom zdravljenja z zdravilom XGEVA®. Hipokalcemija se lahko pojavi kadar koli med zdravljenjem z zdravilom XGEVA®. Kontrolno koncentracijo kalcija je treba izvesti (i) pred prvim odmerkom zdravila XGEVA®, (ii) v dveh tednih po prvem odmerku, (iii) če se pojavijo simptomi, sumljivi za hipokalcemijo. O dodatnih kontrolah koncentracije kalcija med zdravljenjem je treba razmisliti pri bolnikih, ki imajo dejavne tveganja za hipokalcemijo, ali če so takšne kontrole sicer umestne glede na bolnikovo klinično stanje. Bolnikom je treba naročiti, naj zdravniku obvestijo o simptomih, ki kažejo na hipokalcemijo. Če se med prejetjem zdravila XGEVA® pojavijo hipokalcemija, je lahko potrebno dodatno dodajanje kalcija in dodatne kontrole. Bolniki s hudo okviro ledvic (očistek kreatinina < 30 ml/min) ali bolniki na dializi imajo večje tveganje za pojav hipokalcemije. Tveganje za pojav hipokalcemije in spremljajočega zvišanja paratiroidnega hormona se poveča s povečano stopnjo okvare ledvic. Pri takšnih bolnikih so redne kontrole koncentracije kalcija posebej pomembne. Pri bolnikih, ki imajo nezazeleno lezijo mehkih tkiv v ustih, je treba začetek zdravljenja/nov ciklus zdravljenja odložiti. Pred zdravljenjem z zdravilom XGEVA® je priporočljivo opraviti zobozdravstveni pregled in preventivno zobozdravstveno oskrbo ter individualno oceno koristi in tveganja. Pri ocenjevanju bolnikovega tveganja za pojav osteonekroze čeljustine je treba upoštevati naslednje dejavne tveganja: moč zdravila, ki zavira resorpcijo kosti (tveganje je večje z zelo močnimi spojinami), pot uporabe (tveganje je večje v primeru parenteralne uporabe) in kumulativni odmerki zdravila, uporabljenega za zdravljenje resorpcije kosti, rak, sočasne bolezni (npr. anemija, koagulopacije, okužbi), kajenje, sočasna zdravljenja (kortikosteroidi, kemoterapija, zaviralci angiotenzinov, radioterapija glave in vratu, slabo ustno higieno, periodično obsevanje, slabo prilegoče se zobne proteze, že obstoječo zobno bolezen, invazivne zobozdravstvene posege, npr. ekstrakcije zob). Vsem bolnikom je treba naročiti, da morajo med zdravljenjem z zdravilom XGEVA® izdrževati dobro ustno higieno, redno opravljati zobozdravniške preglede in nemudoma obvestiti zdravnika, če se pojavi kakršni koli simptom v ustih, na primer majanje zob, bolečina, oteklina, rana, ki se ne celi, ali izcedek. Med zdravljenjem je izvajanje invazivnih zobozdravniških posegov dovoljeno le po skrbnem razmisleku in se jim je treba izogniti v bližini termina za odmerjanje zdravila XGEVA®. Načrt vodenja bolnikov, ki se jim pojavi osteonekroza čeljustine, je treba oblikovati na podlagi tesnega sodelovanja med lečnim zdravnikom in zobozdravnikom ali ustnim kirurgom, ki ima izkušnje z osteonekrozo čeljustine. Razmisliški je treba očasnem prenehanju zdravljenja z zdravilom XGEVA®, dokler se to stanje ne razreši in se sovpletni dejavniki tveganja ublažijo, če je mogoče. Med močnejše dejavne tveganja za osteonekrozo zunanjega slušnega kanala spadajo uporaba steroidov in kemoterapija in/ali lokalni dejavniki tveganja. Kot sta okužba ali poškodba. Na možnost osteonekroze zunanjega slušnega kanala je potrebno pomisliti pri bolnikih, ki prejmejo denosumab in pri katerih se pojavijo simptomi boleznih ušes, vključno s kroničnimi ušesni ušes. Atipični zlomi stegenice se lahko pojavijo že ob majhni poškodbi ali celo brez poškodbe, in sicer v subtrohanterem in distalnem predelu stegenice. Za te dogodke so značilni radiografski znaki. O njih so poročali tudi pri bolnikih z določenimi sočasnimi boleznimi stani (npr. s pomanjkanjem vitamina D, revmatoidnim artritisom, hipofosfatemijo) in med uporabo določenih zdravil (npr. bisfosfonatov, glukokortikoidov, zaviralcev protonске črpalke). Ti dogodki so se pojavili tudi brez antiresorpcijskega zdravljenja. Podobni zlomi, opisani v zvezi z bisfosfonati, so pogosto obojestranski, zato je treba pri bolnikih, ki se zdravijo z denosumabom in so imeli zlom srednjega dela stegenice, opraviti tudi pregled druge stegenice. Pri bolnikih, pri katerih obstaja sum na atipičen zlom stegenice, je treba razmisliti o prenehanju uporabe zdravila XGEVA® ob vrednotenju bolnika glede na individualno oceno koristi in tveganja. Bolnikom je treba naročiti, da morajo med zdravljenjem z zdravilom XGEVA® zdravniku poročati o novi ali nenavadni bolečini v stegnu, kolku ali dimljah. Bolnike s takimi simptomi je treba preskati glede nepopolnega zloma stegenice. Zdravilo XGEVA® ni priporočljivo pri bolnikih, ki se jim sklet se razvija. Bolniki, zdravljeni z zdravilom XGEVA®, sočasno na smelo prejemati drugih zdravil, ki vsebujejo denosumab (za indikacije pri osteoporozi), in bisfosfonatov. Malignost pri gigantocelularnem kostnem tumorju ali nepredovanje do metastatske boleznii je redki dogodek in je znano tveganje pri bolnikih z gigantocelularnim kostnim tumorjem. Bolnike je treba kontrolirati glede radioloških znakov malignosti, nove radioložnosti ali osteolize. Razpoložljivi klinični podatki ne kažejo povečanega tveganja za malignost pri bolnikih z gigantocelularnim kostnim tumorjem, zdravljenih z zdravilom XGEVA®. Zdravilo XGEVA® vsebuje sorbitol. Bolniki z redko prirojeno motnjo intolerancije za fruktozo ne smejo uporabljati zdravila XGEVA®. Zdravilo vsebuje manj kot 1 mmol natrija (23 mg) na 120 mg, kar pomeni, da je praktično »brez natrija«. **INTERAKCIJE:** Studij medsebojnega delovanja niso izvedli. Sočasna kemoterapija in/ali hormonsko zdravljenje ali predhodna intravenska izpostavljenost bisfosfonatom niso klinično pomembno spremenili najnižje koncentracije denosumaba v serumu in farmakodinamične denosumaba (N-telopeptid v urinu, prilagojen na kreatinin, uNTX/Ch). **POVZETEK NEŽELENIH UČINKOV:** Zelo pogosti (≥ 1/10), dispneja, driska, mišično-skeletna bolečina. Pogosti (≥ 1/100 do < 1/10): hipokalcemija, hipofosfatemija, elektralizacija zoba, hipotenzija, osteonekroza čeljustine. Redki (1/10.000 do < 1/1000): preobčutljivost na zdravilo, anafilaktična reakcija, osteonekroza zunanjega slušnega kanala. **FARMAKETSKE POBUDE:** Shranjujte v hladnihrani (2°C – 8°C). Ne zamrzujte. **NAČIN IN REŽIM PREDPISOVANJA TER IZDAJE ZDRAVILA:** Predpisovanje in odajba zdravila je na recept s posebnim režimom – ZC. **IMETNIK DOVOLJENJA ZA PROMET:** Amgen Europe S.V., Ministerium 7001, NL-6372 ZK Breda, Nizozemska. **Dodatna pojasnila lahko dobite v lokalni pisarni:** Amgen zdravila d.o.o., Šmartinska 140, SI-1000 Ljubljana. **DATUM ZADNJE REVIZIJE BESEDILA:** Junij 2017. Podrobne informacije o zdravilu so objavljene na spletni strani Evropske agencije za zdravila <http://www.ema.europa.eu>. **LITERATURA:** 1. Lipton A et al. Eur J Cancer. 2012; 48: 3082–3092.

AMGEN, XGEVA, DENOSUMAB, NARANČASTA KAPLJICA, AMGEN, XGEVA, DENOSUMAB, NARANČASTA KAPLJICA



# Iclusig<sup>®</sup> ▼ (ponatinib)

Ključ do učinkovitega zdravljenja bolnikov s KML in Ph + ALL



**Zdravilo Iclusig<sup>®</sup> je peroralni zaviralec tirozin-kinaze (TKI) za doziranje enkrat dnevno z učinkovitim delovanjem pri odraslih bolnikih s KML in Ph+ ALL<sup>1</sup>**

**ICLUSIG<sup>®</sup>**  
(ponatinib) tablete

## Za bolnike s kronično mieloidno levkemijo (KML) v kronični, pospešeni ali blastni fazi, ki:

- so odporni na dasatinib ali nilotinib **ali**
- ne prenašajo dasatiniba ali nilotiniba in pri katerih nadaljnje zdravljenje z imatinibom ni klinično ustrezno **ali**
- imajo mutacijo T315I

## Za bolnike z akutno limfoblastno levkemijo s prisotnim kromosomom Philadelphia (Ph+ ALL), ki:

- so odporni na dasatinib **ali**
- ne prenašajo dasatiniba in pri katerih nadaljnje zdravljenje z imatinibom ni klinično ustrezno **ali**
- imajo mutacijo T315I

### SKRAJŠAN POVZETEK GLAVNIH ZNAČILNOSTI ZDRAVILA Iclusig 15 mg, 30 mg in 45 mg filmsko obložene tablete

Pred predpisovanjem natančno preberite celoten Povzetek glavnih značilnosti zdravila.

Samo za strokovno javnost.

▼ Za to zdravilo se izvaja dodatno spremljanje varnosti. Tako bodo hitreje na voljo nove informacije o njegovi varnosti. Zdravstvene delavce naprošamo, da poročajo o katerem koli domnevem neželenem učinku zdravila.

**Sestava:** Ena filmsko obložena tableta vsebuje 15mg, 30mg ali 45 mg ponatiniba (v obliki ponatinibijevega klorida). **Indikacije:** Zdravilo Iclusig je indicirano pri odraslih bolnikih s kronično mieloidno levkemijo (KML) v kronični fazi, pospešeni fazi ali blastni fazi, ki so odporni na dasatinib ali nilotinib; ki ne prenašajo dasatiniba ali nilotiniba in pri katerih nadaljnje zdravljenje z imatinibom ni klinično ustrezno; ali ki imajo mutacijo T315I ter pri odraslih bolnikih z akutno limfoblastno levkemijo s prisotnim kromosomom Philadelphia (Ph+ ALL), ki so odporni na dasatinib; ki ne prenašajo dasatiniba in pri katerih nadaljnje zdravljenje z imatinibom ni klinično ustrezno; ali ki imajo mutacijo T315I. **Odmerjanje in način uporabe:** Terapijo mora uvesti zdravnik z izkušnjami v diagnosticiranju in zdravljenju bolnikov z levkemijo. Med zdravljenjem se lahko bolniku nudi hematološka podpora, če je to klinično indicirano. Pred začetkom zdravljenja s ponatinibom je treba oceniti kardiovaskularni status bolnika, vključno z anamnezo in telesnim pregledom, in aktivno obravnavati kardiovaskularne dejavnike tveganja. Kardiovaskularni status je treba še naprej spremljati in med zdravljenjem s ponatinibom optimizirati zdravljenje z zdravili in podporno zdravljenje stanj, ki prispevajo h kardiovaskularnim tveganjem.

**Odmerjanje:** Priporočeni začetni odmerek ponatiniba je 45 mg enkrat na dan. Potrebno je razmisлити o ukinitvi ponatiniba, če v 3 mesecih ni celovitega hematološkega odgovora. Z zdravljenjem je treba prenehati, če se pojavijo znaki napredovanja bolezni ali v primeru hudih neželenih učinkov. **Prilagoditev odmerjanja:** tveganje za žilni okluzivni dogodek je verjetno povezano z odmerkom. Zdravljenje z zdravilom Iclusig je treba pri sumu, da se je pri bolniku razvil arterijski ali venški okluzivni dogodek, takoj prekiniti. Ko se dogodek razreši, je treba pri odločitvi o ponovni uvedbi zdravljenja upoštevati oceno koristi in tveganj. Pri obravnavi hematoloških in nehematoloških učinkov je treba razmisлити o prilagoditvi ali prekinitvi odmerjanja. V primeru hudih neželenih učinkov je treba z zdravljenjem prekiniti. Prilagajanje odmerka je priporočljivo v primeru nevtropenije ali trombocitopenije, ki nista povezani z levkemijo; pri pankreatitisu in zvišani ravni lipaze/amilaze. **Način uporabe:** tablete je treba pogoltniti cele, ne sme se jih drobiti ali raztapljati, lahko pa se jih jemlje s hrano ali brez nje.

**Kontraindikacije:** Preobčutljivost na ponatinib ali katero koli pomožno snov. **Posebna opozorila in previdnostni ukrepi:** **Mielosupresija** – Zdravilo Iclusig je povezano s hudo trombocitopenijo, nevtropenijo in anemijo. Prve 3 mesece je treba vsaka 2 tedna opraviti pregled celotne krvne slike, nato pa mesečno ali kot je klinično indicirano. **Žilna okluzija** – Pojavili so se arterijski in venska tromboza in okluzija, vključno s smrtnim miokardnim infarktom, možgansko kapjo, retinalna žilna okluzija, v nekaterih primerih povezana s trajno okvaro vida ali slepoto, stenozo velikih arterijskih žil v možganih, hudo periferno žilno boleznijo in potrebo po nujnem postopku revaskularizacije.

Zdravilo Iclusig se ne sme uporabljati pri bolnikih z miokardnim infarktom, predhodno revaskularizacijo ali možgansko kapjo v anamnezi, razen če so možne koristi zdravljenja večje od možnih tveganj. Med zdravljenjem s ponatinibom je treba spremljati znake tromboembolije in žilne okluzije in zdravljenje je treba takoj prekiniti, če se pojavi žilna okluzija. V primeru, da se pojavi poslabšanje vida ali zamegljen vid, je treba opraviti oftalmološki pregled (vključno s fundoskopijo). **Hipertenzija** – Pri zdravljenju z zdravilom Iclusig, se je pojavila z zdravljenjem povezana hipertenzija (vključno s hipertenzivno krizo), ki lahko prispeva k tveganju arterijskih trombotičnih dogodkov. Zato je treba ob vsakem obisku zdravnika spremljati krvni tlak. Zdravljenje z zdravilom Iclusig je treba prekiniti, če hipertenzija ni pod zdravniškim nadzorom. **Kongestivno srčno popuščanje** – Pojavilo se je smrtno in resno srčno popuščanje ter dogodki, povezani s predhodnimi vaskularnimi okluzivnimi dogodki. Bolnike je treba spremljati in jih zdraviti, kot je klinično ustrezno, vključno s prekinitvijo zdravljenja z zdravilom Iclusig. Pri bolnikih, pri katerih se razvije resno srčno popuščanje, je treba razmisлити o ukinitvi ponatiniba. **Pankreatitis in serumska lipaza** – Pogostna pojava pankreatitisa je večja prva 2 meseca uporabe. Prva 2 meseca vsaka 2 tedna preverjajte serumsko lipazo, nato pa periodično. Morda bo treba odmerek prekiniti ali zmanjšati. Če zvišanje ravni lipaz spremljajo abdominalni simptomi, je treba z uporabo zdravila Iclusig prenehati in preveriti, ali ima bolnik pankreatitis. Pri bolnikih s pankreatitisom ali zlomom alkohola v anamnezi se priporoča previdnost. Bolnike s hudo ali zelo hudo hipertrigliceridemijo je treba ustrezno obravnavati. **Laktatoza** – Zdravilo Iclusig vsebuje laktazo monohidrat. Bolniki z redkimi dednimi težavami neprežiranja galaktoze, laponsko obliko zmanjšane aktivnosti laktaze ali slabo absorpcijo glukoze-galaktoze ne smejo jemati tega zdravila. **Podaljšanje intervala QT** – Klinično pomembnih učinkov na interval QT ni mogoče izključiti. **Hepatotoksičnost** – Lahko se zvišajo ravni ALT, AST, bilirubina in alkalne fosfataze. Opazili so jetrno odpoved (vključno s smrtnim izidom). Teste delovanja jeter je treba opraviti pred uvedbo zdravljenja in nato periodično, kot je klinično indicirano. **Krvavitve** – Pojavili so se smrtni ter resni hemoragični dogodki. Pri resni ali hudi krvavitvi je treba zdravljenje z zdravilom Iclusig prekiniti. **Okvara jeter** – Pri bolnikih s hudo okvaro jeter se priporoča previdnost. **Okvara ledvic** – Pri bolnikih z ocenjenim očistkom kreatinina < 50 ml/min ali ledvično boleznijo v zadnjem stadiju se priporoča previdnost. **Starejši bolniki** – Verjetnost neželenih učinkov je večja. **Pediatrska populacija** – Varnost in učinkovitost zdravila Iclusig pri bolnikih starih do 18 let še nista bili dokazani. **Medsebojno delovanje z drugimi zdravili in druge oblike interakcij:** Sočasni uporabi zdravila Iclusig z močnimi induktorji CYP3A4 se je treba izoginiti; pri sočasni uporabi ponatiniba z zdravili proti stjevanju krvi pri bolnikih, pri katerih obstaja tveganje za krvavitve, je potrebna previdnost. **Plodnost, nosečnost in dojenje:** Zenskam v rodni dobi je treba svetovati, da naj v času zdravljenja z zdravilom Iclusig ne zanosijo, moškim pa, da naj v času zdravljenja ne zaplodijo otroka. Med zdravljenjem je treba uporabljati

alternativno ali dodatno metodo kontracepcije. Ni zadostnih podatkov o uporabi zdravila Iclusig pri nosečnicah. Studije na živalih so pokazale vpliv na sposobnost razmnoževanja. Če se zdravilo uporablja med nosečnostjo, je treba bolnico obvestiti o možnem tveganju za plod. Z dojenjem je treba med zdravljenjem z zdravilom Iclusig prenehati. **Vpliv na sposobnost vožnje in upravljanja s stroji:** Pri vožnji ali upravljanju strojev je potrebna previdnost. **Neželeni učinki:** Zelo pogosti ( $\geq 1/10$ ): okužba zgornjih dihal, nespečnost, anemija, zmanjšanje števila trombocitov, zmanjšanje števila nevtrofilcev, zmanjšani apetit, glavobol, omotica, hipertenzija, dispneja, kašelj, bolečine v trebuhu, driska, bruhanje, zaprtje, navzea, zvišanje ravni lipaz, zvišanje ravni alanin aminotransferaze, zvišanje ravni aspartat-aminotransferaze, izpuščaji, suha koža, bolečine v kosteh, artralgija, mialgija, bolečine v okončinah, bolečine v hrbtu, mišični krči, utrujenost, astenija, periferni edem, pireksija, bolečine. Pogosti ( $\geq 1/100$  do  $< 1/10$ ): pljučnica, sepsa, folikulitis, pancitopenija, febrilna nevtropenija, zmanjšanje števila levkocitov, dehidracija, zastajanje tekočine, hipokalcemija, hiperglikemija, hiperurikemija, hipofosfatemija, hipertrigliceridemija, hipokaliemija, zmanjšanje telesne mase, cerebrovaskularni dogodki, cerebralni infarkt, periferna nevtropatija, letargija, migrena, hiperestezija, hipoestezija, parestezija, prehodni ishemični napad, zamegljen vid, suhe oči, periorbitalni edem, edem veke, srčno popuščanje, miokardni infarkt, kongestivno srčno popuščanje, bolezen koronarnih arterij, angina pectoris, perikardni izliv, atrijska fibrilacija, zmanjšanje iztisnega deleža, periferna arterijska okluzivna bolezen, periferna ishemija, stenozna periferna arterija, intermitentna kladivacija, globoka venska tromboza, vročinski oblivi, zariplost, pljučna embolija, plevralni izliv, epistaksa, disfonija, pljučna hipertenzija, pankreatitis, zvišanje amilaz v krvi, gastrozofagealna refluksna bolezen, stomatitis, dispnejska, trebušna distenzija, nelagodje v trebuhu, suha usta, zvišanje ravni bilirubina v krvi, zvišanje ravni alkalne fosfataze v krvi, zvišanje ravni gama-glutamilttransferaze, pruritni izpuščaji, ekfoliativni izpuščaji, eritem, alopecija, pruritis, ekfoliacija kože, nočno potenje, hiperhidroza, petehija, ekhimoza, boleča koža, ekfoliativni dermatitis, mišično-skeletne bolečine, bolečine v vratu, mišično-skeletne bolečine v prsnem košu, erektilna disfunkcija, mrzlica, gripi podobna bolezen, nekardiogena bolečina v prsnem košu, tipljivi vozlički, obrabni edem. Občasni ( $\geq 1/1000$  do  $< 1/100$ ): sindrom tumorske lize, cerebralna arterijska stenozna, tromboza mrežnične vene, okluzija mrežnične vene, okluzija mrežnične arterije, okvara vida, miokardna ishemija, akutni koronarni sindrom, kardialno nelagodje, ishemična kardiomiopatija, spazem koronarnih arterij, disfunkcija levega prekata, atrijska undulacija, slaba periferna cirkulacija, vrančni infarkt, venska embolija, venska tromboza, hipertenzivna kriza, krvavitve v želodcu, hepatotoksičnost, odpoved jeter, zlatenica. **Režim izdaje zdravila:** Predpisovanje in izdaja zdravila je le na recept. **Imetnik dovoljenja za promet z zdravilom:** ARIAD Pharma Ltd., Riverbridge House, Guildford Road, Leatherhead, Surrey KT22 9AD, Velika Britanija. **Zadnja revizija besedila:** marec 2016. **Informacija pripravljena:** april 2016. Podrobnejše informacije o zdravilu Iclusig so na voljo pri predstavniku imetnika dovoljenja za promet z zdravilom: Angelini Pharma d.o.o., Koprška ulica 108A, 1000 Ljubljana, Tel.: +386 1 544 65 79, E-pošta: info@angelini.si



Predstavnik:  
Angelini Pharma d.o.o.  
Koprška ulica 108 A, Ljubljana

➤ PRVA REGISTRIRANA TERAPIJA  
V 2. LINIJI ZA ZDRAVLJENJE  
ADENOKARCINOMA ŽELODCA ALI  
GASTRO-EZOFAGEALNEGA PREHODA<sup>1</sup>

  
**CYRAMZA™**  
(ramucirumab)

**UKREPAJTE ZDAJ**



**USPOSOBLJENI  
ZA SPREMEMBE,  
ZA NEPRIMERLJIVE  
IZKUŠNJE**

**Skrajšan povzetek glavnih značilnosti zdravila**

▼ Za to zdravilo se izvaja dodatno spremljanje varnosti. Tako bodo hitreje na voljo nove informacije o njegovi varnosti. Zdravstvene delavce naprošamo, da poročajo o katerem koli domnevem neželenem učinku zdravila.

**Cyramza 10 mg/ml koncentrat za raztopino za infundiranje**

En mililiter koncentrata za raztopino za infundiranje vsebuje 10 mg ramucirumaba. Ena 10-mililitrska viala vsebuje 100 mg ramucirumaba. **Terapevtske indikacije** Zdravilo Cyramza je v kombinaciji s paklitakselom indicirano za zdravljenje odraslih bolnikov z napredovalim rakom želodca ali adenokarcinomom gastro-efozagealnega prehoda z napredovalo boleznijo po predhodni kemoterapiji, ki je vključevala platino in fluoropirimidin. Monoterapija z zdravilom Cyramza je indicirana za zdravljenje odraslih bolnikov z napredovalim rakom želodca ali adenokarcinomom gastro-efozagealnega prehoda z napredovalo boleznijo po predhodni kemoterapiji s platino ali fluoropirimidinom, za katere zdravljenje v kombinaciji s paklitakselom ni primerno. Zdravilo Cyramza je v kombinaciji s shemo FOLFIRI indicirano za zdravljenje odraslih bolnikov z metastatskim kolorektalnim rakom (mCRC), z napredovanjem bolezni ob ali po predhodnem zdravljenju z bevacizumabom, oksaliplatinom in fluoropirimidinom. Zdravilo Cyramza je v kombinaciji z docetakselom indicirano za zdravljenje odraslih bolnikov z lokalno napredovalim ali metastatskim nedrobnočelničnim pljučnim rakom, z napredovanjem bolezni po kemoterapiji na osnovi platine. **Odmerjanje in način uporabe** Zdravljenje z ramucirumabom morajo uvesti in nadzirati zdravniki z izkušnjami v onkologiji. **Odmerjanje Rak želodca in adenokarcinomom gastro-efozagealnega prehoda** Priporočeni odmerek ramucirumaba je 8 mg/kg 1. in 15. dan 28-dnevnega cikla, pred infuzijo paklitaksela. Priporočeni odmerek paklitaksela je 80 mg/m<sup>2</sup> in se daje z intravenskim infundiranjem, ki traja približno 60 minut, 1., 8. in 15. dan 28-dnevnega cikla. Pred vsakim infundiranjem paklitaksela je treba pri bolnikih pregledati celotno krvno sliko in izvide kemičnih preiskav krvi, da se oceni delovanje jeter. Priporočeni odmerek ramucirumaba kot monoterapije je 8 mg/kg vsaka 2 tedna. **Kolorektalni rak** Priporočeni odmerek ramucirumaba je 8 mg/kg vsaka 2 tedna, dan z intravensko infuzijo pred dajanjem sheme FOLFIRI. Pred kemoterapijo je treba bolnikom odvzeti kri za popolno krvno sliko. **Nedrobnočelični pljučni rak (NSCLC)** Priporočeni odmerek ramucirumaba je 10 mg/kg na 1. dan 21-dnevnega cikla, pred infuzijo docetakselo. Priporočeni odmerek docetakselo je 75 mg/m<sup>2</sup>, dan z intravensko infuzijo v približno 60 minutah na 1. dan 21-dnevnega cikla. **Premedikacija** Pred infundiranjem ramucirumaba je priporočljiva premedikacija z antagonistom histaminskih receptorjev H1. **Način uporabe** Po redčenju se zdravilo Cyramza daje kot intravenska infuzija v približno 60 minutah. Zdravila ne dajajte v obliki intravenskega bolusa ali hitre intravenske injekcije. Da boste dosegli zahtevano trajanje infundiranja približno 60 minut, največja hitrost infundiranja ne sme preseči 25 mg/minuto, saj morate sicer podaljšati trajanje infundiranja. Bolnika je med infundiranjem treba spremljati glede znakov reakcij, povezanih z infuzijo, zagotoviti pa je treba tudi razpoložljivost ustrezne opreme za oživiljanje. **Kontraindikacije** Pri bolnikih z NSCLC je ramucirumab kontraindiciran, kjer gre za kavitacijo tumorja ali prepletenost tumorja z glavnimi žilami. **Posebna opozorila in previdnostni ukrepi** Trajno prekinite zdravljenje z ramucirumabom pri bolnikih, pri katerih se pojavijo resni arterijski tromboembolični dogodki, gastrointestinalne perforacije, krvavitve stopnje 3 ali 4, če zdravstveno pomembne hipertenzije ni mogoče nadzirati z antihipertenzivnim zdravljenjem ali če se pojavi fistula, raven beljakovin v urinu > 3 g/24 ur ali v primeru nefrotskega sindroma. Pri bolnikih z neuravnavano hipertenzijo zdravljenja z ramucirumabom ne smete uvesti, dokler oziroma v kolikor obstoječa hipertenzija ni uravnavana. Pri bolnikih s ploščatocelično histologijo obstaja večje tveganje za razvoj resnih pljučnih krvavitve. Če se pri bolniku med zdravljenjem razvijejo zapleti v zvezi s celjenjem rane, prekinite zdravljenje z ramucirumabom, dokler rana ni povsem zaceljena. V primeru pojava stomatitisa je treba takoj uvesti simptomatsko zdravljenje. Pri bolnikih, ki so prejeli ramucirumab in docetaksel za zdravljenje napredovalnega NSCLC z napredovanjem bolezni po kemoterapiji na osnovi platine, so opazili trend manjše učinkovitosti z naraščajočo starostjo. **Plodnost, nosečnost in dojenje** Ženskam v rodni dobi je treba svetovati, naj se izognejo zanositvi med zdravljenjem z zdravilom Cyramza in jih je treba seznaniti z možnim tveganjem za nosečnost in plod. Ni znano, ali se ramucirumab izloča v materino mleko. **Neželeni učinki** **Želo pogosti (≥ 1/10)** nevtropenija, levkopenija, trombocitopenija, hipoalbuminemija, hipertenzija, epistaksa, gastrointestinalne krvavitve, stomatitis, driska, proteinurija, utrujenost/astenija, periferni edem, bolečina v trebuhu. **Pogosti (≥ 1/100 do < 1/10)** hipokaliemija, hiponatriemija, glavobol. **Rok uporabnosti** 3 leta **Posebna navodila za shranjevanje** Shranjujte v hladilniku (2 °C–8 °C). Ne zamrzujte. Vialo shranjujte v zunanji ovojnini, da zagotovite zaščito pred svetlobo. **Pakiranje** 2 viali z 10 ml **IMETNIK DOVOLJENJA ZA PROMET Z ZDRAVILOM** Eli Lilly Nederland B.V., Papendorpseweg 83, 3528 BJ Utrecht, Nizozemska **DATUM ZADNJE REVIZIJE BESEDILA** 25.01.2016

Režim izdaje: Predpisovanje in izdaja zdravila je le na recept, zdravilo pa se uporablja samo v bolnišnicah.

**Pomembno obvestilo:**

Pričujoče gradivo je namenjeno **samo za strokovno javnost**. Zdravilo Cyramza se izdaja le na recept. Pred predpisovanjem zdravila Cyramza vas vljudno prosimo, da preberete celotni Povzetek glavnih značilnosti zdravila Cyramza. Podrobnejše informacije o zdravilu Cyramza in o zadnji reviziji besedila Povzetka glavnih značilnosti zdravila so na voljo na sedežu podjetja Eli Lilly (naslov podjetja in kontaktni podatki spodaj) in na spletni strani European Medicines Agency (EMA): [www.ema.europa.eu](http://www.ema.europa.eu). in na spletni strani European Commission <http://ec.europa.eu/health/documents/community-register/html/alfregister.htm>.

**Eli Lilly farmacevtska družba, d.o.o.**, Dunajska cesta 167, 1000 Ljubljana, telefon: (01) 5800 010, faks: (01) 5691 705

**Referenca:** 1. Cyramza, Povzetek glavnih značilnosti zdravila, zadnja odobrena verzija.

EERAM00010a, 12.02.2016.



Zdravilo za predhodno že zdravljene bolnike z mKRR

# Več časa za trenutke, ki štejejo

**Lonsurf**  
trifluridin/tipiracil

## Spremeni zgodbo predhodno že zdravljenih bolnikov z mKRR

LONSURF® (trifluridin/tipiracil) je indiciran za zdravljenje odraslih bolnikov z metastatskim kolorektalnim rakom (mKRR), ki so bili predhodno že zdravljeni ali niso primerni za zdravljenja, ki so na voljo. Ta vključuje kemoterapijo na osnovi fluoropirimidina, oksaliplatina in irinotekana, zdravljenje z zaviralci žilnega endotelijskega rastnega dejavnika (VEGF) in zaviralci receptorjev za epidermalni rastni dejavnik (EGFR).

mKRR = metastatski kolorektalni rak

Družba Servier ima licenco družbe Taiho za zdravilo Lonsurf®. Pri globalnem razvoju zdravila sodelujeta obe družbi in ga tržita v svojih določenih področjih.



TAIHO PHARMACEUTICAL CO., LTD.



### Skrajšan povzetek glavnih značilnosti zdravila: Lonsurf 15 mg/6,14 mg filmsko obložene tablete in Lonsurf 20 mg/8,19 mg filmsko obložene tablete

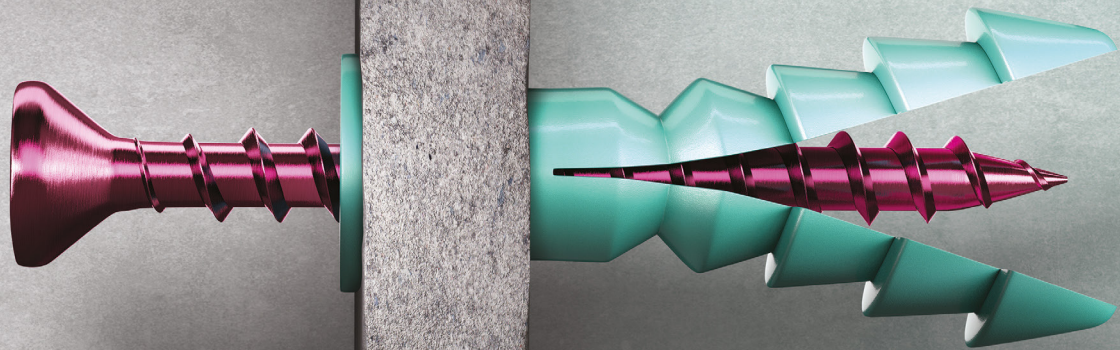
▼ Za to zdravilo se izvaja dodatno spremljanje varnosti. **SESTAVA**: Lonsurf 15 mg/6,14 mg: Ena filmsko obložena tableta vsebuje 15 mg trifluridina in 6,14 mg tipiracila (v obliki klorida). Lonsurf 20 mg/8,19 mg: Ena filmsko obložena tableta vsebuje 20 mg trifluridina in 8,19 mg tipiracila (v obliki klorida). **TERAPEVTSKE INDIKACIJE**: Zdravilo Lonsurf je indicirano za zdravljenje odraslih bolnikov z metastatskim kolorektalnim rakom, ki so bili predhodno že zdravljeni ali niso primerni za zdravljenja, ki so na voljo. Ta vključuje kemoterapijo na osnovi fluoropirimidina, oksaliplatina in irinotekana, zdravljenje z zaviralci žilnega endotelijskega rastnega dejavnika (VEGF - Vascular Endothelial Growth Factor) in zaviralci receptorjev za epidermalni rastni dejavnik (EGFR - Epidermal Growth Factor Receptor). **ODMERJANJE IN NAČIN UPORABE**: Odmerjanje: Priporočeni začetni odmerek zdravila Lonsurf pri odraslih je 35 mg/m<sup>2</sup>/odmerek peroralno dvakrat dnevno na 1. do 5. dan in 8. do 12. dan vsakega 28-dnevnega cikla zdravljenja, najpozneje 1 uro po zaključku jutranjega in večernega obroka. Odmerjanje, izračunano glede na telesno površino, ne sme preseči 80 mg/odmerek. Možne prilagoditve odmerka glede na varnost in prenašanje zdravila: dovoljena so največ 3 zmanjšanja odmerka na najmanjši odmerek 20 mg/m<sup>2</sup> dvakrat dnevno. Potem ko je bil odmerek zmanjšan, povečanje ni dovoljeno. **KONTRAINDIKACIJE**: Preobčutljivost na zdravilni učinkovini ali katero koli pomožno snov. **OPOMORILO IN PREVIDNOSTNI UKREPI**: Supresija kostnega mozga: Pred uvedbo zdravljenja, pred vsakim ciklom zdravljenja in po potrebi je treba pregledati celotno krvno sliko. Zdravljenja ne smete začeti, če je absolutno število nevtrofilcev < 1,5 x 10<sup>9</sup>/l, če je število trombocitov < 75 x 10<sup>9</sup>/l ali če se je pri bolniku zaradi predhodnih zdravljenj pojavila klinično pomembna nehematološka toksičnost 3. ali 4. stopnje, ki še traja. Bolnike je treba skrbno spremljati zaradi morebitnih okužb, uvesti je treba ustrezne ukrepe, kot je klinično indicirano. Toksičnost za prebavila: Potrebna je uporaba antiemetikov, antiidiaroidov ter drugih ukrepov, kot je klinično indicirano. Če je potrebno, prilagodite odmerke. Ledvična okvara: Zdravilo Lonsurf ni primerno za uporabo pri bolnikih s hudo ledvično okvaro ali končno stopnjo ledvične okvare. Bolnike z zmerno ledvično okvaro je treba zaradi hematološke toksičnosti bolj pogosto spremljati. Jetrna okvara: Uporaba zdravila Lonsurf pri bolnikih z obstoječo zmerno ali hudo jetrno okvaro ni priporočljiva. Proteinurija: Pred začetkom zdravljenja in med njim je priporočljivo spremljanje proteinurije z urinskimi testnimi lističi. Pomožne snovi: Vsebujejo laktozo. **INTERAKCIJE**: Zdravila, ki medsebojno delujejo z nukleozidnimi prenašalci CNT1, ENT1 in ENT2, zaviralci OCT2 ali MATE1, substrati humane timidin-kinaze (npr. zidovudinom), hormonskimi kontraceptivi. **PLODNOST, NOSEČNOST IN DOJENJE**: Ni priporočljivo. **KONTRACELIJA**: Zenske in moški morajo uporabljati učinkovito metodo kontracepcije med zdravljenjem in do 6 mesecev po zaključku zdravljenja. **VPLIV NA SPOSOBNOST VOZNIJE IN UPRAVLJANJA S STROJI**: Med zdravljenjem se lahko pojavijo utrujenost, omotica ali splošno slabo počutje. **NEŽELENI UČINKI**: Zelo pogosti: nevropenija, levkopenija, anemija, trombocitopenija, zmanjšan apetit, diareja, navzea, bruhanje, utrujenost. **Pogosti**: okužba spodnjih dihal, okužba zgornjih dihal, febrilna nevropenija, limfopenija, monocitoza, hipobalbuminemija, nespečnost, disgevgija, periferna nevropatija, omotica, glavobol, vročinski oblivi, dispneja, kašelj, bolečina v trebuhu, zaprtje, stomatitis, boleznine ustne votline, hiperbilirubinemija, sindrom palmarne plantarne eritrodizestezijske, izpuščaji, alopecija, pruritus, suha koža, proteinurija, piroksija, edem, vnetje sluznice, splošno slabo počutje, zvišanje jetrnih encimov, zvišanje alkalne fosfataze v krvi, zmanjšanje telesne mase. **Občasni**: septični šok, infekcijski enteritis, pljučnica, okužba žolčevoda, gripa, okužba sečil, vnetje dlesni, herpes zoster, tinea pedis, kandidiaza, bakterijska okužba, okužba, bolečina zaradi raka, pancitopenija, granulocitopenija, monocitopenija, eritropenija, levkocitoza, dehidracija, hiperglikemija, hiperkalemija, hipokalemija, hipofosfatemija, hipernatriemija, hiponatriemija, hipokalcemija, protin, anksioznost, nevrotoksičnost, disestezijska, hiperestezijska, hipostezijska, sinkopa, parestezijska, pekoč občutek, letargija, zmanjšana ostrina vida, zamegljen vid, diplopija, katarakta, konjunktivitis, suho oko, vrtoglavica, neugodje v ušesu, angina pectoris, aritmija, palpitacije, embolija, hipertenzija, hipotenzija, pljučna embolija, plevralni izliv, izcedek iz nosu, disfonija, orofaringealna bolečina, epistaksa, hemoragični enterokolitis, krvavitve v prebavilih, akutni pankreatitis, ascites, ileus, subileus, kolitis, gastritis, refluksni gastritis, ezofagitis, moleno praznjenje želodca, abdominalna distenzija, analno vnetje, razjede v ustih, dispepsija, gastroezofagealna refluksna bolezen, proktalgija, bukalni polip, krvavitve dlesni, glositis, parodontalna bolezen, bolezen zob, siljenje na bruhanje, flatulenca, slab zadah, hepatotoksičnost, razširitev žolčnih vodov, luščenje kože, urtikarija, preobčutljivostne reakcije na svetlobo, eritem, akne, hiperhidroza, žulji, boleznine nohtov, otekanje sklepov, artralgija, bolečina v kosteh, migalga, mišično-skeletna bolečina, mišična oslabelost, mišični krči, bolečina v okončinah, občutek teže, ledvična odpoved, neinfektivni cistitis, motnje mikcije, hematurija, levkociturija, motnje menstruacije, poslabšanje splošnega zdravstvenega stanja, bolečina, občutek spremembe telesne temperature, keseroza, zvišanje kreatinina v krvi, podaljšanje intervala QT na elektrokardiogramu, povečanje mednarodnega umernega zmerja (INR), podaljšanje aktiviranega parcialnega tromboloplastinskega časa (aPTC), zvišanje sečnine v krvi, zvišanje laktatne dehidrogenaze v krvi, znižanje celokupnih proteinov, zvišanje C-reaktivnega proteina, zmanjšanje hematokrit. **Post-marketingne izkušnje**: pri bolnikih, zdravljenih z zdravilom Lonsurf na Japonskem, so poročali o primerih intersticijske bolezni pljuč. **PREVELIKO ODMERJANJE**: Neželeni učinki, o katerih so poročali v povezavi s prevelikim odmerjanjem, so bili v skladu z uveljavljenim varnostnim profilom. Glavni pričakovani zaplet prevelikega odmerjanja je supresija kostnega mozga. **FARMAKODINAMIČNE LASTNOSTI**: Farmakoterapevtska skupina: zdravila z delovanjem na novotvorbe, antimetaboliti, oznaka ATC: L01BC59. Zdravilo Lonsurf sestavlja antineoplastični timidinski nukleozidni analog, trifluridin, in zaviralec timidin-fostforilaze (TPaze), tipiraciljev klorid. Po prizvemu v rakave celice timidin-kinaza fostforilira trifluridin. Ta se v celicah nato presnovi v substrat deoksiribonukleinske kisline (DNA), ki se vgradi neposredno v DNA ter tako preprečuje celično proliferacijo. TPaza hitro razgradi trifluridin in njegova presnova po peroralni uporabi je hitra zaradi učinka prvega prehoda, zato je v zdravilo vključen zaviralec TPaze, tipiraciljev klorid. **PAKIRANJE**: 20 filmsko obloženih tablet. **NAČIN PREDPISOVANJA IN IZDAJANJA ZDRAVILA**: Rp/Spec. **Imetnik dovoljenja za promet z zdravilom**: Les Laboratoires Servier, 50, rue Carnot, 92284 Suresnes cedex, Francija. **Številka dovoljenja za promet z zdravilom**: EU/1/16/1096/001 (Lonsurf 15 mg/6,14 mg), EU/1/16/1096/004 (Lonsurf 20 mg/8,19 mg). \* Pred predpisovanjem preberite celoten povzetek glavnih značilnosti zdravila. Datum zadnje revizije besedila: marec 2017. **Celoten povzetek glavnih značilnosti zdravila in podrobnejše informacije so na voljo pri: Servier Pharma d.o.o., tel: 01 563 48 11, www.servier.si.**

Datum priprave informacije: april 2017.  
LNF16/17C2AD2 Samo za strokovno javnost.



# SKUPAJ

# MOČNEJŠA



Kombinacija zdravil  
Cotellic<sup>®</sup> ▼ in Zelboraf<sup>®</sup>  
za zdravljenje odraslih bolnikov  
z neoperabilnim ali metastatskim  
melanomom, ki ima mutacijo  
BRAF V600.<sup>1,2</sup>

1 Povzetek glavnih značilnosti zdravila Cotellic. Dostopano julij 2017 na: [http://www.ema.europa.eu/docs/sl\\_SI/document\\_library/EPAR\\_-\\_Product\\_Information/human/003960/WC500198563.pdf](http://www.ema.europa.eu/docs/sl_SI/document_library/EPAR_-_Product_Information/human/003960/WC500198563.pdf)  
2 Povzetek glavnih značilnosti zdravila Zelboraf. Dostopano julij 2017 na: [http://www.ema.europa.eu/docs/sl\\_SI/document\\_library/EPAR\\_-\\_Product\\_Information/human/002409/WC500124317.pdf](http://www.ema.europa.eu/docs/sl_SI/document_library/EPAR_-_Product_Information/human/002409/WC500124317.pdf)



**THE MOST ADVANCED  
ELECTROPORATION TECHNOLOGY**  
for treatment of tumour nodules located to the  
skin, subcutaneous tissue, parenchyma and bone.

# Zdravljenje trombemboličnih bolezni, na katerega se lahko zanesete<sup>1</sup>

**FRAXIPARINE<sup>®</sup> FORTE**  
kalcijev nadroparinat

**Fraxiparine<sup>®</sup>**  
kalcijev nadroparinat

**aspEN**  
EUROPE

1. Povzetek glavnih značilnosti zdravila Fraxiparine in Fraxiparine Forte

## Skrajšan povzetek glavnih značilnosti zdravila

**FRAXIPARINE<sup>®</sup> 2850 i.e. anti-Xa/0,3 ml raztopina za injiciranje, FRAXIPARINE<sup>®</sup> 3800 i.e. anti-Xa/0,4 ml raztopina za injiciranje, FRAXIPARINE<sup>®</sup> 5700 i.e. anti-Xa/0,6 ml raztopina za injiciranje, FRAXIPARINE<sup>®</sup> 7600 i.e. anti-Xa/0,8 ml raztopina za injiciranje, FRAXIPARINE<sup>®</sup> 9500 i.e. anti-Xa/1,0 ml raztopina za injiciranje**

**Sestava:** Zdravilna učinkovina je kalcijev nadroparinat. Ena mililitr raztopine za injiciranje ustreza 9500 i.e. anti-Xa. FRAXIPARINE<sup>®</sup> 2850 i.e. anti-Xa/0,3 ml raztopina za injiciranje: Ena napolnjena injekcijska brizga vsebuje 0,3 ml raztopine za injiciranje, kar ustreza 2850 i.e. anti-Xa. FRAXIPARINE<sup>®</sup> 3800 i.e. anti-Xa/0,4 ml raztopina za injiciranje: Ena napolnjena injekcijska brizga vsebuje 0,4 ml raztopine za injiciranje, kar ustreza 3800 i.e. anti-Xa. FRAXIPARINE<sup>®</sup> 5700 i.e. anti-Xa/0,6 ml raztopina za injiciranje: Ena umerjena napolnjena injekcijska brizga vsebuje 0,6 ml raztopine za injiciranje, kar ustreza 5700 i.e. anti-Xa. FRAXIPARINE<sup>®</sup> 7600 i.e. anti-Xa/0,8 ml raztopina za injiciranje: Ena umerjena napolnjena injekcijska brizga vsebuje 0,8 ml raztopine za injiciranje, kar ustreza 7600 i.e. anti-Xa. FRAXIPARINE<sup>®</sup> 9500 i.e. anti-Xa/1,0 ml raztopina za injiciranje: Ena umerjena napolnjena injekcijska brizga vsebuje 1,0 ml raztopine za injiciranje, kar ustreza 9500 i.e. anti-Xa. **Terapevtske indikacije:** Preprečevanje trombemboličnih zapletov v splošni ali ortopedski kirurgiji, pri interstističnih bolnikih z velikim tveganjem (respiratorna insuficienca in/ali okužba dihal in/ali srčno popuščanje), ki so hospitalizirani in se zdravijo v enoti intenzivne medicine, zdravljenje trombemboličnih bolezni, preprečevanje nastanka krvnih strdkov med hemodializo, zdravljenje nestabilne angine pectoris in miokardnega infarkta brez zoba Q. **Odmerjanje in način uporabe:** Med zdravljenjem se kalcijev nadroparinat in drugih nizkomolekularnih heparinov ne sme zamenjavati. Z umernimi napolnjenimi injekcijskimi brizgami je možno odmerek prilagoditi bolnikovi telesni masi. Zdravilo ni namenjeno za intramuskularno uporabo. Zdravilo se daje subkutano, običajno pod kožo na področju desne ali leve strani trebušne stene, lahko pa tudi na področju stegna. **Odrasli: Preprečevanje trombemboličnih bolezni:** Priporočeni odmerek zdravila FRAXIPARINE<sup>®</sup> je 0,3 ml (2850 i.e. anti-Xa) na dan operacije 2 do 4 ure pred posegom, v dneh po operaciji pa enkrat na dan. Profilaktično zdravljenje mora trajati najmanj sedem dni in celotno obdobje tveganja, dokler se bolnik ne začne gibati. **Ortopedska kirurgija:** Bolnik zdravilo FRAXIPARINE<sup>®</sup> prejema subkutano. Odmerek je treba prilagoditi bolnikovi telesni masi (glejte celoten SmPC). Ciljni odmerek je 38 i.e. anti-Xa na kilogram telesne mase. Četiri dni po operaciji se odmerek poveča za 50 %. Prvi odmerek bolnik prejme 12 ur pred operacijo, drugi odmerek pa 12 ur po koncu operacije. Profilaktično zdravljenje se nato nadaljuje enkrat na dan, najmanj 10 dni, in traja celotno obdobje tveganja. **Interstistični bolniki z velikim tveganjem, ki se zdravijo v enoti intenzivne medicine:** Zdravilo se daje subkutano enkrat na dan, odmerek je treba prilagoditi bolnikovi telesni masi (glejte celoten SmPC). Ciljni odmerek je 86 i.e. anti-Xa na kilogram telesne mase. **Preprečevanje nastanka krvnih strdkov med hemodializo:** Odmerek je treba prilagoditi vsakemu posameznemu bolniku. Upoštevati je treba tudi tehnične pogoje dialize. Zdravilo se običajno daje v obliki enkratnega odmerka v arterijsko linijo na začetku vsake dialize. Priporočeni začetni odmerki so prilagojeni telesni masi, pri bolnikih brez povečanega tveganja za krvavitve. Bolniki s telesno maso < 50 kg prejmejo FRAXIPARINE<sup>®</sup> 0,3 ml (2850 anti-Xa i.e.), bolniki s telesno maso med 50 do 69 kg prejmejo FRAXIPARINE<sup>®</sup> 0,4 ml (3800 anti-Xa i.e.), bolniki s telesno maso > 70 kg prejmejo FRAXIPARINE<sup>®</sup> 0,6 ml (5700 anti-Xa i.e.). Običajno zadostuje za štiriurno dializo. Pri dializi, ki traja dlje kot 4 ure, lahko bolnik med dializo prejme še dodaten manjši odmerek. Pri naslednjih dializah je odmerek treba prilagoditi glede na opažen učinek. Bolniki s povečanim tveganjem za krvavitve s povečanim tveganjem za krvavitve smejo prejeti le polovični odmerek. Glejte celoten SmPC. **Zdravljenje nestabilne angine pectoris in miokardnega infarkta brez zoba Q:** Priporočeno odmerjanje je dvakrat na dan (vsakih 12 ur). Zdravljenje običajno traja šest dni. Bolnik začetni odmerek prejme v obliki bolusa intravensko, poznejše odmerke pa subkutano. Odmerek je treba prilagoditi bolnikovi telesni masi (glejte celoten SmPC). Ciljni odmerek je 86 i.e. anti-Xa na kilogram telesne mase. **Otroci in mladostniki:** Zaradi nezadostnih podatkov odmerjanje pri bolnikih, mlajših od 18 let, ni bilo določeno in uporabe tega zdravila ne priporočamo. **Starostniki:** Pri starostnikih z normalnim delovanjem ledvic odmerkov ni treba prilagajati. **Okvara ledvic: Preprečevanje trombemboličnih bolezni:** Pri bolnikih z blago okvaro ledvic pri profilaktičnem zdravljenju odmerkov ni treba prilagajati. Pri bolnikih z zmerno okvaro ledvic mora zdravnik na osnovi individualnih dejavnikov tveganja za pojav krvavitve in trombembolije presoditi o ustreznosti zmanjšanja odmerka in odmerek zmanjšati za 25 do 33 %. **Zdravljenje trombemboličnih bolezni, nestabilne angine pectoris in miokardnega infarkta brez zoba Q:** Pri bolnikih z blago okvaro ledvic ni treba prilagajati. Pri bolnikih z zmerno okvaro ledvic mora zdravnik na osnovi individualnih dejavnikov tveganja za pojav krvavitve in trombembolije presoditi o ustreznosti zmanjšanja odmerka in odmerek zmanjšati za 25 do 33 %. Pri bolnikih s hudo okvaro ledvic je uporaba zdravila kontraindicirana. **Okvara jeter:** Pri bolnikih z okvaro jeter študije niso bile izvedene. **Kontraindikacije:** preobčutljivost za kalcijev nadroparinat ali katerokoli pomožni snov zdravila; anamneza s kalcijevim nadroparinatom povzročene trombotične pojave; aktivne krvavitve ali povečano tveganje za krvavitve zaradi motenj hemostaze, razen v primeru diseminirane intravaskularne koagulacije, ki ni povzročena s heparinom; organske lezije, ki rade krvavijo (npr. aktivni peptični ulkusi), hemoragični cerebrovaskularni dogodki, akutni infekcijski endokarditis; huda okvara ledvic, in sicer pri zdravljenju trombemboličnih bolezni, nestabilne angine pectoris in miokardnega infarkta brez zoba Q. Pri bolnikih, ki nizkomolekularni heparin dobivajo terapevtsko, je pri elektivnih kirurških posegih kontraindicirana lokalna in/ali regionalna anestezija. **Posebna opozorila in previdnostni ukrepi: S heparinom povzročena trombotična:** Zaradi možnosti pojasa s heparinom povzročene trombotične pojave je treba število trombocitov nadzirati vs čas zdravljenja z zdravilom FRAXIPARINE<sup>®</sup>. **Povečano tveganje za krvavitve je pri:** opovedi jeter; hudi arterijski hipertenziji; anamnezi peptičnega ulkusa ali drugih organskih lezij, ki rade krvavijo; okvarah žilja, žilnice in mrežnice; obdobju po operaciji na možganih, hrbtnjači ali obeh. **Okvara ledvic:** Tveganje za pojav krvavitve obstaja, zato je potrebna previdnost. **Starostniki:** Pred začetkom zdravljenja priporočamo oceno ledvičnega delovanja. **Hiperkaliemija:** Povečano tveganje pri bolnikih, ki že imajo povečane plazemske vrednosti kalija, ali bolnikih, pri katerih obstaja tveganje za povečanje plazemskih vrednosti kalija, ali bolnikih, ki jemljejo zdravila, ki lahko povzročijo hiperkaliemijo. Tveganje za hiperkaliemijo se s trajanjem zdravljenja povečuje, vendar pa je običajno reverzibilno. **Spinalna/epiduralna anestezija, spinalna/lumbalna punkcija in sočasna uporaba zdravil:** Uporaba nizkomolekularnih heparinov je pri bolnikih, ki so prejeli spinalno ali epiduralno anestezijo, redko povezana s hematomi, ki lahko povzročijo podaljšano ali trajno paralizno. Tveganje za spinalno/epiduralne hematome je večje pri bolnikih, ki imajo vstavljen epiduralni kateter oziroma sočasno dobivajo tudi druga zdravila, ki lahko vplivajo na hemostazo. Tveganje je večje tudi pri travmatski ali ponavljajoči se epiduralni ali spinalni punkciji. **Salicilati, nesteroidna protivnetna zdravila in zaviralci agregacije trombocitov:** Sočasna uporaba ni priporočljiva. **Nekroza kože:** Pred nekrozo kože se pojavi purpura ali infiltrirane ali boleče eritematozne eflorescence s splošnimi znaki ali brez njih. V takih primerih je treba zdravljenje nemudoma prekiniti. **Alergija na lateks:** Ščitnik injekcijske igle v napolnjeni injekcijski brizgi lahko vsebuje suho naravno lateksno gumo, ki lahko pri na lateks preobčutljivih posameznikih povzroči alergijske reakcije. **Medsedebno delovanje z drugimi zdravili in druge oblike interakcij:** Zdravilo je treba dajati previdno bolnikom, ki se zdravijo s peroralnimi antikoagulanti, sistemskimi (gluko-) kortikosteroidi in dekstrani. Pri bolnikih, ki prejemanjo to zdravilo in se jim uvede peroralno antikoagulačno zdravljenje, je treba zdravilo nadaljevati s tem zdravilom nadaljevati, dokler se INR ne ustavi v ciljnem območju. Sočasna uporaba acetilsalicilne kisline (ali drugih salicilatov), nesteroidnih protivnetnih zdravil in zaviralcev agregacije trombocitov ni priporočena, saj lahko povečajo tveganje za krvavitve. **Nosečnost in dojenje:** Uporabe med nosečnostjo in dojenjem ne priporočamo. Če koristi zdravila ne prevažajo nad možgimi tveganji. **Neželeni učinki: Zelo pogosti:** krvavitve na različnih mestih (vključno s primeri spinalnih hematovov), ki so pogostejše pri bolnikih z drugimi dejavniki tveganja, majhni hematomi na mestu injiciranja. **Pogosti:** povečanje vrednosti transaminaz, običajno prehodno, reakcija na mestu injiciranja. **Redki:** trombotična (vključno s heparinom povzročeno trombotično), ki je večših trombotična, trombotična, izpuščaj, urtikarija, eritem, pruritus, kalcinosis na mestu injiciranja. **Zelo redki:** ezoinfilija, reverzibilna po prekinitvi zdravljenja, preobčutljivostne reakcije (vključno z angioedemom in kožnimi reakcijami), anafilaktoidna reakcija, reverzibilna hiperkaliemija zaradi s heparinom povzročene zaviranja izločanja aldosterona, še posebej pri bolnikih s tveganjem, priazipem, nekroza kože, običajno na mestu injiciranja. **Način in režim izdaje:** H/Rp - Predpisovanje in izdaja zdravila je le na recept, zdravilo pa se uporablja samo v bolnišnicah. Izjemoma se lahko uporablja pri nadaljevanju zdravljenja na domu ob odpuštu iz bolnišnice in nadaljnjem zdravljenju. **Imetnik dovoljenja za promet:** Aspen Pharma Trading Limited, 3016 Lake Drive, Citywest Business Campus, Dublin 24, Irsko. **Datum zadnje revizije besedila:** 11.09.2015. **Številka dovoljenja za promet z zdravilom:** H/99/00658/001-005.

## Skrajšan povzetek glavnih značilnosti zdravila

**FRAXIPARINE<sup>®</sup> FORTE 11400 i.e. anti-Xa/0,6 ml raztopina za injiciranje, FRAXIPARINE<sup>®</sup> FORTE 15200 i.e. anti-Xa/0,8 ml raztopina za injiciranje, FRAXIPARINE<sup>®</sup> FORTE 19000 i.e. anti-Xa/1,0 ml raztopina za injiciranje**

**Sestava:** Zdravilna učinkovina je kalcijev nadroparinat. Ena mililitr raztopine za injiciranje ustreza 19.000 i.e. anti-Xa. FRAXIPARINE<sup>®</sup> FORTE 11400 i.e. anti-Xa/0,6 ml raztopina za injiciranje: Ena umerjena napolnjena injekcijska brizga vsebuje 0,6 ml raztopine za injiciranje, kar ustreza 11.400 i.e. anti-Xa. FRAXIPARINE<sup>®</sup> FORTE 15200 i.e. anti-Xa/0,8 ml raztopina za injiciranje: Ena umerjena napolnjena injekcijska brizga vsebuje 0,8 ml raztopine za injiciranje, kar ustreza 15.200 i.e. anti-Xa. FRAXIPARINE<sup>®</sup> FORTE 19000 i.e. anti-Xa/1,0 ml raztopina za injiciranje: Ena umerjena napolnjena injekcijska brizga vsebuje 1,0 ml raztopine za injiciranje, kar ustreza 19.000 i.e. anti-Xa. **Terapevtske indikacije:** Zdravljenje trombemboličnih bolezni. **Odmerjanje in način uporabe:** Med zdravljenjem se kalcijev nadroparinat in drugih nizkomolekularnih heparinov ne sme zamenjavati. Z umernimi napolnjenimi injekcijskimi brizgami je možno odmerek prilagoditi bolnikovi telesni masi. Zdravilo ni namenjeno za intramuskularno uporabo. Zdravilo se daje subkutano, običajno pod kožo na področju desne ali leve strani trebušne stene, lahko pa tudi na področju stegna. **Odrasli: Zdravljenje trombemboličnih bolezni:** Priporočamo, da se zdravilo daje enkrat na dan. Zdravljenje običajno traja deset dni. Odmerek je treba prilagoditi bolnikovi telesni masi (glejte celoten SmPC). **Otroci in mladostniki:** Zaradi nezadostnih podatkov o varnosti in učinkovitosti odmerjanje pri bolnikih, mlajših od 18 let, ni bilo določeno in uporabe tega zdravila ne priporočamo. **Starostniki:** Pri starostnikih z normalnim delovanjem ledvic odmerkov ni treba prilagajati. **Okvara ledvic:** Pri bolnikih z blago okvaro ledvic pri profilaktičnem zdravljenju odmerkov ni treba prilagajati. Pri bolnikih z zmerno okvaro ledvic mora zdravnik na osnovi individualnih dejavnikov tveganja za pojav krvavitve in trombembolije presoditi o ustreznosti zmanjšanja odmerka in odmerek zmanjšati za 25 do 33 %. Pri bolnikih s hudo okvaro ledvic je uporaba zdravila kontraindicirana. **Okvara jeter:** Pri bolnikih z okvaro jeter študije niso bile izvedene. **Kontraindikacije:** preobčutljivost za kalcijev nadroparinat ali katerokoli pomožni snov zdravila; anamneza s kalcijevim nadroparinatom povzročene trombotične pojave; aktivne krvavitve ali povečano tveganje za krvavitve zaradi motenj hemostaze, razen v primeru diseminirane intravaskularne koagulacije, ki ni povzročena s heparinom; organske lezije, ki rade krvavijo (npr. aktivni peptični ulkusi); hemoragični cerebrovaskularni dogodki; akutni infekcijski endokarditis; huda okvara ledvic, in sicer pri zdravljenju trombemboličnih bolezni, nestabilne angine pectoris in miokardnega infarkta brez zoba Q. Pri bolnikih, ki nizkomolekularni heparin dobivajo terapevtsko, je pri elektivnih kirurških posegih kontraindicirana lokalna in/ali regionalna anestezija. **Posebna opozorila in previdnostni ukrepi: S heparinom povzročena trombotična:** Zaradi možnosti pojasa s heparinom povzročene trombotične pojave je treba število trombocitov nadzirati vs čas zdravljenja z zdravilom FRAXIPARINE<sup>®</sup> FORTE. **Povečano tveganje za krvavitve je pri:** opovedi jeter; hudi arterijski hipertenziji; anamnezi peptičnega ulkusa ali drugih organskih lezij, ki rade krvavijo; okvarah žilja, žilnice in mrežnice; obdobju po operaciji na možganih, hrbtnjači ali obeh. **Okvara ledvic:** Tveganje za pojav krvavitve, zato je potrebna previdnost. **Starostniki:** Pred začetkom zdravljenja priporočamo oceno ledvičnega delovanja. **Hiperkaliemija:** Povečano tveganje pri bolnikih, ki že imajo povečane plazemske vrednosti kalija, ali bolnikih, ki jemljejo zdravila, ki lahko povzročijo hiperkaliemijo. Tveganje za hiperkaliemijo se s trajanjem zdravljenja povečuje, vendar pa je običajno reverzibilno. **Spinalna/epiduralna anestezija, spinalnolumbalna punkcija in sočasna uporaba zdravil:** Uporaba nizkomolekularnih heparinov je pri bolnikih, ki so prejeli spinalno ali epiduralno anestezijo, redko povezana s hematomi, ki lahko povzročijo podaljšano ali trajno paralizno. Tveganje za spinalno/epiduralne hematome je večje pri bolnikih, ki imajo vstavljen epiduralni kateter oziroma sočasno dobivajo tudi druga zdravila, ki lahko vplivajo na hemostazo. Tveganje je večje tudi pri travmatski ali ponavljajoči se epiduralni ali spinalni punkciji. **Salicilati, nesteroidna protivnetna zdravila in zaviralci agregacije trombocitov:** Sočasna uporaba ni priporočljiva. **Nekroza kože:** Pred nekrozo kože se pojavi purpura ali infiltrirane ali boleče eritematozne eflorescence s splošnimi znaki ali brez njih. V takih primerih je treba zdravljenje nemudoma prekiniti. **Alergija na lateks:** Ščitnik injekcijske igle v napolnjeni injekcijski brizgi lahko vsebuje suho naravno lateksno gumo, ki lahko pri na lateks preobčutljivih posameznikih povzroči alergijske reakcije. **Medsedebno delovanje z drugimi zdravili in druge oblike interakcij:** Zdravilo je treba dajati previdno bolnikom, ki se zdravijo s peroralnimi antikoagulanti, sistemskimi (gluko-) kortikosteroidi in dekstrani. Pri bolnikih, ki prejemanjo to zdravilo in se jim uvede peroralno antikoagulačno zdravljenje, je treba zdravilo nadaljevati s tem zdravilom nadaljevati, dokler se INR ne ustavi v ciljnem območju. Sočasna uporaba acetilsalicilne kisline (ali drugih salicilatov), nesteroidnih protivnetnih zdravil in zaviralcev agregacije trombocitov ni priporočena, saj lahko povečajo tveganje za krvavitve. **Nosečnost in dojenje:** Uporabe med nosečnostjo in dojenjem ne priporočamo. Če koristi zdravila ne prevažajo nad možgimi tveganji. **Neželeni učinki: Zelo pogosti:** krvavitve na različnih mestih (vključno s primeri spinalnih hematovov), ki so pogostejše pri bolnikih z drugimi dejavniki tveganja, majhni hematomi na mestu injiciranja. **Pogosti:** povečanje vrednosti transaminaz, običajno prehodno, reakcija na mestu injiciranja. **Redki:** trombotična (vključno s heparinom povzročeno trombotično), ki je večših trombotična, trombotična, izpuščaj, urtikarija, eritem, pruritus, kalcinosis na mestu injiciranja. **Zelo redki:** ezoinfilija, reverzibilna po prekinitvi zdravljenja, preobčutljivostne reakcije (vključno z angioedemom in kožnimi reakcijami), anafilaktoidna reakcija, reverzibilna hiperkaliemija zaradi s heparinom povzročene zaviranja izločanja aldosterona, še posebej pri bolnikih s tveganjem, priazipem, nekroza kože, običajno na mestu injiciranja. **Način in režim izdaje:** Predpisovanje in izdaja zdravila je le na recept s posebnim režimom-H/Rp. **Imetnik dovoljenja za promet:** Aspen Pharma Trading Limited, 3016 Lake Drive, Citywest Business Campus, Dublin 24, Irsko. **Datum zadnje revizije besedila:** 11.09.2015. **Številka dovoljenja za promet z zdravilom:** H/03/00658/007-009.

O neželenih učinkih pri zdravljenju s tem zdravilom poročajte v skladu s Pravilnikom o farmakovigilanci zdravil za uporabo v humani medicini. Za informacije o varnosti teh zdravil se obrnite na: DUB-GM-Drugsafety@e.aspenpharma.com. Za medicinske informacije se obrnite na: e-pošta: Aspenmedinfo@professionalinformation.co.uk; telefon: +386 (0)1 888 8201. Pred predpisovanjem preberite celoten Povzetek glavnih značilnosti zdravila, ki je na voljo pri naših strokovnih sodelavcih ali na www.cbz.si.

**Datum priprave informacije:** 12/7/2017. **Samo za strokovno javnost.** Aspen Europe GmbH, Podružnica Ljubljana, Železna cesta 8A, 1000 Ljubljana, www.aspenpharma.com, www.aspenpharma.eu.

SLO-NAD-0717-0124



# Instructions for authors

## The editorial policy

Radiology and Oncology is a multidisciplinary journal devoted to the publishing original and high quality scientific papers and review articles, pertinent to diagnostic and interventional radiology, computerized tomography, magnetic resonance, ultrasound, nuclear medicine, radiotherapy, clinical and experimental oncology, radiobiology, radiophysics and radiation protection. Therefore, the scope of the journal is to cover beside radiology the diagnostic and therapeutic aspects in oncology, which distinguishes it from other journals in the field.

The Editorial Board requires that the paper has not been published or submitted for publication elsewhere; the authors are responsible for all statements in their papers. Accepted articles become the property of the journal and, therefore cannot be published elsewhere without the written permission of the editors.

## Submission of the manuscript

The manuscript written in English should be submitted to the journal via online submission system Editorial Manager available for this journal at: [www.radioloncol.com](http://www.radioloncol.com).

In case of problems, please contact Sašo Trupej at [saso.trupej@computing.si](mailto:saso.trupej@computing.si) or the Editor of this journal at [gsera@onko-i.si](mailto:gsera@onko-i.si)

All articles are subjected to the editorial review and when the articles are appropriated they are reviewed by independent referees. In the cover letter, which must accompany the article, the authors are requested to suggest 3-4 researchers, competent to review their manuscript. However, please note that this will be treated only as a suggestion; the final selection of reviewers is exclusively the Editor's decision. The authors' names are revealed to the referees, but not vice versa.

Manuscripts which do not comply with the technical requirements stated herein will be returned to the authors for the correction before peer-review. The editorial board reserves the right to ask authors to make appropriate changes of the contents as well as grammatical and stylistic corrections when necessary. Page charges will be charged for manuscripts exceeding the recommended length, as well as additional editorial work and requests for printed reprints.

Articles are published printed and on-line as the open access ([www.degruyter.com/view/j/raon](http://www.degruyter.com/view/j/raon)).

All articles are subject to 700 EUR + VAT publication fee. Exceptionally, waiver of payment may be negotiated with editorial office, upon lack of funds.

Manuscripts submitted under multiple authorship are reviewed on the assumption that all listed authors concur in the submission and are responsible for its content; they must have agreed to its publication and have given the corresponding author the authority to act on their behalf in all matters pertaining to publication. The corresponding author is responsible for informing the coauthors of the manuscript status throughout the submission, review, and production process.

## Preparation of manuscripts

Radiology and Oncology will consider manuscripts prepared according to the Uniform Requirements for Manuscripts Submitted to Biomedical Journals by International Committee of Medical Journal Editors ([www.icmje.org](http://www.icmje.org)). The manuscript should be written in grammatically and stylistically correct language. Abbreviations should be avoided. If their use is necessary, they should be explained at the first time mentioned. The technical data should conform to the SI system. The manuscript, excluding the references, tables, figures and figure legends, must not exceed 5000 words, and the number of figures and tables is limited to 8. Organize the text so that it includes: Introduction, Materials and methods, Results and Discussion. Exceptionally, the results and discussion can be combined in a single section. Start each section on a new page, and number each page consecutively with Arabic numerals.

*The Title page* should include a concise and informative title, followed by the full name(s) of the author(s); the institutional affiliation of each author; the name and address of the corresponding author (including telephone, fax and E-mail), and an abbreviated title (not exceeding 60 characters). This should be followed by the abstract page, summarizing in less than 250 words the reasons for the study, experimental approach, the major findings (with specific data if possible), and the principal conclusions, and providing 3-6 key words for indexing purposes. Structured abstracts are required. Slovene authors are requested to provide title and the abstract in Slovene language in a separate file. The text of the research article should then proceed as follows:

*Introduction* should summarize the rationale for the study or observation, citing only the essential references and stating the aim of the study.

*Materials and methods* should provide enough information to enable experiments to be repeated. New methods should be described in details.

*Results* should be presented clearly and concisely without repeating the data in the figures and tables. Emphasis should be on clear and precise presentation of results and their significance in relation to the aim of the investigation.

*Discussion* should explain the results rather than simply repeating them and interpret their significance and draw conclusions. It should discuss the results of the study in the light of previously published work.

### Charts, Illustrations, Images and Tables

Charts, Illustrations, Images and Tables must be numbered and referred to in the text, with the appropriate location indicated. Charts, Illustrations and Images, provided electronically, should be of appropriate quality for good reproduction. Illustrations and charts must be vector image, created in CMYK color space, preferred font "Century Gothic", and saved as .AI, .EPS or .PDF format. Color charts, illustrations and Images are encouraged, and are published without additional charge. Image size must be 2.000 pixels on the longer side and saved as .JPG (maximum quality) format. In Images, mask the identities of the patients. Tables should be typed double-spaced, with a descriptive title and, if appropriate, units of numerical measurements included in the column heading. The files with the figures and tables can be uploaded as separate files.

### References

References must be numbered in the order in which they appear in the text and their corresponding numbers quoted in the text. Authors are responsible for the accuracy of their references. References to the Abstracts and Letters to the Editor must be identified as such. Citation of papers in preparation or submitted for publication, unpublished observations, and personal communications should not be included in the reference list. If essential, such material may be incorporated in the appropriate place in the text. References follow the style of Index Medicus, DOI number (if exists) should be included.

All authors should be listed when their number does not exceed six; when there are seven or more authors, the first six listed are followed by "et al.". The following are some examples of references from articles, books and book chapters:

Dent RAG, Cole P. In vitro maturation of monocytes in squamous carcinoma of the lung. *Br J Cancer* 1981; **43**: 486-95. doi:10.1038/bjc.1981.71

Chapman S, Nakielny R. *A guide to radiological procedures*. London: Bailliere Tindall; 1986.

Evans R, Alexander P. Mechanisms of extracellular killing of nucleated mammalian cells by macrophages. In: Nelson DS, editor. *Immunobiology of macrophage*. New York: Academic Press; 1976. p. 45-74.

### Authorization for the use of human subjects or experimental animals

When reporting experiments on human subjects, authors should state whether the procedures followed the Helsinki Declaration. Patients have the right to privacy; therefore the identifying information (patient's names, hospital unit numbers) should not be published unless it is essential. In such cases the patient's informed consent for publication is needed, and should appear as an appropriate statement in the article. Institutional approval and Clinical Trial registration number is required. Retrospective clinical studies must be approved by the accredited Institutional Review Board/Committee for Medical Ethics or other equivalent body. These statements should appear in the Materials and methods section.

The research using animal subjects should be conducted according to the EU Directive 2010/63/EU and following the Guidelines for the welfare and use of animals in cancer research (*Br J Cancer* 2010; **102**: 1555 – 77). Authors must state the committee approving the experiments, and must confirm that all experiments were performed in accordance with relevant regulations.

These statements should appear in the Materials and methods section (or for contributions without this section, within the main text or in the captions of relevant figures or tables).

### Transfer of copyright agreement

For the publication of accepted articles, authors are required to send the License to Publish to the publisher on the address of the editorial office. A properly completed License to Publish, signed by the Corresponding Author on behalf of all the authors, must be provided for each submitted manuscript.

The non-commercial use of each article will be governed by the Creative Commons Attribution-NonCommercial-NoDerivs license.

### Conflict of interest

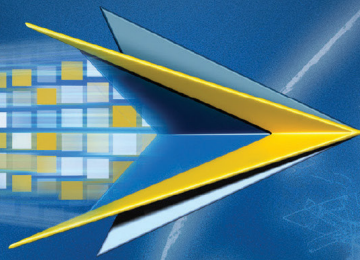
When the manuscript is submitted for publication, the authors are expected to disclose any relationship that might pose real, apparent or potential conflict of interest with respect to the results reported in that manuscript. Potential conflicts of interest include not only financial relationships but also other, non-financial relationships. In the Acknowledgement section the source of funding support should be mentioned. The Editors will make effort to ensure that conflicts of interest will not compromise the evaluation process of the submitted manuscripts; potential editors and reviewers will exempt themselves from review process when such conflict of interest exists. The statement of disclosure must be in the Cover letter accompanying the manuscript or submitted on the form available on [www.icmje.org/coi\\_disclosure.pdf](http://www.icmje.org/coi_disclosure.pdf)

### Page proofs

Page proofs will be sent by E-mail to the corresponding author. It is their responsibility to check the proofs carefully and return a list of essential corrections to the editorial office within three days of receipt. Only grammatical corrections are acceptable at that time.

### Open access

Papers are published electronically as open access on [www.degruyter.com/view/j/raon](http://www.degruyter.com/view/j/raon), also papers accepted for publication as E-ahead of print.



# XALKORI® - prvi zaviralec ALK, odobren za I. linijo zdravljenja napredovalega, ALK pozitivnega nedrobnoceličnega pljučnega raka<sup>1</sup>

ALK = anaplasična limfomska kinaza

## BISTVENI PODATKI IZ POVZETKA GLAVNIH ZNAČILNOSTI ZDRAVILA

### XALKORI 200 mg, 250 mg trde kapsule

▼ Za to zdravilo se izvaja dodatno spremljanje varnosti. Tako bodo hitreje na voljo nove informacije o njegovi varnosti. Zdravstvene delavce naprošamo, da poročajo o kateremkoli domnevnem neželenem učinku zdravila. Glejte poglavje 4.8 povzetka glavnih značilnosti zdravila, kako poročati o neželenih učinkih. **Sestava in oblika zdravila:** Ena kapsula vsebuje 200 mg ali 250 mg krizotiniba. **Indikacije:** Prva linija zdravljenja odraslih bolnikov z napredovalim nedrobnoceličnim pljučnim rakom (NSCLC - Non-Small Cell Lung Cancer), ki je ALK (anaplasična limfomska kinaza) pozitiven. Zdravljenje odraslih bolnikov s predhodno zdravljenim, napredovalim NSCLC, ki je ALK pozitiven. Zdravljenje odraslih bolnikov z napredovalim NSCLC, ki je ROS1 pozitiven. **Odmernje in način uporabe:** Zdravljenje mora uvesti in nadzorovati zdravnik z izkušnjami z uporabo zdravil za zdravljenje rakavih bolezni. **Preverjanje prisotnosti ALK in ROS1:** Pri izbiri bolnikov za zdravljenje je treba pred zdravljenjem opraviti točno in validirano preverjanje prisotnosti ALK ali ROS1. **Odmernje:** Priporočeni odmerek je 250 mg dvakrat na dan (500 mg na dan), bolniki pa morajo zdravilo jemati brez prekinitev. Če bolnik pozabi vzeti odmerek, ga mora vzeti takoj, ko se spomni, razen če do naslednjega odmerka manjka manj kot 6 ur. V tem primeru bolnik pozabljenega odmerka ne sme vzeti. **Prilaganje odmerkov:** Glede na varnost uporabe zdravila pri posameznem bolniku in kako bolnik zdravljenje prenaša, utegne biti potrebna prekinitev in/ali zmanjšanje odmerka zdravila na 200 mg dvakrat na dan, če je potrebno še nadaljnje zmanjšanje, pa znaša odmerek 250 mg enkrat na dan. Za prilaganje odmerkov pri hematološki in nehematološki (povečanje vrednosti AST, ALT, bilirubina; ILD/pnevmonitis; podaljšanje intervala QTc, bradikardija, bolezi oči) toksičnosti glejte preglednici 1 in 2 v povzetku glavnih značilnosti zdravila. **Okvara jeter:** Pri blagi in zmerni okvari je zdravljenje treba izvajati previdno, pri hudi okvari se zdravila ne sme uporabljati. **Okvara ledvic:** Pri blagi in zmerni okvari prilaganje začetnega odmerka ni priporočeno. Pri hudi okvari ledvic (ki ne zahteva peritonealne dialize ali hemodialize) je začetni odmerek 250 mg peroralno enkrat na dan; po vsaj 4 tednih zdravljenja se lahko poveča na 200 mg dvakrat na dan. **Starejši bolniki (U 65 let):** Prilaganje začetnega odmerka ni potrebno. **Pediatrična populacija:** Varnost in učinkovitost nista bili dokazani. **Način uporabe:** Kapsule je treba pogoltniti cele, z nekaj vode, s hrano ali brez nje. Ne sme se jih združiti, raztopiti ali odpreti. Izogibati se je treba uživanju grenivk, grenivkega soka ter uporabi šentjanževke. **Kontraindikacije:** Preobčutljivost na krizotinib ali katerokoli pomožni snov. Huda okvara jeter. **Posebna opozorila in previdnostni ukrepi:** Določanje statusa ALK in ROS1: Pomembno je izbrati dobro validirano in robustno metodologijo, da se izognemo lažno negativnim ali lažno pozitivnim rezultatom. **Hepatotoksičnost:** V kliničnih študijah so poročali o hepatotoksičnosti, ki jo je povzročilo zdravilo (vključno s primeri s smrtnim izidom). Delovanje jeter, vključno z ALT, AST in skupnim bilirubinom, je treba preveriti enkrat na teden v prvih 2 mesecih zdravljenja, nato pa enkrat na mesec in kot je klinično indicirano. Ponovite preverjanj morajo biti pogostejše pri povečanih vrednostih stopnje 2, 3 ali 4. **Intersticijska bolezen pljuč (ILD)/pnevmonitis:** Lahko se pojavi huda, življenjsko nevarna ali smrtna ILD/pnevmonitis. Bolnike s simptomi ILD/pnevmonitisa, je treba spremljati, zdravljenje pa prekiniti ob sumu na ILD/pnevmonitis. **Podaljšanje intervala QTc:**

Opažali so podaljšanje intervala QTc. Pri bolnikih z obstoječo bradikardijo, podaljšanjem intervala QTc v anamnezi ali predispozicijo zanj, pri bolnikih, ki jemljejo antiaritmike ali druga zdravila, ki podaljšujejo interval QT, ter pri bolnikih s pomembno obstoječo srčno boleznijo in/ali motnjami elektrolitov je treba krizotinib uporabljati previdno; potrebno je redno spremljanje EKG, elektrolitov in delovanja ledvic; preiskavi EKG in elektrolitov je treba opraviti čim bližje uporabi prvega odmerka, potem se priporoča redno spremljanje. Če se interval QTc podaljša za 60 ms ali več, je treba zdravljenje s krizotinibom začasno prekiniti in se posvetovati s kardiologom. **Bradikardija:** Lahko se pojavi simptomatska bradikardija (lahko se razvije več tednov po začetku zdravljenja); izogibati se je treba uporabi krizotiniba v kombinaciji z drugimi zdravili, ki povzročajo bradikardijo; pri simptomatski bradikardiji je treba prilagoditi odmerek. **Srčno popuščanje:** Poročali so o hudih, življenjsko nevarnih ali smrtnih neželenih učinkih srčnega popuščanja. Bolnike je treba spremljati glede pojavov znakov in simptomov srčnega popuščanja in ob pojavu simptomov zmanjšati odmerjanje ali prekiniti zdravljenje. **Nevtropenija in levkopenija:** V kliničnih študijah so poročali o nevtropeniji, levkopeniji in febrilni nevtropeniji; spremljati je treba popolno krvno sliko (pogostejše preiskave, če se opazijo abnormalnosti stopnje 3 ali 4 ali če se pojavi povišana telesna temperatura ali okužba). **Perforacija v prebavilih:** V kliničnih študijah so poročali o perforacijah v prebavilih, v obdobju trženja pa o smrtnih primerih perforacij v prebavilih. Krizotinib je treba pri bolnikih s tveganjem za nastanek perforacije v prebavilih uporabljati previdno; bolniki, pri katerih se razvije perforacija v prebavilih, se morajo prenehati zdraviti s krizotinibom; bolnike je treba poučiti o prvih znakih perforacije in jim svetovati, naj se nemudoma posvetujejo z zdravnikom. **Vplivi na ledvice:** V kliničnih študijah so opazili zvišanje ravnih kreatininov v krvi in zmanjšanje očistka kreatinina. V kliničnih študijah in v obdobju trženja so poročali tudi o odpovedi ledvic, akutni odpovedi ledvic, primerih s smrtnim izidom, primerih, ki so zahtevali hemodializo in hiperkalemiji stopnje 4. **Vplivi na vid:** V kliničnih študijah so poročali o izgubi vidnega polja stopnje 4 z izgubo vida. Če se na novo pojavi huda izguba vida, je treba zdravljenje prekiniti in opraviti oftalmološki pregled, če so motnje vida trdovratne ali se poslabšajo, je priporočilo oftalmološki pregled. **Histološka preiskava, ki ne nakazuje adenokarcinoma:** Na voljo so le omejeni podatki pri NSCLC, ki je ALK in ROS1 pozitiven in ima histološke značilnosti, ki ne nakazujejo adenokarcinoma, vključno s ploščatoceličnim karcinomom (SCC). **Medsebojno delovanje z drugimi zdravili in druge oblike interakcij:** Zdravilo, ki lahko povečajo koncentracije krizotiniba v plazmi (močni zaviralci CYP3A4, npr. atazanavir, indinavir, neflavinol, ritonavir, sakvinavir, itrakonazol, ketokonazol, vorikonazol, klaritromicin, telitromicin, troleandomicin), tudi grenivke in grenivkin sok. Zdravila, ki lahko zmanjšajo koncentracije krizotiniba v plazmi (močni induktorji CYP3A4, npr. karbamazepin, fenobarbital, fenitoin, rifampicin, šentjanževka). Zmerni induktorji CYP3A4, npr. efavirenz in rifabutin. Zdravila, katerih koncentracije v plazmi lahko krizotinib spremeni (midazolam, alfentanil, cisaprid, ciklosporin, derivati ergot alkaloidov, fentanyl, pimizid, kinidin, sirolimus, takrolimus, bupropion, efavirenz, peroralni kontraceptivi, raltegravir, inderin, morfin, nalokson, digoksin, dabigatran, kolhicin, pravastatin, meflokin, prokainamid). Zdravila, ki podaljšujejo interval QT ali ki lahko



povzročijo Torsades de pointes (antiaritmiki skupine IA (kinidin, disopiramid), antiaritmiki skupine III (amiodaron, sotalol, dofetilid, ibutilid), metadon, cisaprid, moksifloksacin, antipsihotiki). Zdravila, ki povzročajo bradikardijo (nedihidropiridinski zaviralci kalcijevih kanalčkov (verapamil, diltiazem), antagonisti adrenergičnih receptorjev beta, klonidin, gvanfacin, digoksin, meflokin, antiholinesteraze, pilokarpin). **Plodnost, nosečnost in dojenje:** Ženske v rodni dobi se morajo izogibati zanositvi. Med zdravljenjem in najmanj 90 dni po njem je treba uporabljati ustrezno kontracepcijo (velja tudi za moške). Zdravilo lahko škoduje plodu in se ga med nosečnostjo ne sme uporabljati, razen če klinično stanje matere ne zahteva takega zdravljenja. Matere naj se med jemanjem zdravila dojenju izogibajo. Zdravilo lahko zmanjša plodnost moških in žensk. **Vpliv na sposobnost vožnje in upravljanja strojev:** Lahko se pojavijo simptomatska bradikardija (npr. sinkopa, omotica, hipotenzija), motnje vida ali utrujenost; potrebna je previdnost. **Neželeni učinki:** Najresnejši neželeni učinki so bili hepatotoksičnost, ILD/pnevmonitis, nevtropenija in podaljšanje intervala QT. Najpogostejši neželeni učinki (U 25 %) so bili motnje vida, navzea, diareja, bruhanje, edem, zaprtje, povečane vrednosti transaminaz, utrujenost, pomanjkanje apetita, omotica in nevtropatija. Ostali lete pogosti (U 1/10 bolnikov) neželeni učinki so: nevtropenija, anemija, levkopenija, disgevgzija, bradikardija, bolečina v trebuhu in izpuščaji. **Način in režim izdaje:** Predpisovanje in izdaja zdravila je le na recept, zdravilo pa se uporablja samo v bolnišnicah. Izjemoma se lahko uporablja pri nadaljevanju zdravljenja na domu ob odpustu iz bolnišnice in nadaljnjem zdravljenju. **Imetnik dovoljenja za promet:** Pfizer Limited, Ramsgate Road, Sandwich, Kent CT13 9NJ, Velika Britanija. **Datum zadnje revizije besedila:** 11.11.2016 **Pred predpisovanjem se seznanite s celotnim povzetkom glavnih značilnosti zdravila.**

Vir: 1. Povzetek glavnih značilnosti zdravila Xalkori, 11.11.2016



Pfizer Luxembourg SARL, GRAND DUCHY OF LUXEMBOURG, 51, Avenue J.F. Kennedy, L-1855, Pfizer podružnica Ljubljana, Letališka cesta 3c, 1000 Ljubljana

